The Carboniferous Bowland Shale gas study: geology and resource estimation

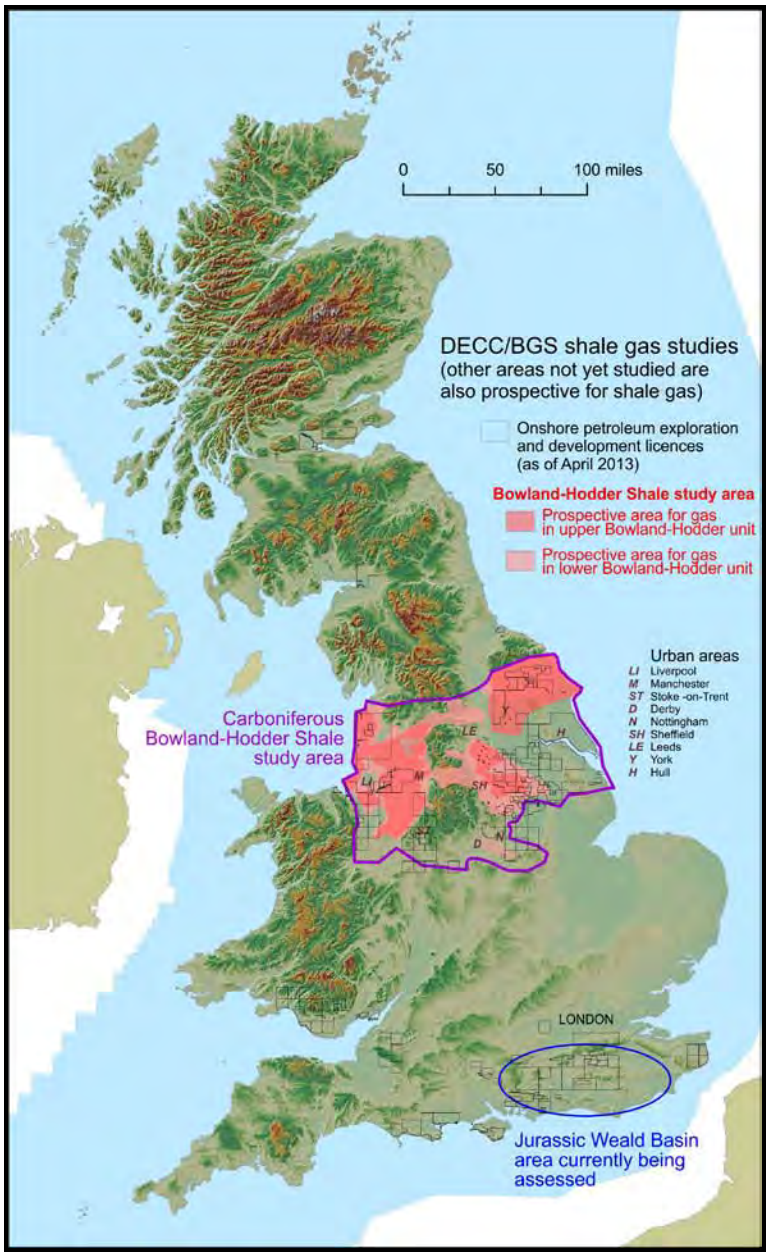

British Geological Survey
NATURAL ENVIRONMENT RESEARCH COUNCIL

Department of Energy & Climate Change

Disclaimer

Suggested citation:

Andrews, I.J. 2013. *The Carboniferous Bowland Shale gas study: geology and resource estimation*. British Geological Survey for Department of Energy and Climate Change, London, UK.

Requests and enquiries should be addressed to:

Toni Harvey
Senior Geoscientist - UK Onshore
Email: toni.harvey@decc.gsi.gov.uk

Foreword

This report has been produced under contract by the British Geological Survey (BGS). It is based on a recent analysis, together with published data and interpretations.

Additional information is available at the Department of Energy and Climate Change (DECC) website. https://www.gov.uk/oil-and-gas-onshore-exploration-and-production. This includes licensing regulations, maps, monthly production figures, basic well data and where to view and purchase data. Shale gas related issues including hydraulic fracturing, induced-seismicity risk mitigation and the information regarding the onshore regulatory framework can also be found on this webpage.

Interactive maps, with licence data, seismic, relinquishment reports and stratigraphic tops for many wells are available at www.ukogl.org.uk.

A glossary of terms used and equivalences is tabled at the end of the report (see page 48).

All of the figures in this report are attached in A4 or larger format; thumbnails are also included in the text for reference.

Acknowledgements

The author would like to thank the many contributors to this report, most notably Sue Stoker[1], Kevin Smith[3], Nigel Smith[4], Mike Sankey[3], Chris Vane[4], Mike McCormac[3], Ceri Vincent[4], Vicky Moss-Hayes[4], Toni Harvey[2] and Joy Gray[2], and reviewers Al Fraser[5], Nick Riley[4] and Don Cameron[3].

[1] Formerly of British Geological Survey, Edinburgh, UK
[2] Department of Energy and Climate Change, London, UK
[3] British Geological Survey, Edinburgh, UK
[4] British Geological Survey, Keyworth, UK
[5] Department of Earth Science and Engineering, Imperial College, London, UK

With minor typographic changes, July 2013.

Contents

List of figures

Figure 14. The Early Carboniferous basins and platforms of central Britain (modified after Fraser *et al*. 1990, Kirby *et al*. 2000). CLH = Central Lancashire High; HH = Holme High. Note: the presence of Early Carboniferous basins beneath the Permo-Triassic Cheshire Basin (Smith *et al*. 2005 cf. Waters *et al*. 2009) and a putative Humber Basin (Kent 1966, Hodge 2003) are both debatable (see text).

Figure 15. Lithostratigraphical framework of the Bowland-Hodder unit in central Britain (after Waters *et al*. 2009). Note: away from the outcrops, the platform carbonates in the Wessenden 1 and Roddlesworth 1 boreholes are termed Holme High Group and Trawden Group respectively (Waters *et al*. 2011). No formal lithostratigraphic framework has yet been applied to strata in the subsurface Cleveland Basin. In pre-2009 terminology, the Craven Group equates to the combined Worston Shale and Bowland Shale groups, excluding the Clitheroe Limestone Formation. Note: the use of Upper Chadian follows Riley (1990), but the Chadian has been partly redefined by Waters *et al*. (2011). Also, the Cleveland Basin sequence is poorly known and it is likely to have non-sequences that are not yet unrecognized.

Figure 16. Schematic diagram showing the relationship between hemipelagic basinal shales and platform carbonates within the Bowland-Hodder unit. Note that basin shales also occur interbedded with the sandstones of the overlying Millstone Grit.

Figure 17. Depth (ft) to the top of the Bowland-Hodder unit, central Britain. The location of regional cross-sections is indicated (see Figure 19).

Figure 18. Thickness (ft) of the Bowland-Hodder unit, central Britain. The interval was not mapped across the Derbyshire High where there are no seismic data (and the unit comprises platform carbonate rocks) (see Figure 19C & E). The location of example seismic profiles is indicated (see Figures 20-25).

Figure 19. Generalised depth cross-sections through the Bowland Basin, Cheshire Basin, Widmerpool Trough, Gainsborough Trough and Edale Basin. For location of the sections, see Figure 17.

Figure 20. Seismic example across the deepest-buried part of the Bowland Basin showing thickening of the Bowland-Hodder unit towards the basin depocentre. The Thistleton 1 well terminated in Brigantian-aged shales and sandstones and the lower Bowland-Hodder unit was not reached. However, the Hodder Mudstone Formation is at least 3000 ft (900 m) thick in the Plantation Farm Anticline outcrop section located 25 km ENE of Thistleton 1 (Riley 1990), and a section of similar thickness is expected to be present in the area overlain by Permo-Triassic strata. For location of the section, see Figure 18.

Figure 21. Seismic example across a folded and uplifted part of the Bowland Basin. The Pendle Line and associated monocline mark the southern boundary of the Bowland Basin; Westphalian Coal Measures crop out in the south-east. For location of the section, see Figure 18.

Figure 22. Seismic example across the Edale Basin where very thick basinal shales are interpreted. On the adjacent Derbyshire High, the Bowland-Hodder unit comprises platform carbonates topped by relatively thin upper Bowland-Hodder shales. For location of the section, see Figure 18.

Figure 23. Seismic example across the Gainsborough Trough. The Grove 3 well is located on the East Midlands Shelf and illustrates the platform limestone-dominated nature of the Bowland-Hodder unit

1. Summary

The assessment of shale gas resources in the UK is in its infancy. This report summarises the background geological knowledge and methodology which has enabled a preliminary in-place gas resource calculation to be undertaken for the Bowland-Hodder (Carboniferous) shale gas play[1] across a large area of central Britain (Figure 1).

Marine shales were deposited in a complex series of tectonically active basins across central Britain during the Visean and Namurian epochs[2] of the Carboniferous (c.347-318 Ma). In all of these basins, deep-water marine shales pass laterally into shallow-water shelf limestones and deltaic sandstones. Contemporary basins extend offshore beneath the East Irish Sea and the Southern North Sea.

The marine shales attain thicknesses of up to 16,000 ft (5000 m) in basin depocentres (i.e. the Bowland, Blacon, Gainsborough, Widmerpool, Edale and Cleveland basins), and they contain sufficient organic matter to generate considerable amounts of hydrocarbons. Conventional oil and gas fields around most of these basins attest to their capability to produce hydrocarbons.

The organic content of the Bowland-Hodder shales is typically in the range 1-3%, but can reach 8%.

The maturity of the Bowland-Hodder shales is a function of burial depth, heat flow and time, but subsequent uplift complicates this analysis. Where they have been buried to sufficient depth for the organic material to generate gas, the Bowland-Hodder shales have the potential to form a shale gas resource analogous to the producing shale gas provinces of North America (e.g. Barnett Shale, Marcellus Shale). Where the shales have been less-deeply buried, there is potential for a shale oil resource (but, as yet, there is inadequate geotechnical data to estimate the amount of oil in-place).

In this study, shales are considered mature for gas generation (vitrinite reflectance > 1.1%) at depths greater than c. 9500 ft (2900 m) (where there has been minimal uplift). However, central Britain has experienced a complex tectonic history and the rocks here have been uplifted and partially eroded at least once since Carboniferous times. Because of this, the present-day depth to the top of the gas window is dependent on the amount of uplift, and can occur significantly shallower than 9500 ft.

The total volume of potentially productive shale in central Britain was estimated using a 3D geological model generated using seismic mapping, integrated with outcrop and deep borehole information. This volume was truncated upwards at a depth of 5000 ft (1500 m) below land surface (a suggested US upper limit for thermogenic shale gas production) or the depth at which the shale is mature for gas generation (whichever was the shallowest).

The volume of potentially productive shale was used as one of the input parameters for a statistical calculation (using a Monte Carlo simulation) of the in-place gas resource (see Appendix A).

[1] The Bowland-Hodder shale gas play (or Bowland-Hodder shales) is the term used in this report for an amalgamation of shales of Visean to early Namurian age that includes the Bowland Shale Formation (and its equivalents) together with older shales which equate to the Hodder Mudstone Formation. The definition of the unit is discussed in more detail within this report.

[2] See Section 5 for a comparison of the Carboniferous chronostratigraphies used by European and North American/international geologists.

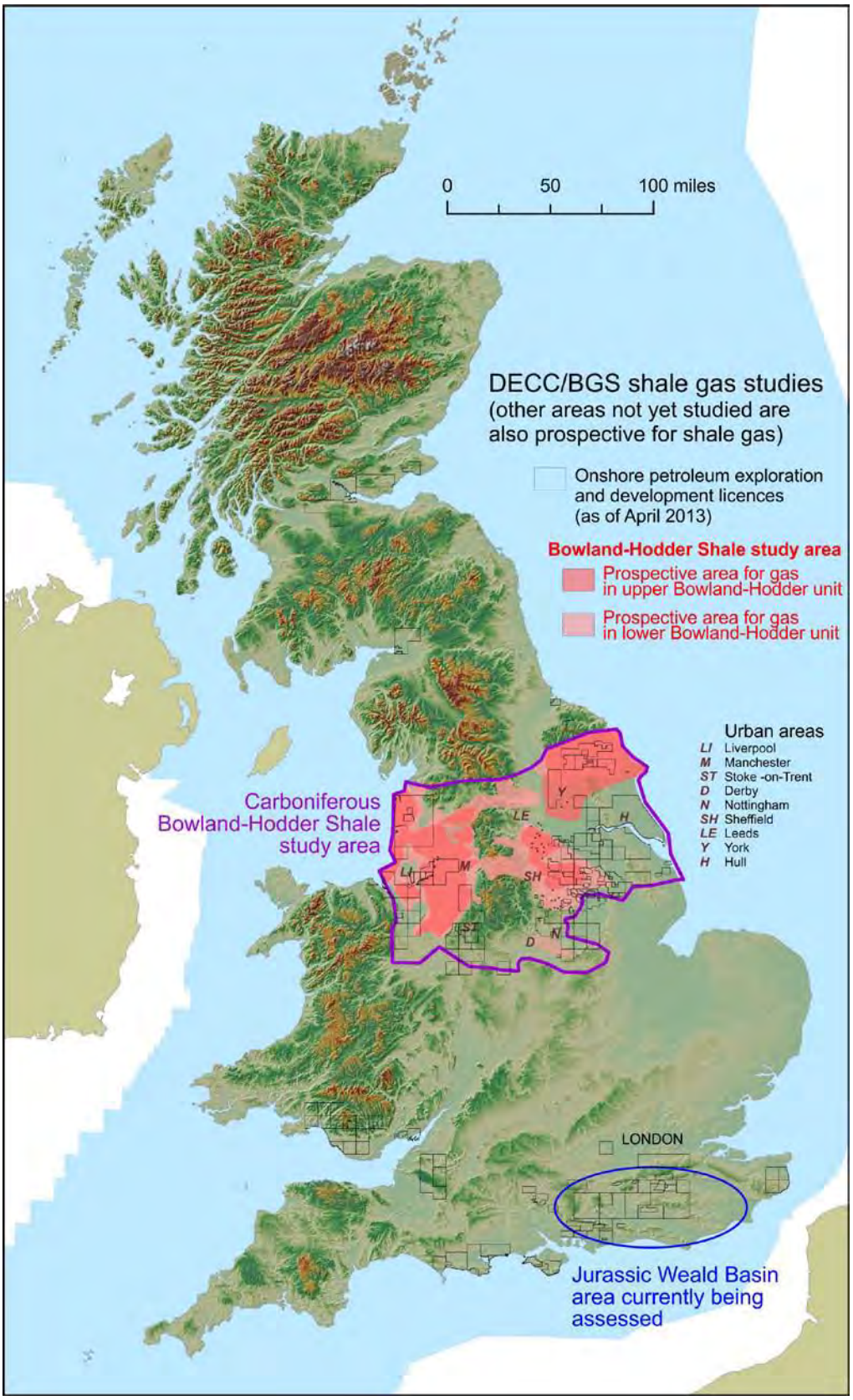

Figure 1. Location of the DECC/BGS study area in central Britain, together with prospective areas for shale gas, currently licensed acreage and selected urban areas. Other shale gas and shale oil plays may exist.

For the purposes of resource estimation, the Bowland-Hodder unit is divided into two units: an upper post-rift unit in which laterally contiguous, organic-rich, condensed zones can be mapped, even over the platform highs, and an underlying syn-rift unit, expanding to thousands of feet thick in fault-bounded basins, where the shale is interbedded with mass flow clastic sediments and re-deposited carbonates.

The upper unit is more prospective, primarily due to the better well control which demonstrates its closer resemblance to the prolific North American shale gas plays, in which the productive zones are hundreds of feet thick. The lower unit is largely undrilled, but where it has been penetrated it contains organic-rich shale intervals, whose lateral extent is unknown.

This study offers a range of total in-place gas resource estimates for the upper Bowland-Hodder unit shales across central Britain of 164 – 264 – 447 tcf (4.6 – 7.5 – 12.7 tcm) (P90 – P50 – P10). It should be emphasised that these 'gas-in-place' figures refer to an estimate for the entire volume of gas contained in the rock formation, not how much can be recovered.

There is considerable upside potential in the lower unit, but the resource estimation for this unit has a much higher uncertainty due to the paucity of well data so far and potentially less favourable lithologies. The estimated range of gas in place for this thick unit is 658 – 1065 – 1834 tcf (18.7 – 31.2 – 51.9 tcm). The total range for estimated gas in place is 822 – 1329 – 2281 tcf (23.3 – 37.6 – 64.6 tcm) (P90 – P50 – P10) for the combined upper and lower parts of the Bowland-Hodder unit.

	Total gas in-place estimates (tcf)			Total gas in-place estimates (tcm)		
	Low (P90)	Central (P50)	High (P10)	Low (P90)	Central (P50)	High (P10)
Upper unit	164	264	447	4.6	7.5	12.7
Lower unit	658	1065	1834	18.6	30.2	51.9
Total	822	1329	2281	23.3	37.6	64.6

This large volume of gas has been identified in the shales beneath central Britain, but not enough is yet known to estimate a recovery factor, nor to estimate potential reserves (how much gas may be ultimately produced). An estimate was made in the previous DECC-commissioned BGS report (2010a) that the Carboniferous Upper Bowland Shale, if equivalent to the Barnett Shale of Texas, could potentially yield up to 4.7 tcf (133 bcm) of shale gas. In the absence of subsurface volumes of potential gas-bearing shale, this early estimate was based on the relative areal extent of the basins. Now, after detailed subsurface analysis, a "bottom-up" resource assessment of gas in-place has be made, which more accurately reflects the area's shale gas potential. However, it is still too early to use a more refined methodology, like the USGS's Technically Recoverable Resource "top-down" estimates which require production data from wells. In time, the drilling and testing of new wells will give an understanding of achievable, sustained production rates. These, combined with other non-geological factors such as gas price, operating costs and the scale of development agreed by the local planning system, will allow estimates of the UK's shale gas reserves to be made.

Other areas in the UK have shale gas and shale oil potential, and later in 2013 the Jurassic shales in the Weald Basin of southern England will be the subject of a further BGS/DECC study.

2. Introduction to shale gas and resource estimation

2.1. History of oil and gas exploration and production in the UK

Exploration for oil and gas in the UK began onshore in the late 19th century, but subsequent land-based activity has been episodic, with six principal phases yielding variable success (Evans 1990, Decc 2010b). The earliest reports of hydrocarbons date from 1836, and a well drilled at Heathfield in Sussex in 1895 produced sufficient gas to fuel a gas light for the railway station. The history of exploration through subsequent decades is detailed in DECC (2010b), with the largest gas fields discovered being Saltfleetby (Lincolnshire) and Kirby Misperton (North Yorkshire). Wytch Farm with associated gas (Dorset), Welton (Lincolnshire), Stockbridge (Hampshire) and Eakring (Nottinghamshire) have produced the most oil (DECC 2010b). Wytch Farm is the largest onshore oil field in Europe, but the total onshore production is small compared with offshore production and contributes only 1.5% of overall UK oil and gas total. Over 2100 wells have been drilled onshore for oil and gas. There are currently (April 2013) 30 oil fields and 8 gas fields producing onshore, plus 3 coalbed methane and 18 vent gas (extraction of methane from abandoned coal mines) fields producing gas.

In recent years (Figure 2), there has been a decline in the number of exploration and appraisal wells drilled for conventional oil and gas onshore, with a shift to coalbed methane (CBM), vent gas and most recently, to wells drilled for shale gas exploration.

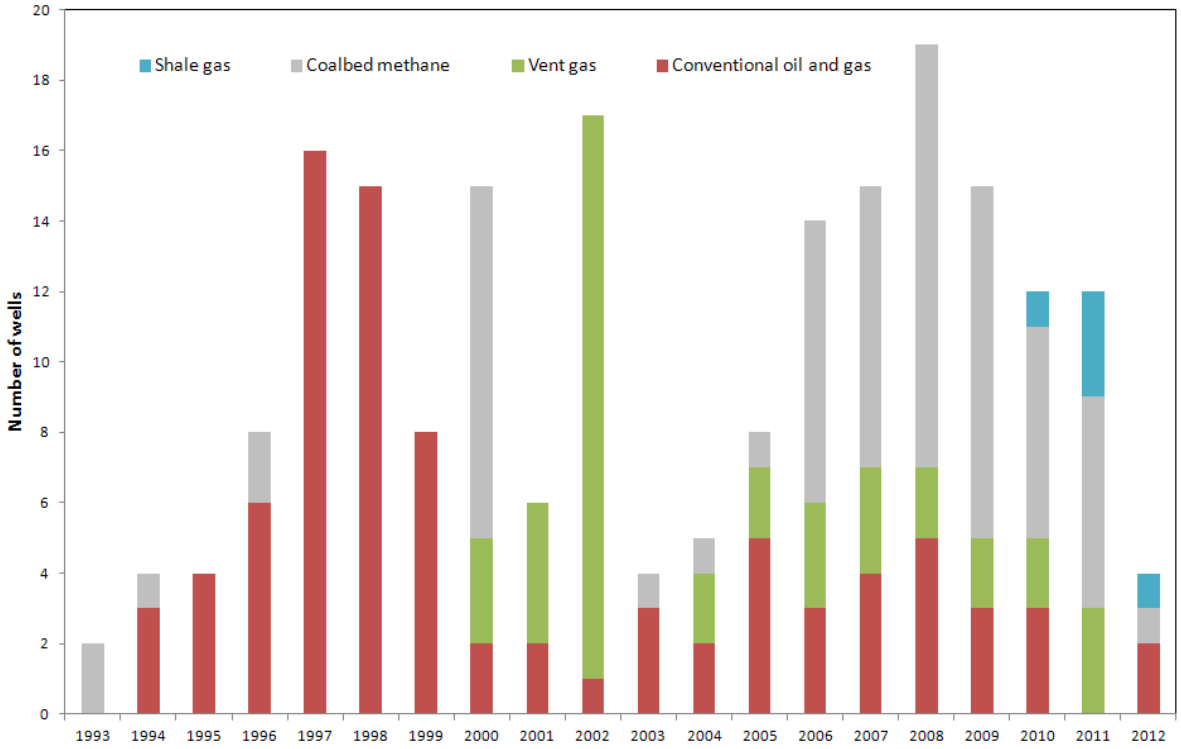

Figure 2. Numbers of onshore exploration and appraisal wells drilled in the past 20 years.

Within the study area, significant amounts of gas have been discovered in conventional plays in the Bowland, Cleveland, Edale, Gainsborough, Humber and Widmerpool basins (Figure 3). There was also a natural build-up of methane in the Wyresdale Tunnel, Lancashire, which lead to the fatal Abbeystead explosion in May 1984 (Wilson *et al*. 1985, Smith *et al*. 2010). These occurrences provide

evidence for working petroleum systems in all of the sub-basins and the expulsion of gas from source rocks which have reached the gas window in the vicinity of the fields.

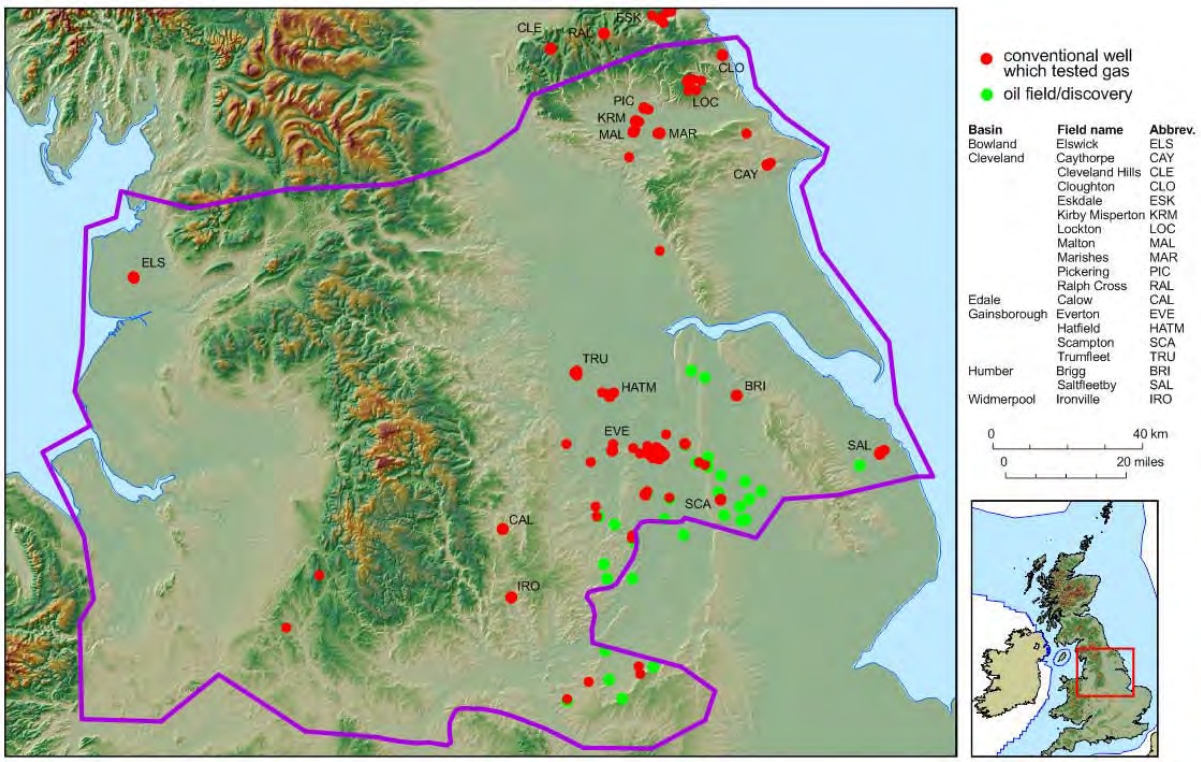

Figure 3. Distribution of wells (not including coal-related CBM or vent gas) which have tested gas and oil in central Britain (from DECC data).

Oil was commercially produced from Carboniferous oil shales in West Lothian between 1859 and the 1940s, and although shale gas potential was highlighted in the 1980s (Selley 1987, 1996, 2005) it was only in the 13th Onshore Licensing Round in 2008 that companies specifically sought to explore for shale gas. Only one shale gas well has been hydraulically fractured, Cuadrilla's Preese Hall 1 well during 2011, but that test was suspended before completion of the fracturing programme after two small earthquakes were induced (Green *et al*. 2012).

2.2. Resources vs. reserves

In simple terms, the resource estimate for any shale gas play is the amount of gas in the ground (some of which might never be produced), while the reserve estimate is a more speculative measure which describes the amount of gas that you might be able to extract given appropriate technology, economics and other factors. The recovery factor is an estimate of the proportion of the total gas resource that might be extracted, and it is generally expressed as a percentage. Recently, the Parliamentary Office of Science and Technology published a POSTbox note for policymakers to address the distinction between reserves and resources, which have often been confused by the media (POSTbox 2013).

To some extent our ability to obtain reserve or resource figures in any hydrocarbon province is determined by the stage of exploration and the degree of production uncertainty. Gas in-place (GIP), original gas in-place (OGIP) or gas initially in-place (GIIP) are all the same estimate and these figures

are normally derived early in an exploration phase perhaps even before drilling takes place, for the benefit of shareholders and investors. These speculative values often find their way into the media. When substantive data from drilling and production rates become available, more reliable figures for reserves and resources can be estimated. But if only a few wells are drilled, there is a risk that the data they reveal may not be representative of large undrilled areas. A large variability in shale gas well productivity has been experienced in North America, where the gas from wells in 'sweet spots' far exceed the average recovery from wells across the play area.

A third measure of the amount of gas is the concept of 'technically recoverable resources' (TRR) which the US Geological Survey (e.g. Charpentier & Cook 2011) use to estimate how much gas is likely to be extracted. The USGS methodology was modified for coalbed methane and shale gas and oil to use well production information (estimated ultimate recovery and well spacing) to better constrain estimates of recoverable volumes compared with their previous recovery factor based methodology used for conventional oil and gas. The US Energy Information Administration (EIA) estimates of TRR for shale gas and tight oil have changed significantly in recent years as new well performance data and USGS resource assessments have been integrated (USEIA 2012). However, a wide variety of other methodologies of estimating resource and reserve potential have been used by other organizations and these described by Pearson *et al.* (2012) along with the factors determining the viability of development. Technically or economically recoverable resources will fluctuate in time according to technological advances and commercial factors.

In the US, the SPE Petroleum Resource Management System nomenclature (Figure 4, SPE 2007) defines total petroleum initially-in-place as that quantity of petroleum that is estimated to exist in naturally occurring accumulations. It includes that quantity of petroleum that is estimated, as of a given date, to be contained in known accumulations prior to production plus those estimated quantities in accumulations yet to be discovered (equivalent to 'total resources') and goes on to describe 'contingent resources' for which key conditions or contingencies that prevent commercial development must be clarified or proved to be viable.

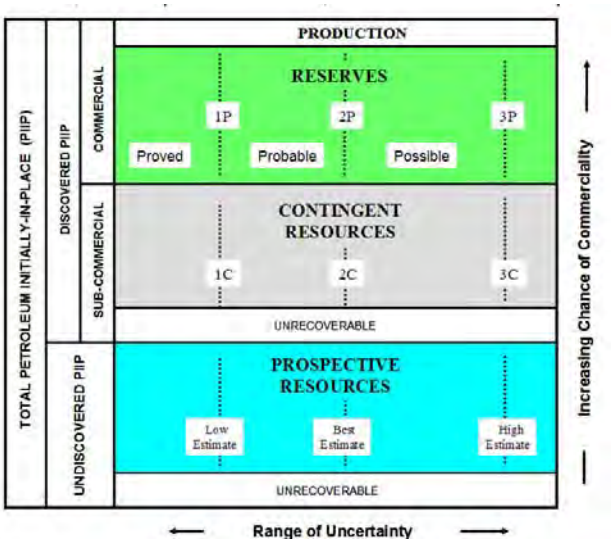

Figure 4. The Society of Petroleum Engineers' framework for petroleum resource classification (SPE 2007).

For the Bowland-Hodder shale, a number of hurdles must be overcome to economically produce gas. A way to describe the current state of understanding is illustrated by the diagram presented by the IEA (2011) (Figure 4a) which indicates five factors determining the viability of commercial development, or reserves. This report addresses only the resource size, the first stage of this process.

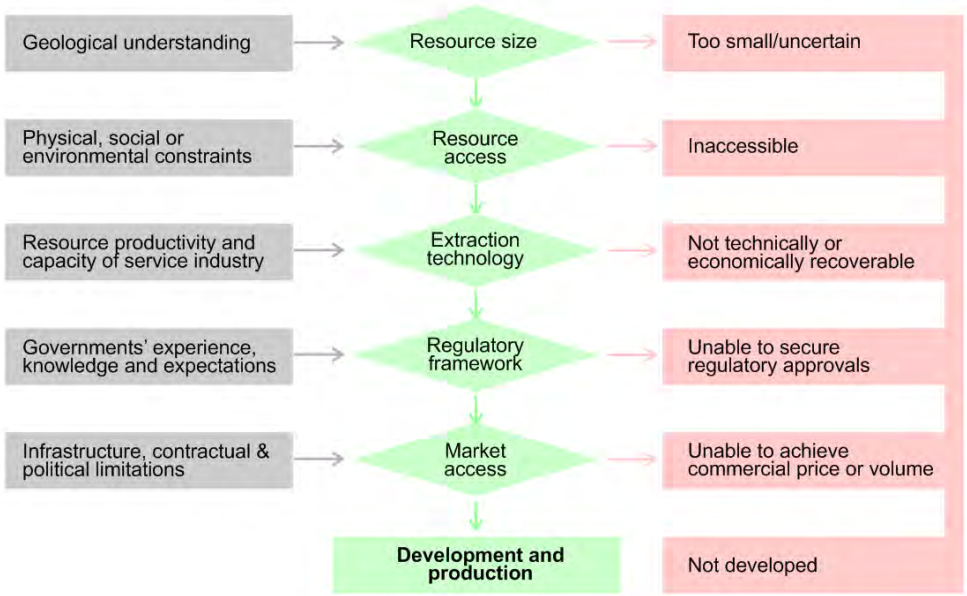

Figure 4a. Factors determining the viability of natural gas developments (IEA 2011).

2.3. Shale as a source and reservoir rock

In conventional oil and gas accumulations, shales comprise the source rock from which hydrocarbons are generated following burial. Through geological time, these hydrocarbons migrate from the source rock, through carrier beds and ultimately accumulate in porous reservoirs (typically sandstone or carbonate) in discrete traps. These traps are typically located in structural highs on the margins of the basin centres.

In the case of unconventional hydrocarbon accumulations (such as shale gas), this perceived wisdom is turned on its head – with shales acting as both source and reservoir rock, and the extensive basin centres becoming the exploration targets. Also, it is only within the last few decades that technology has enabled shale gas reservoirs to be exploited more economically.

Exploration for shale gas presents a series of new challenges; not least the collection of a different suite of geological, petrophysical and geotechnical data across previously little understood and poorly studied parts of hydrocarbon provinces.

In shale gas plays, biogenic[3] or thermogenic gas is present as two components: either adsorbed onto kerogen or clay particles, or present as free gas in pore spaces and natural fractures.

Shale is predominantly comprised of very fine-grained clay particles deposited in a thinly laminated texture, but shale gas production may also come from layers of re-deposited limestone or thin clastic beds within the gross shale sequence. The clay particles fall out of suspension and become interspersed with organic matter, which is measured as the rock's total organic carbon content (TOC). Through deep burial these muddy strata are compacted, and the pore water is expelled, resulting in a low-permeability layered rock called 'shale', which describes the very fine-grained and laminar nature of the sediment, not the rock composition, which is layered. Each of these layers creates a barrier to fluid migration, and this stacked system, called 'composite layering' is an effective vertical seal.

Matrix permeabilities (the ability of fluids to pass through them) of typical shale are very low compared to conventional oil and gas reservoirs (<0.1 mD in shales versus >1 mD in conventional reservoir sandstones) which means that, in shale, hydrocarbons are effectively trapped and unable to flow or be extracted under normal circumstances, and they are usually only able to migrate to conventional traps over geological time.

2.4. What defines a shale gas play?

Table 2 summarises some of the most important geological, geochemical and geotechnical criteria that are widely used to define a successful shale gas play; some criteria are essential, others are desirable. The criteria are based on data from analogous shale gas plays in the USA, which are known to vary considerably from one another.

Criteria	Range of data and definitions	UK data (availability and gaps) and definitions used in this report
Organic matter content (TOC)	Shales should be rich in organic matter, with total organic carbon (TOC) values > 2% (TNO 2009, Charpentier & Cook 2011, Gilman & Robinson 2011). >4% (Lewis *et al*. 2004). Jarvie (2012) uses a cut-off of just 1% present-day TOC, and quotes averages for the 10 top US systems as 0.93-5.34% TOC.	Some legacy data available, augmented by data from a study commissioned by DECC (Appendix B). A cut-off of TOC > 2% is used for a potentially viable shale gas resource.
Gamma-ray values	High gamma radiation is typically an indication of high organic carbon content. Gamma log response should preferably be 'high' (Charpentier & Cook 2011); 20 API above shale baseline (Schmoker 1980); >230 API (NPC 1980); >180 API (DECC 2010a); >150 API, but lower if TOC is demonstrably high (D. Gautier, USGS, pers. comm.).	The cut-off used has been selected on a well-by-well basis taking into account TOC and background shale gamma-log values, but is typically in the range 150 to 200 API.

[3] Natural gas can be created by two mechanisms: biogenic and thermogenic. Biogenic gas is created by micro-organisms that produce methane as a metabolic by-product in anoxic conditions such as in marshes, bogs, landfills, and shallow sediments. At depth, at greater temperature and pressure, thermogenic gas is created through the maturation of buried organic material. Biogenic gas can be encountered even if the underlying source rocks have not entered the thermogenic gas generation window.

Criteria	Range of data and definitions	UK data (availability and gaps) and definitions used in this report
Kerogen type	Kerogen should be of Type I, II or IIS (Charpentier & Cook 2011). Ideally, II (Jarvie 2012). This indicates a planktonic, marine origin.	Information on kerogen type is incomplete. Ewbank *et al*. (1993) identify Type II and III kerogen in various basins. Note: immature Type II kerogen can plot in the Type III field when matured for gas generation (Jarvie *et al.* 2005).
Original hydrogen index (HI_o)	HI_o preferably >250 mg/g (TNO, 2009, Charpentier & Cook 2011); 250-800 mg/g (Jarvie 2012). Note: it is important to have information on original, rather than present day, HI values. This conversion relies heavily on kerogen type.	Only present day HI values are available for UK basins.
Mineralogy/clay content	Clay content should be low (< 35%) to facilitate fracking and hence gas extraction. Jarvie (2012) stresses the requirement of a significant silica content (>30%) with some carbonate, and presence of non-swelling clays.	USEIA (2011a) quote 'medium/high' clay contents. There is scope for further work to bring together data from disparate sources and for new analyses.
Net shale thickness	Moderate shale thicknesses are considered ideal; >50 ft (15 m) (Charpentier & Cook 2011); >20 m (TNO 2009); >150 ft (Jarvie 2012). Conventional wisdom is that the 'thicker the better', but this may not necessarily be the case (Gilman & Robinson 2011); >25 m in <200 m gross section (Bent 2012). Thick shale sequences (100s of metres) tend to be regarded as 'basin centre gas' plays rather than shale gas plays.	Net potentially productive shale in the upper Bowland-Hodder unit is 200-3000 ft (60-900 m) thick; the lower Bowland-Hodder unit is up to 10,000 ft (3000 m thick) (with the possibility of thin units of higher-than-background TOC). These latter thicknesses are much greater than in the US analogues.
Shale oil precursor	A shale oil precursor should ideally be identified.	Oil and gas fields sourced from the Bowland-Hodder unit are both present in central Britain.
Thermally maturity	The shale should be mature for gas generation; R_o = 1.1 – 3.5% is widely accepted as the 'gas window'. Charpentier & Cook (2011) use a cuff-off of R_o >1.1%. Smith *et al*. (2010) use 1.1% as it demarcates the prospective area in the Fort Worth Basin; Jarvie (2012) quotes a higher cut-off of R_o >1.4%; 1.2 – 3.5% (BGR 2012); <3.3% (TNO 2009). Conventional wisdom is 1.25 – 2%, but 'empirical wisdom' is 1.75 – 3% (Gilman & Robinson 2011).	In this study, the shale is considered to be mature for gas generation above an R_o value of 1.1%.
Gas content/saturation	Gas should be present as free gas (in matrix and fractures) and adsorbed gas. Gas contents should be 60-200 bcf/section (Bent 2012) or >100 bcf/section (Jarvie 2012).	There is no published information on gas contents. Data from US analogues has been used.
Depth minimum	Depth >5000 ft (>1500 m) (Charpentier & Cook 2011). Lower pressures generally encountered at shallower depths result in low flow rates.	Shale resources shallower than 5000 ft (1500 m) below land surface have been excluded from this study.
Shale porosity	Typically 4-7%, but should be less than 15% (Jarvie 2012).	Not known.
Overpressure	Slightly to highly overpressured (Charpentier & Cook 2011, Jarvie 2012). The Barnett Shale is slightly overpressured (Frantz *et al.* 2005).	Not known, but Smith *et al*. (2010) mention 'the lack of overpressure' in the Bowland Shale. However, recently-uplifted shales in central England should in theory be mildly overpressured. In resource calculations the pressure is assumed to be hydrostatic to give a conservative estimate of gas in place.
Tectonics and burial history	Preferably in large, stable basins, without complex tectonics (Charpentier & Cook 2011). Wells should be drilled away from faults where possible.	Britain is located at the junction of several structural terrains and has undergone a complex geological history; the basins are also generally small. Locally, faulting occurs at high densities.

Table 2. Criteria that are widely used to define a successful shale gas play.

2.5. Shale gas around the world

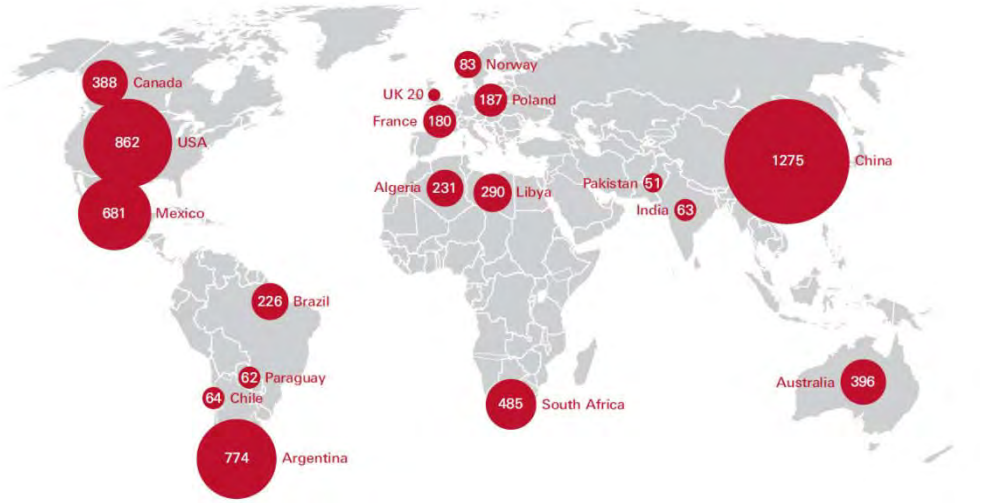

Figure 5. Estimates of technically recoverable shale gas resources (tcf) for selected shale formations in 32 countries (USEIA 2011a; Bickle et al. 2012). Note: data were not available for Russia, Central Asia, Middle East, South-east Asia and central Africa. The figure of 20 tcf for the UK includes 19 tcf for the Bowland Shale and 1 tcf for the Liassic shales of the Weald Basin.

The distribution of potential shale gas plays covers the globe (Figure 5), but it is only within North America that large-scale commercial extraction has been achieved to date. In the USA, ten shale gas plays hold the vast majority of the country's technically recoverable reserves, and these are the only shale gas plays currently being exploited (USEIA 2011b, Jarvie 2012).

2.6. How to estimate how much gas?

Two fundamentally different methodologies are used to assess shale gas basins worldwide:

1. In-place resource estimates based on a geological model, volumetrics and gas contents ('bottom-up approach', as used by TNO and BGR), and

2. Technically recoverable resource estimates based on well technology, well performance, well density ('top-down approach', as used by the USGS).

In-place estimates with a robust connection to geological studies are widely considered an excellent tool for initial estimates, and BGS/DECC have employed this methodology. TNO (2009) and BGR (2012) also used this approach to make their preliminary assessments of shale gas resources in the Netherlands and Germany. While the second approach has been shown to be more reliable based on the US experience, no shale gas production data are yet available in the UK.

USEIA (2011a) subsequently de-risked their equivalent gas in-place figure by a factor that 'account[s] for the current level of knowledge of the resource and the capability of the technology to eventually tap into the resource'. This approach is not followed here because of the relative infancy of the UK shale gas industry.

3. Estimating the total in-place gas resource of the Bowland-Hodder unit in central Britain

3.1. Introduction

Carboniferous organic-rich basinal marine shales are present across a large part of central Britain and the study area extends from Merseyside to Humberside and Loughborough to Pickering (Figure 6). The shales are either buried at depth or occur at outcrop. These organic-rich shales are recognised to be excellent source rocks, in which oil and gas matured before some of it migrated into conventional oil and gas fields (e.g. UK Midlands area, East Irish Sea) (DECC 2010b). The Bowland shale gas study area is bounded by complete erosion of the potentially prospective shales over highs to the south, by uplift in several areas where the prospective units are at outcrop, and by a facies change in the north and north-east to contemporary deltaic deposits.

Figure 6. Location of the BGS/DECC shale gas study area, central Britain. Contains Ordnance Survey data © Crown copyright and database right 2013.

3.2. Seismic, well and outcrop data

This assessment of the Carboniferous basin shales of central Britain is based upon detailed seismic mapping using all available hydrocarbon well and stratigraphic borehole information along with outcrop geology.

Although several thousand wells and boreholes have been drilled within the assessment area, only 64 of these reached sufficient depths to record more than 50 ft (15 m) of net shale in the Early

Carboniferous section (Figure 7). Very few wells have drilled more than 1000 feet (300 m) of the section of interest. Key wells are discussed further in Section 3.6.

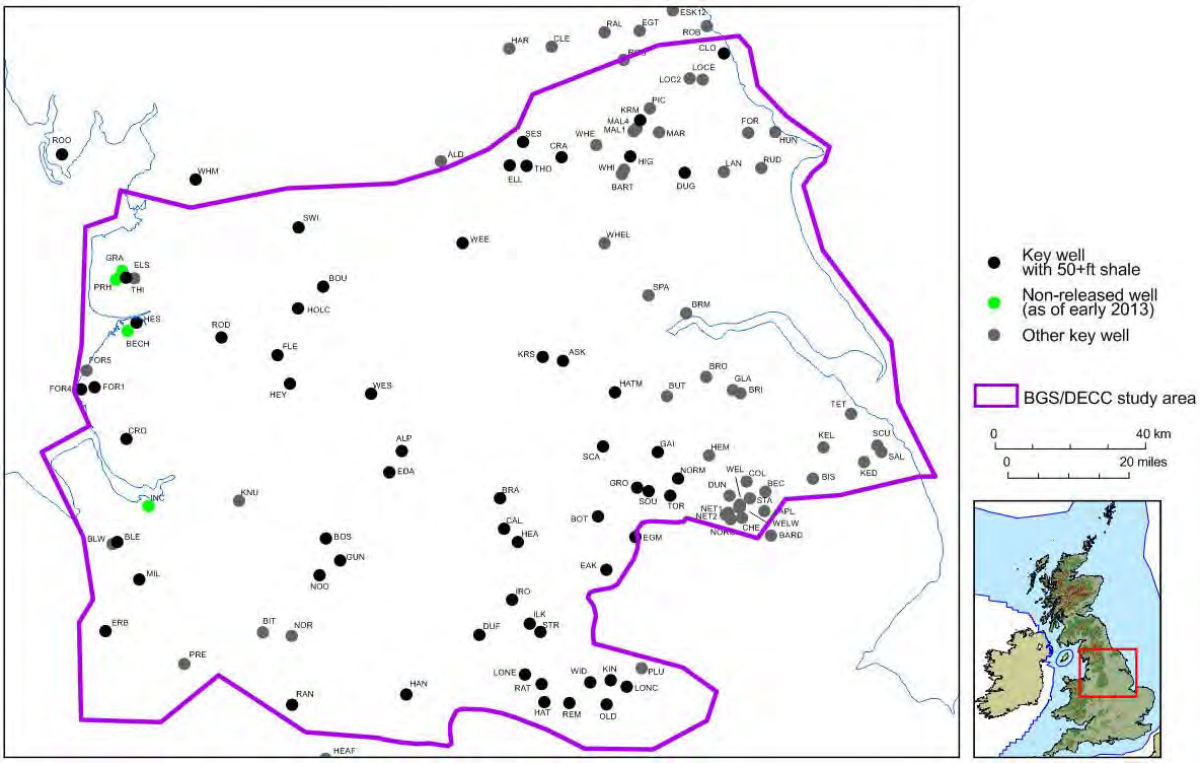

Figure 7. Location of key wells, non-released wells and other wells providing important stratigraphic information used to assess the shale gas potential of central Britain. See Appendix C for details of well name abbreviations and stratigraphic information.

All of the available seismic data was obtained from the UK Onshore Geophysical Library (UKOGL www.ukogl.org.uk). A total of c. 23,500 km (14,700 miles) of 2D and 1000 km² (390 mile²) of 3D seismic data (Figure 8) was loaded on an interpretive workstation. This mixed vintage data is of variable quality and often short line lengths (because seismic data onshore UK can only be shot over extant licences). An iterative approach was employed, finding seismic lines with the good evidence for horizon mapping, then circling back through the poorer quality lines, with an interpretation that was consistent with the detailed BGS outcrop mapping and the geological model.

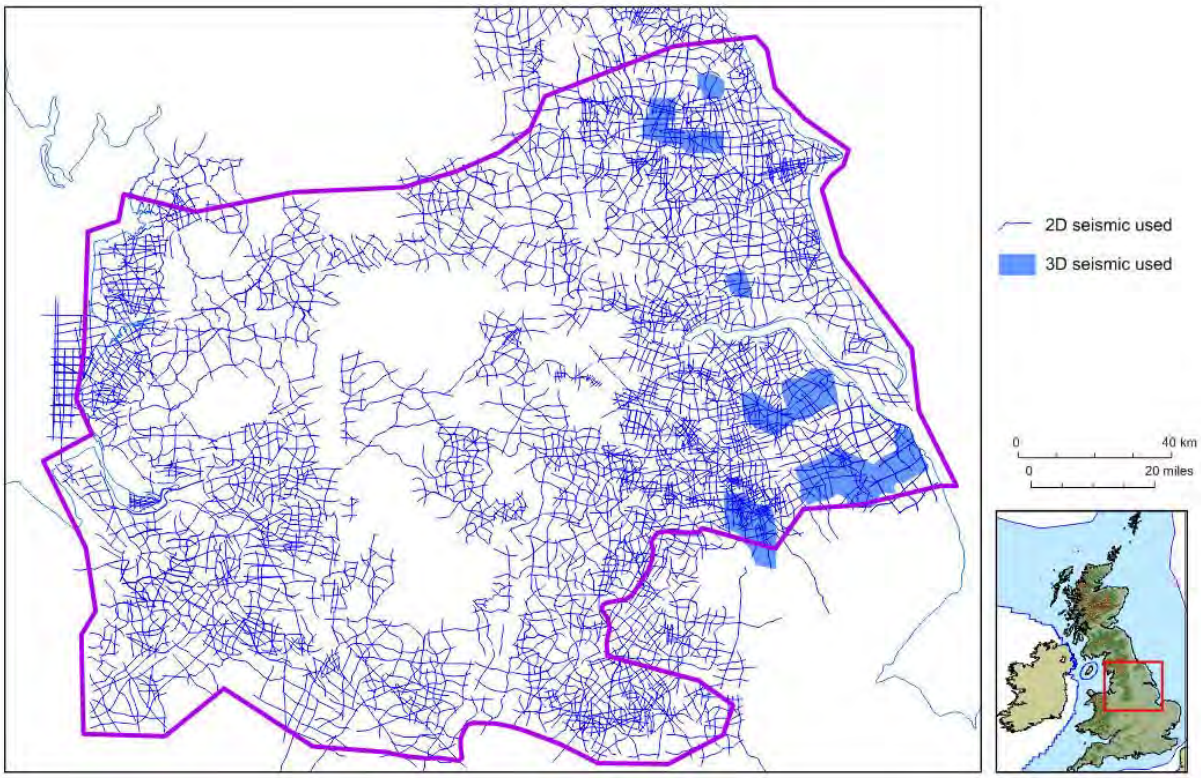

Figure 8. Location of 2D seismic profiles and 3D surveys used to assess the shale gas potential of central Britain.

The Bowland-Hodder shales (of the Craven Group, see section 3.4) are at outcrop in the Lancashire Forest of Bowland, Derbyshire Peak District, North Wales, at Gleaston (Cumbria) and a small area near Harrogate (Figure 9). These outcrops fringe areas where post-Carboniferous uplift has brought older rocks to the surface (e.g. the Derbyshire Dome and the Clitheroe and Slaidburn anticlines). These have been mapped by the BGS over a period of c.150 years and a large amount of literature has been published, but this has often concentrated on the sandstones, fossils and bed-by-bed stratigraphy. Since 2000, BGS has published three subsurface memoirs within the study area (Kirby *et al.* 2000, Smith *et al.* 2005, Pharaoh *et al.* 2011) (Figure 10).

Lee (1991) and others have interpreted the regional gravity and magnetic data (Figures 11 and 12). In the northern half of the area, gravity lows correlate more closely with known rift basins, such as the Widmerpool and Edale gulfs and the Gainsborough Trough (GL7, GL8 and GL9 respectively). Anomaly GL 10, however, is thought to be related to the postulated concealed Market Weighton Granite adjacent to the lineaments associated with known basement highs, such as the Nocton and Askern-Spital highs, and ESE-trending lineaments associated with faults which controlled sedimentation, such as the fault on the southern margin of the Widmerpool Gulf. Licence operators have acquired proprietary high-resolution gravity gradiometry surveys which better image the structural fabric of the Carboniferous rift basins, but these are not yet in the public domain.

Although the shales are widely distributed, their outcrops are not extensive and occur mainly in river and road cuttings (Figure 13).

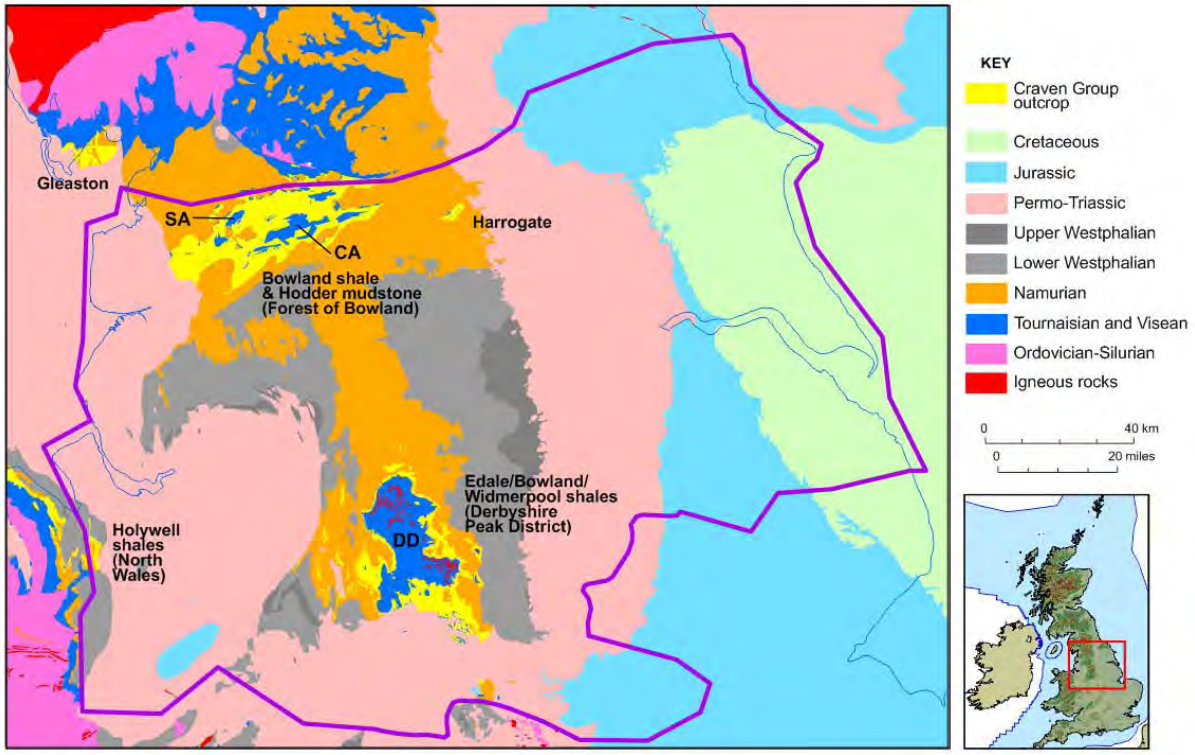

Figure 9. The five main Craven Group outcrops in central Britain (from BGS 1:50,000 mapping). DD = Derbyshire Dome; CA = Clitheroe Anticline; SA = Slaidburn Anticline.

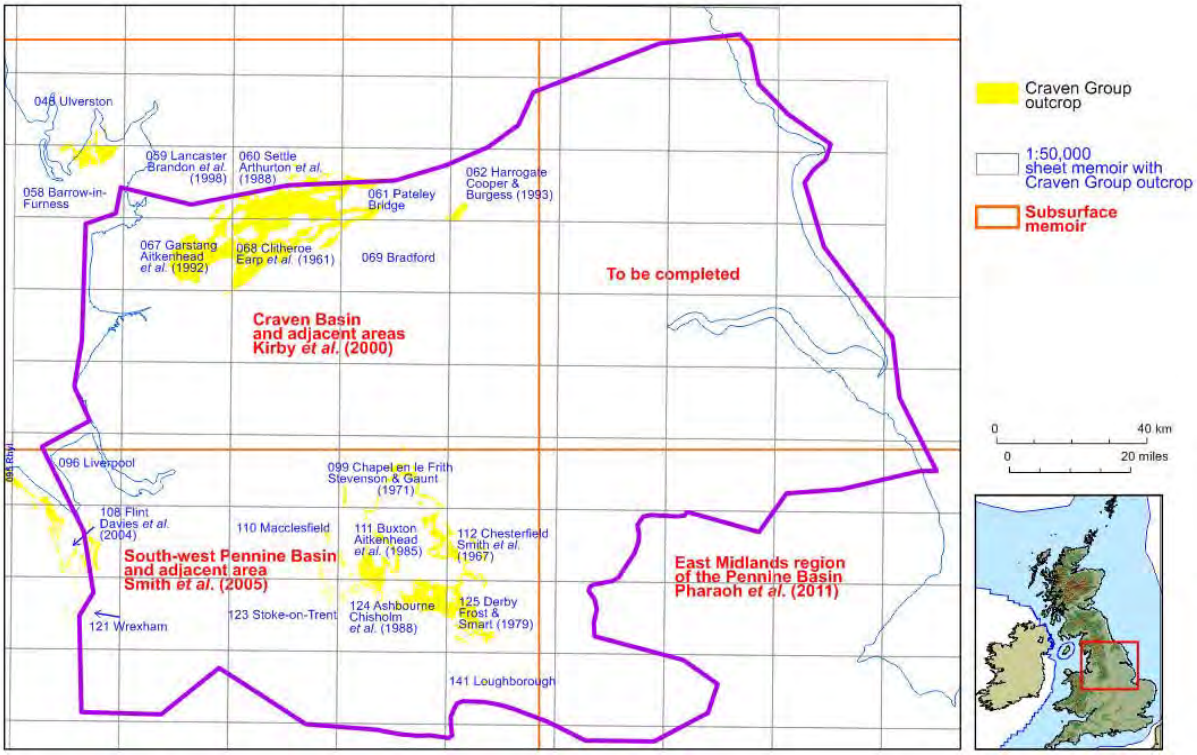

Figure 10. Location of relevant BGS map sheets and memoirs across central Britain. See references for further details.

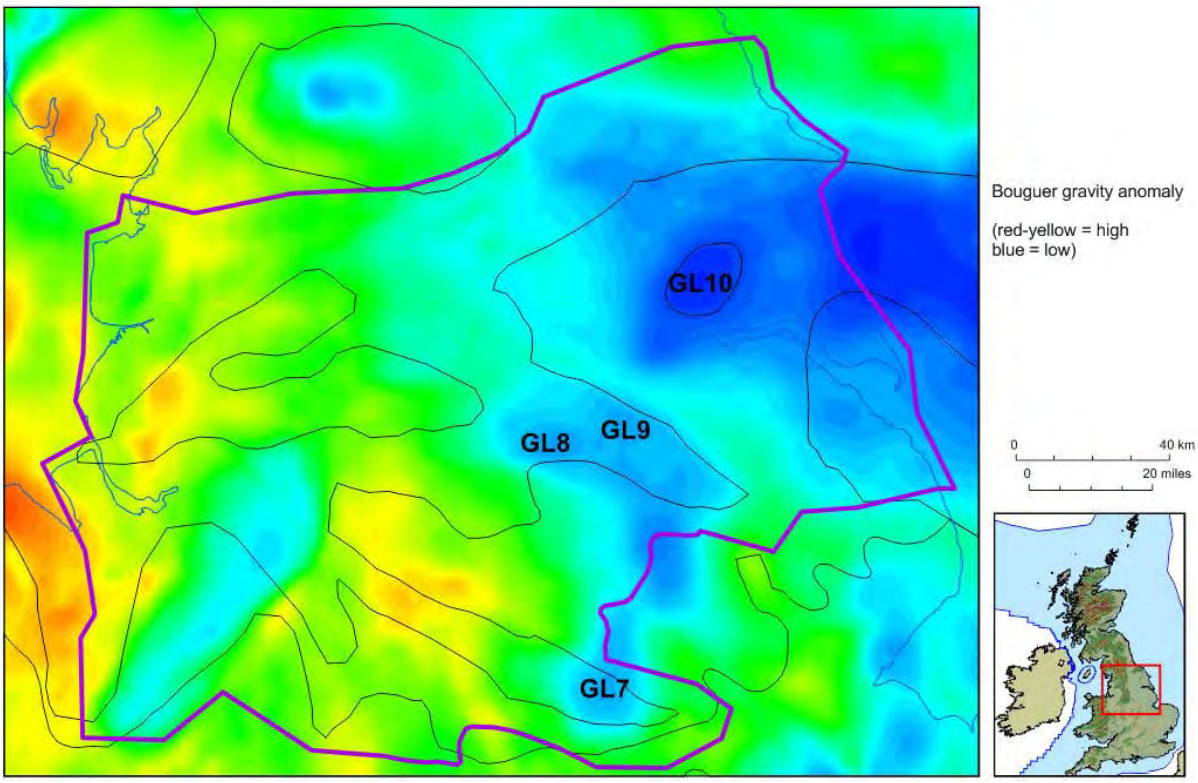

Figure 11. Bouguer gravity anomaly map for central Britain (from BGS mapping). Gravity low (GL) numbering from Lee et al. (1991). The Early Carboniferous structural framework lines are from Figure 14.

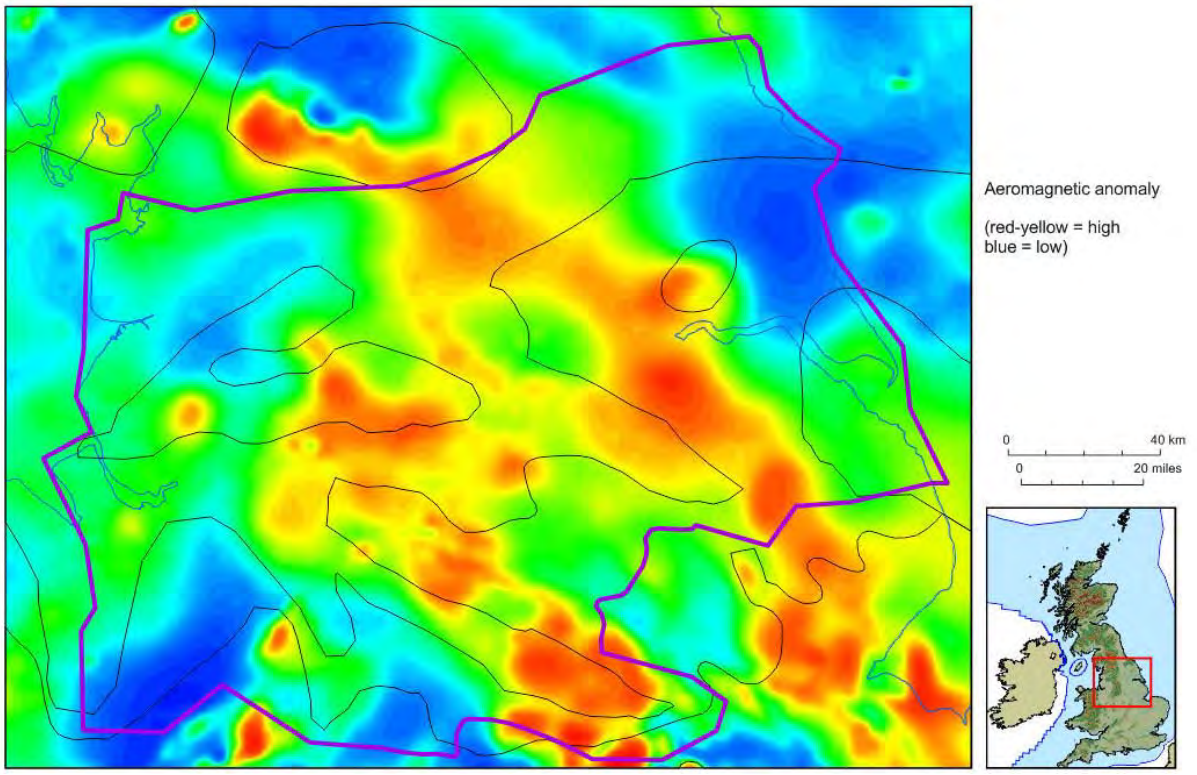

Figure 12. Magnetic anomaly map for central Britain (from BGS mapping). The Early Carboniferous structural framework lines are from Figure 14.

Figure 13. Typical outcrop of shale showing a slope deposit comprising imbricated rafted blocks of Hodder Mudstone Formation (Arundian age) on the flank of Ashnott High, Bowland Basin, Lancashire. © N.J. Riley/BGS

3.3. Paleogeography and basin inversion

Palaeomagnetic evidence suggests that Britain was situated in near-equatorial latitudes during Visean times, and the Carboniferous was a period of glacial eustasy, with sea-level fluctuations likely to have had a significant impact on deposition. Marine shales were deposited in a complex series of tectonically active basins across central Britain during the Visean and Namurian. A phase of Late Devonian to Early Carboniferous rifting produced a marked palaeo-relief with numerous basins occupying subsiding grabens and half-grabens and emergent highs associated with horsts and tilt-block highs (Leeder 1982, 1988) (Figure 14). In general terms, hemipelagic marine shales (with mass flow deposits) were deposited in the basins and these pass laterally into extensive platform carbonates over the East Midlands Shelf and Derbyshire High. Equivalent basins occur offshore beneath the East Irish Sea (Jackson *et al.* 1995) and the Southern North Sea (Cameron *et al.* 1992). Cessation of most rifting processes occurred across large parts of the UK in the late Visean to be followed by a period of regional subsidence during which the pre-existing basins were generally filled in completely by more widespread marine deposition.

The Early Carboniferous basin model has become increasingly well defined, with supporting evidence coming from both the interpretation of seismic data and well penetrations (e.g. Kent 1966, Leeder 1982, 1988, Smith *et al*. 1985, Fraser *et al.* 1990, Fraser & Gawthorpe 1990, 2003). The exceptions are the basin beneath the Permo-Triassic Cheshire Basin[4] where the thickness is unconstrained and in the Humber Basin, where the interpretation is tenuous due to the lack of well penetrations and poor seismic control (Figure 14).

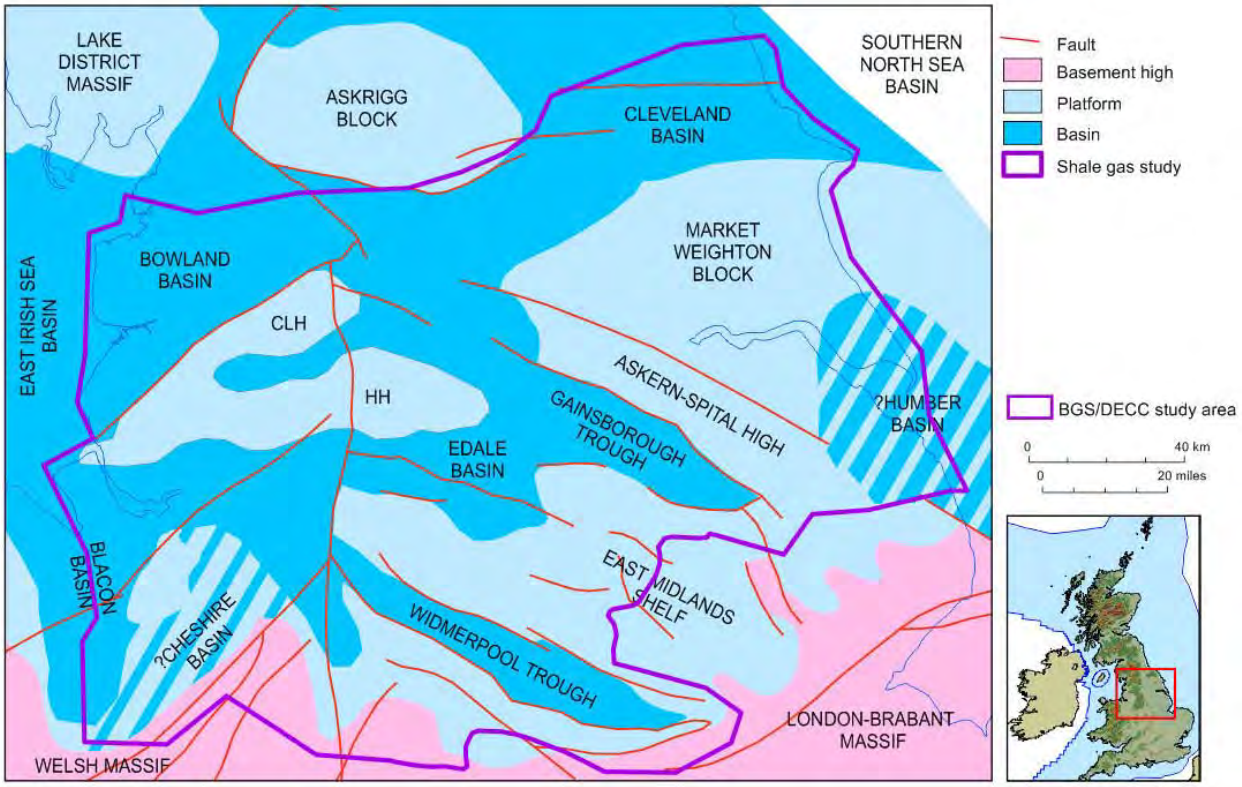

Figure 14. The Early Carboniferous basins and platforms of central Britain (modified after Fraser et al. 1990, Kirby et al. 2000). CLH = Central Lancashire High; HH = Holme High. Note: the presence of Early Carboniferous basins beneath the Permo-Triassic Cheshire Basin (Smith et al. 2005 cf. Waters et al. 2009) and a putative Humber Basin (Kent 1966, Hodge 2003) are both debatable (see text).

The Blacon East 1 and Milton Green 1 wells in the Blacon Basin penetrate basinal facies of late Visean, Brigantian age (Smith *et al.* 2005) and Davies *et al.* (2004) indicate basinal facies extending south as far as the Dee Estuary and Wirral. There are no well data further east and the seismic data is of insufficient quality to provide evidence for the thickness of the unit. Smith *et al.* (2005, Fig. 27) show that deep-water sediments with limestone turbidites were deposited across the Cheshire Basin area during the Asbian-Brigantian, with platform carbonates to the west and also south-east of the Red Rock Fault. On the other hand, Mikkelsen & Floodpage (1997) and Fraser & Gawthorpe (2003) show carbonate shelf facies extending broadly across an area that Waters *et al.* (2009; Fig. 1) label as the 'Holme High'. To avoid confusion, this report introduces the term 'Blacon Basin' for the Early Carboniferous basin which lies beneath the western part of the Permo-Triassic Cheshire Basin.

[4] The term Cheshire Basin is restricted to the Permo-Triassic basin; the presence of a poorly-defined Carboniferous depocentre, offset to the west, informally referred to as the 'Blacon Basin', is postulated.

The Humber Basin was first mentioned by Kent (1966) and is shown by Fraser & Gawthorpe (2003) and Hodge (2003). There are no well or seismic data to support this suggestion. Seismic interpretation reveals the presence of a Namurian-Westphalian thickening in the vicinity of the Tetney Lock 1 well. It could be interpolated that the Visean exhibits similar depositional thickening in this area, but importantly there is no evidence from the seismic data for a large-scale Visean half-graben (although seismic data quality is poor at this level). Hodge (2003) alluded to basinal shales being the source for the gas in the Saltfleetby field; this could be the most compelling evidence for the existence of the Visean-Namurian Humber Basin. More well penetrations or better seismic resolution will be necessary to assess the extent of the prospective shale in the Humber Basin.

The Bowland Basin[5] is one of the largest basins in the assessment area (Figure 14), and it continues westwards beneath the Irish Sea. Near the coast the Bowland Basin is buried beneath a layer of thick Permo-Triassic rocks, whilst farther east, the centre of the same basin has been uplifted and eroded such that rocks of the Bowland-Hodder unit crop out at the surface. The Edale Basin is a fault-bounded structure (Gutteridge 1991) that has a preserved cover of Millstone Grit and a relatively thin overlying unit of late Carboniferous Coal Measures locally also. The Gainsborough and Widmerpool troughs are broadly similar faulted basins to the Edale Basin, but the western, deepest part of the Widmerpool Trough was inverted and partially eroded prior to deposition of Permo-Triassic rocks. Over the crest of the Widmerpool Trough basin inversion, all of the overlying Coal Measures and Millstone Grit sections were eroded along with the uppermost part of the Bowland-Hodder unit (see Figure 24).

Late Carboniferous uplift occurred in a number of phases across central Britain, associated with the Variscan orogeny. The areas of greatest uplift largely followed the axis of the earlier depocentres, so that, for example, the oldest basinal strata of the Bowland-Hodder unit are exhumed in the centre of the inversion axis in the Bowland Basin.

3.4. Stratigraphy

Historically, the Early Carboniferous organic-rich basin shales have been given many names (e.g. Bowland Shale, Hodder Mudstone, Worston Shales, Widmerpool Formation, Sabden Shale, Caton Shale, Long Eaton Formation, Edale Shales, Lask Edge Shales and Holywell Shales etc.), and all of these shale units are now encompassed within the Craven Group (Waters *et al.* 2009) (Figure 15).

The interval mapped in this study is of Visean to early Namurian age, and has been interpreted on the seismic data in terms of sequence boundaries, and therefore includes both shales and laterally-equivalent platform limestones (Figures 15 and 16). The non-prospective platform deposits were subsequently excluded from the model using estimated net shale mapping (see Section 3.7).

In this study, this interval of interest is informally termed the 'Bowland-Hodder unit' (Figures 15 and 16) since this is the key stratigraphic interval within the Bowland Basin that was targeted by the Preese Hall 1 well in western Lancashire (Figure 7), the UK's first shale gas exploration well.

The age of the Bowland-Hodder unit extends from the late Chadian to the Pendleian (and locally Arnsbergian), within the Visean and Namurian epochs.

[5] The term Bowland Basin is used in this report in preference to the synonym Craven Basin (Hudson 1933). It was formerly known as the Bowland Trough (e.g. Kent 1966).

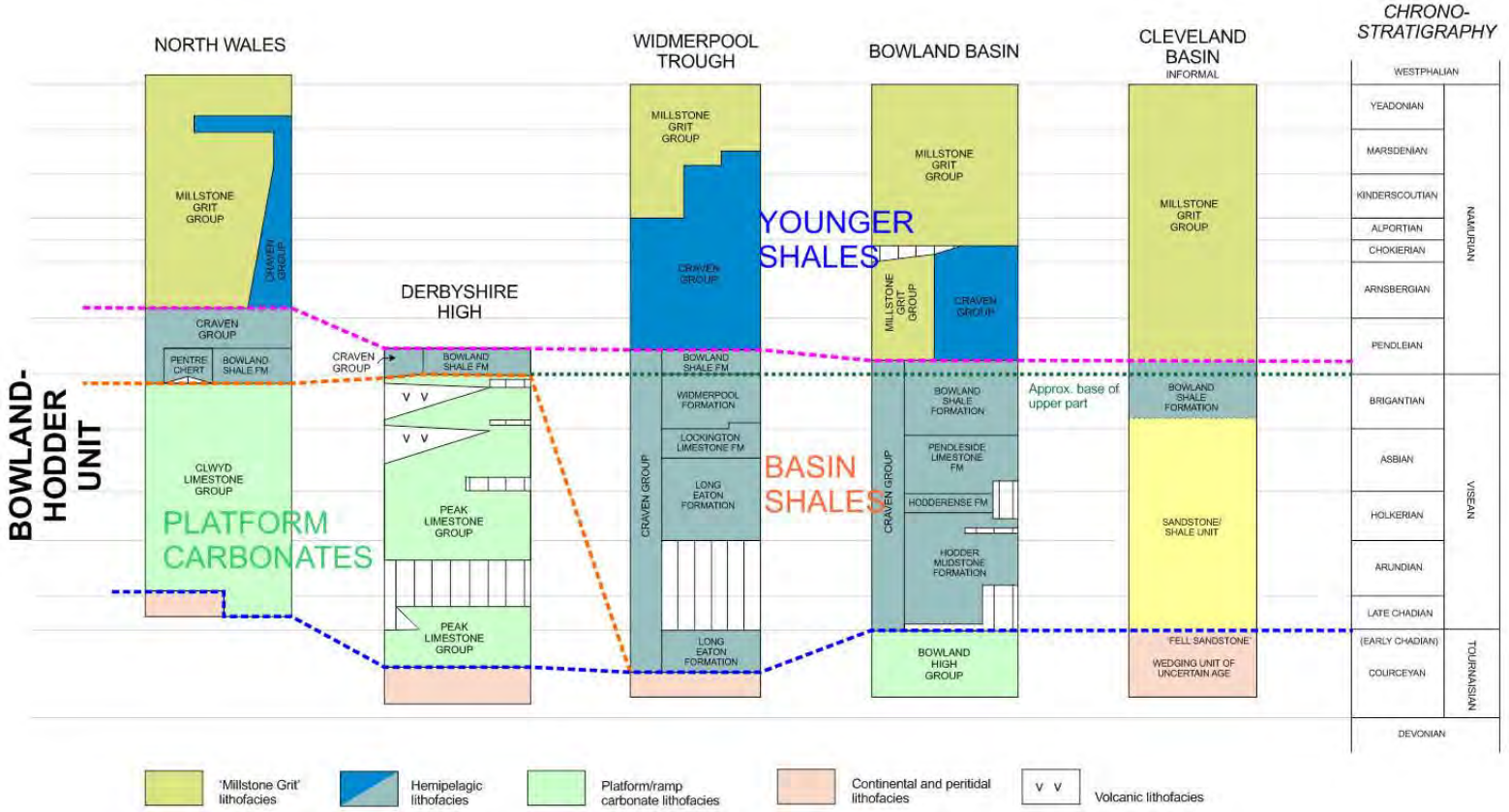

Figure 15. Lithostratigraphical framework of the Bowland-Hodder unit in central Britain (after Waters et al. 2009). Note: away from the outcrops, the platform carbonates in the Wessenden 1 and Roddlesworth 1 boreholes are termed Holme High Group and Trawden Group respectively (Waters et al. 2011). No formal lithostratigraphic framework has yet been applied to strata in the subsurface Cleveland Basin. In pre-2009 terminology, the Craven Group equates to the combined Worston Shale and Bowland Shale groups, excluding the Clitheroe Limestone Formation. Note: the use of Upper Chadian follows Riley (1990), but the Chadian has been partly redefined by Waters et al. (2011). Also, the Cleveland Basin sequence is poorly known and it is likely to have non-sequences that are not yet unrecognized.

The base of the Bowland-Hodder unit is defined in the basins as the top of the 'EC2/Chadian' carbonates identified in the Widmerpool Trough (Fraser *et al.* 1990). Outside this half-graben, it has only been penetrated on the highs and platforms. In the Cleveland Basin, the Kirby Misperton 1 well terminated in a sandstone (termed the 'Fell Sandstone' on the company log), the top of which is taken to approximately equate to the base of the Bowland-Hodder unit. The overlying shales have been only imprecisely dated using palynology , but on regional sequence stratigraphical grounds it is likely that the top of the Fell Sandstone is overlain by Holkerian strata, with the equivalent boundary being the top of the Ashfell Sandstone (Stainmore Trough) and Twiston Sandstone in the Bowland Basin.

The top of the Bowland-Hodder unit corresponds to the base of the sandstone-dominated Millstone Grit sequences. In outcrop, the Bowland Shale – Pendle Grit (oldest Millstone Grit unit) boundary is gradational and rather arbitrary, being part of an upward-coarsening sequence (Brandon *et al.* 1998). It is taken at either the base of the first massive sandstone, or where the sandstones predominate over siltstones and mudstones. This transition is younger in the north, due to the progradation of deltaic sequences from the north and north-east.

It should be noted that younger potential shale gas units, such as the Arnsbergian-Kinderscoutian Sabden Shale in Lancashire and much of the 'Holywell shales' in North Wales, which occur within Millstone Grit sandstone sequences, are excluded from this study (Figure 6). The Sabden Shale reaches a thickness of 1300 ft (400 m) in the Ribchester Syncline (Aitkenhead *et al.* 1992) and 2000 ft (610 m) south-east of Clitheroe (Earp *et al.* 1961), but it is not sufficiently deeply buried onshore to be considered as a source of shale gas.

Older 'limestone-with-shales' of Courceyan age are also excluded from the Bowland-Hodder unit, and these represent the deposits of the initial phase of rifting within the basin. These include the Haw Bank Limestone-with-Shales (Hudson 1944, Arthurton *et al.* 1988), the Gisburn Cotes Beds (Earp *et al.* 1961) and 2156 ft (657 m) of undated muddy limestones in the Swinden 1 borehole (Charsley 1984). They may reach a thickness in excess of 10,000 ft (3000 m) based on geophysical modelling (Arthurton *et al.* 1988). This depocentre coincides with the location of the greatest uplift and inversion and where the Bowland High Group crops out in the core of the anticline.

The integration of outcrop, well and seismic data has shown that the Bowland-Hodder unit can be divided into lower and upper parts (Figure 16). These correspond respectively to the EC3-EC6 syn-rift sequences and part of the LC1 post-rift sequence of Fraser *et al.* (1990). This subdivision provides a useful framework for the breakdown of the resource estimation into the less understood (and higher risk) lower unit and the better well-controlled (and lower risk) upper unit (see Section 5). It should be noted that although this division is valid as a generalized model, there is evidence that local syn-depositional faulting continued into the Arnsbergian (e.g. Brandon *et al*. 1998 p.55).

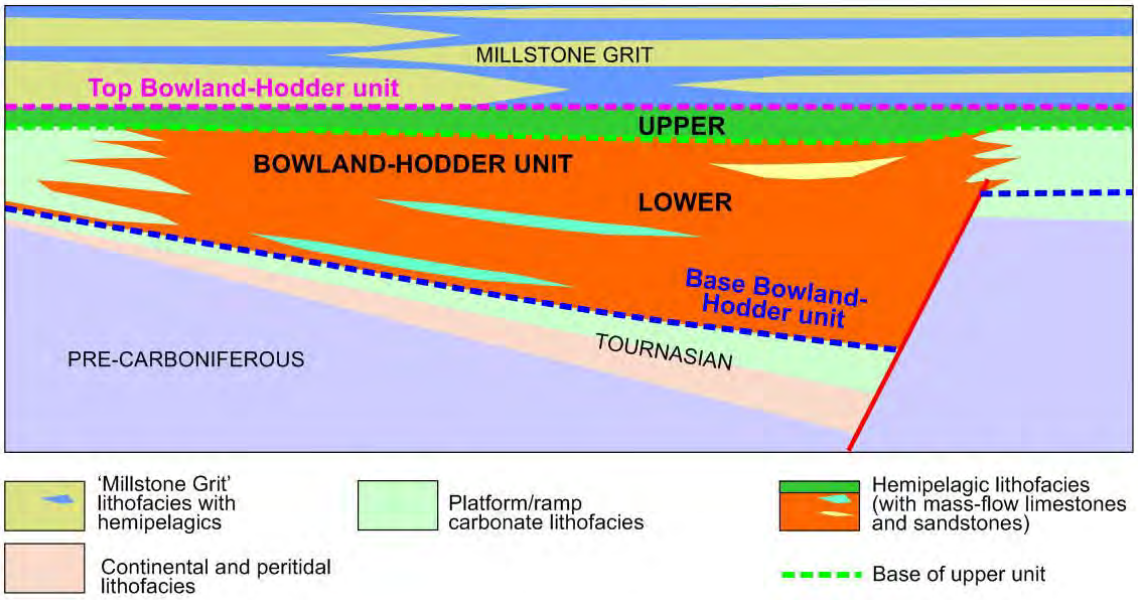

Figure 16. Schematic diagram showing the relationship between hemipelagic basinal shales and platform carbonates within the Bowland-Hodder unit. Note that basin shales also occur interbedded with the sandstones of the overlying Millstone Grit.

The lower part of the Bowland-Hodder unit comprises a thick, syn-rift, shale-dominated facies which passes laterally to age-equivalent limestones that were deposited over the adjacent highs and platforms (Figure 16). The presence of slumps, debris flows and gravity slides (Gawthorpe & Clemmey 1985, Riley 1990) are evidence for relatively steep slopes, which may have been the result of instability induced by tectonic activity. A combination of syn-depositional tectonics, fluctuating sea levels, climate change, and evolution of the carbonate ramps/platforms surrounding the basin resulted in a variety of sediments being fed into the basin at different times. Localised breccias are present close to the basin-bounding faults (Smith *et al*. 1985, Arthurton *et al*. 1988). This lower unit is dated as late Chadian to Brigantian in age.

There is some evidence that marine transgressions, represented by high gamma, high TOC intervals, also occasionally flooded the platform highs (e.g. Arundian shales in the Plungar 8A well). However, there is so little well control for the lower unit in the deep basins, that it is unclear how regionally correlative these intervals are.

The upper part of the Bowland-Hodder unit comprises basinal shales that were deposited both in the basins and across most of the platforms, following the drowning of the highs. These condensed zones are laterally continuous, rather than enclosed within basins, but are considerably thicker and richer in organic material within the basins which had a stratified water column. Within the Bowland Basin, individual beds can be easily correlated between (currently unreleased) wells, providing further evidence of relative stability in the upper unit. This unit is dated as latest Brigantian to Pendleian (locally up to Arnsbergian) in age.

Evidence as to whether the onset of high-gamma shale deposition is always coincident with the Visean-Namurian boundary (*Emstites leion* Marine Band) requires further research. In most cases, there is a good correlation between these boundaries. However, in several wells, Brigantian ages have been assigned to the lowest part of the upper unit.

In the Harrogate outcrop (Cooper & Burgess 1993) and wells in the Cleveland Basin (this study), the boundary between the lower and upper parts of the Bowland-Hodder unit (and the top of the Visean) is taken near the base of the Harrogate Roadstone (of the Pendleton Formation).

Biostratigraphic control will be particularly important in interpreting the depositional controls on shale gas prospectivity and obtaining a terminal core to constrain the maximum stratigraphical penetration is most desirable. Cores of shale over zones of interest can be used not only for gas desorption tests and analysis, but also to gain the high resolution stratigraphical knowledge and geophysical log/seismic calibration necessary to inform subsequent exploration and development (e.g. prediction of shale net to gross, lithological and diagenetic controls on shale characterisation, lateral distribution of most productive zones and identify faults and their displacement).

3.5. Regional depth and isopach maps

The top of the Bowland-Hodder unit lies at depths of up to 16,000 ft (4750 m) across the assessment area (Figure 17), with the greatest depth of burial occurring in the Bowland Basin of Lancashire, beneath the Permo-Triassic Cheshire Basin and in eastern Humberside.

The thickness of the Bowland-Hodder unit (Figure 18) mirrors the regional Early Carboniferous structural configuration (Figure 14), with greatly expanded sections in the syn-rift basins.

From outcrop data, the Bowland Basin is estimated to contain up to 880 ft (268 m) of Bowland Shale (Brandon *et al*. 1998) and 3000 ft (900 m) of Hodder Mudstone (Riley 1990). In the subsurface, seismic interpretation suggests the complete Bowland-Hodder unit reaches a thickness of up to 6300 ft (1900 m) (Figure 18) in the same basin. This may be a conservative approximation, as Kirby *et al.* (2000) and Aitkenhead *et al.* (2002) estimated Tournaisian-Visean thicknesses of 13,000 ft (4000 m) and 8200 ft (2500 m) respectively (although both apparently include the Courceyan Chatburn Limestone Group and are thus not directly comparable to the Bowland-Hodder unit). The Thistleton 1 well drilled 2911 ft (887 m) of the Bowland-Hodder unit, but terminated in Brigantian-aged shales and sandstones (N.J. Riley pers. comm.) and the lower part of the unit was not reached.

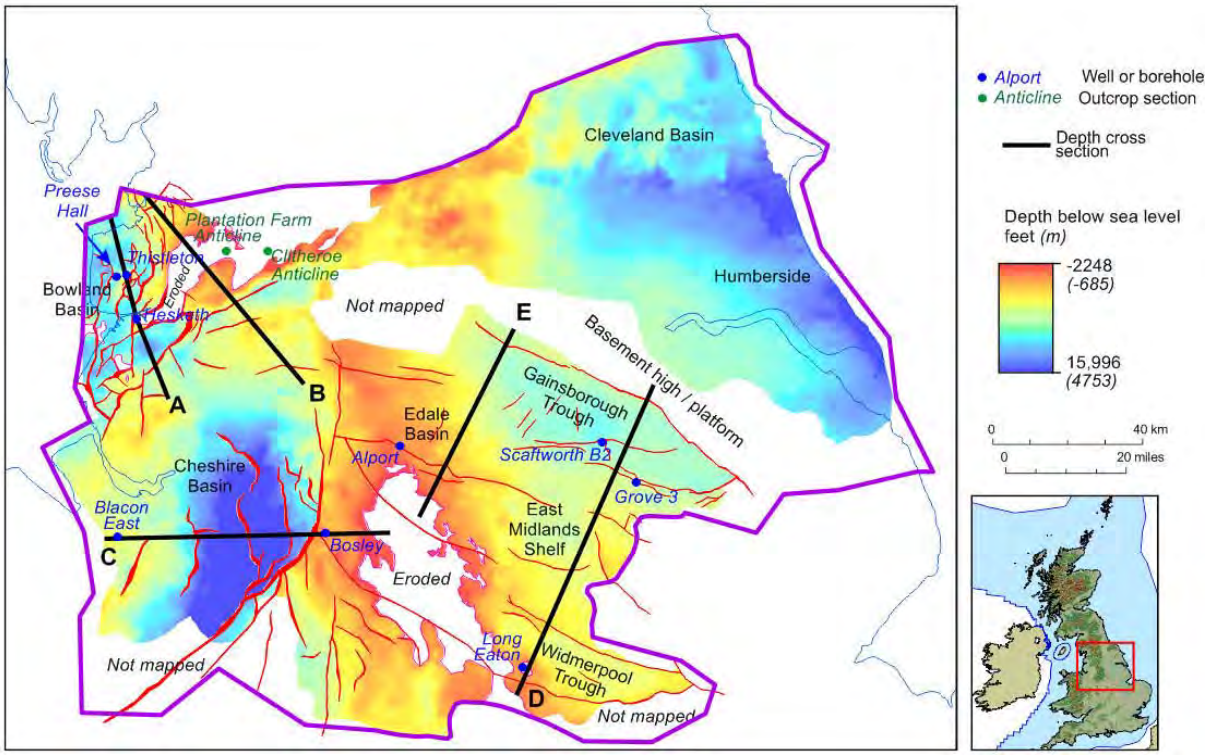

Figure 17. Depth (ft) to the top of the Bowland-Hodder unit, central Britain. The location of regional cross-sections is indicated (see Figure 19).

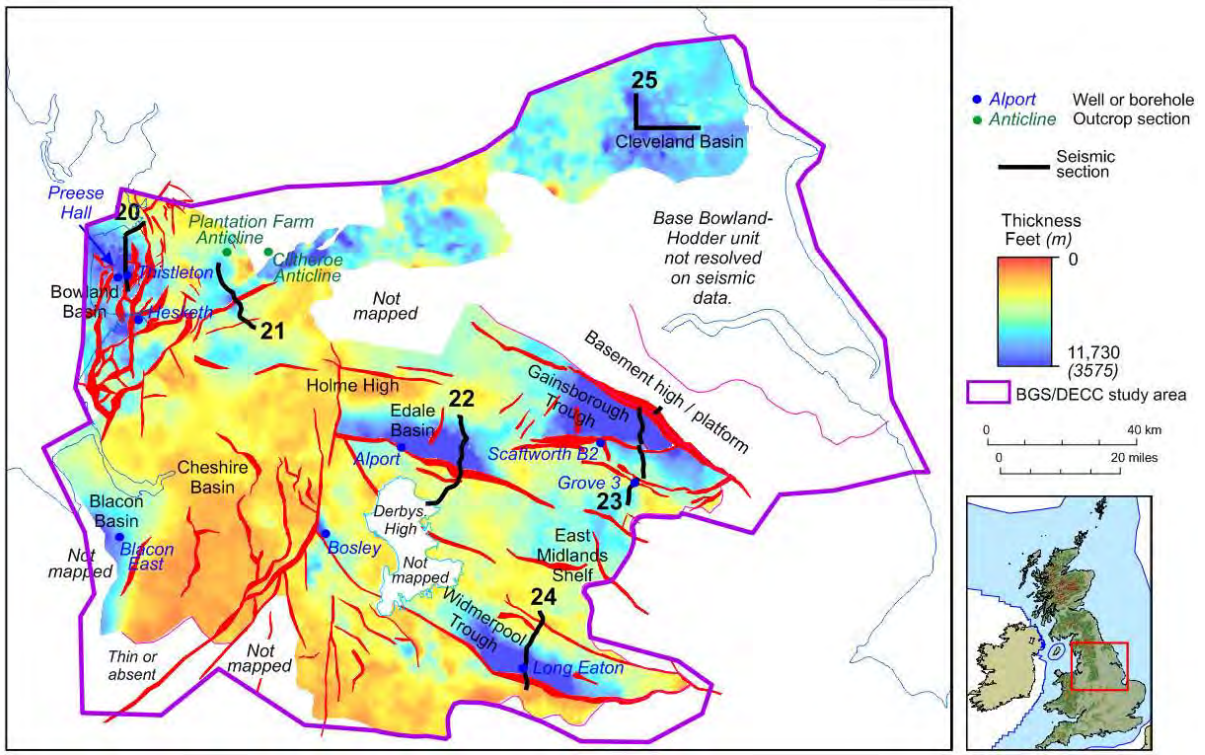

Figure 18. Thickness (ft) of the Bowland-Hodder unit, central Britain. The interval was not mapped across the Derbyshire High where there are no seismic data (and the unit comprises platform carbonate rocks) (see Figure 19C & E). The location of example seismic profiles is indicated (see Figures 20-25).

The Bowland-Hodder unit is equally thick, or thicker, within the narrow, fault-bounded Gainsborough, Edale and Widmerpool basins (Figure 18) with up to 10,000 ft (3000 m), 11,500 ft (3500 m) and 9500 ft (2900 m) respectively. The Cleveland Basin maintains a more uniform thickness, with the distribution of net shale controlled by facies changes to the north and south. Kirky Misperton 1 drilled a complete Bowland-Hodder unit thickness of 4598 ft (1401 m).

The organic-rich upper part of the Bowland-Hodder unit is typically up to c.500 ft (150 m) thick, but locally reaches 2900 ft (890 m). The syn-rift lower part of the Bowland-Hodder unit is considerably thicker, reaching 10,000 ft (3000 m) in the depocentres.

A selection of seismic-based depth cross-sections (Figure 19) and example seismic profiles (Figures 20-25) illustrate various aspects of the deep geology of the study area. Expanded captions provide additional information.

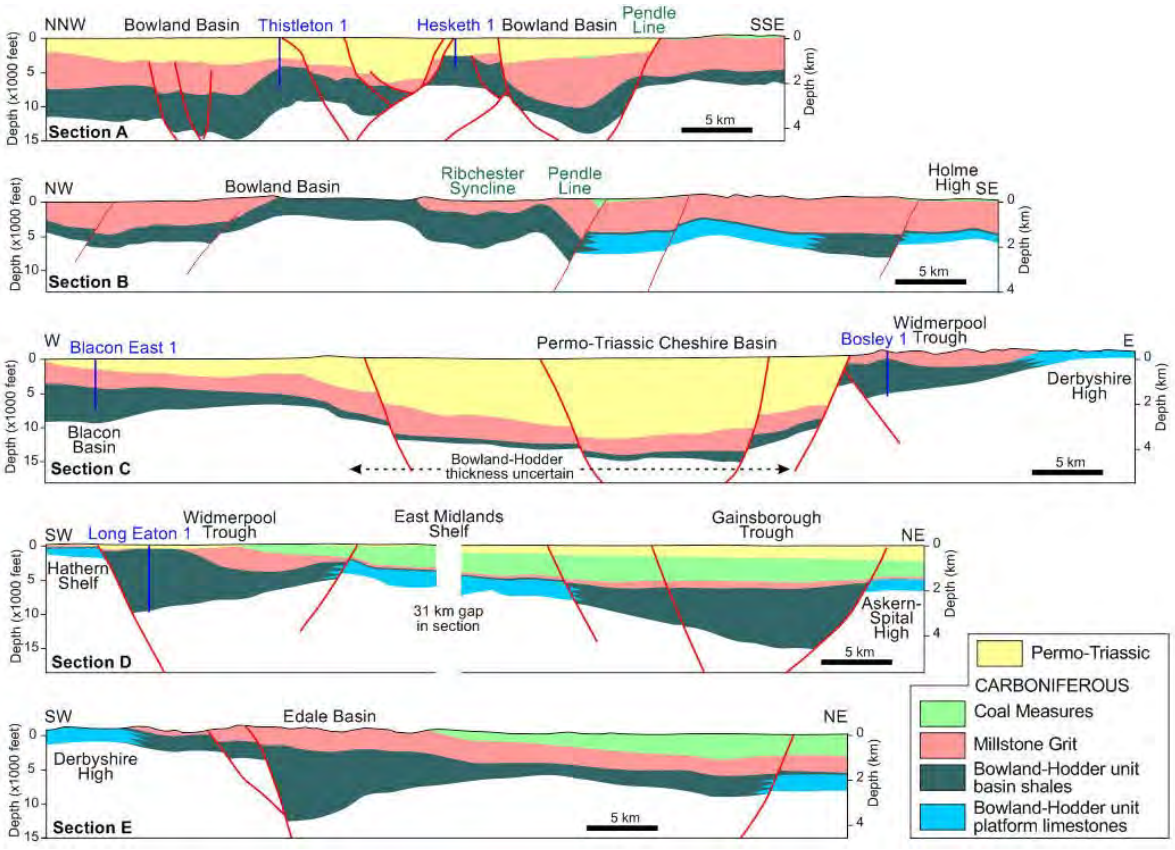

Figure 19. Generalised depth cross-sections through the Bowland Basin, Cheshire Basin, Widmerpool Trough, Gainsborough Trough and Edale Basin. For location of the sections, see Figure 17.

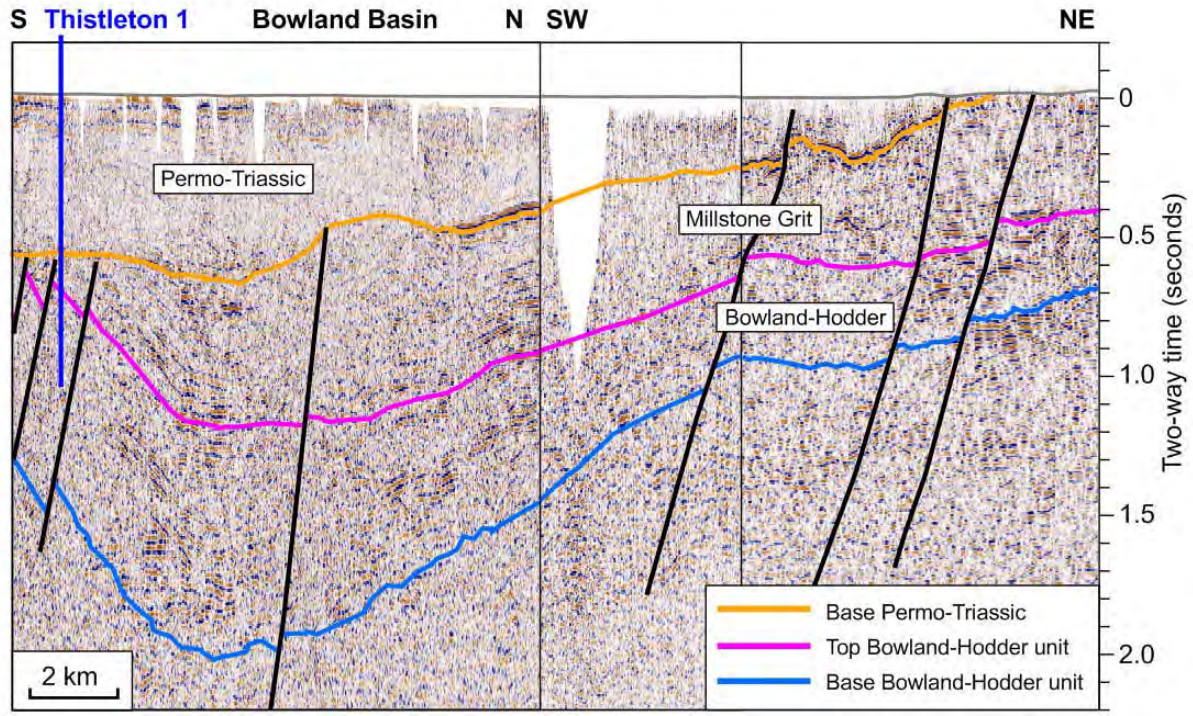

Figure 20. Seismic example across the deepest-buried part of the Bowland Basin showing thickening of the Bowland-Hodder unit towards the basin depocentre. The Thistleton 1 well terminated in Brigantian-aged shales and sandstones and the lower Bowland-Hodder unit was not reached. However, the Hodder Mudstone Formation is at least 3000 ft (900 m) thick in the Plantation Farm Anticline outcrop section located 25 km ENE of Thistleton 1 (Riley 1990), and a section of similar thickness is expected to be present in the area overlain by Permo-Triassic strata. For location of the section, see Figure 18.

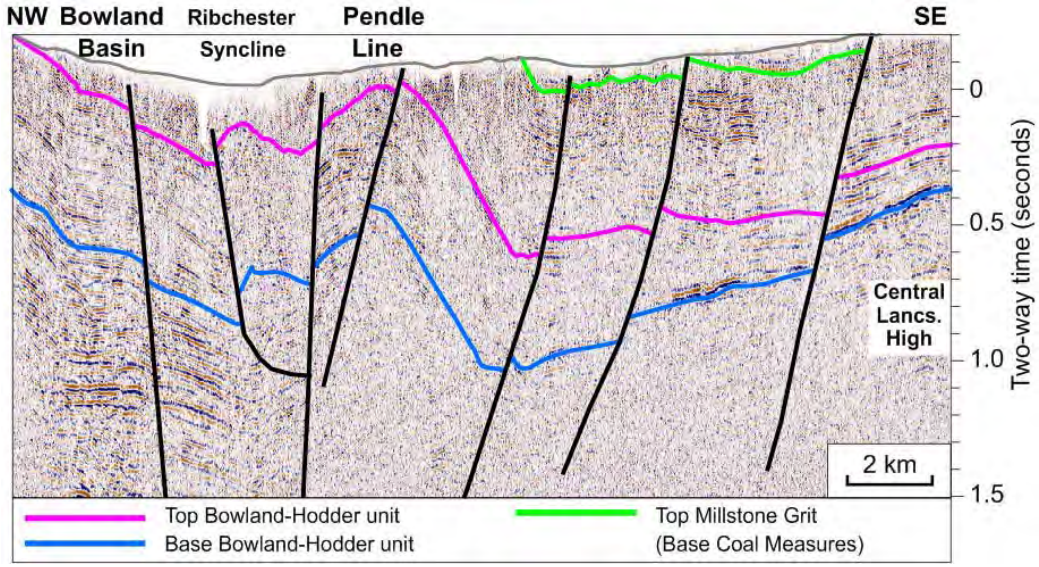

Figure 21. Seismic example across a folded and uplifted part of the Bowland Basin. The Pendle Line and associated monocline mark the southern boundary of the Bowland Basin; Westphalian Coal Measures crop out in the south-east. For location of the section, see Figure 18.

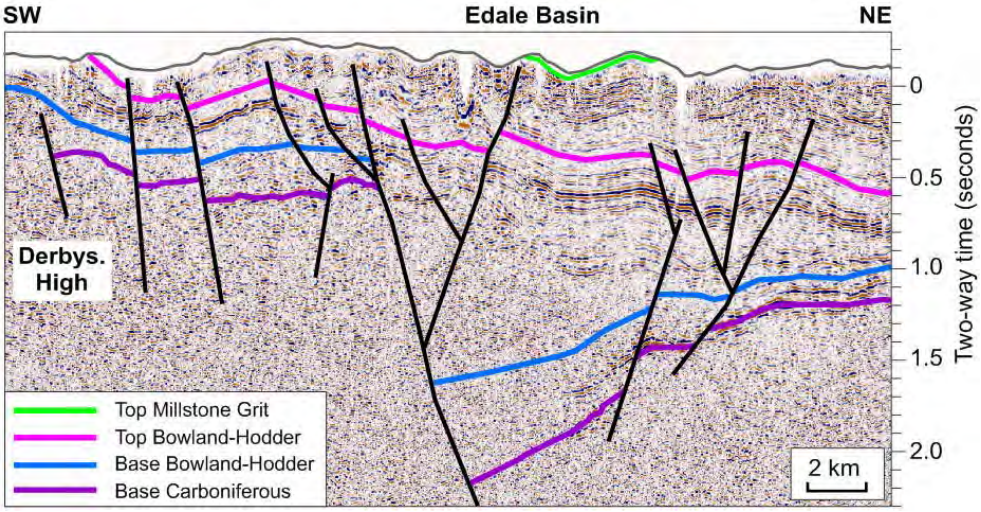

Figure 22. Seismic example across the Edale Basin where very thick basinal shales are interpreted. On the adjacent Derbyshire High, the Bowland-Hodder unit comprises platform carbonates topped by relatively thin upper Bowland-Hodder shales. For location of the section, see Figure 18.

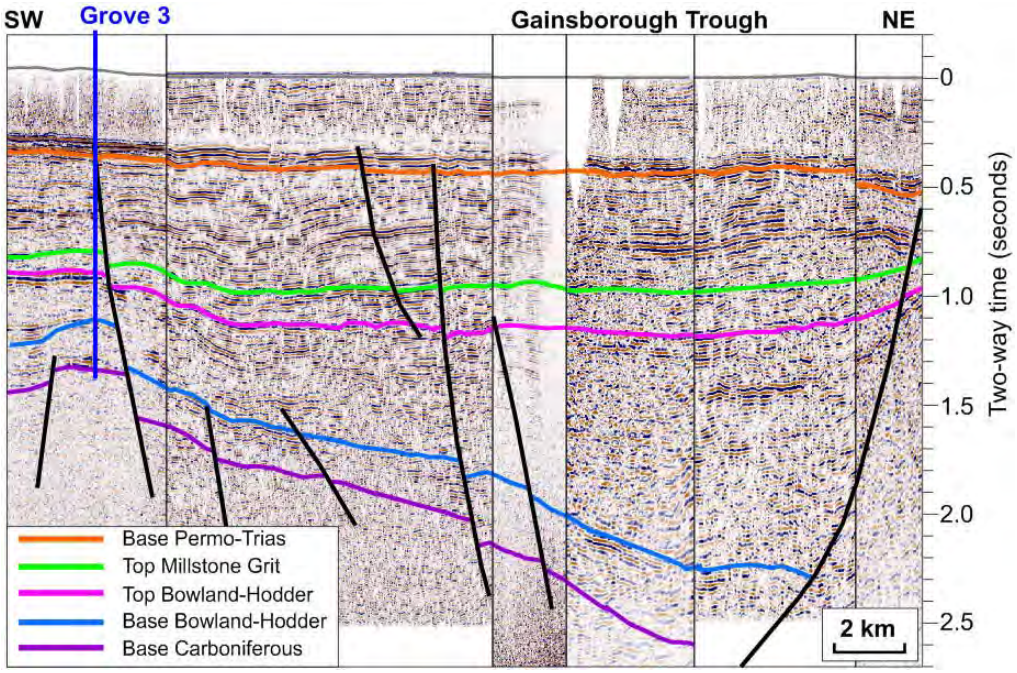

Figure 23. Seismic example across the Gainsborough Trough. The Grove 3 well is located on the East Midlands Shelf and illustrates the platform limestone-dominated nature of the Bowland-Hodder unit that was deposited on an Early Carboniferous platform high area. For location of the section, see Figure 18.

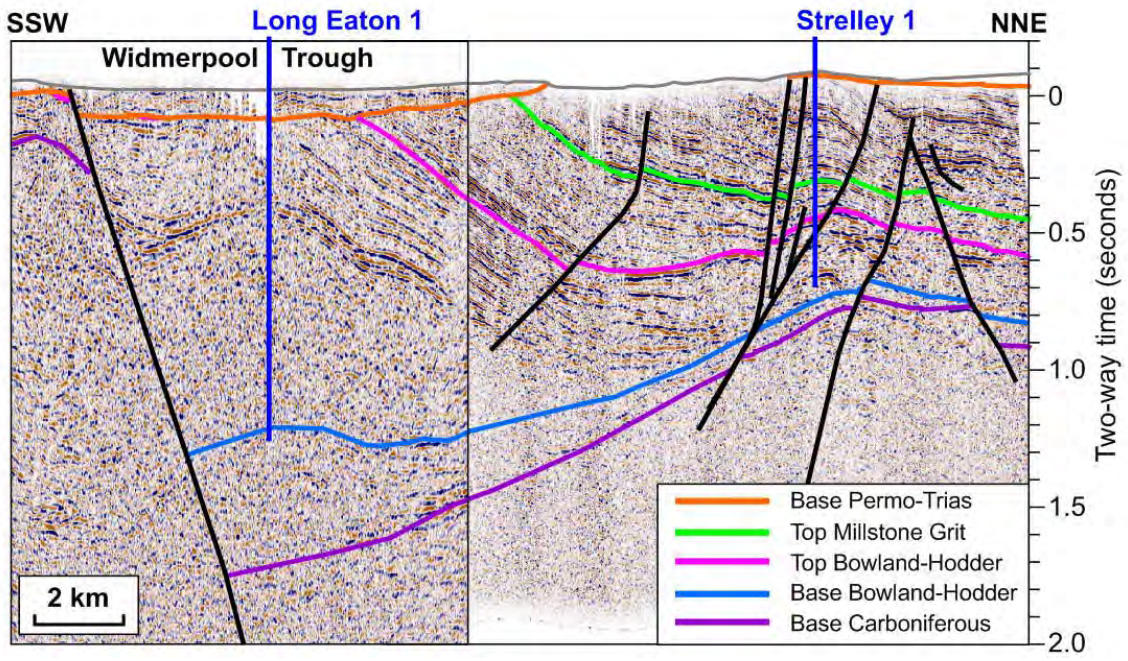

Figure 24. Seismic example across the Widmerpool Trough, showing inversion of the basin depocentre and localised erosion of the upper part of the Bowland-Hodder unit beneath the base Permian unconformity. The Long Eaton 1 well penetrated 8028 ft (2447 m) of the Bowland-Hodder unit before reaching a limestone of possible Chadian age. For location of the section, see Figure 18.

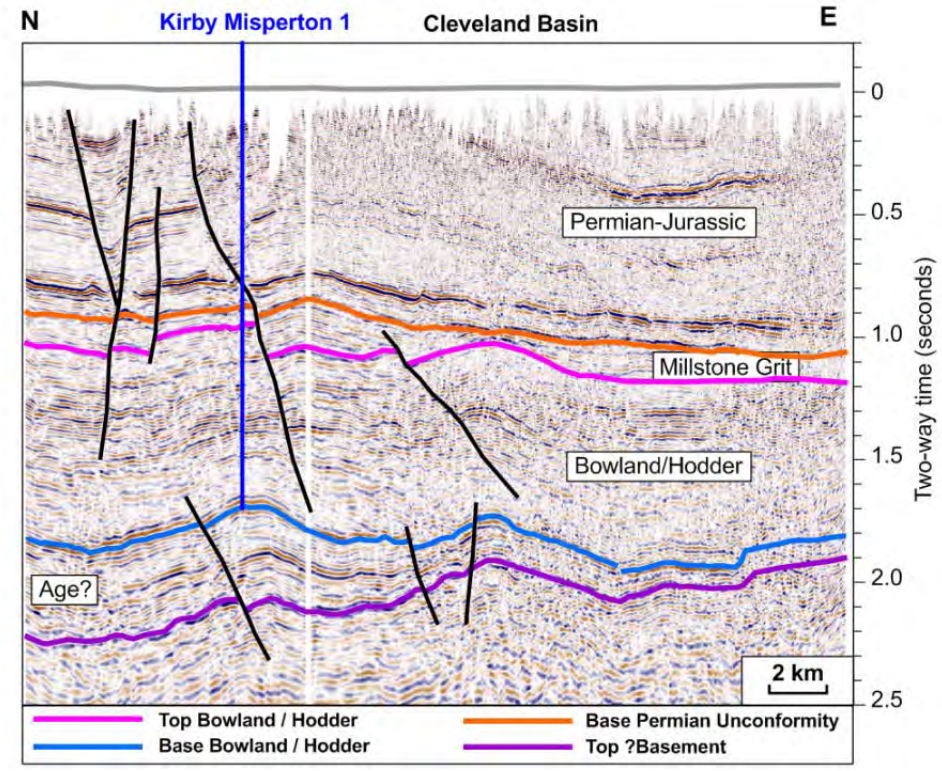

Figure 25. Seismic example across the Cleveland Basin, showing the presence of older wedging strata (of unknown age) beneath the Bowland-Hodder unit. The Kirby Misperton 1 well terminates in the 'Fell Sandstone', but the older part of the Bowland-Hodder unit is also sand-prone in this well. For location of the section, see Figure 18.

3.6. Key wells

Of the many wells drilled within the assessment area, only 64 reached sufficient depths to record more than 50 ft (15 m) of net shale in the Early Carboniferous section (Figures 7, 26 and 28, Appendix C).

Few wells have penetrated the full Bowland-Hodder succession within the deep basins, but several have drilled sections of more than 5000 ft (1500 m). Detailed well correlations are included in Appendix D (Figure 26) and Figure 27 compares the sections encountered in some of the key wells and outcrops in the study. Note that most wells do not encounter the base of the unit, and only a few penetrate significantly into the lower Bowland-Hodder unit.

In addition to wells drilled under hydrocarbon legislation, there are a number boreholes drilled for mineral and geothermal investigation which are relevant to the understanding of the Bowland-Hodder shale play. For example, the BGS Duffield (Aitkenhead 1977) and Roosecote boreholes, the Cominco boreholes described by Arthurton *et al*. (1988), the BP minerals boreholes described by Aitkenhead *et al*. (1992) and Brandon *et al*. (1998) and the unpublished BGS Clitheroe geothermal borehole (SD 755 409). Note also, that many borehole samples, thin sections and macrofossil (ammonoids, bivalves) and microfossil (conodonts, foraminifera and palynology) preparations are held in the biostratigraphy/palaeontology collections at BGS. Contact *enquiries@bgs.ac.uk* for further details.

Dating and correlation of the Bowland-Hodder unit requires a multidisciplinary approach. Standard industry techniques such as palynology are of limited use due to the poor preservation of miospores in the hemipelagic marine shales and the broad stratigraphic range of the miospore zones. The highest resolution stratigraphy is provided by glacio-eustatic flooding surfaces. These form the backbone for all the marine event stratigraphy and biostratigraphic correlation through the Bowland-Hodder unit, particularly in the upper part (Bowland Shales). Major flooding surfaces successively introduce new marine faunas, especially ammonoids (hence the need to take cores for definitive dating). Accessory taxa, such as hemipelagic bivalves, trilobites, foraminifera and conodonts, provide additional tools for correlation and understanding depositional environments, as well as elucidating the interplay between basinal facies and sediments sourced from surrounding areas (with implications on predicting shale quality and distribution). This knowledge is particularly important in deciphering the origin, cause and distribution of gravity-fed deposits within the hemipelagic sequence, and corresponding carbonate, silicate and organic-rich zones.

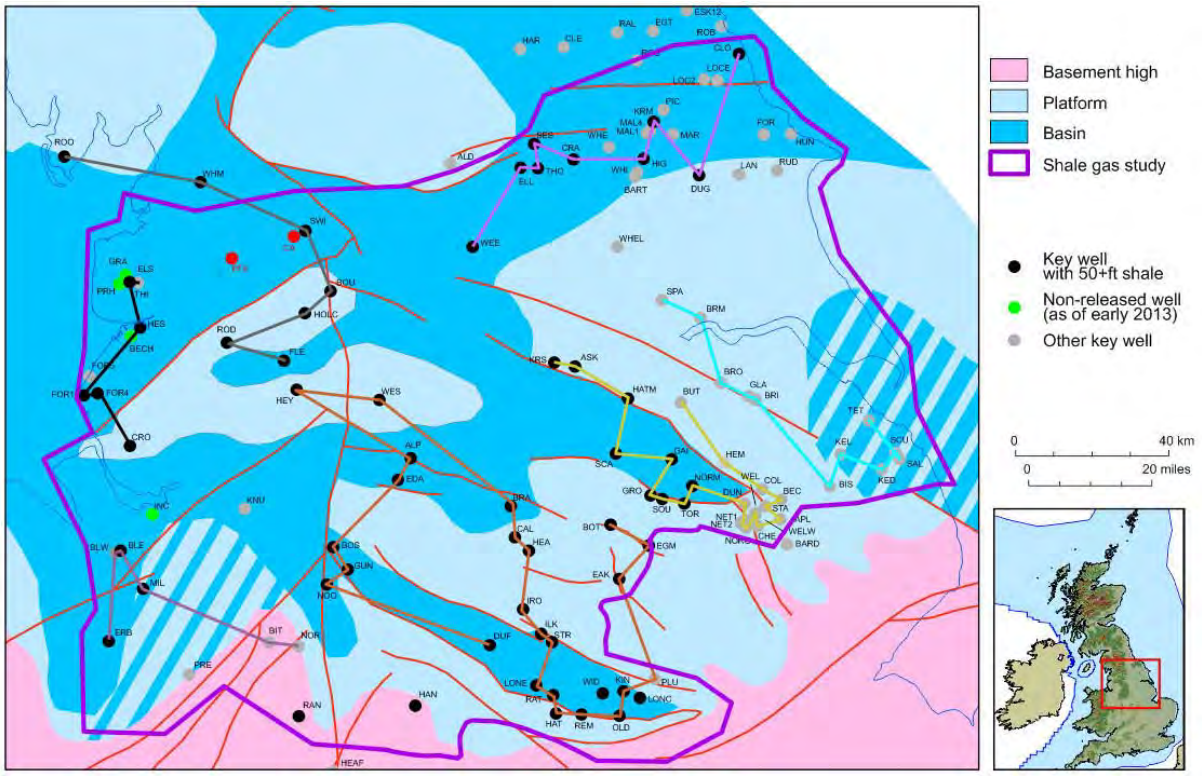

Figure 26. Location of well correlation lines included in Appendix D.

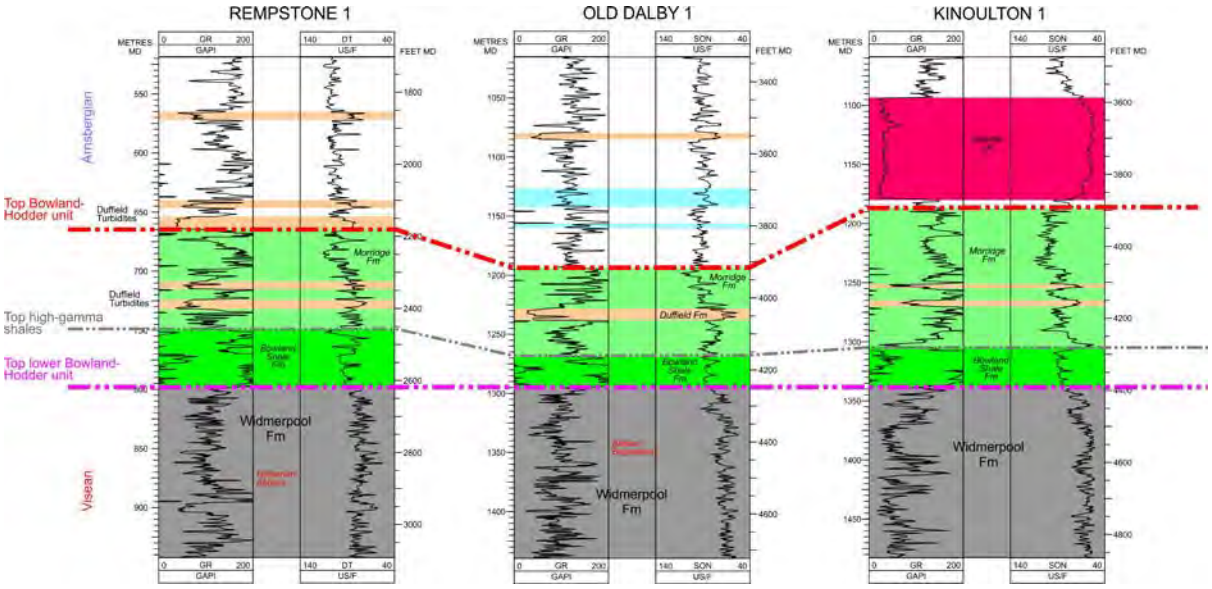

Figure 27. Geophysical well-log correlation of the upper Bowland-Hodder unit between Rempstone 1, Old Dalby 1 and Kinoulton 1 located in the Widmerpool Gulf (see Appendix D iv for the complete correlation diagram). The upper part of the Bowland-Hodder unit contains correlateable units.

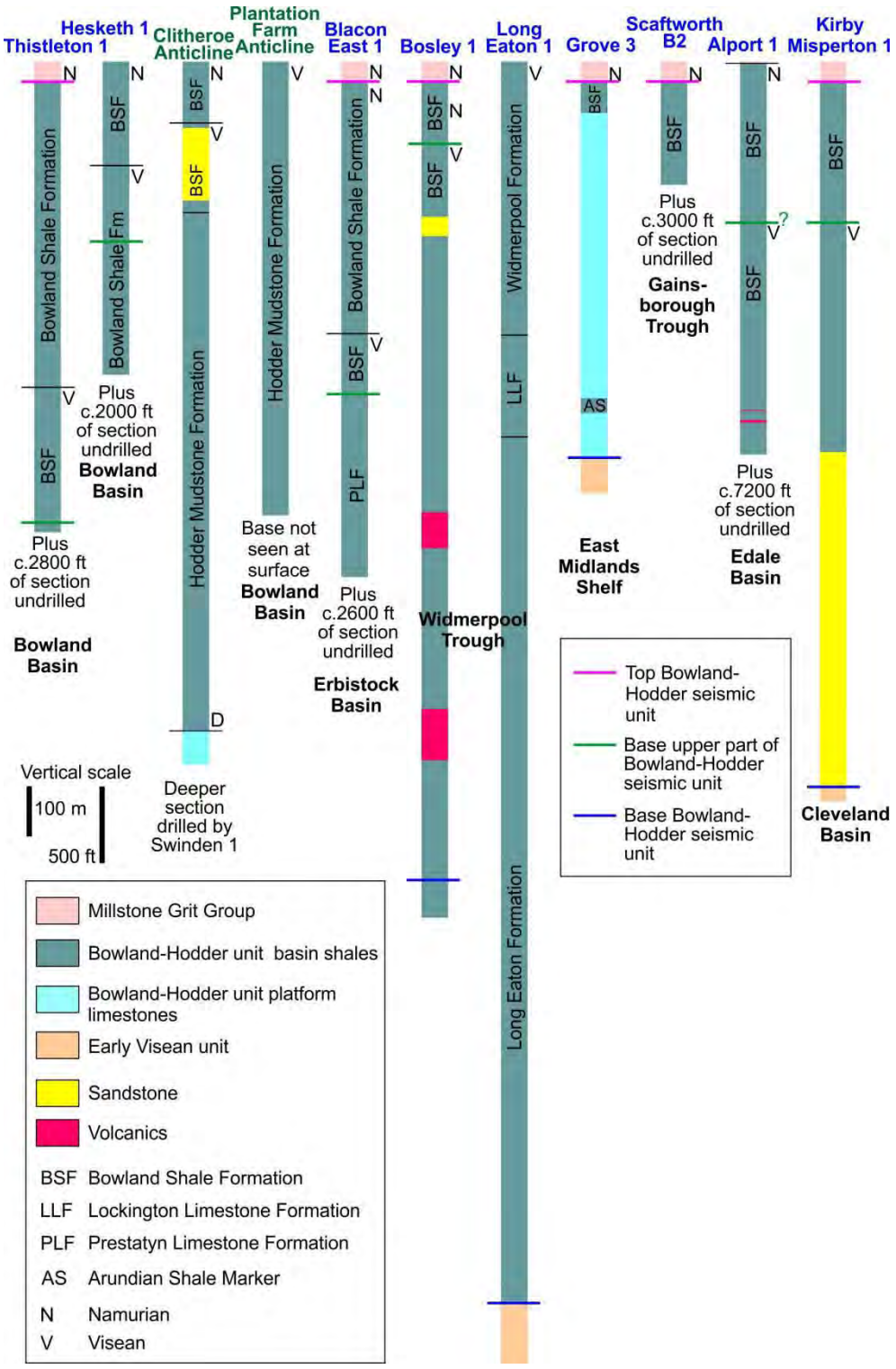

Figure 28. Craven Group basinal shale sections recorded from wells and outcrops, central Britain. At the Clitheroe and Plantation Farm anticlines, the outcrop section has been measured along the ground. In the wells, only the part drilled down from just above the top of the Bowland-Hodder unit is shown. See Figure 26 for the location of the wells and outcrop localities. The estimated thickness of the unit which remains undrilled below the terminal depth of each well is also indicated; this is based on seismic interpretation. Note the early incoming of clastic sediments in the northernmost well, Kirby Misperton 1.

3.7. Regional distribution of shale

The mapping of the Bowland-Hodder interval as a seismically defined unit necessitated the use of a sequence stratigraphic approach. As a result, the mapped unit is constrained by time lines, between which there are a variety of basinal and platform facies. To ensure that the 3D volume model used to calculate the potential amount of gas in-place within the Bowland-Hodder unit only included shale lithologies (and not the platform limestones, nor sandstones and limestone turbidites within the basins), it was necessary to map the predicted lateral variation in shale percentage. The distribution of shale in the lower part of the Bowland-Hodder unit (Figure 29) was mapped using a shale analysis of key wells (using an appropriate gamma log cut-off) integrated into the regional palaeogeographic model (Figure 14). The distribution of shale in the upper part shows little variation across the study area.

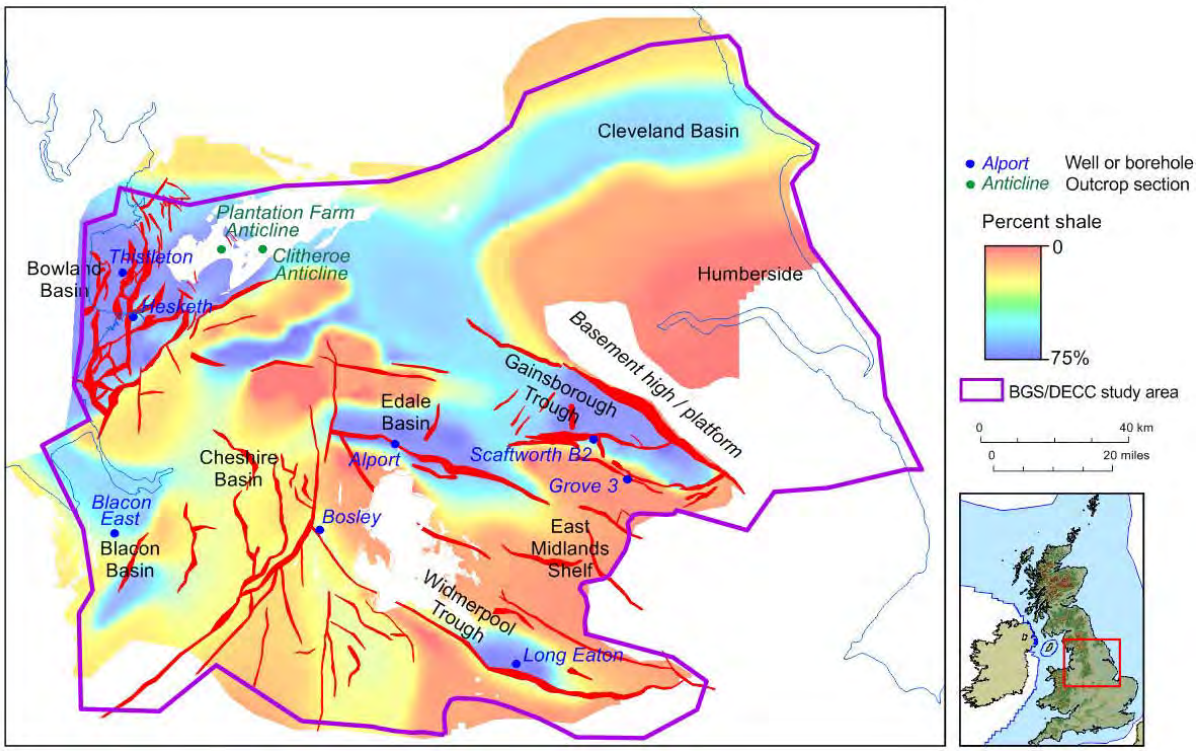

Figure 29. Predicted shale percentages within the lower part of the Bowland-Hodder seismic unit used to condition the 3D volume during the calculation of in-place gas resources.

3.8. Geochemical evaluation

Many central Britain outcrop, core and cuttings samples of Visean and Namurian shales have undergone geochemical analysis, mainly when studying source rocks in conventional petroleum systems. Relatively little analysis has specifically targeted its shale gas plays.

Data from 161 well and outcrop locations (3420 samples) were available to this study. Many reports are available through the general release of hydrocarbon well data from DECC's data release agents. Data has also been extracted from Petra-Chem (1983a, b, c) and RRI (1987). Rock-Eval analysis of an additional 109 core samples was commissioned as part of this study (Appendix B). Confidential data available to DECC was integrated into the study, but it is not published in this report. Under UK

onshore licence terms, well data is held confidential for four or five years before it can be released into the public domain by DECC's release agents.

Geochemical data were also available from strata higher in the Carboniferous succession, and these have proved useful in determining maturation trends with depth and burial history.

Organic carbon content

There are only limited published data on organic carbon contents in the Bowland-Hodder unit (DECC 2010a, Smith *et al*. 2010). These published data suggest that Namurian marine shales have generally higher TOC values (average 4.5%) compared to non-marine shales, which have an average value of 2.7% (Spears & Amin 1981). Maynard *et al.* (1991) found that two thin Namurian black shale marine bands have a TOC of between 10 and 13%, whereas values within interbedded strata ranged between 2 and 3%. The Namurian Holywell Shale of North Wales has TOC values in the range 0.7-5%, with an average of 2.1% (Armstrong *et al.* 1997). More recently, the Ince Marshes 1 well encountered shales with TOC values of 1.18 – 6.93% (average 2.73%) in the 'Bowland Shale' (iGas 2012). Könitzer *et al.* (2011) record Arnsbergian shales with 1-7% TOC in the Carsington C4 borehole [SK 251 530].

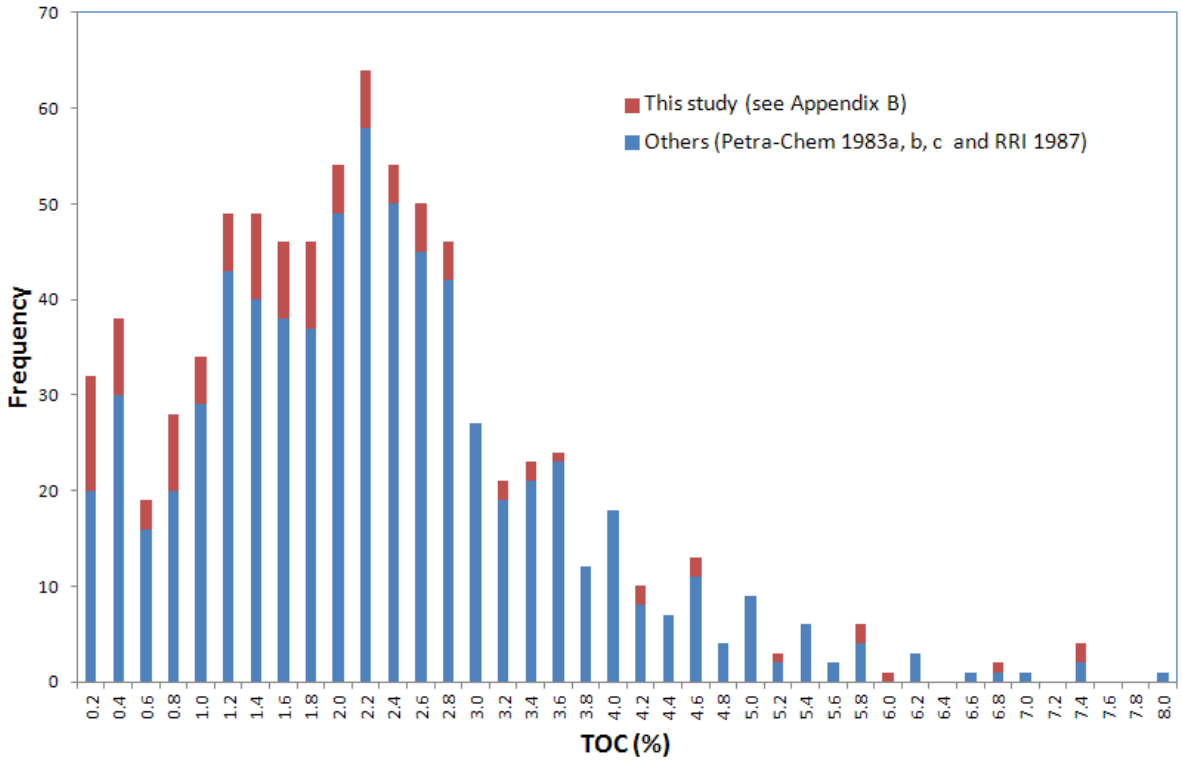

Figure 30. Summary of total organic carbon analyses from the Bowland-Hodder unit in central Britain. There are seven data points with TOC >8%. Some data may be from adjacent horizons and some non-shale lithologies are included.

A review of all available total organic carbon data from the Bowland-Hodder unit in central Britain is summarised in Figure 30. Most samples are from the upper part of the Bowland-Hodder unit. Values fall in the range >0.2 to 8%, with most shale samples in the range 1-3% TOC. Smith *et al*. (2010) give

a similar range up to 10%. The results of the new Rock-Eval analyses commissioned as part of this study (shown in red on Figure 30 and listed in full in Appendix B) mirror this conclusion.

For comparison, USEIA (2011a) quote an 'average TOC' for the Bowland shale play of 5.8%.

The down-hole gamma-log response is generally considered to be a good proxy for organic carbon content where geochemical analyses are lacking. TOCs in excess of 1-3% typically correlate with gamma log values of greater than 150 API.

The gamma-log responses of the shales within the upper Bowland-Hodder unit indicate significant intervals having >2% TOC (see well correlations in Appendix D).

While there are some data for the lower Bowland-Hodder unit, the well penetrations are mostly within the uppermost 100 feet, so few wells sample the full expanded section in the narrow rifted basins. The exceptions indicate consistently high TOC values in the Widmerpool Gulf, with average TOCs of 3.5%, 4.9% and 5% over sampled intervals in Old Dalby 1, Ratcliffe-on-Soar 1 and Rempstone 1 respectively (Appendix B). There are no analysed samples from the lower unit in the Gainsborough Trough.

The observed range of TOC values in the Bowland-Hodder unit (average 1-3%, maximum 8%) is comparable to many of the producing North American shale-gas analogues (Table 3).

Formation	Age	HI_o (mg/g)	TOC_{pd} Low (wt. %)	TOC_{pd} High (wt. %)	TOC_{pd} Average (wt. %)
Barnett	Early Carboniferous	434	0.02	9.94	3.74
Fayetteville	Early Carboniferous	404	0.71	7.13	3.77
Woodford	Devonian	503	0.26	11.27	5.34
Bossier	Late Jurassic	419	0.46	4.11	1.64
Haynesville	Late Jurassic	722	0.23	6.69	3.01
Marcellus	Devonian	507	0.41	9.58	4.67
Muskwa	Devonian	532	0.01	5.97	2.16
Montney	Triassic	354	0.01	4.78	1.95
Utica	Ordovician	379	0.19	3.06	1.33
Eagle Ford	Late Cretaceous	411	0.58	5.6	2.76

Table 3. Comparison of present-day total organic carbon contents (TOC_{pd}) for the top 10 shale gas plays in North America (Jarvie 2012).

Kerogen type

Four basic categories of kerogen are recognised in organic matter (Tissot *et al*. 1974). Type I and II kerogens have the potential to generate both oil and gas. Type III kerogens mainly generate gas, with only a small amount of oil, while Type IV kerogens have little or no remaining potential to generate hydrocarbons.

The type of kerogen present is also an indication of the environment in which the interval was deposited. Algae seen in Type I samples indicate a lacustrine (or marine environment), whereas Type II is deposited exclusively in marine conditions and contains plant spores, exines, resins and bacterially degraded algal matter. During initial maturation, Type II source rocks generate mainly oil and only a limited amount of gas. As maturation proceeds through higher temperatures, secondary cracking in these source rocks cracks the generated oil into gas. Type III organic material is comprised of vitrinite and is typically woody material found in continental rocks deposited in rivers and deltas, but it can also be found in marine environments where it is washed in from a nearby

shelf. Type IV contains inertinite, where oxidation of woody material has occurred, either before it is deposited or in situ.

Ewbank *et al*. (1993) reported Type II kerogen in the Widmerpool Gulf, Edale Basin, Goyt Trough and mudstones interbedded with carbonates on the Derbyshire High; Type III was also present. However, little additional data are available to establish the original composition of the kerogen in the Bowland-Hodder unit. The identification of kerogen type using geochemical cross-plots is complicated by the fact that various ratios can reduce during the maturation process (Jarvie *et al.* 2005, 2008). A significant number (but still a minority) of samples plot in the Type II field (Figure 31; Appendix B) which is in general agreement with the deep-water marine, hemipelagic depositional environment of the Bowland-Hodder unit. One explanation as to why many samples plot as Type III is that their geochemistry has been altered during maturation.

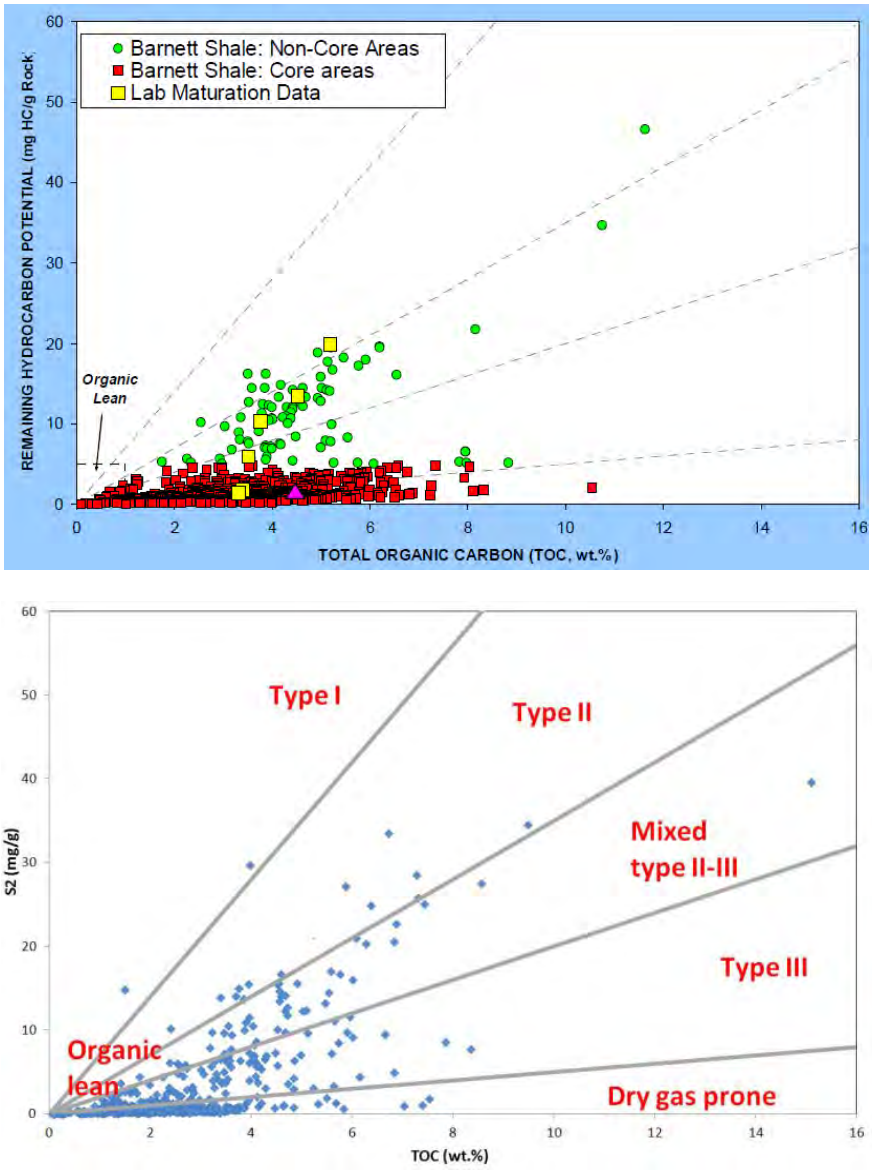

Figure 31. Remaining hydrocarbon potential (S2) versus TOC plot for (a) the Barnett Shale (from Jarvie 2008) and (b) all available data from this study. There are close similarities, although the larger range of TOCs in the Barnett Shale is evident.

Further data relevant to kerogen typing and maturation are shown in Figures 32 and 33.

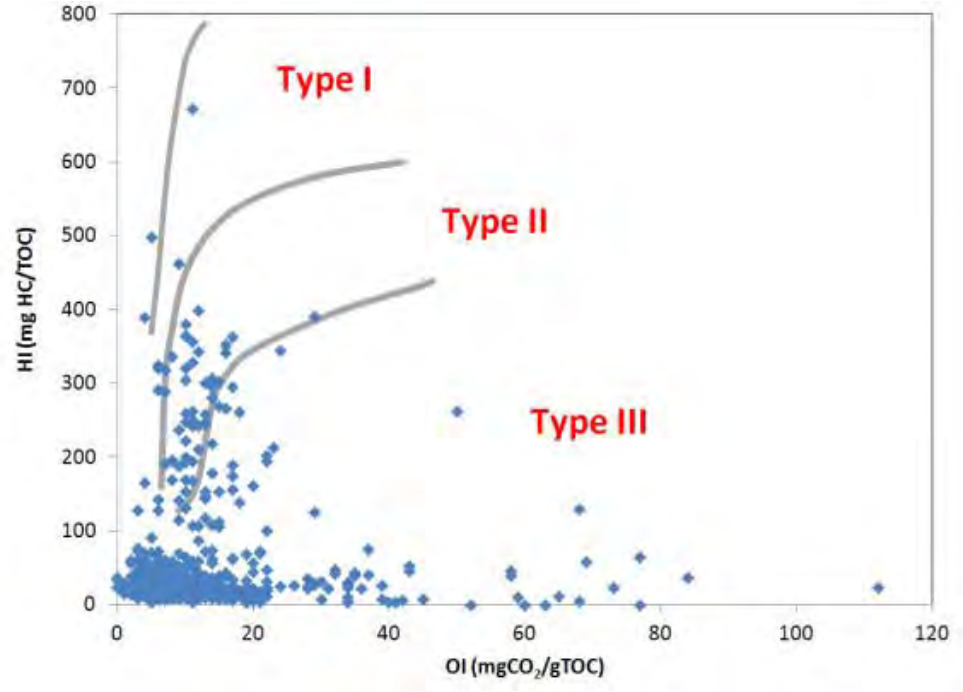

Figure 32. Modified van Krevelen diagram (HI versus OI plot) for all available data from this study. A significant number of samples fall in the Type II field.

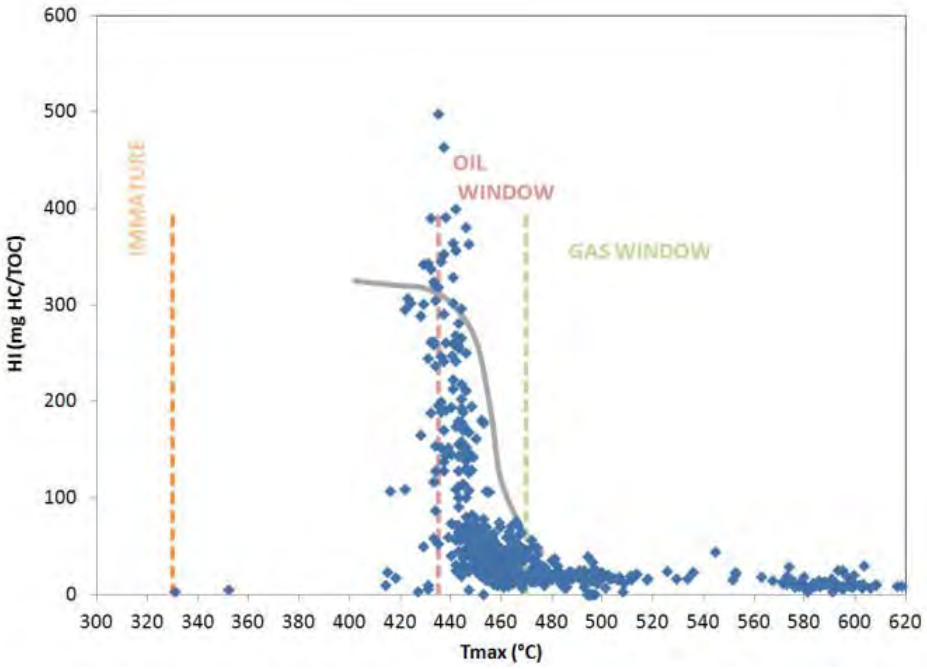

Figure 33. Hydrogen Index versus T_{max} plot for all available data from this study.

Thermal maturity and uplift

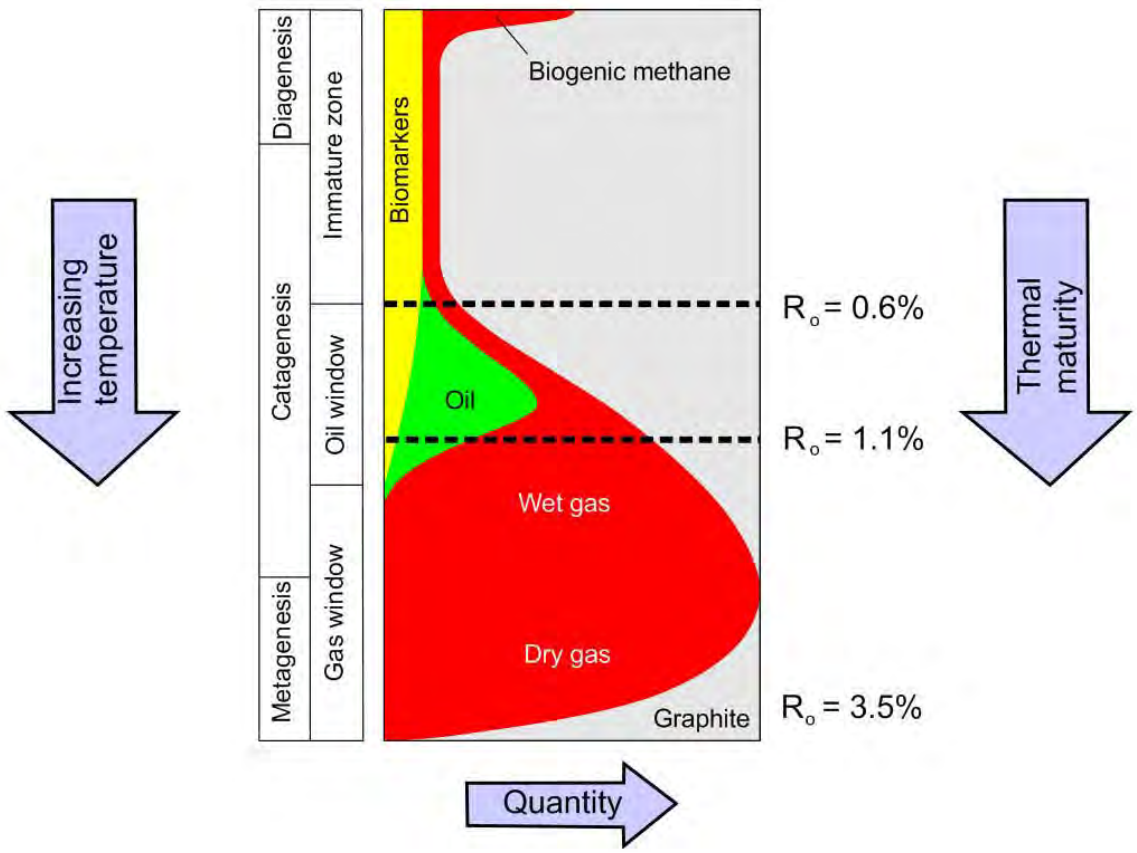

Figure 34. *Relationship between temperature, vitrinite reflectance of organic material and phases of hydrocarbon generation (modified from Tissot et al. 1974 and McCarthy et al. 2011).*

The thermal generation of oil and gas from organic material (Figure 34) generally takes place at temperatures between 50°C and 225°C. At lower temperatures, the organic material is immature and no oil or gas will be thermally generated from the source rock; at much higher temperatures, the organic material is overmature and all possible oil and gas will have been generated. The timing of generation is dependent on the kerogen type and the exact composition of the organic material.

Vitrinite reflectance (R_o) and measurements of the temperature of maximum release of S2 hydrocarbons (T_{max}) at outcrop and in boreholes provide a widely accepted proxy for thermal maturity and extent of hydrocarbon generation. An equivalent to R_o can be calculated from T_{max} using the following formula (Jarvie *et al.* 2001):

$$T_{maxeq}\%R_o = 0.018(T_{max}) - 7.16 \qquad [\text{where } T_{max} \text{ is in } °C]$$

From an analysis of all available maturity data of the Bowland-Hodder unit in the study area, it can be deduced that an R_o of 1.1% (equating to the onset of significant gas production) can be reached at a present-day depth of anything between outcrop and 9500 ft (2900 m) (Figure 35). This variability occurs because the simple R_o vs. depth relationship is overprinted by the multiphase subsidence and inversion experienced across the study area.

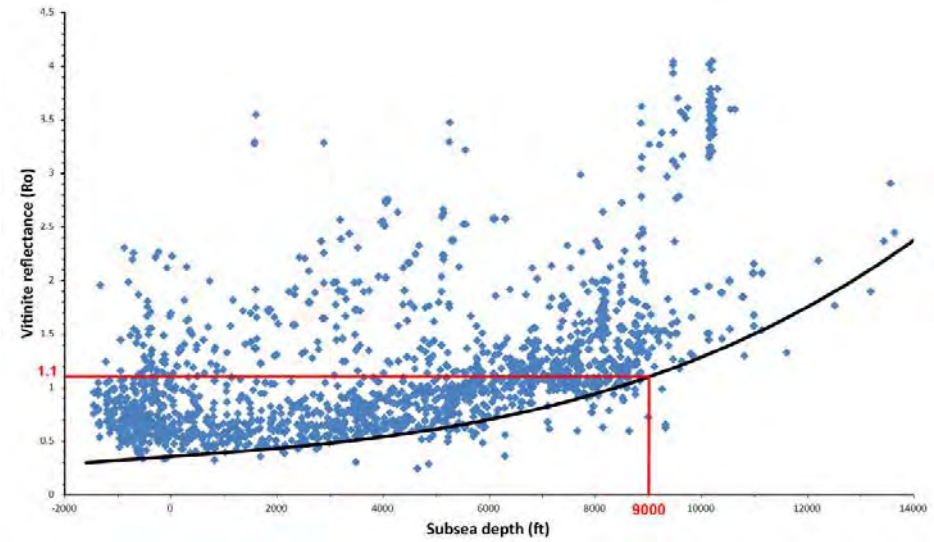

Figure 35. Chart showing all available vitrinite reflectance data (R_o and equivalent data calculated from T_{max}) plotted against present-day sub-sea depth for the Bowland-Hodder unit (and some younger strata) across central Britain. The curve shows a conservative best-fit baseline (i.e. a minimal uplift baseline); data points lying well above the baseline are affected by the highest amounts of uplift.

In the absence of quantitative data on uplift, the data summarised in Figure 35 have been used to set a baseline with minimal uplift to subsequently obtain a best-guess estimate of uplift at well locations. Data points lying above the baseline are primarily affected by uplift, so by adjusting the best-fit baseline curve to fit the data for a given well, the depth at which this curve intersects R_o = 1.1% can be identified (Figure 36).

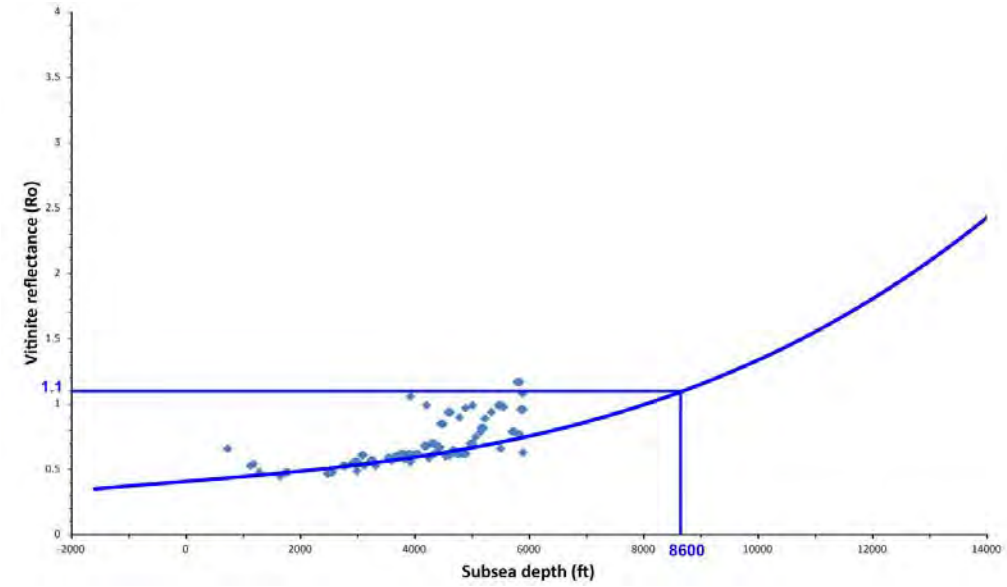

Figure 36. Chart showing the vitrinite reflectance data from Widmerpool 1. The baseline from Figure 35 has been adjusted upwards to fit the spread of the data. The depth at which R_o is expected to reach 1.1% is 8600 ft, i.e. the top of the gas window lies at c.8600 ft at this well location.

This approach is qualitative and should be treated with considerable caution, but it achieves some credence in its broad geographical conformance to other uplift models (e.g. Fraser *et al.* 1990, Kirby *et al.* 2000). At least two phases of uplift have been recognised: the first during the latest Carboniferous and early Permian (Variscan uplift) and the second during the Tertiary (Alpine uplift).

Appendix E contains details of a 1D and 2D basin modelling study, which includes uplift curves for wells and maturity models for 2D profiles. An example from the Kirk Smeaton 1 well is shown as Figure 37.

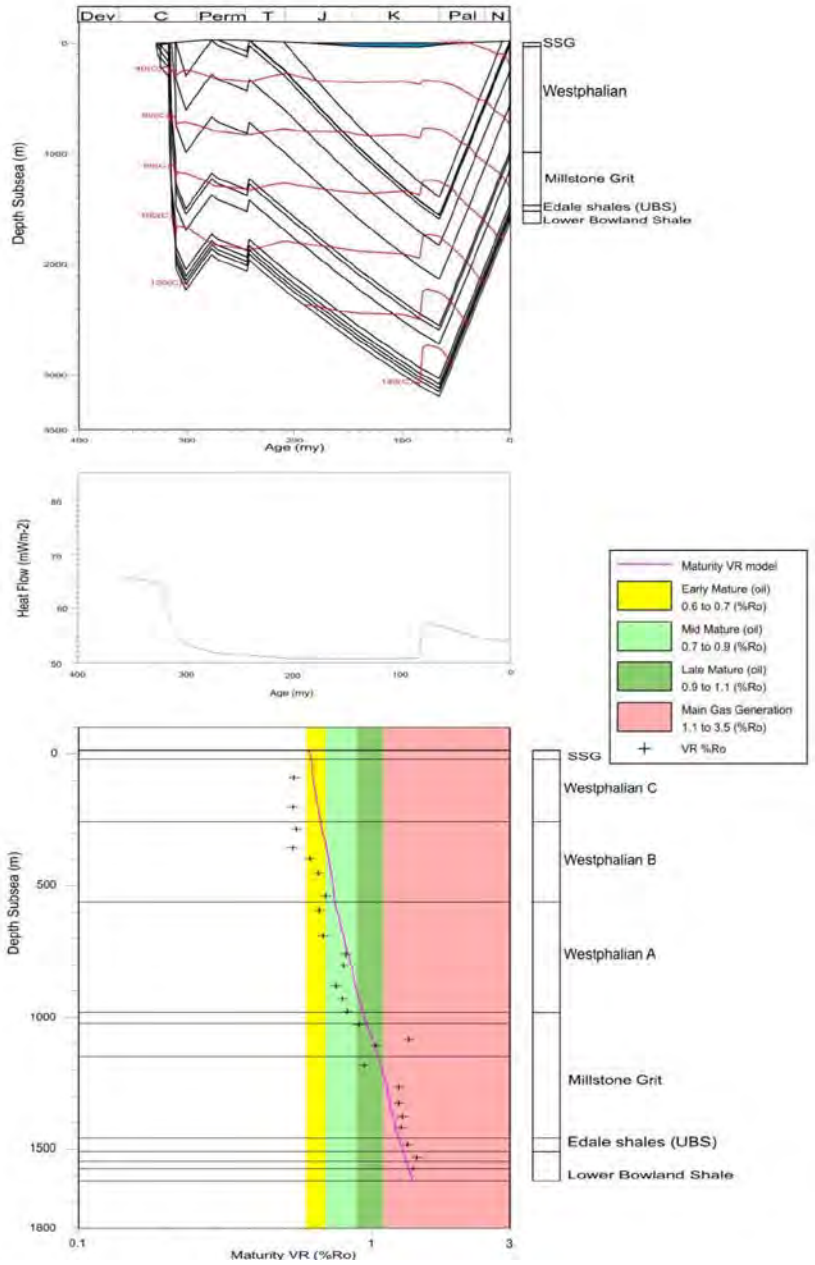

Figure 37. 1-D basin model for the Kirk Smeaton 1 well taken from Appendix E. (top) shows the depositional history, (centre) shows the modelled palaeo-heat flow and (bottom) shows the modelled vitrinite reflectance (VR) maturity curve and raw VR data.

This procedure was carried out for all well and outcrop data and the resulting depths contoured to derive a depth surface to the top of the gas window throughout the study area (Figure 37).

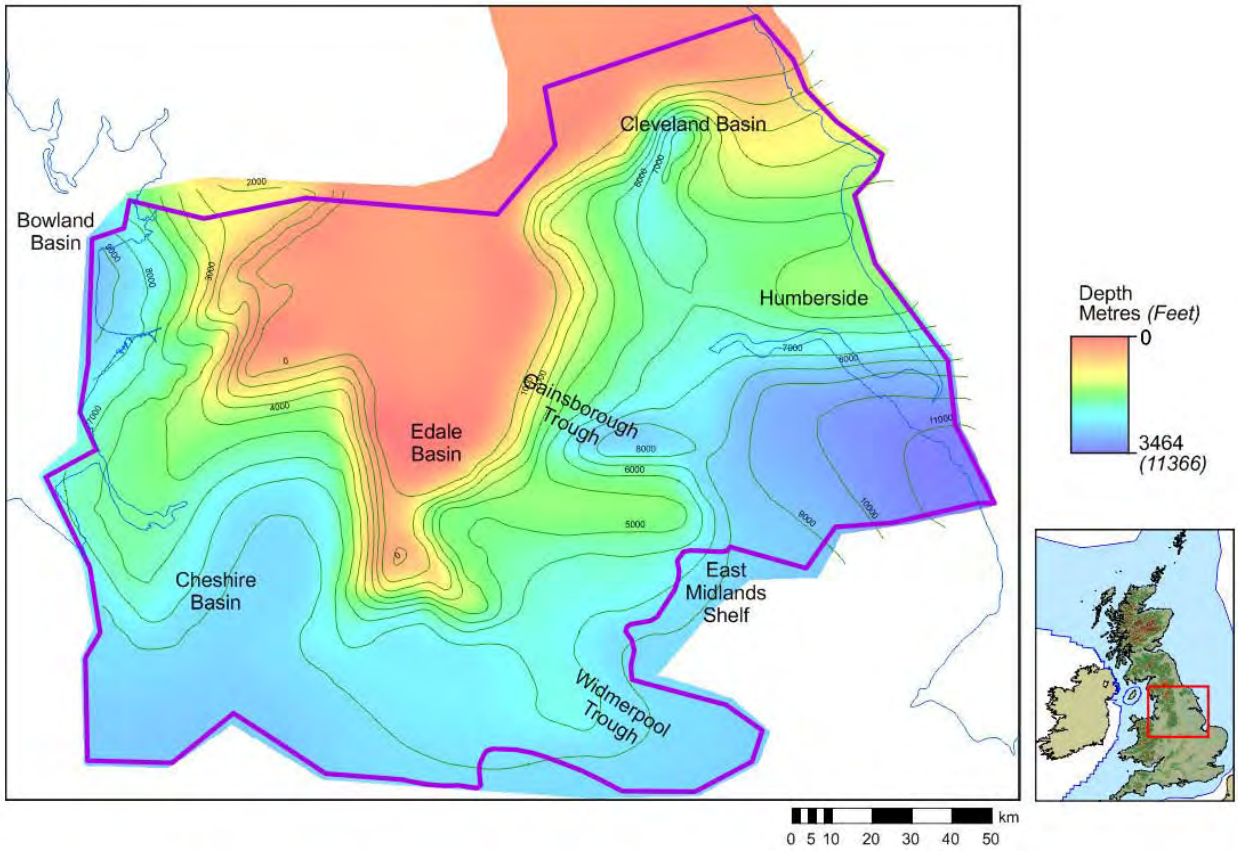

Figure 38. Estimated present-day depth (feet) to the top of the gas window (R_o = 1.1%), central Britain. Note: the shallowest colour includes areas where this isomaturity surface is above sea-level and also above the land surface.

3.9. Calculating gas-mature shale volumes

The work flow used to estimate the in-place gas resource in this study is shown in Figure 39. This shows the processes (large arrow) as well as the data sources (in blue). Some data was not available from the study area, so data from US analogies was used. There is a significant range of uncertainty of the shale volume, and greater uncertainty in the range of free and adsorbed gas used to calculate the total in-place gas volume. No attempt was made to estimate the potential liquid resource, for which the thermal maturity criteria would result in a different gross rock volume.

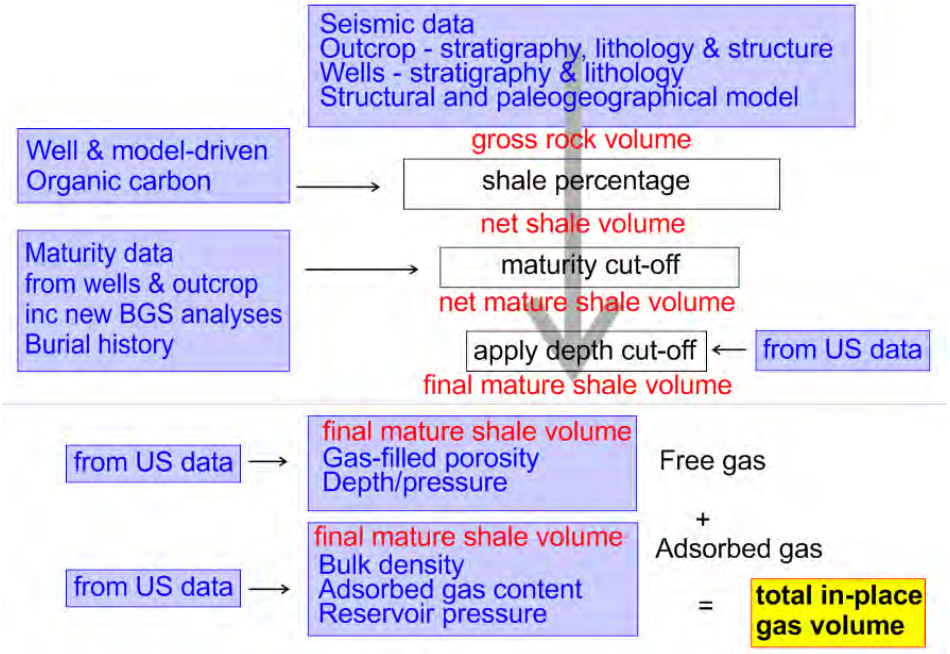

Figure 39. Workflow used in this study to estimate the in-place shale gas resource.

The calculation of the net gas-mature shale volume in the study area used the following basic screening criteria:

Identification of potentially prospective shale gas units from well information

- Mapping the top and base of units to enter into a 3D model
- Mapping the shale component as a proportion of the seismically mapped unit
- Minimum depth cut-off of 5000 ft (1500 m) below land surface
- Minimum cut-off where R_o > 1.1% (max cutoff of R_o > 3.5% never exceeded)

The volumes of shale in the upper and lower parts of the Bowland-Hodder unit were calculated using the following formula:

Net shale volume (m^3) = gross rock volume[1] (m^3) x proportion of shale

[1] below the depth where R_o = 1.1% or 5000 ft, whichever is the deeper.

The thermal maturity surface (Figure 38) was integrated with the depth structure mapping and shale proportion distribution (Figure 29) to calculate the volume of Bowland-Hodder shale in the gas window. Areas where the Bowland-Hodder shale is less than 5000 ft (1500 m) below the land

surface were removed from the potentially prospective volume. North American experience has shown that there is not adequate pressure to economically produce shale gas at shallow depths (with the exception of the biogenic gas in the Antrim Basin in Michigan).

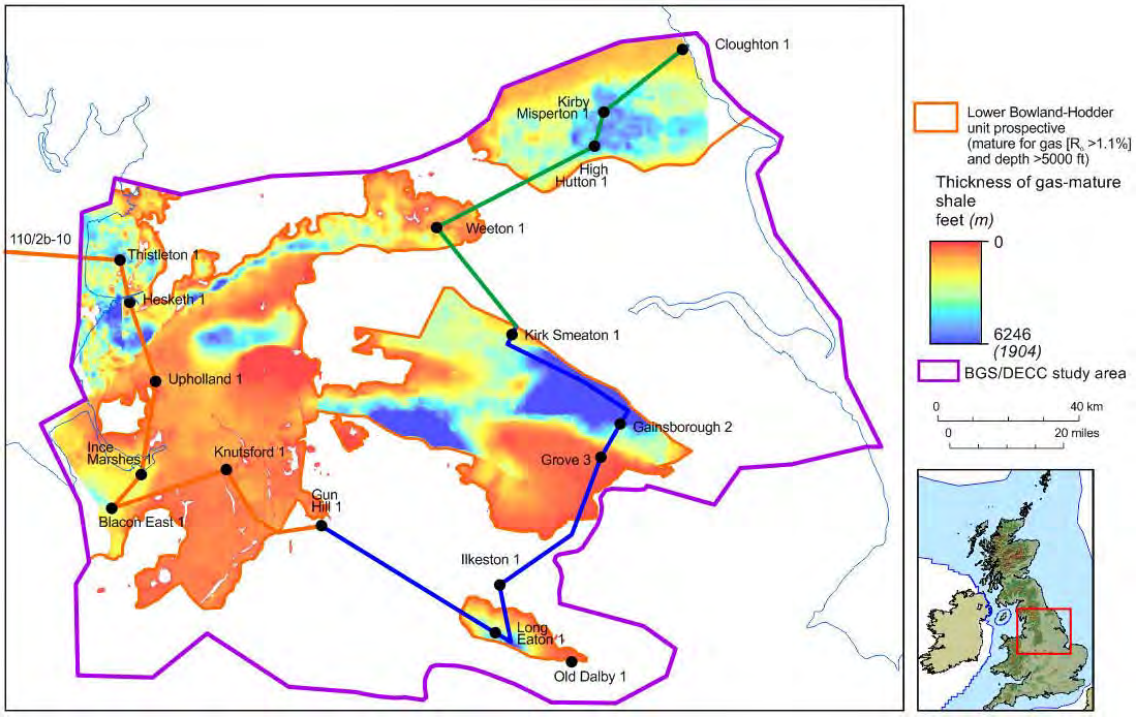

Figure 40. Thickness and distribution of shales of the lower Bowland-Hodder unit that are within the gas window and at a depth greater than 5000 ft.

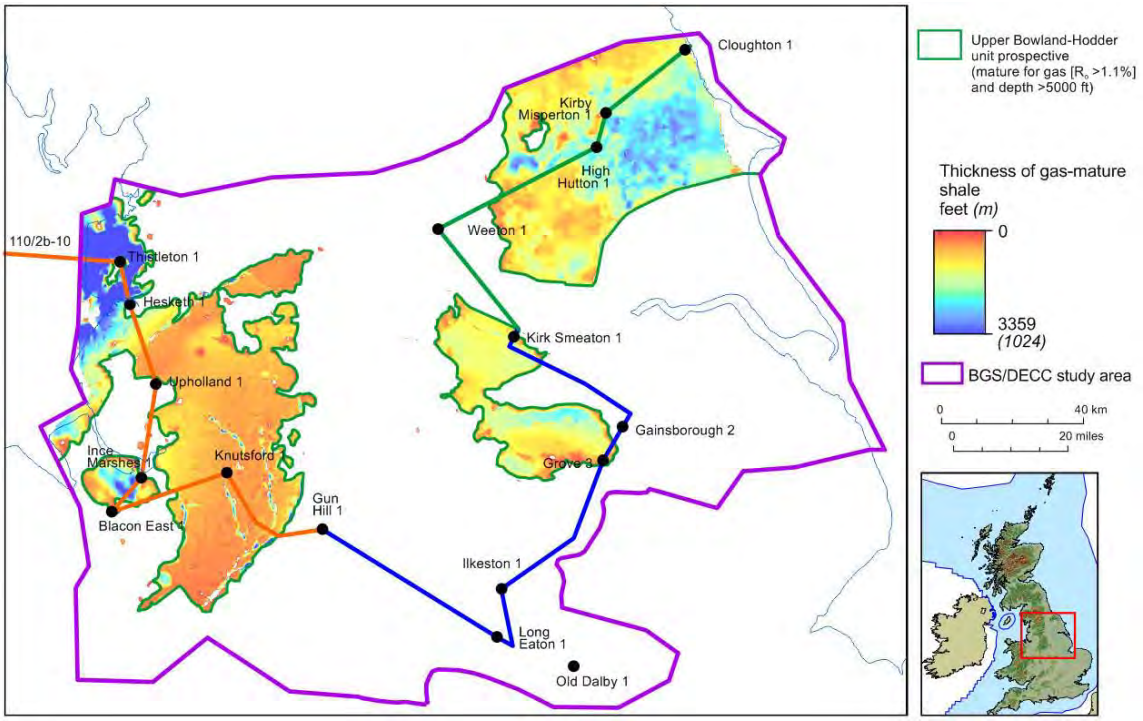

Figure 41. Thickness and distribution of shales of the upper Bowland-Hodder unit that are within the gas window and at a depth greater than 5000 ft.

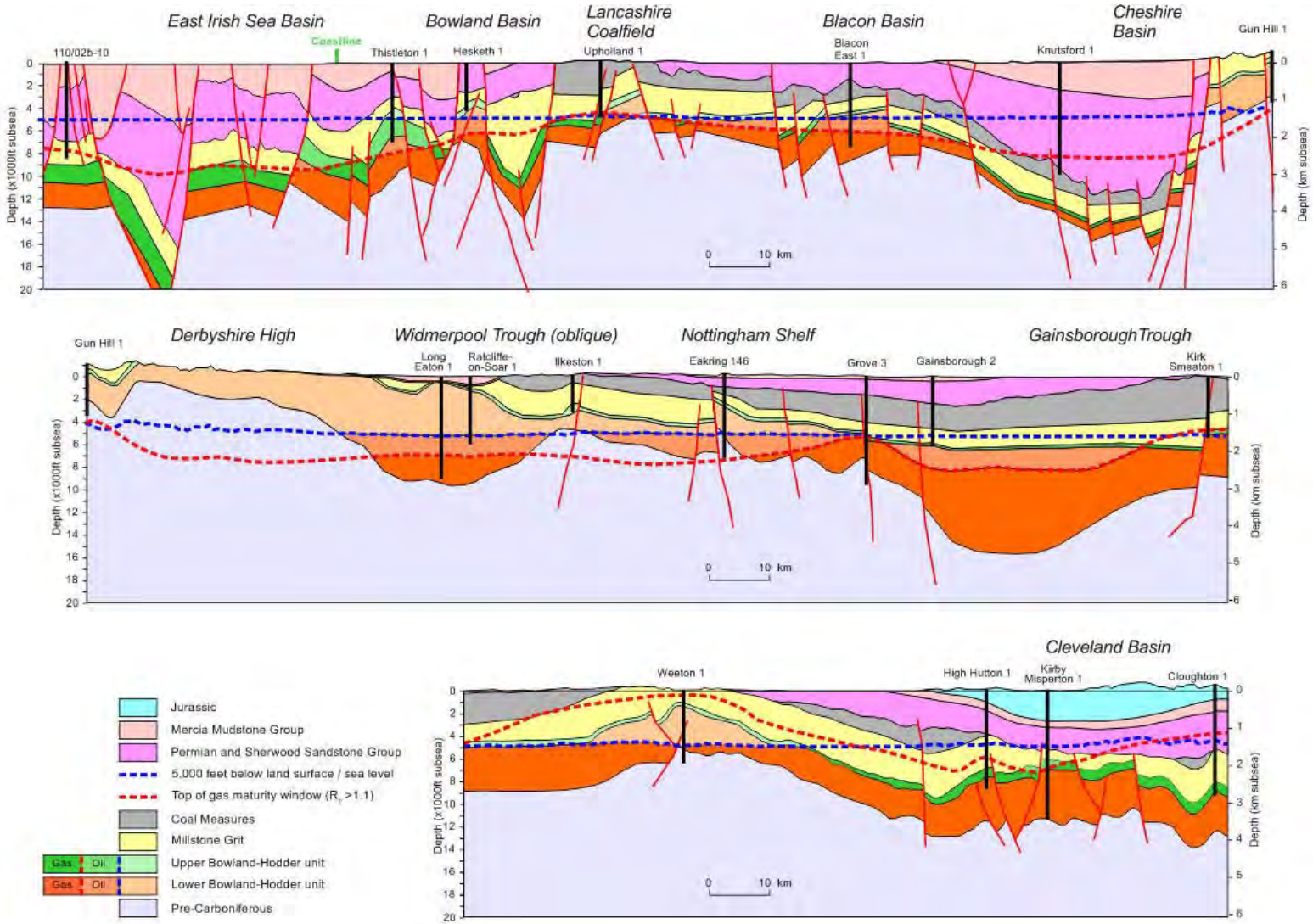

Figure 42. Schematic geological cross-sections indicating where the Bowland-Hodder unit might be considered a shale gas target (labelled 'Gas' in the key). Liquids potential, where not thermally mature for gas (labelled "Oil"), are not considered within the scope of this study. For location of the section, see Figure 40 or 41.

This interpretation is consistent with the detailed core analysis from wells (see Appendix B). In Old Dalby 1 in the Widmerpool Trough, high organic contents and high hydrogen indices (interpreted as Type II kerogen) are encountered, but the calculated R_o values of 0.6-0.7% at 4239-4450 ft sub-sea indicate that the lower Bowland-Hodder shales are immature for gas generation (Figure 40).

In Blacon East 1, in the Blacon Basin, the calculated R_o values of 1.0-1.1% at 6075-6100 ft sub-sea and 1.6-1.9% at 7423-7433 ft indicate that the upper shales are at the lower limit of the gas window, whilst the lower unit is within the gas window (Figures 40 and 41). In Grove 3, located on the East Midlands Shelf, a shale within the lower unit carbonates is also within the gas window (calculated R_o values of 1.8% at 7354-7384 ft sub-sea) (Figure 40).

The resultant maps and cross-sections show the areal extent of the upper and lower shale gas plays together with the estimated thickness of gas-mature shale (Figures 40-42). There are indications that there is a significant volume of gas-mature Bowland-Hodder shale in the Bowland, Cleveland, Edale and Blacon basins and the Gainsborough Trough. The shales in the Widmerpool Trough and Nottingham Shelf are not mature for gas, but contain a significant volume of shale that is thermally within the oil window, where liquids may be prospective, but this is outside the scope of this study.

While liquids associated with shale gas are highly sought after in North America, the recovery of liquids is lower yield than gas and therefore with the current high gas price in Europe it is anticipated that shale gas will be more commercially viable than producing liquids. However, the economics of both plays need more study once the results of wells are available.

Figure 43 shows that there is extant acreage which falls into the highly prospective areas for shale gas, so shale gas drilling and testing does need not wait upon the award of new licences. An update to DECC's 2010 Strategic Environmental Assessment is currently being undertaken and a full consultation is planned to form the basis for the next onshore licensing round.

Some of the most prospective areas are in environmentally sensitive areas or under urban centres. Exploration and potential development will likely progress at a much slower pace to fully consider how adverse impacts can be mitigated and to obtain surface landowner access permissions (both for well sites and under the path of all deviated wells), but shale gas development of the Barnett Shale in the densely populated Dallas-Fort Worth Basin proves that it is not impossible.

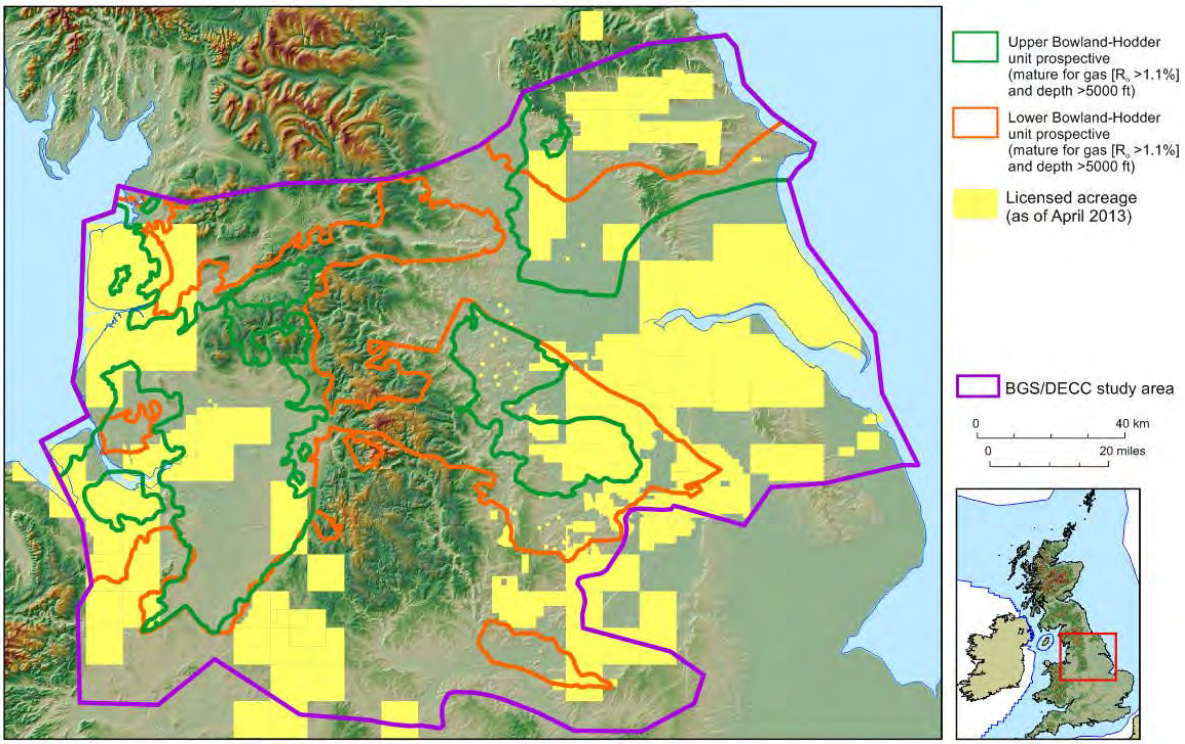

Figure 43. Summary of areas prospective for gas in the upper and lower parts Bowland-Hodder unit in central Britain with currently licensed acreage shown.

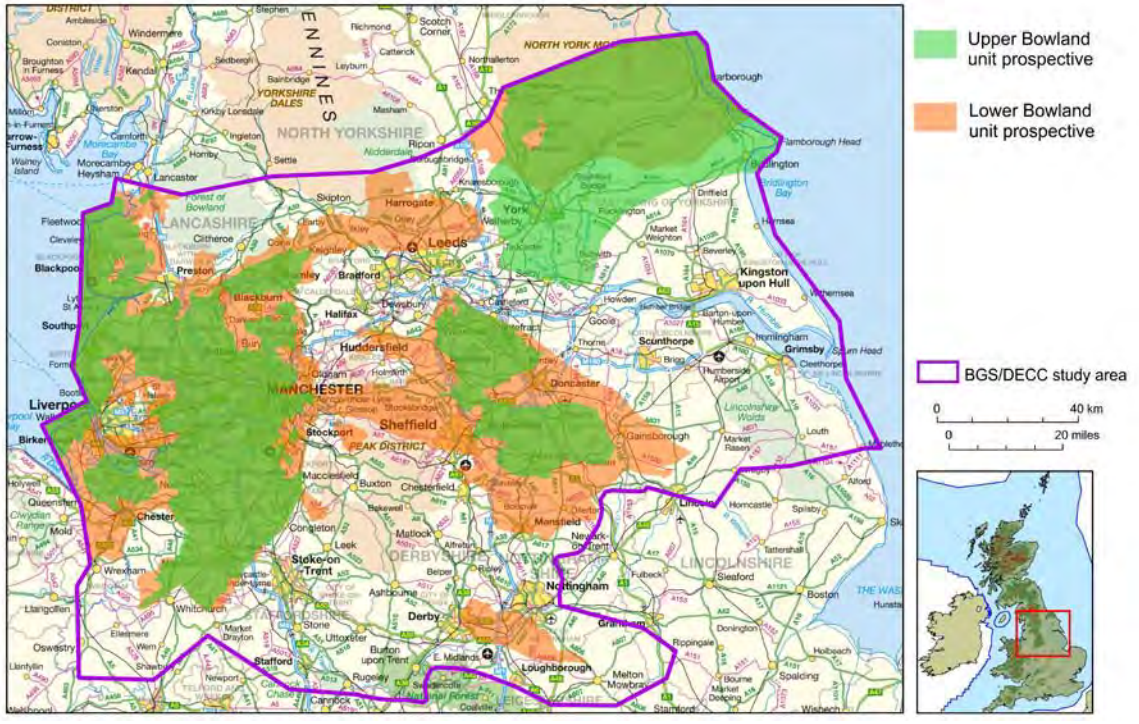

Figure 44. Summary of areas prospective for gas in the upper and lower parts Bowland-Hodder unit in relation to the urban areas of central Britain. Contains Ordnance Survey data © Crown copyright and database right 2013.

4. Resource estimation

In 2010, a DECC-commissioned BGS study estimated that, by a simple scaled basin-size analogy with similar producing shale gas plays in North America, that the UK Carboniferous Upper Bowland Shale (i.e. upper Bowland-Hodder unit) gas play, if analogous to the Barnett Shale of Texas, could potentially yield up to 4.7 tcf of gas or if analogous to the Antrim Shale, 2.1 tcf (DECC 2010a, BGS 2012).

Now, based on this detailed work undertaken in 2012-13, a rigorous gas-in-place resource estimation can be made for the Bowland-Hodder unit in central Britain. The details of this study's calculation and its results are presented in Appendix A.

This study concludes that the stacked Bowland-Hodder unit can be separated into two genetically defined intervals, with different probabilities of success, largely due to the limited well penetrations of the deeper interval. The upper unit is well constrained with borehole penetrations, core analyses and moderate seismic control. It is a condensed interval characterised by high organic content, with evidence of gas in boreholes and high gamma ray signature in well logs which can be correlated over a large area, even flooding over the carbonate platforms at the basin margins. There are a number of intervals greater than 200 ft thick that could potentially be developed using horizontal drilling technology. **The estimated range of Gas in Place (GIIP) for the upper Bowland-Hodder unit is 164 – 264 – 447 tcf.**

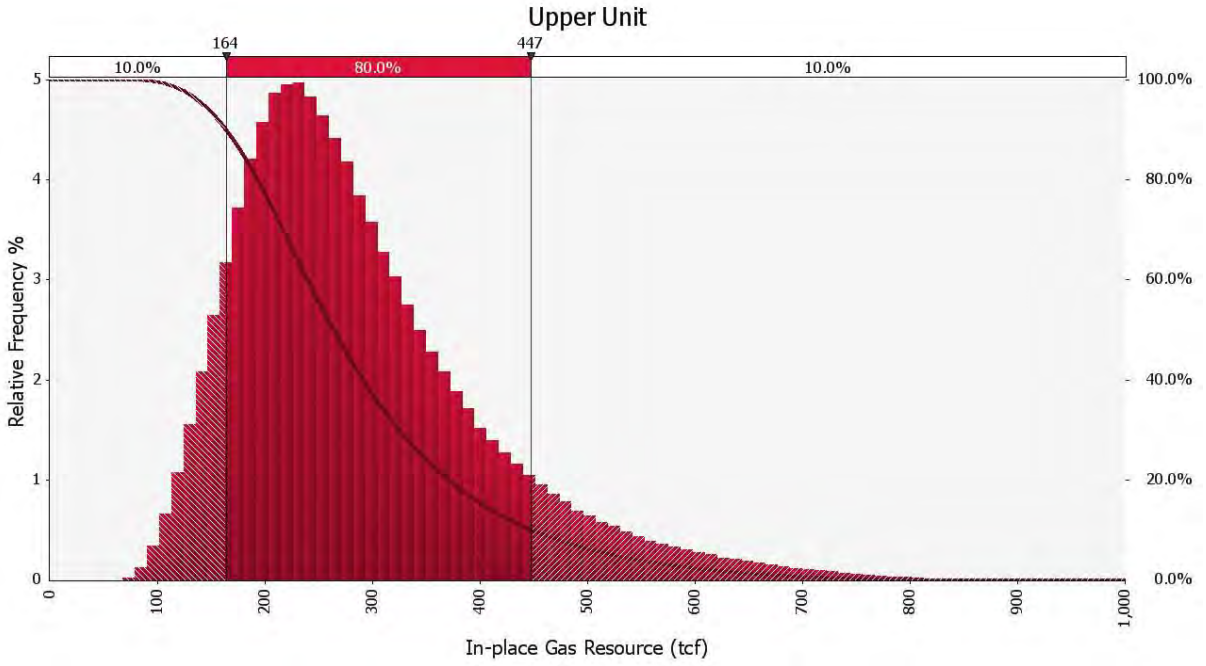

Figure 45. Probabilistic distribution and cumulative probability curve representing the result of a Monte Carlo analysis for the in-place resource estimation of shale gas in the upper Bowland-Hodder unit.

The lower unit's expanded sequence must be viewed as a higher risk resource as it is much less explored – there are few well penetrations and it is poorly imaged on seismic data in the deepest, potentially most prospective basins (Widmerpool Gulf, Edale Basin and Gainsborough Trough),

where thicknesses can reach 10,000 ft. The few deep well penetrations do show some high organic content, high gamma log prospective intervals that may prove to be laterally contiguous. The presence of large-scale slumps in the lower unit may also present challenges for shale gas exploration and production. In addition, the lower unit thickness, complex syn-rift structure and stratigraphy do not have any producing analogies in North America. Consequently, the estimated range of gas in-place for this thick sequence is 658 – 1065 – 1834 tcf, with a lower assumption of gas yield than the upper unit.

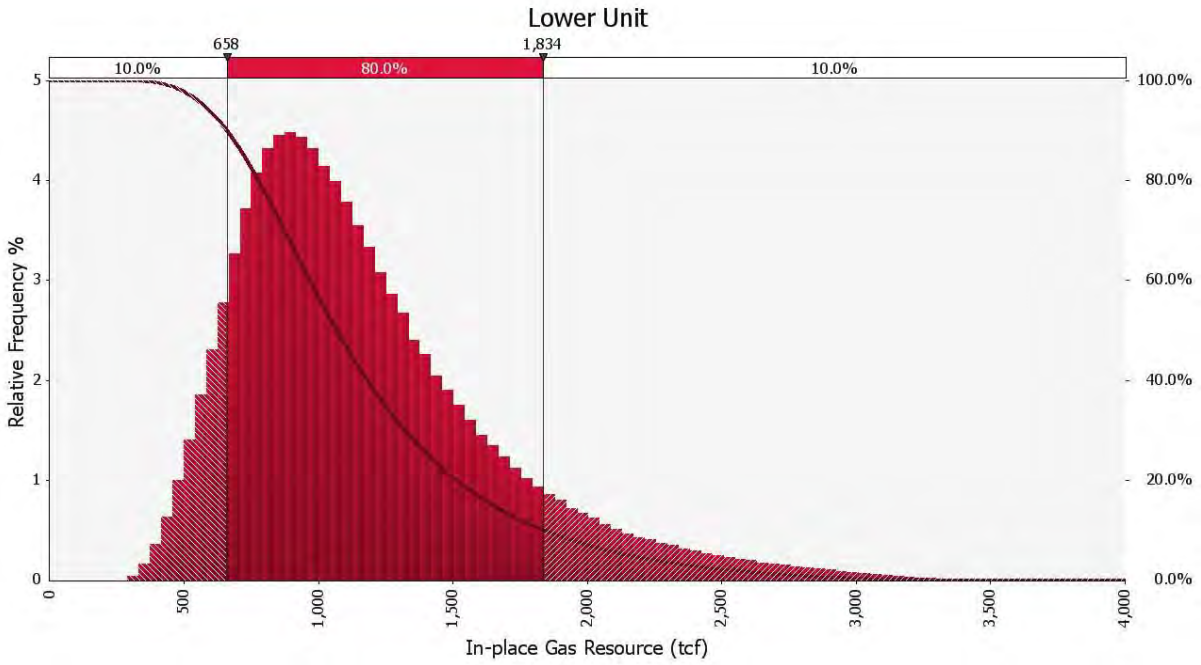

Figure 46. Probabilistic distribution and cumulative probability curve representing the result of a Monte Carlo analysis for the in-place resource estimation of shale gas in the lower Bowland-Hodder unit.

The total range of estimated gas-in-place for the combined upper and lower units is 822 – 1329 – 2281 tcf. No estimate is made for the potential for liquid hydrocarbons, which is outside the scope of this study.

	Total gas in-place estimates (tcf)			Total gas in-place estimates (tcm)		
	Low (P90)	Central (P50)	High (P10)	Low (P90)	Central (P50)	High (P10)
Upper unit	164	264	447	4.6	7.5	12.7
Lower unit	658	1065	1834	18.6	30.2	51.9
Total	822	1329	2281	23.3	37.6	64.6

This estimate is a gas in-place (GIP) estimate, because a reliable estimate of recoverable shale gas cannot be made at this time (see Section 2.2). DECC does not include any onshore or offshore shale gas potential in the published estimates for Undiscovered Resources , where detailed mapping has identified undrilled prospectivity in basins where the uncertainties in evaluating prospectivity are much better understood.

It must be noted that this Bowland Shale gas in-place (GIP) estimate is very large when compared with the total ultimate recovery of gas (i.e. gas reserves plus cumulative production) from the offshore UK, which is currently estimated at 92.7 - 101.4 - 109.0 tcf. Of this total, the cumulative amount of gas produced to the end of 2011 was 84.0 tcf. (See https://www.gov.uk/government/uploads/system/uploads/attachment_data/file/16096/6313-appendix-1-reserves-2012l.pdf)

However, only with further shale gas exploration drilling and testing over an extended period, and optimization of the extraction process, will it be possible to determine whether this identified shale gas prospectivity can be exploited commercially – and how significant a contribution it could make to the future UK energy mix.

5. Glossary

Unit/abbreviation	Full name
API	standard (American Petroleum Institute) measure of natural gamma radiation typically in a borehole
bcf	billion (10^9) cubic feet
B_g	gas expansion factor
ft	foot/feet
ft^3 or scf	(standard) cubic foot/feet
GIIP	gas initially in place
HI_o	original hydrogen index
HI_{pd}	present-day hydrogen index
km	kilometre(s)
km^2	square kilometre(s)
m	metre(s) (1 m = 3.28084 ft)
m^3	cubic metre(s) (1 m^3 = 35.31467 ft^3)
Ma	million years before present
mD	millidarcy
MPa	megapascal(s) (1 MPa = 145 psi)
mmcfd	million (10^6) cubic feet of gas per day
$mile^2m$	a volume occupying an area of 1 square mile with a thickness of 1 metre (1 $mile^2m$ = 2,589,988 m^3)
R_o	vitrinite reflectance (in oil) (%)
tcf	trillion (10^{12}) cubic feet
tcm	trillion (10^{12}) cubic metres
TOC	total organic carbon (%)

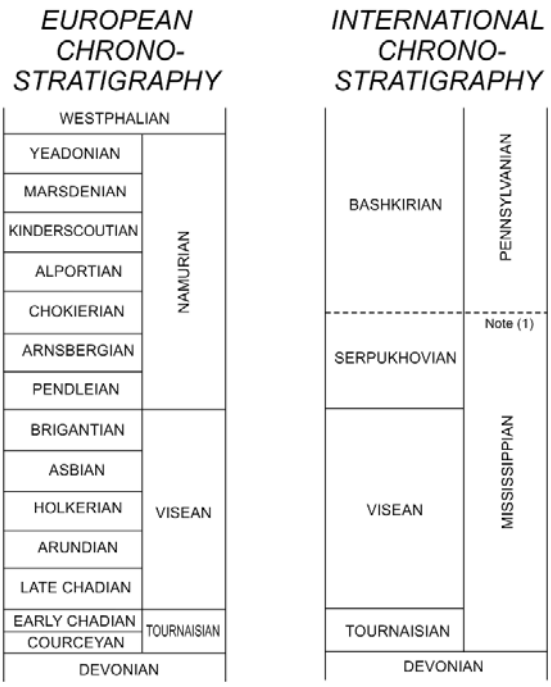

Note (1) As the Global Stratotype for the base Pennsylvanian contains numerous non-sequences (Barnett & Wright 2008), precise correlation is not possible.

6. References

Aitkenhead, N. 1977. The Institute of Geological Sciences Borehole at Duffield, Derbyshire. *Bulletin of the Geological Survey G.B.* 59: 1-38.

Aitkenhead, N., Chisholm, J.I. & Stevenson, I.P. 1985. Geology of the country around Buxton, Leek and Bakewell. *Memoir of the British Geological Survey*, Sheet 111 (England and Wales).

Aitkenhead, N., Bridge, D. McC., Riley, N.J. & Kimbell, S.F. 1992. Geology of the country around Garstang. *Memoir of the British Geological Survey*, Sheet 67 (England and Wales).

Aitkenhead, N., Barclay, W.J. Brandon, A., Chadwick, R.A., Chisholm, J.I., Cooper A.H. & Johnson E.W. 2002. *British regional geology: the Pennines and adjacent areas* (4th edition). British Geological Survey, Nottingham.

Armstrong, J.P., Smith, J., d'Elia, V.A. A. & Trueblood, S.P. 1997. The occurrence and correlation of oils and Namurian source rocks in the Liverpool Bay-North Wales area. In: Meadows, N.S., Trueblood, S.P., Hardman, M. & Cowan, G. (eds) Petroleum geology of the Irish Sea and adjacent areas. *Geological Society Special Publication* 124: 195-211.

Arthurton, R.S., Johnston, E.W. & Mundy, D.J.C. 1988. Geology of the country around Settle. *Memoir of the British Geological Survey*, Sheet 60 (England and Wales).

BGS. 2012. The Impact of Shale Gas on Energy Markets. Written evidence submitted by the British Geological Survey (ISG 17) to the UK Commons Select Committee, October 2012. www.publications.parliament.uk/pa/cm201213/cmselect/cmenergy/writev/isg/m17.htm

Barnett, A.J. & Wright, V.P. 2008. A sedimentological and cyclostratigraphic evaluation of the completeness of the Mississippian-Pennsylvanian (Mid-Carboniferous) Global Stratotype Section and Point, Arrow Canyon, Nevada, USA. *Journal of the Geological Society* 165: 859-873.

Balmer, R. 2008. Abbeystead explosion. *New Civil Engineer* 20 February 2008.

Bent, A. 2012. What will it take to replicate the shale gas revolution outside North America? Oral presentation at PETEX 2012 conference, London, 20-22 November 2012.

Bickle, M., Goodman, D., Mair, R., Roberts, R., Selley, R.C., Shipston, Z., Thomas, H. & Younger, P. 2012. Shale gas extraction in the UK: a review of hydraulic fracturing. Royal Society & Royal Academy of Engineering 105pp. royalsociety.org/uploadedFiles/Royal_Society_Content/policy/projects/shale-gas/2012-06-28-Shale-gas.pdf

Brandon, A., Aitkenhead, N., Crofts, R.G., Ellison, R.A., Evans, D.J. & Riley, N.J. 1998. Geology of the country around Lancaster. *Memoir of the British Geological Survey*, Sheet 59 (England & Wales).

Bundesanstalt für Geowissenschaften und Rohstoffe (BGR). 2012. Abschätzung des Erdgaspotenzials aus dichten Tongesteinen (Schiefergas) in Deutschland.

www.bgr.bund.de/DE/Themen/Energie/Downloads/BGR_Schiefergaspotenzial_in_Deutschland_2012.pdf

Cameron, T.D.J., Crosby, A., Balson, P.S., Jeffery, D.H., Lott, G.K., Bulat, J. & Harrison, D. 1992. *United Kingdom offshore regional report: the geology of the southern North Sea*. HMSO for BGS, London.

Carney, J.N., Ambrose, K., Brandon, A., Lewis, M.A., Royles, C.P. & Sheppard, T.H. 2004. Geology of the Melton Mowbray district. *Memoir of the British Geological Survey*, Sheet 142 (England and Wales).

Chadwick, R.A. & Evans, D.J. 2005. A seismic atlas of southern Britain – images of subsurface structure. *British Geological Survey Occasional Publication* No. 7.

Charpentier, R.R. & Cook, T.A. 2011. *USGS Methodology for Assessing Continuous Petroleum Resources*. U.S. Geological Survey Open-File Report 2011-1167.

Charsley, T.J. 1984. Early Carboniferous rocks of the Swinden No. 1 Borehole, west of Skipton, Yorkshire. *Report of the British Geological Survey* 84/1: 5-12.

Chisholm, J.I., Charsley, T.J. & Aitkenhead, N. 1988. Geology of the country around Ashbourne and Cheadle. *Memoir of the British Geological Survey*, Sheet 124 (England and Wales).

Church, K.D. & Gawthorpe, R.L. 1994. High resolution sequence stratigraphy of the late Namurian in the Widmerpool Gulf (East Midlands, UK). *Marine and Petroleum Geology* 11: 528–544.

Cooper, A.H. & Burgess, I.C. 1993 Geology of the country around Harrogate. *Memoir of the British Geological Survey*, Sheet 62 (England and Wales).

Creaney, S. 1982. Vitrinite reflectance determinations from the Beckermonds Scar and Raydale boreholes, Yorkshire. *Proceedings of the Yorkshire Geological Society* 44(1/7): 99-102.

Curtis, J. B., 2002. Fractured shale gas systems: *AAPG Bulletin* 86(11): 1921–1938.

Davies, J.R., Wilson, D. & Williamson, I.T. 2004. Geology of the country around Flint. *Memoir of the British Geological Survey*, Sheet 108 (England and Wales).

de Pater C.J. & Baisch, S. 2011. Geomechanical study of Bowland Shale seismicity (synthesis report). Report by StrataGen/Q-con for Cuadrilla Resources Ltd. www.cuadrillaresources.com/wp-content/uploads/2012/02/Geomechanical-Study-of-Bowland-Shale-Seismicity_02-11-11.pdf

DECC. 2010a. The unconventional hydrocarbon resources of Britain's onshore basins - shale gas. DECC Promote website, December 2010. https://www.gov.uk/government/uploads/system/uploads/attachment_data/file/66172/uk-onshore-shalegas.pdf

DECC. 2010b. The hydrocarbon prospectivity of Britain's onshore basins. DECC Promote website, December 2010. https://www.gov.uk/government/uploads/system/uploads/attachment_data/file/66170/uk-onshore-prospectivity.pdf

Earp, J.R., Macgraw, D., Poole, E.G., Land, D.H. & Whiteman, A.J. 1961. Geology of the country around Clitheroe and Nelson. *Memoir of the British Geological Survey*, Sheet 68 (England and Wales).

Egan, F. & Clarke, H. 2012. Lessons from the front line: investing in a license to operate. UK Shale Summit, London, 26-27 September 2012.

Evans, W.E. 1990. Development of the petroleum exploration scene in the UK onshore area; a struggle over the last 75 years. In: Ala-M., Hatamian, H., Hobson, G.D., King, M.S. & Williamson, I. (eds). *Seventy-five years of progress in oil field science and technology*. A.A. Balkema, Rotterdam, 49-54.

Evans, D.J. & Kirby, G.A. 1999. The architecture of concealed Dinantian carbonate sequences over the Central Lancashire and Holme highs, northern England. *Proceedings of the Yorkshire Geological Society* 52(3): 297-312.

Ewbank, G., Manning, D.A.C. & Abbott, G.D. 1993. An organic geochemical study of bitumens and their potential source rocks from the South Pennine Orefield, central England. *Organic Geochemistry* 20: 579–598.

Floodpage, J., Newman, P. & White, J. 2001. Hydrocarbon prospectivity in the Irish Sea area: insights from recent exploration of the Central Irish Sea, Peel and Solway basins. In: Shannon, E.M., Haughton, P.D.W. & Corcoran, D.V. (eds) The Petroleum Exploration of Ireland's Offshore Basins. *Geological Society Special Publication* 188: 107-134.

Frantz, J.H., Waters, G.A. & Jochen, V.A. 2005. Operators re-discover shale gas value. *E&P*, 1 October 2005.

Fraser, A.J. & Gawthorpe, R.L. 1990. Tectono-stratigraphic development and hydrocarbon habitat of the Carboniferous in northern England. In: Hardman, R.F.P. & Brooks, J. (eds). *Tectonic events responsible for Britain's Oil and Gas Reserves. Geological Society Special Publication* 55: 49-86.

Fraser, A.J. & Gawthorpe, R.L. 2003. An atlas of Carboniferous basin evolution in Northern England. *Geological Society Memoir* 28.

Fraser, A.J., Nash, A.J., Steele, R.P. & Ebdon, C.C. 1990. A regional assessment of the intra-Carboniferous play of northern England. In: J. Brooks, J. (ed.) *Classic Petroleum Provinces. Geological Society Special Publication* 50: 417-440.

Frost, D.V. & Smart, J.G.O. 1979. Geology of the country north of Derby. *Memoir of the British Geological Survey*, Sheet 125 (England and Wales).

Gawthorpe, R.L. 1986. Sedimentation during carbonate ramp-to-slope evolution in a tectonically active area: Bowland Basin (Dinantian), northern England. *Sedimentology* 33: 185-206.

Gawthorpe, R.L. 1987. Tectono-sedimentary evolution of the Bowland Basin, northern England, during the Dinantian. *Journal of the Geological Society (London)* 144: 59-71.

Gawthorpe, R.L. & Clemmey, H. 1985. Geometry of submarine slides in the Bowland Basin (Dinantian) and their relation to debris flows. *Journal of the Geological Society of London* 142: 555-565.

Gilman, J. & Robinson, C. 2011. Success and failure in shale gas exploration and development: attributes that make the difference. Oral presentation at AAPG International Conference and Exhibition, Calgary, Alberta, September 12-15, 2011. http://www.searchanddiscovery.com/documents/2011/80132gilman/ndx_gilman.pdf

Green, C.A., Styles, P. & Baptie, B.J. 2012. Preese Hall shale gas fracturing: review and recommendations for induced seismic mitigation. Report for DECC. www.decc.gov.uk/assets/decc/11/meeting-energy-demand/oil-gas/5055-preese-hall-shale-gas-fracturing-review-and-recomm.pdf

Gutteridge, P. 1991. Aspects of Dinantian sedimentation in the Edale Basin, North Derbyshire. *Geological Journal* 26: 245-269.

Hodge, T. 2003. The Saltfleetby Field, Block L 47/16, Licence PEDL 005, Onshore UK. Gluyas, J.G. & Hichens, H.M. (eds) *United Kingdom Oil and Gas Fields, Commemorative Millennium Volume*. Geological Society, London, Memoir 20: 911-919.

Hudson, R.G.S. 1933. The scenery and geology of North-West Yorkshire. *Proceedings of the Geologists' Association* 44: 228-255.

Hudson, R.G.S. 1944. The Carboniferous of the Broughton Anticline, Yorkshire. *Proceedings of the Yorkshire Geological Society* 25: 190-214.

iGas. 2012 Results presentation and shale update. Online presentation. www.igasplc.com/uploads/analystpresentationjune2012final.pdf

International Energy Agency (IEA). 2011. *Are we entering the Golden Age of Gas?* World Energy Outlook Special Report. www.worldenergyoutlook.org/media/weowebsite/2011/WEO2011_GoldenAgeofGasReport.pdf

International Energy Agency (IEA). 2012. *Golden Rules for a Golden Age of Gas*. World Energy Outlook Special Report on Unconventional Gas. www.worldenergyoutlook.org/goldenrules/.

Jackson, D.I., Jackson, A.A., Evans, D., Wingfield, R.T.R, Barnes, R.P. & Arthur, M.J. 1995. *United Kingdom offshore regional report: the geology of the Irish Sea*. HMSO for BGS, London.

Jarvie, D. M. 2008. Geochemical comparison of shale-resource systems. Insight Shale Gas Summit, Dallas, Texas, 6-7 May 2008. http://wwgeochem.com/resources/Final+Jarvie+-+Insight+Dallas+May+2008.pdf

Jarvie, D. M., 2012. Shale resource systems for oil and gas: Part 1—Shale-gas resource systems, in J. A. Breyer (ed.). *Shale reservoirs—Giant resources for the 21st century*. *AAPG Memoir* 97: 69–87.

Jarvie, D.M., Burgess, J.D., Morelos, A., Mariotti, P.A. & Lindsey, R. 2001, Permian Basin petroleum systems investigations; inferences from oil geochemistry and source rocks. *AAPG Bulletin* 85(9): 1693-1694.

Jarvie, D. M., Hill, R. J. & Pollastro, R. M. 2005. Assessment of the gas potential and yields from shales: the Barnett Shale model. In: Cardott, B. J. (Ed.) *Unconventional energy resources in the southern Midcontinent, 2004 Symposium*. Oklahoma Geological Survey Circular 110: 37-50. http://wwgeochem.com/resources/Jarvie+et+al.+2005+OGS+Circ.+110+Barnett+paper.pdf

Kent, P.E. 1966. The structure of the concealed Carboniferous rocks of north-east England. *Proceedings of the Yorkshire Geological Society* 35(3): 323-352.

Kirby, G.A., Baily, H.E., Chadwick, R.A., Evans, D.J., Holliday, D.W., Holloway, S., Hulbert, A.G., Pharaoh, T.C., Smith, N.J.P., Aitkenhead, N. & Birch, B. 2000. The structure and evolution of the Craven Basin and adjacent areas. *Subsurface Memoir of the British Geological Survey*.

Könitzer, S.F., Davies S.J., Stephenson, M.H., Leng, M.J., Gabbott, S.E., Angiolini, L., Macquaker, J.H.S., Vane, C.H., Millward, D. & Kane, I.A. 2011. Primary Controls on Organic Carbon Content in UK Upper Mississippian Gas Shales. Adapted from ePoster presentation at AAPG Annual Convention and Exhibition, Houston, Texas, USA, April 10-13, 2011. www.searchanddiscovery.com/documents/2011/80175konitzer/ndx_konitzer.pdf

Langford, F.F. & Blanc-Valleron, M.M. 1990. Interpreting Rock-Eval pyrolysis data using graphs of pyrolizable hydrocarbons vs. total organic carbon. *AAPG Bulletin* 74(6): 799-804.

Lawrence, S.R., Coster, P.W. & Ireland, R.J. 1987. Structural development and petroleum potential of the northern flanks of the Bowland Basin (Carboniferous), North-west England. In: Brooks, J. & Glennie, K. (eds). *Petroleum Geology of North West Europe*. Graham & Trotman. 225-233.

Lee, M.K., Pharaoh, T.C. & Green, C.A. 1991. Structural trends in the concealed basement of eastern England from images of regional potential field data. *Annales de la Société Géologique de Belgique* 114: 45-62.

Leeder, M.R. 1982. Upper Palaeozoic basins of the British Isles: Caledonide inheritance versus Hercynian plate margin processes. *Journal of the Geological Society of London* 139: 481–494.

Leeder, M.R. 1988. Recent developments in Carboniferous geology: a critical review with implications for the British Isles and NW Europe. *Proceedings of the Geologists' Association* 99: 73–100.

Lewis, R., Ingraham, D., Pearcy, M., Williamson, J., Sawyer, W. & Frantz, J. 2004. New evaluation techniques for gas shale reservoirs. Reservoir Symposium 2004. www.sipeshouston.com/presentations/pickens%20shale%20gas.pdf

Magraw, D. & Ramsbottom, W.H.C. 1957. A deep borehole for oil at Croxteth Park, near Liverpool. *Geological Journal* 1(6): 512-535.

Maynard, J.R., Wignall, P.B. & Varker, W.J. 1991. A 'hot' new shale facies from the Upper Carboniferous of Northern England. *Journal of the Geological Society* 148: 805-808.

McCarthy, K., Rojas, K., Palmowski, D., Peters, K. & Stankiewicz, A. 2011. Basic petroleum geochemistry for source rock evaluation. *Oilfield Review* 23(2): 32-43. www.slb.com/resources/publications/industry_articles/oilfield_review/2011/or2011sum03_basic_petroleum.aspx

Mikkelsen, P.W. & Floodpage, J.B. 1997. The hydrocarbon potential of the Cheshire Basin. In: Meadows, N.S., Trueblood, S.E, Hardman, M. & Cowan, G. (eds) Petroleum Geology of the Irish Sea and Adjacent Areas. *Geological Society Special Publication* 124: 161-183.

National Petroleum Council, 1980. *Unconventional Gas Sources, Volume III – Devonian Shale*. National Petroleum Council, Washington, DC.

Pearson, I.L.G., Zeniewski, P., Gracceva, F., Zastera, P., McGlade, C., Sorrell, S., Spiers, J. & Thonhauser, G. 2012. *Unconventional gas: potential energy market impacts in the European Union*. A report by the Energy Security Unit of the European Commission's Joint Research Centre. ec.europa.eu/dgs/jrc/downloads/jrc_report_2012_09_unconventional_gas.pdf

Pearson, M.J. & Russell, M.A. 2000. Subsidence and erosion in the Pennine Carboniferous Basin, England; lithological and thermal constraints on maturity modelling. *Journal of the Geological Society* 157: 471-482.

Penn, I.E. 1987. Geophysical logs in the stratigraphy of Wales and adjacent offshore and onshore areas. *Proceedings of the Geologists' Association* 98(4): 275-313.

Petra-Chem 1983a. Geochemical evaluation of Carboniferous sediments from five boreholes: Duffield, Wardlow Mires No 2, Knutsford No 1, Holme Chapel No 1 and Knott Copy drilled in Derbyshire, Cheshire, Lancashire and Yorkshire. Unpublished report.

Petra-Chem 1983b. Geochemical evaluation of potential source rocks of Carboniferous age from the Clitheroe district of Lancashire & Yorkshire. Unpublished report.

Petra-Chem 1983c. Geochemical evaluation of potential source rocks of Carboniferous age from Derbyshire. Unpublished report.

Pharaoh, T.C., Vincent, C., Bentham, M.S., Hulbert, A.G., Waters, C.N. & Smith, N.J.P. 2011. Structure and evolution of the East Midlands region of the Pennine Basin. *Subsurface Memoir of the British Geological Survey*.

POSTbox (Parliamentary Office of Science and Technology) 2013. *UK Shale Gas Potential: Shale Gas Resource and Reserve Estimates.*

Riley, N.J. 1994. Lithological log of core 1, Fina plc, Long Eaton 1 Bh. *BGS Technical Report* WH/94/247C.

Riley, N.J. 1997. Foraminiferal biostratigraphy of the Carboniferous interval in Fina Long Eaton 1 Bh. *BGS Technical Report* WH/97/46C.

Riley, N.J. 1990. Stratigraphy of the Worston Shale Group (Dinantian), Craven Basin, north-west England. *Proceedings of the Yorkshire Geological Society* 48(2): 163-187.

Robertson Research International Limited (RRI). 1987. *The Carboniferous of Northern England and Adjacent Areas: petroleum geochemistry and geology*. Report Number EM019, Volume 3.

Roche, I. 2012. Lessons from history – unlocking a new UK shale oil play. Paper presented at the SPE/EAGE European Unconventional Resources Conference and Exhibition, Vienna, March 2012.

Schmoker, J.W. 1980. Defining organic-rich facies in the Devonian shale in the western part of the Appalachian Basin. US Department of the Interior Geological Survey Open-File Report 80-707. http://pubs.usgs.gov/of/1980/0707/report.pdf

Selley, R.C. 1987. British shale gas potential scrutinized. *Oil & Gas Journal*. 15th June 1987: 62-64.

Selley, R.C. 1996. *Elements of Petroleum Geology*. 2nd Edition. Academic Press. [pp. 434-438]

Selley, R.C. 2005. UK shale-gas resources. In: Doré, A.G. & Vining, B.A. (eds.) Petroleum Geology: North-West Europe and Global Perspectives – Proceedings of the 6th Petroleum Geology Conference. Geological Society. London. 707-714.

Selley, R.C. 2011. Shale gas: blessing or curse? *Geoscientist* 21(4): 14-19.

Selley, R.C. 2012. UK shale gas: the story so far. *Marine and Petroleum Geology* 31: 100-109.

Smith, E.G., Rhys, G.H. & Eden, R.A. 1967. Geology of the country around Chesterfield, Matlock and Mansfield. *Memoir of the British Geological Survey*, Sheet 112 (England and Wales).

Smith, K., Smith, N.J.P. & Holliday, D.W. 1985. The deep structure of Derbyshire. *Geological Journal* 20: 215-225.

Smith, N., Turner, P. & Williams, G. 2010. UK data and analysis for shale gas prospectivity. In: Vining, B.A. & Pickering, S.C. (eds) *Petroleum Geology: From Mature Basins to New Frontiers – Proceedings of the 7th Petroleum Geology Conference*, 1087–1098.

Smith, N.J.P., Kirby, G.A. & Pharaoh, T.C. 2005. Structure and evolution of the south-west Pennine Basin and adjacent area. *Subsurface Memoir of the British Geological Survey*.

Society of Petroleum Engineers 2007. Petroleum Resources Management System. http:/www.spe.org/industry/docs/Petroleum_Resources_Management_System_2007.pdf

Spathopoulos, F. & Sephton, M. 2012. Benchmarking the reservoir characteristics of the UK black shale as targets for unconventional production – analysis and comparison with US and European Analogues. UK Shale Summit, London, 26-27 September 2012.

Spears, D.A. & Amin, M.A. 1981. Geochemistry and mineralogy of marine and non-marine Namurian black shales from the Tansley borehole. *Sedimentology* 28: 407-417.

Stevenson, I.P. & Gaunt, G.D. 1971. Geology of the country around Chapel en le Frith. *Memoir of the British Geological Survey*, Sheet 99 (England and Wales).

Tissot, B., Durand, B., Espitalié, J. & Combaz, A. 1974. Influence of nature and diagenesis of organic matter in formation of petroleum. *AAPG Bulletin* 58(3): 499-506.

TNO. 2009. *Inventory non-conventional gas*. TNO-034-UT-2009-00774/B.

Transform Software and Services, Inc. 2012. A Comparative Study of North America's Largest Shale Gas Reservoirs. Online report http://www.transformsw.com/papers-and-presentations/studies.html

U.S. Energy Information Administration (USEIA). 2011a. *World Shale Gas Resources: an initial assessment of 14 regions outside the United States*. Report prepared by Advanced Resources International Inc. www.eia.gov/analysis/studies/worldshalegas/.

U.S. Energy Information Administration (USEIA). 2011b. *Review of Emerging Resources: U.S. shale gas and shale oil plays*. Report prepared by INTEK. ftp://ftp.eia.doe.gov/natgas/usshaleplays.pdf.

Waters, C.N., Waters, R.A., Barclay, W.J. & Davies, J.R. 2009. A lithostratigraphical framework for the Carboniferous successions of southern Great Britain (onshore). *British Geological Survey Research Report* RR/09/01.

Waters, C.N., Somerville, I.D., Jones, N.S. & 16 others. 2011. *A Revised Correlation of Carboniferous Rocks in the British Isles*. Geological Society Special Report No. 26, London.

Wilson, A.A., Brandon, A. & Johnson, E.W. 1985. Abbeystead: geological context of the Wyresdale Tunnel Methane Explosion. *British Geological Survey Technical Report* WA/89/30.

Appendix A: Estimation of the total in-place gas resource in the Bowland-Hodder shales, central Britain

Aim

The aim of this study is to estimate the P10-P50-P90[1] range of **total gas-in-place volumes** for the upper and lower Bowland-Hodder (Early Carboniferous) shale units across the Pennine Basin of central Britain.

This analysis forms the appendix to the main Bowland-Hodder report, which provides the detailed geological background to this shale gas play. This specific study applies a Monte Carlo simulation to a suite of input parameters, some of which come from the geology-based methodology described in the main report, and others which are based on information from published analogues.

Introduction

The total gas content of a shale is made up of two main components:

Free gas – the gas contained in pore spaces; this volume is very pressure dependent, and pressure is related to depth (assuming no overpressure).

Adsorbed gas – the gas which is adsorbed in the organic matter in the shale. The quantity of gas adsorbed is dependent on the quantity, type and distribution of the organic content within the shale, it is largely pressure independent.

In the USA shale gas plays, the ratio of adsorbed gas to free gas varies from 60:40 to 10:90 (Jarvie 2012).

Equations[2]

Free gas at standard conditions is calculated using the equation:

$GIIP_f = A * h * \phi * Bg$

Where A = area
h = thickness
ϕ = gas-filled porosity
B_g = gas expansion factor (depth dependant)

[1] P10, P50 and P90 correspond to the 10%, 50% or 90% probability of more than that amount being present. In the case of P10, there is a 10% probability that the actual result will be higher, or a 90% chance the result will be lower.

[2] In this project, metric units have been used throughout the calculation stages, with the conversion to imperial units only given for the presentation of the output (Table 3b and Figures 1 and 2).

Adsorbed gas is calculated using the equation:

$GIIP_a = A * h * \rho * G$

Where A = area
h = thickness
ρ = rock density
G = adsorbed gas content of shale (volume of gas/weight of shale)

Where experimental analysis of core samples is available, the Langmuir equation is used to calculate G:

$$G = \frac{G_l * P}{P_l + P}$$

Where G_l = Langmuir volume [volume of adsorbed gas at infinite pressure]
P_l = Langmuir pressure [pressure where one-half of the gas at infinite pressure has been desorbed]
P = Reservoir pressure

Total gas in place (GIIP) (at standard conditions) **= Free gas ($GIIP_f$) + Adsorbed gas ($GIIP_a$)**

Values used

Free gas

The controlling factors for free gas are **area**, **thickness**, *gas-filled porosity* and **depth** (and overpressure, if present). Those factors that are estimated in this study are shown in bold; those that rely on analogues are shown in italics.

Rather than inputting parameters for area and thickness separately, a figure for net shale volume has been used. This is the volume of organic-rich shale (TOC>2%) which is considered mature for gas generation (R_o>1.1). The explanation of how this volume was derived can be found in Section 3.9 of the main report. Error bars of ± 15% have been used to take into account uncertainties in the seismic mapping.

Specific information on the gas-filled porosities of UK shales is not available. Reported gas-filled porosities for US gas shales are in the range 1-5% (Curtis 2002) and 2.9-6% (Jarvie 2012) (Table 1). Lewis *et al.* (2004) quotes a figure of 4-6% porosity for gas shales. For an undeveloped play in the Netherlands, TNO (2009) used the Curtis (2002) figures of 1-5% gas-filled porosity. These conservative figures are used in this analysis: a log-normal distribution with a mean of 3% porosity with a two standard-deviation variation and cut-offs at 0.5% and 10%.

The gas expansion factor (B_g) converts the volume of free gas under reservoir conditions into a volume under atmospheric conditions using the formula:

B_g = depth (m) /10.7

It is not known whether the UK shales are overpressured, and hydrostatic pressure has been assumed. Any overpressure would increase the quantity of free gas stored in the pore spaces. Shale gas accumulations in the USA are commonly overpressured.

Adsorbed gas

The controlling factors are **area**, **thickness**, **shale density** and *adsorbed gas content of shale*. Those factors that are estimated in this study are shown in bold; those that rely on analogues are shown in italics.

Langmuir volumes can be obtained experimentally from core samples, but none have been published for shales in the UK. Published values of adsorbed gas contents of shales in the USA are as follows:

Source	Basin/area	Gas-filled porosity (%)	Total gas content (scf/ton)	Adsorbed gas (%)	Adsorbed gas content (scf/ton)	Adsorbed gas content (m^3/ton)
Curtis (2002)	Antrim	4	40 - 100	70	28 - 70	0.8 - 2.0
Curtis (2002)	Ohio	2	60 - 100	50	30 - 50	0.8 - 1.4
Curtis (2002)	New Albany	5	40 - 80	40 - 60	16 - 32	0.5 - 0.9
Curtis (2002)	Barnett	2.5	300 - 350	20	60 - 70	1.7 - 2.0
Curtis (2002)	Lewis	1 - 3.5	15 - 45	60 - 85	9 - 27	0.3 - 0.8
Jarvie (2012)	Marcellus	4	60 - 150	45	27 - 67.5	0.8 - 1.9
Jarvie (2012)	Haynesville	6	100 - 330	25	25 - 82.5	0.7 - 2.3
Jarvie (2012)	Bossier	4	50 - 150	55	27.5 - 82.5	0.8 - 2.3
Jarvie (2012)	Barnett	5	300 - 350	55	165 - 192.5	4.7 - 5.5
Jarvie (2012)	Fayetteville	4.5	60 - 220	50 - 70	30 - 110	0.8 - 3.1
Jarvie (2012)	Muskwa	4	90 - 110	20	18 - 22	0.5 - 0.6
Jarvie (2012)	Woodford	3	200 - 300	60	120 - 180	3.4 - 5.1
Jarvie (2012)	Eagle Ford	4.5	200 - 220	25	50 - 55	1.4 - 1.6
Jarvie (2012)	Utica	2.9	70	60	42	1.2
Jarvie (2012)	Montney	3.5	300	10	30	0.8

Table 1. Summary of parameters for various shales in the USA that are relevant to gas resource calculations in this study (from Curtis 2002, Jarvie 2012).

For the modelling undertaken in this report, a fairly conservative range of adsorbed gas contents of 0.5 to 2.0 m^3/ton (18-71 scf/ton) has been taken. There is a linear relationship between gas contents and TOC values, and the use of a lower gas content value relative to the US examples (which tend to have a slightly higher TOC) is reasonable. See Section 3.8 of the main report for a discussion on UK TOC values.

Published shale densities are in the range 2.4-2.8 g/cm³. This study has used 2.55 – 2.6 – 2.65 g/cm³ as a range of values for calcareous shale. This is supported by downhole geophysical well logs in the study area.

Monte Carlo input parameters

For free gas-in-place ($GIIP_f$)

	Net mature shale volume (m^3)			Median depth (m)			Gas-filled porosity (%)		
	cut-off	ml	cut-off	min	ml	max	cut-off	mean	cut-off
Upper unit	7.90E+11	9.31E+11	1.15E+12	1800	2100	2400	0.5	3	10
Lower unit	2.90E+12	3.45E+12	3.97E+12	2100	2400	2700	0.5	3	10

For adsorbed gas-in-place ($GIIP_a$)

	Net mature shale volume (m^3)			Density (g/cm^3)			Adsorbed gas content (m^3/t)	
	cut-off	ml	cut-off	min	ml	max	min	max
Upper unit	7.90E+11	9.31E+11	1.15E+12	2.55	2.6	2.65	0.5	2
Lower unit	2.90E+12	3.45E+12	3.97E+12	2.55	2.6	2.65	0.5	2

Table 2. Input parameters for the Monte Carlo simulation used to determine the total gas content and total gas in place in the upper and lower parts of the Bowland-Hodder unit, central Britain.

Monte Carlo results

(a) Metric	Total gas content estimates (m^3/m^3)			Total gas in-place estimates (tcm)		
	Low (P90)	Central (P50)	High (P10)	Low (P90)	Central (P50)	High (P10)
Upper unit	3.9	7.9	14.8	4.6	7.5	12.7
Lower unit	4.2	8.7	16.3	18.6	30.2	51.9

(b) Imperial	Total gas content estimates (bcf/mile²m)			Total gas in-place estimates (tcf)		
	Low (P90)	Central (P50)	High (P10)	Low (P90)	Central (P50)	High (P10)
Upper unit	0.36	0.73	1.35	164	264	447
Lower unit	0.39	0.79	1.49	658	1065	1834

Table 3. Results of a Monte Carlo simulation (500,000 iterations) to determine the total gas content and total in-place gas resource in the upper and lower parts of the Bowland-Hodder unit, central Britain. The results are given in (a) metric and (b) imperial units.

Note that USEIA (2001a) used a figure of 48 bcf/mile² with a thickness of 148 ft (45.1 m), which gives an equivalent value of 1.06 bcf/mile²m.

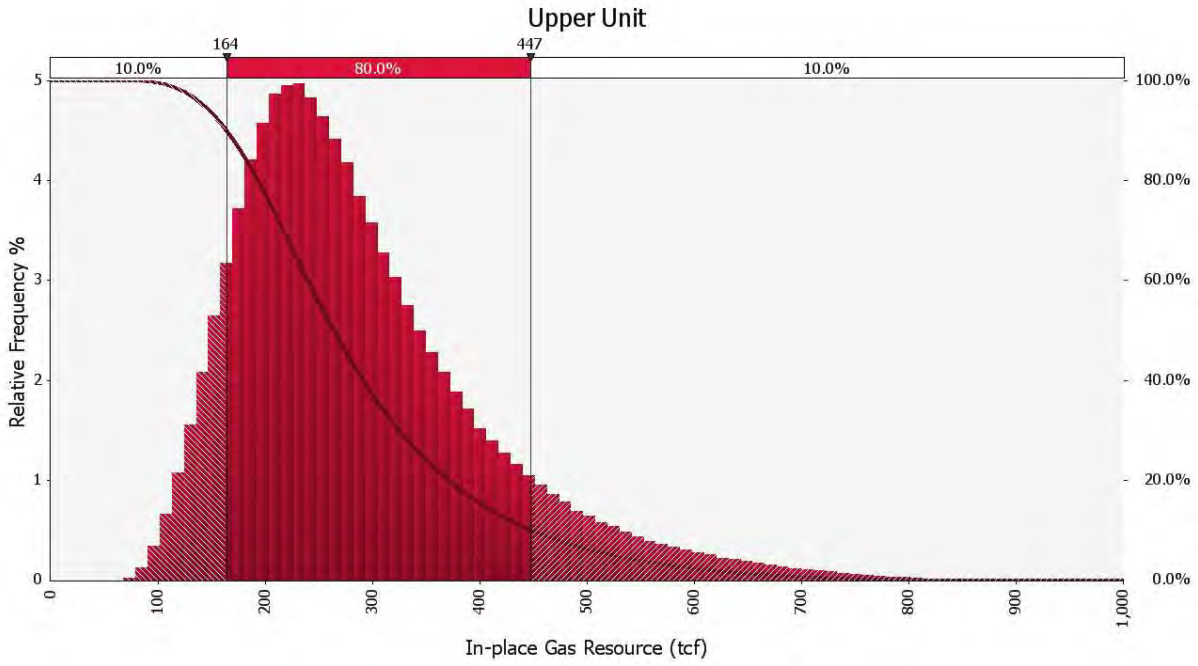

Figure 1. Probabilistic distribution and cumulative probability curve representing the result of a Monte Carlo analysis for the in-place resource estimation of shale gas in the upper Bowland-Hodder unit.

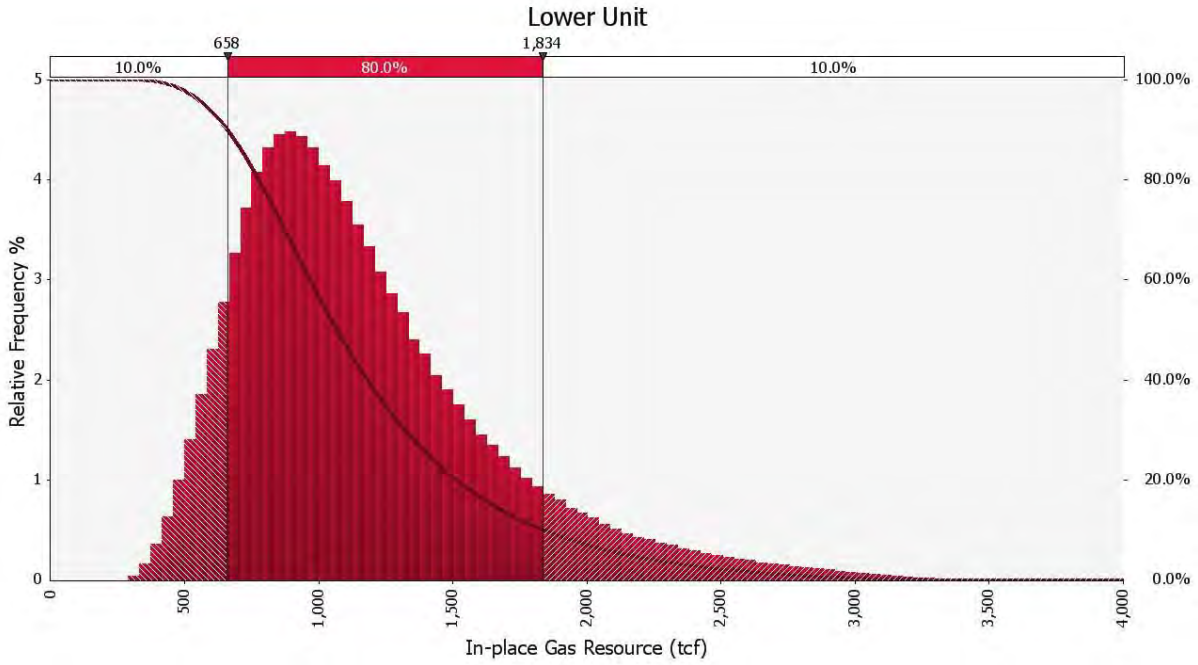

Figure 2. Probabilistic distribution and cumulative probability curve representing the result of a Monte Carlo analysis for the in-place resource estimation of shale gas in the lower Bowland-Hodder unit.

Key variables and their effect on the estimated gas volume

Variable	Uncertainty
Gross rock volume/3D geological model	The 2D seismic data interpreted in the study area is of variable quality, and is generally poor to moderate. A two-standard-deviation variation has been used on the gross rock volume, but it could be greater, resulting in a wider range of estimated gas volumes.
Definition of prospective shale	The definition of net prospective shale used in this report could be optimistic; it includes a wide variety of shales and not just those with the highest gamma-log response (and hence highest TOC). This definition is influenced by the fact that the most suitable shales for current extraction techniques are not necessarily those with the highest TOC. Any approach which is more pessimistic would have the greatest effect on the *lower* Bowland-Hodder unit volumes.
Definition of gas maturity	The use of R_o > 1.1% as the top of the gas window is possibly optimistic. It could be 1.4% which would reduce the estimated gas volume.
Shallow depth cut-off	The use of 5000 ft is based on USGS global screening criteria. If this were deeper, this would reduce the estimated gas volume.
Gas-filled porosity of the shale	The use of a mean of 3% is a conservative estimate. It could be greater, which would increase the estimated gas volume. The large range of values has a significant effect on the calculated in-place gas figure (see Figures 3 & 4).
Reservoir pressure	The assumption that the shales are at hydrostatic pressure is conservative. Any amount of overpressure would increase the estimated gas volume.
Adsorbed gas content	The use of 0.5-2.0 m^3/ton is lower than some US analogues. Any increase in this range of values would increase the estimated gas volume.
Bulk density	The average density of 2.6 g/cm^3 is a robust estimate. If the density is higher this will increase the estimated gas volume (and vice versa).

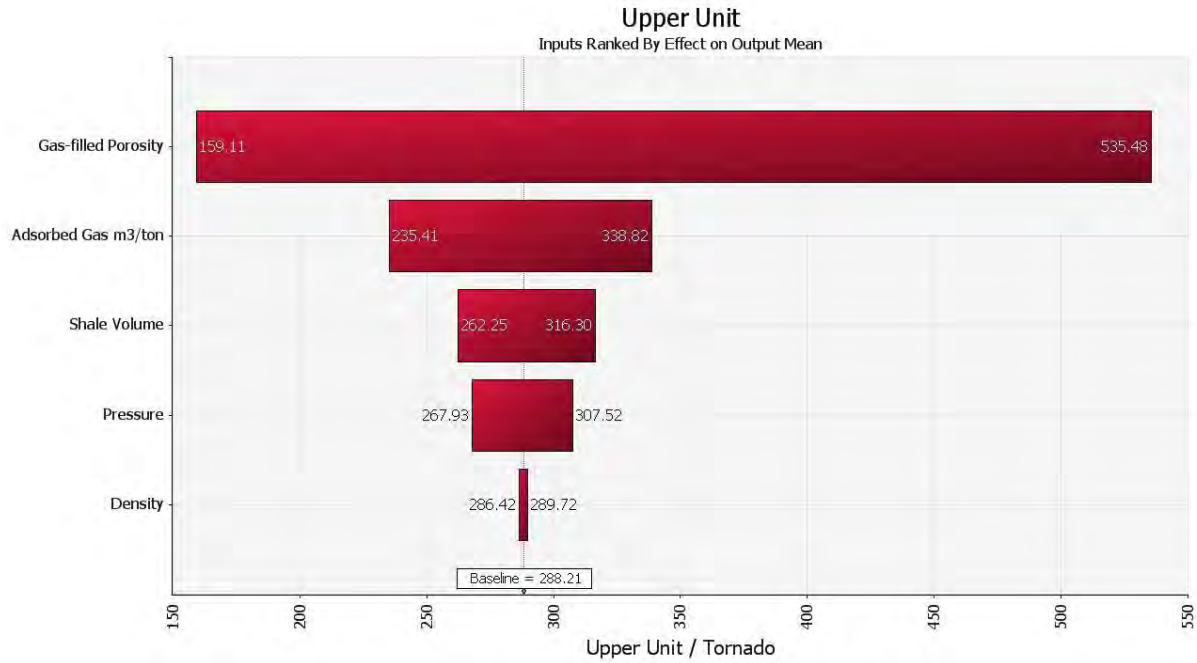

Figure 3. Tornado diagram representing the result of a Monte Carlo analysis for the in-place resource estimation of shale gas in the lower Bowland-Hodder unit.

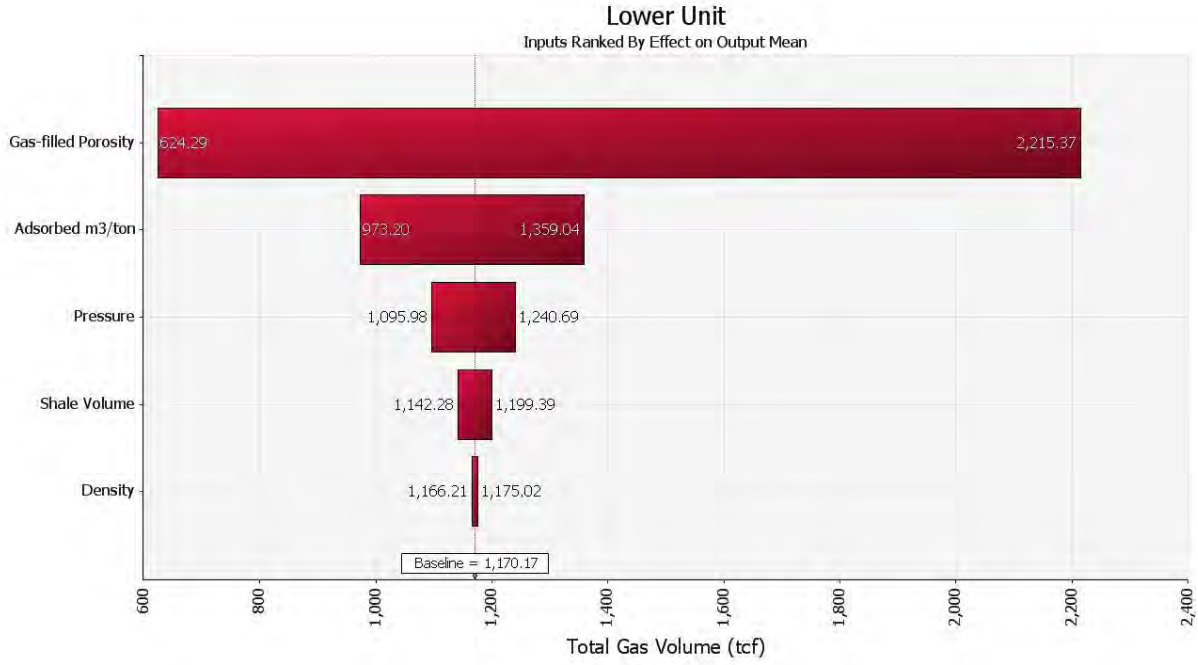

Figure 4. Tornado diagram representing the result of a Monte Carlo analysis for the in-place resource estimation of shale gas in the lower Bowland-Hodder unit.

Conclusion

This study estimates that the **total in-place gas resource** for the Bowland-Hodder (Carboniferous) shales across northern England is 822 – 1329 – 2281 tcf (23.3 – 37.6 – 64.6 tcm) (P90 – P50 – P10). It should be emphasised that this figure is an in-place resource estimate. The amount that could be recovered depends on factors outwith the scope of this report, and could very likely be a small percentage.

References

Curtis, J. B., 2002. Fractured shale gas systems: *AAPG Bulletin* 86(11): 1921–1938.

Jarvie, D. M., 2012. Shale resource systems for oil and gas: Part 1—Shale-gas resource systems, in J. A. Breyer (ed.). *Shale reservoirs—Giant resources for the 21st century*. *AAPG Memoir* 97: 69–87.

Lewis, R., Ingraham, D., Pearcy, M., Williamson, J., Sawyer, W. & Frantz, J. 2004. New evaluation techniques for gas shale reservoirs. Reservoir Symposium 2004. www.sipeshouston.com/presentations/pickens%20shale%20gas.pdf

TNO. 2009. *Inventory non-conventional gas*. TNO-034-UT-2009-00774/B.

BGR. 2012 Abschätzung des Erdgaspotenzials aus dichten Tongesteinen (Schiefergas) in Deutschland. http://www.bgr.bund.de/DE/Themen/Energie/Downloads/BGR_Schiefergaspotenzial_in_Deutschland_2012.pdf

I.J. Andrews, M.J. Sankey, A.L. Harvey & M. McCormac

Appendix B: Rock-Eval geochemical analysis of 109 samples from the Carboniferous of the Pennine Basin, including the Bowland-Hodder unit

Introduction

One hundred and nine core samples were collected from 16 selected wells within the Carboniferous Pennine Basin of central Britain (Figure 1, Table 1) and analysed using the BGS Rock-Eval machine. The spreadsheet of data derived from the Rock-Eval analysis (Appendix 1) records depths and the main parameters measured - S_1 (free hydrocarbons), S_2 (bound hydrocarbons), T_{max} (the temperature at which S_2 peaked), S_3 (carbon dioxide) and the total organic carbon (TOC).

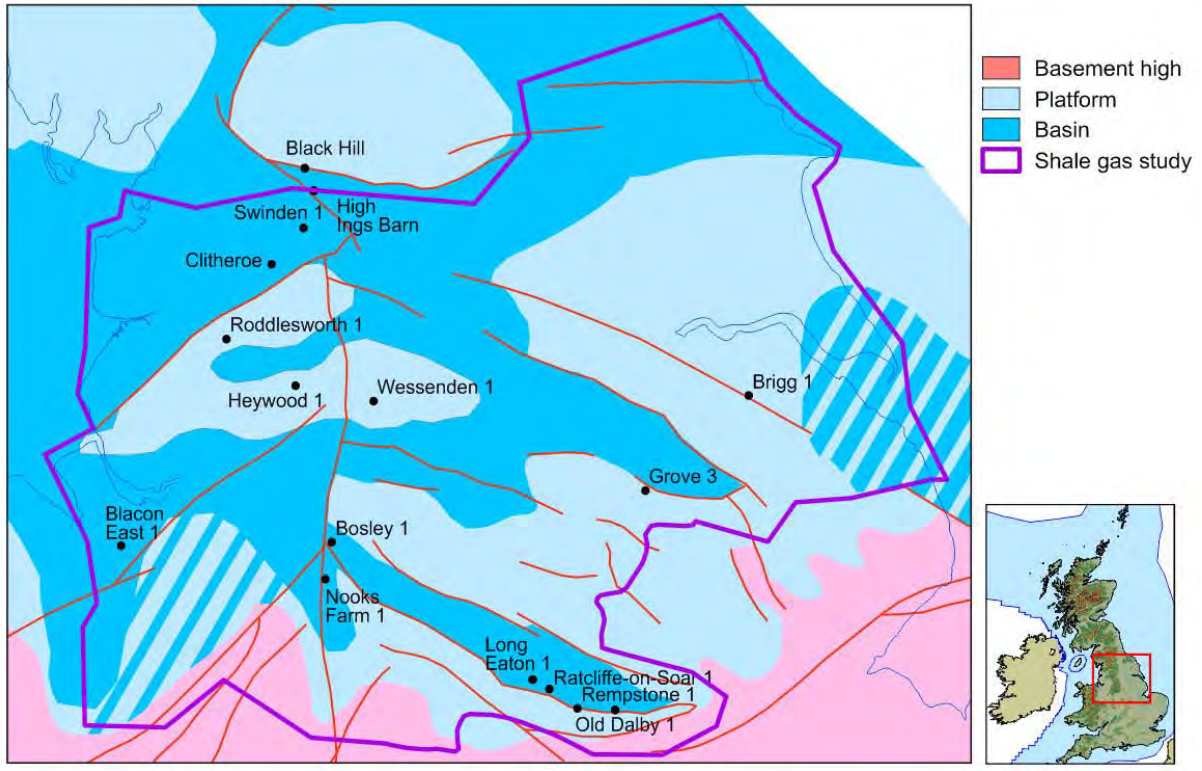

Figure 1. Map of central Britain showing the Early Carboniferous basins and the locations of the 16 sampled wells.

Well name	top sample (ft)	bottom sample (ft)	Chronostratigraphy	Lithostratigraphy	Unit (this report)
Black Hill	218.2	246.1	Namurian (Marsdenian?)	Millstone Grit	Millstone Grit
Blacon East 1	6122.0	6147.6	Visean (Brigantian)	Bowland Shale Fm	Upper BHU
	7423.0	7432.6	Visean (?Asbian)	Clwyd Limestone Group	?shelf limestone
Bosley 1	6568.9	6582.7	Chadian		Lower BHU?
Brigg 1	6328.4	6336.9	Visean	Carboniferous limestone	shelf limestone
Clitheroe	403.2	761.8	Visean	Hodder Mudstone	Lower BHU
Grove 3	7564.6	7594.0	Visean (Chadian)	Carboniferous limestone	shelf limestone
Heywood 1	5249.2	5260.2	Visean (Asbian-Brigantian)	Carboniferous limestone	shelf limestone
High Ings Barn	313.3	719.5	Visean	Carboniferous limestone	shelf limestone
Long Eaton 1	5871.0	5901.0	Visean (Arundian-Holkerian)	Long Eaton Fm	Lower BHU
Nooks Farm 1A	1401.0	1531.0	Visean (Asbian-Brigantian)	Onecote Sandstone	Lower BHU
Old Dalby 1	4562.3	4773.6	Visean (Asbian-Brigantian)	Widmerpool Fm	Lower BHU
Ratcliffe-on-Soar 1	891.4	949.8	Namurian (Arnsbergian)	Rempstone Fm	Millstone Grit
Rempstone 1	2181.8	2191.6	Namurian (Arnsbergian)	Upper Bowland Shale	Upper BHU
Roddlesworth 1	4226.0	4281.0	Visean (Asbian-Brigantian)	Carboniferous limestone	shelf limestone
Swinden 1	98.4	2065.3	Tournasian (Courceyan)	Carboniferous limestone	shelf limestone
Wessenden 1	3505.0	3513.0	Tournasian (Courceyan)	Carboniferous limestone	shelf limestone

Table 1. Wells analysed in this study, together with stratigraphic information. BHU = Bowland-Hodder unit, as used in the main shale gas assessment report.

In addition, the principal useful parameters derived from the data include Production Index (PI), present-day Hydrogen Index (HI_{pd}) and Oxygen Index (OI). PI is the sum of the S_1 and S_2 hydrocarbons. HI_{pd} is derived by the ratio of S_2 mg HC per gram of organic carbon and values above 350 are generally rated to be good source rocks (for conventional hydrocarbons, Tissot & Welte 1978, Fig. V.1.11). OI is the ratio of mg carbon dioxide per g organic carbon. HI and OI are plotted to be comparable with the van Krevelen diagram, showing the branching of the different kerogen types I (lacustrine, algal, oil prone), II (marine, oil prone), III (terrestrial, gas prone) and IV (oxidised or inertinite). From the work of Jarvie, in particular, it seems that these types cannot be fixed on such diagrams because there is a progressive change with increasing maturity (Jarvie *et al.* 2005). The immature Barnett Shale is Type II kerogen which has been converted to plot in the Type III field within the gas window fairway (Jarvie *et al.* 2005). Kerogen, of any type, once deeply buried or heated becomes gas prone and this explains the difference between conventional and unconventional plays. Carbon and hydrogen are lost during hydrocarbon generation. Gas is present in the source rock at lower maturities (R_o = 1.1% in the Newark East shale gas field (Texas), Smith *et al.* 2011) than in conventional gas fields (gas window R_o >1.3%) because it has not migrated. Overmaturity is a well-worn phrase in conventional exploration, effectively writing off some areas which deserve to be re-evaluated for unconventional hydrocarbons.

Total organic carbon (TOC)

Of the 16 wells, notably the Grove 3 and Brigg 1 samples were visually very light coloured, because they were from conventional reservoirs and give low TOC values (Figure 2). Samples from the other 14 wells had the appearance of dark grey and black shales containing probable organic matter. Rempstone 1, Ratcliffe-on-Soar 1 and Old Dalby 1, located in the Widmerpool Gulf, the southern sub-basin within the Pennine Basin, all had fairly consistent characters including consistently high TOC (Figure 2).

The Barnett Shale at crop has very high TOC (13.08%, Jarvie *et al.* 2005). During maturation organic matter is inevitably destroyed (Jarvie 2008). Jarvie *et al.* (2005) reported that 'artificially maturing' immature samples from one well reduced TOC by approximately 36% from its original value, whereas at peak oil maturity this had only been reduced by 18%. This could explain why the three Widmerpool Gulf wells had the highest TOC values and are immature (Figure 2).

Comparing the Pennine Basin samples with the Barnett Shale makes it clear that the former are slightly leaner (Figure 5).

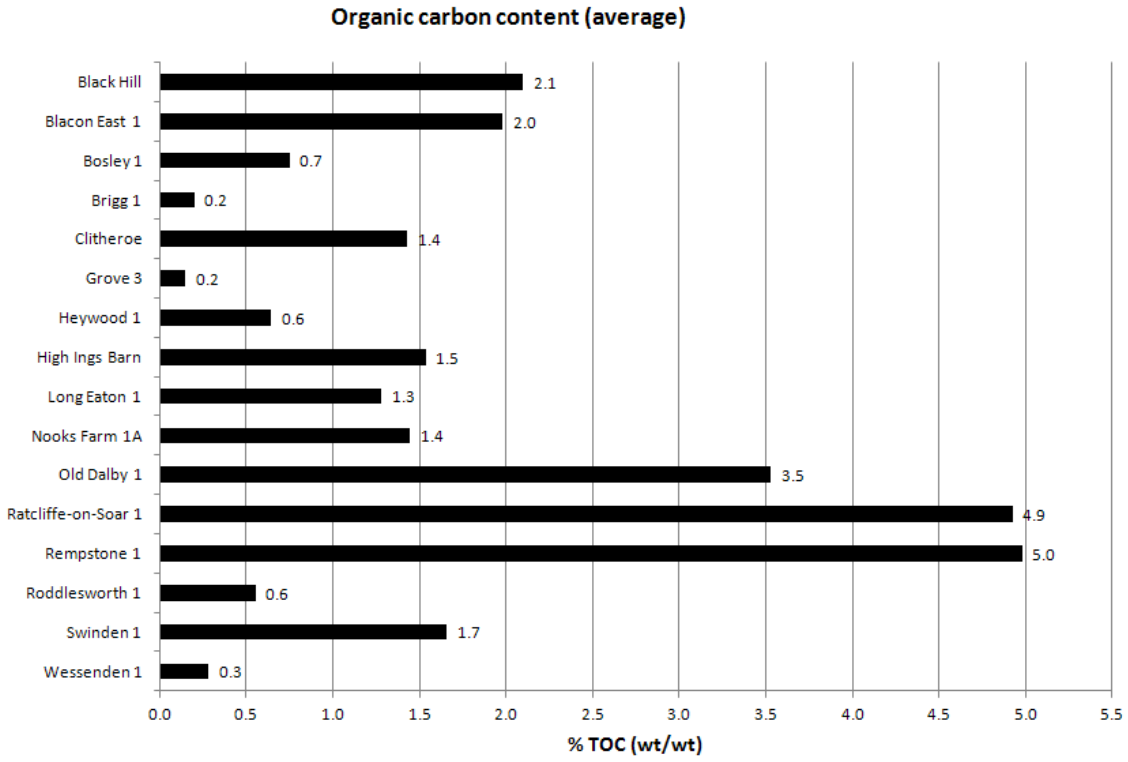

Figure 2. Average total organic carbon content of samples from the 16 selected wells.

Kerogen type

Kerogen types are identified by plotting on a modified van Krevelen diagram (Figure 3). Typical Type I (algal, lacustrine Green River Shale), Type II (oil prone Toarcian of Paris Basin) and Type III (gas prone Tertiary of Greenland) have been included. Some publications show the Type III curve emerging at about HI=100 (*e.g.* Tissot & Welte 1978, fig. V.1.12), nearer to the Greenland example (Figure 3, blue cross), which would seem preferable, so that the Paris Basin example plots in the Type II field. Some other publications have a Type IV kerogen (also near to HI=0) (Boyer *et al.* 2006). Type IV kerogens may have lost all generative potential at an early stage, perhaps as a result of oxidation or combustion.

Roche (2012, Fig. 7) showed Thistleton 1 samples as being Type III kerogens, mostly in the oil window, whereas Bowland outcrop samples plotted at immature or early oil window as Type II kerogens.

However, many Barnett Shale samples also plot near the base of modified van Krevelen diagrams and are considered to have been originally Type II kerogens, based on Barnett low maturity outcrops in the southern margin of the Fort Worth Basin *e.g.* at Lampasas (Jarvie *et al.* 2005). The samples in deeper parts of the basin are interpreted to have 'matured' to positions with very low HI (Figure 3). Similarly, the DECC samples differentiate into Widmerpool Gulf well samples, which plot in the Type II field, and the Craven Basin well samples that plot near the base of the graph. One interpretation is that they may have originated as the same Type II kerogens, but 'migrated' to the base of this diagram as they matured.

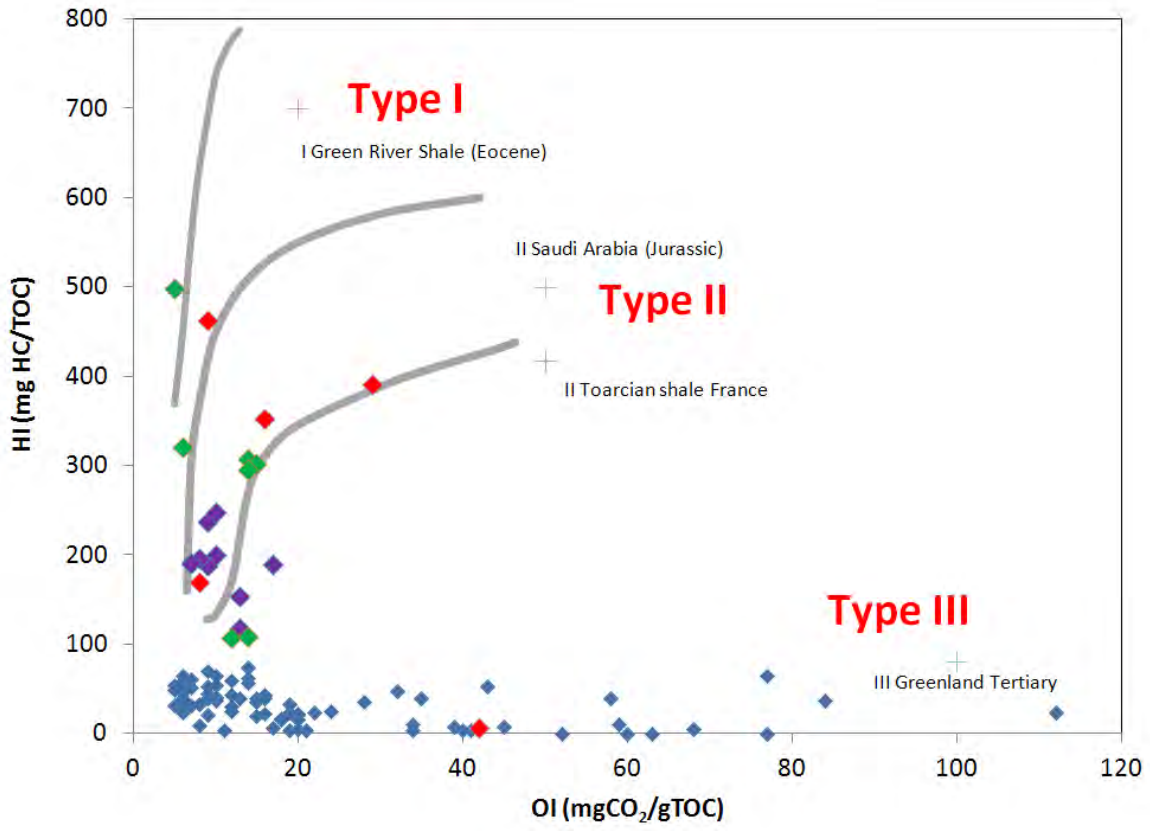

Figure 3. Modified van Krevelen diagram showing examples of Types I-III kerogens and relationship to the samples [Red = Rempstone 1; green = Ratcliffe-on-Soar 1; purple =Old Dalby 1; blue = remainder (see Fig. 1 for well locations)]

T_{max} (measured in degrees centigrade)

T_{max} is the Rock-Eval equivalent of vitrinite reflectance (R_o), similarly indicating the maturity of the sample. Conversion of T_{max} to vitrinite reflectance is by the following formula (Jarvie *et al.* 2005):

$$\text{Calculated } R_o\ \% = 0.018 \times T_{max} - 7.16$$

In the spreadsheet (Appendix 1), the various maturity windows have been indicated by the cell background colour. Immature samples have a background yellow, oil window samples are green, shale wet gas window samples are orange and shale dry gas samples are red.

Very low T_{max} is recorded for two samples. The Heywood sample (T_{max} = 352) and one Swinden sample (T_{max} = 331) are not shown on Figure 4. These two samples might be comparable with Barnett Shale and Bossier Shale Type III gas-prone sediments (Jarvie *et al.* 2007), but the rest of the Swinden 1 samples are within the dry gas window. T_{max} becomes more erratic at high maturity. The current samples conform quite closely to the pattern established for the Barnett Shale (Jarvie *et al.* 2005). The low Swinden T_{max} of 331 should perhaps be disregarded. Four samples at about 410-430 T_{max} might indicate both immaturity and low HI, possibly indicating non-prospective shale. These samples are from Heywood 1, Bosley 1 and Ratcliffe-on-Soar 1 (2) wells, although other samples from Bosley 1 and Ratcliffe-on-Soar 1 plot more uniformly with the Barnett Shale model.

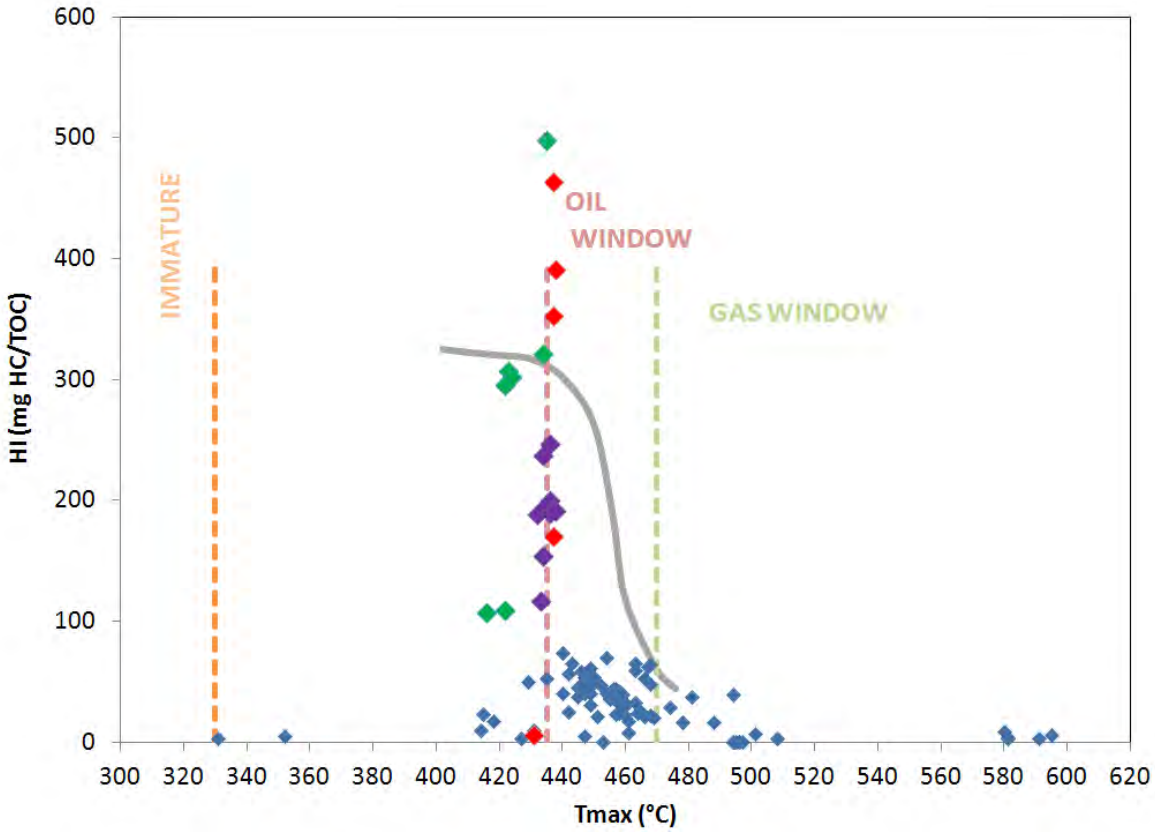

Figure 4. Plot of Hydrogen Index versus T_{max}. This is known as a modified Espitalie kerogen type and maturity plot.

Hydrogen Index

The HI of 500 to about 160 obtained from the Widmerpool Gulf samples from wells Rempstone 1, Ratcliffe-on-Soar 1 and Old Dalby 1 defines this group as Type II, comparable with the Mitcham well of the Barnett Shale kerogen (Figure 4). This is supported by other studies showing Type II (HI = 248.5) and some Type III (HI = 46.1) in the Pennine Basin (Ewbank *et al.* 1993). With increasing maturity the HI decreases, so that above T_{max} = 460 (at the onset of gas window maturity) the HI values of this study and the Barnett wells are mainly below 50 (Figure 4).

Remaining hydrocarbon potential (S_2)

Plotting S_2 against TOC, as done for the Barnett Shale (Jarvie & Lundell 1991, Jarvie *et al.* 2005), shows that a similar pattern occurs for the current Pennine Basin (DECC) data (Figure 5). The types of kerogen are shown, together with the organic lean area (TOC <1%) and the Barnett Shale maturation trend. This trend shows that during maturation, TOC declines (Mitcham well, Jarvie *et al.* 2005), incidentally creating porosity within the thermally more mature sections.

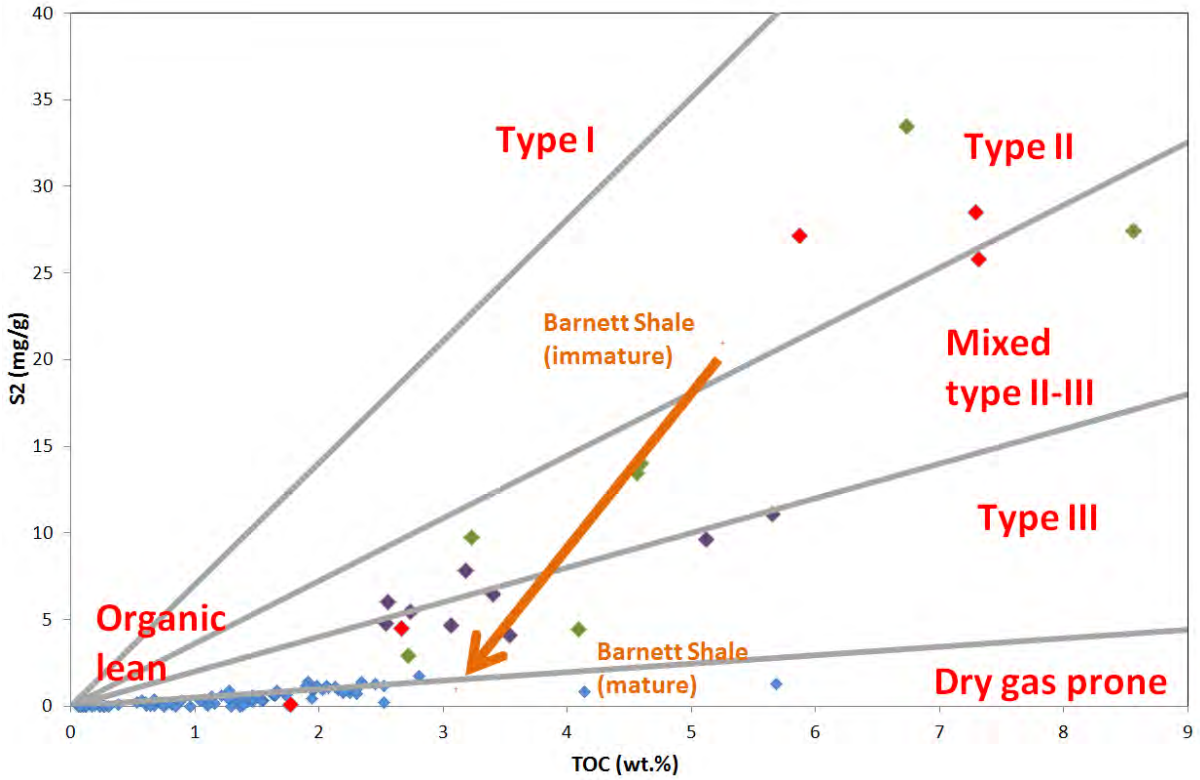

Figure 5. Remaining hydrocarbon potential (S_2) v TOC (cf. Jarvie & Lundell 1991). The orange arrow shows the Barnett Shale maturation trend (from Jarvie 2008). The current data, combining different sub-basins, collectively shows a gentler trend, resulting in residually lower TOC than the Barnett Shale. [Red = Rempstone 1; green = Ratcliff- on-Soar 1; purple =Old Dalby 1; blue = remainder]

Production index

The production index is the ratio of free hydrocarbons to the total free and bound hydrocarbons ($S_1/S_1 + S_2$). Values of 0.1 up to 0.4 define the oil window. Hence in the Widmerpool Gulf (Figure 6), Long Eaton 1, west of Nottingham, is more mature than Rempstone 1, Old Dalby 1 and Ratcliffe-on-Soar 1, which are south of Nottingham. Long Eaton 1 lies within the gas window at the levels of the samples, confirmed by its position on the van Krevelen diagram (Figure 3), whereas the others plot within the oil window.

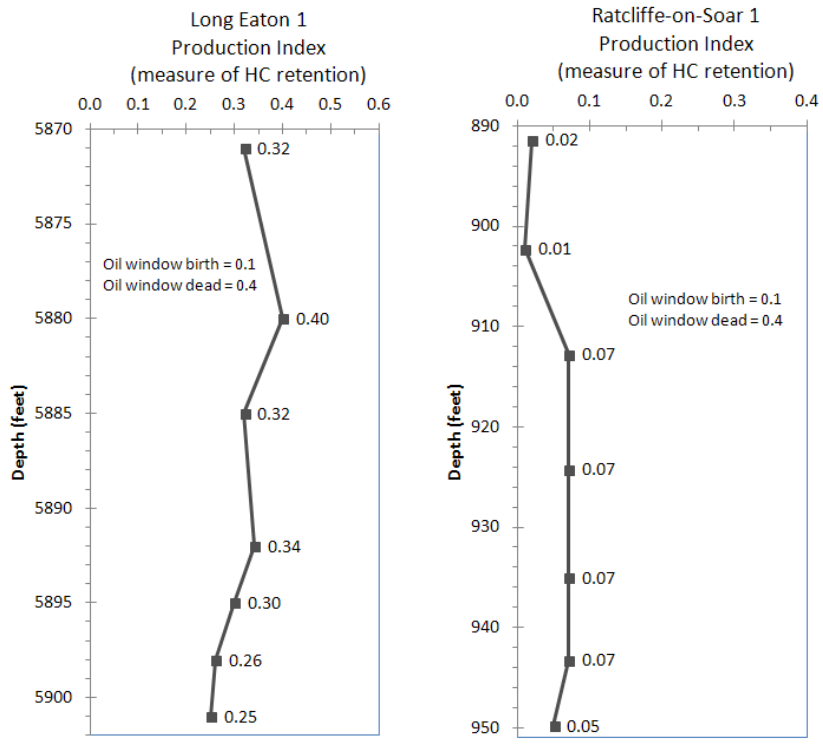

Figure 6. Widmerpool Gulf wells showing the onset of the conventional gas window maturity (Long Eaton 1) and the conventional oil window maturity (Ratcliffe-on-Soar 1).

Conclusions

For the Barnett Shale, Jarvie *et al.* (2005) concluded that although the shale currently plots in the gas window in the Type III kerogen part of the field in a modified van Krevelen diagram, the original kerogen had been Type II. This was based on outcrop data and data from immature wells. This important conclusion showed that during maturation the type of kerogen appears to change and the TOC decreases. An almost identical situation has been proven for the Craven Basin samples of this study with respect to the less-mature Widmerpool Gulf wells (with the notable exception of Long Eaton 1). The samples that do not fit the Barnett model are those which have a low T_{max} (*i.e.* are pre- or early oil window), but these also have a low hydrogen index. Apart from the Heywood well, these are wells with samples that otherwise plot within the Barnett model.

This geochemical evidence supports the comparison made by Smith *et al.* 2011 between the UK Upper Bowland Shale and the US Barnett Shale and the previous decision to compare the potential productivity of the UK Carboniferous Pennine Basin Upper Bowland Shale with the ongoing production from the Fort Worth Basin's Barnett Shale (DECC 2010). However, it should be emphasised that the Upper Bowland Shale is organically leaner than the Barnett Shale.

References

Boyer, C., Kieschnick, J., Suarez-Rivera, R., Lewis, R. E. & Waters, G. 2006. Producing gas from its source. *Oilfield Review* Autumn 2006: 36-49.

DECC. 2010. The unconventional hydrocarbon resources of Britain's onshore basins - shale gas. DECC Promote website, December 2010. https://www.og.decc.gov.uk/UKpromote/onshore_paper/UK_onshore_shalegas.pdf

Ewbank, G., Manning, D. A. C. & Abbott, G. D. 1993. An organic geochemical study of bitumens and their potential source rocks from the South Pennine Orefield, central England. *Organic Geochemistry* 20(5): 579-598.

Jarvie, D. M., & Lundell, L.L. 1991. Hydrocarbon generation modelling of naturally and artificially matured Barnett Shale, Fort Worth Basin, Texas. Southwest Regional Geochemistry Meeting, September 8– 9, 1991, The Woodlands, Texas, 1991. www.humble-inc.com/Jarvie_Lundell_1991.pdf

Jarvie, D. M., Hill, R. J. & Pollastro, R. M. 2005. Assessment of the gas potential and yields from shales: the Barnett Shale model. In: Cardott, B. J. (Ed.) *Unconventional energy resources in the southern Midcontinent, 2004 Symposium*. Oklahoma Geological Survey Circular 110: 37-50. http://wwgeochem.com/resources/Jarvie+et+al.+2005+OGS+Circ.+110+Barnett+paper.pdf

Jarvie, D. M., Hill, R. J., Ruble, T. E. & Pollastro, R. M. 2007. Unconventional shale gas systems: the Mississippian Barnett Shale of north-central Texas as one model for thermogenic shale gas assessment. *Bulletin of the American Association of Petroleum Geologists* 91(4): 475-499.

Jarvie, D. M. 2008. Geochemical comparison of shale-resource systems. Insight Shale Gas Summit, Dallas, Texas, 6-7 May 2008. http://wwgeochem.com/resources/Final+Jarvie+-+Insight+Dallas+May+2008.pdf

Roche, I. 2012. Lessons from history - unlocking a new UK shale oil play. *Society of Petroleum Engineers*, SPE 150933.

Smith, N., Turner, P. & Williams, G. 2011. UK data and analysis for shale gas prospectivity. In: Vining, B. A. & Pickering, S. C. (Eds) *Petroleum Geology: from mature basins to new frontiers – Proceedings of the 7th Petroleum Geology Conference*, Geological Society, London, 1087-1098.

Tissot, B.P. & Welte, D.H. 1978. *Petroleum Formation and Occurrence: A New Approach to Oil and Gas Exploration*. Springer-Verlag. 538pp.

N.J.P. Smith, C. Vane, V. Moss-Hayes & I.J. Andrews

Appendix A1. Selected output from the Rock-Eval analysis of 16 wells in central Britain. The various maturity windows are indicated by the cell background colour: yellow = immature, green = oil window, orange = shale wet gas window, red = shale dry gas.

Well	BGS sample number	Depth (m)	Depth (ft)	S_1 (mg/g)	S_2 (mg/g)	PI	T_{max} (°C)	S_3 (mg/g)	$S_{3'}$ (mg/g)	PC (%)	RC (%)	TOC (%)	HI	OICO	OI	pyroMINC (%)	oxiMINC (%)	MINC (%)
Black Hill	13003-0001	66.5	218.2	0.19	1.22	0.14	467	0.27	7	0.13	1.85	1.98	62	9	14	0.19	0.07	0.26
Black Hill	13003-0002	68.8	225.7	0.3	0.99	0.23	450	0.11	1.9	0.12	1.91	2.03	49	3	5	0.06	0.07	0.13
Black Hill	13003-0003	69.6	228.3	0.4	1.33	0.23	450	0.12	4.3	0.15	2.3	2.45	54	5	5	0.12	0.21	0.33
Black Hill	13003-0004	70.5	231.3	0.23	0.82	0.22	456	0.13	1.3	0.1	2.15	2.25	36	5	6	0.04	0.1	0.13
Black Hill	13003-0005	71.4	234.3	0.32	0.97	0.25	445	0.19	3	0.12	2.03	2.15	45	4	9	0.09	0.35	0.44
Black Hill	13003-0006	72.3	237.2	0.45	1.42	0.24	449	0.17	1.6	0.17	2.17	2.34	61	6	7	0.05	0.19	0.24
Black Hill	13003-0007	73.2	240.2	0.32	1.16	0.22	447	0.21	3.6	0.14	1.99	2.13	54	3	10	0.1	0.41	0.51
Black Hill	13003-0008	74.1	243.1	0.34	1.41	0.19	440	0.26	5.6	0.16	1.75	1.91	74	4	14	0.16	0.46	0.61
Black Hill	13003-0009	75.0	246.1	0.29	0.93	0.24	442	0.24	13	0.11	1.55	1.66	56	2	14	0.36	2.91	3.27
Blacon East	13003-0010		6122.0	0.03	0.11	0.21	461	0.12	3.70	0.02	0.63	0.65	17	5	18	0.10	0.17	0.27
Blacon East	13003-0011		6134.0	0.10	0.31	0.24	460	0.22	5.00	0.04	1.36	1.40	22	2	16	0.14	0.32	0.46
Blacon East	13003-0012		6139.0	0.28	0.85	0.25	451	0.38	14.20	0.11	4.03	4.14	21	3	9	0.39	2.66	3.05
Blacon East	13003-0013		6147.6	0.48	1.30	0.27	457	0.33	8.40	0.16	5.52	5.68	23	1	6	0.24	1.14	1.37
Blacon East	13003-0014		7423.0	0.01	0.19	0.06	488	0.21	7.20	0.03	1.13	1.16	16	3	18	0.20	7.86	8.06
Blacon East	13003-0015		7428.0	0.00	0.05	0.04	501	0.30	10.40	0.01	0.66	0.67	7	4	45	0.28	3.51	3.79
Blacon East	13003-0016		7432.6	0.00	0.00	0.60	496	0.26	3.80	0.01	0.16	0.17	0	24	153	0.10	9.18	9.28
Bosley	13003-0017	2002.2	6568.9	0.00	0.00	0.76	497	0.28	9.5	0.01	0.22	0.23	0	13	122	0.26	11.11	11.37
Bosley	13003-0018	2003.0	6571.5	0.01	0.11	0.08	431	0.37	10.6	0.02	1.07	1.09	10	3	34	0.29	6	6.3
Bosley	13003-0019	2003.7	6573.8	0.01	0.03	0.21	581	0.38	7.7	0.02	0.94	0.96	3	5	40	0.21	10.03	10.24
Bosley	13003-0020	2004.0	6574.8	0.00	0.00	0.29	495	0.39	4.5	0.01	0.09	0.1	0	50	390	0.12	11.28	11.41
Bosley	13003-0021	2005.8	6580.7	0.02	0.04	0.31	447	0.51	7.5	0.03	0.72	0.75	5	15	68	0.21	9.9	10.11
Bosley	13003-0022	2006.4	6582.7	0.01	0.04	0.22	591	0.46	11.2	0.02	1.34	1.36	3	7	34	0.31	5.44	5.75
Brigg 1	13003-0023	1928.9	6328.4	0.08	0.37	0.18	443	0.44	2.90	0.05	0.52	0.57	65	7	77	0.08	0.01	0.09
Brigg 1	13003-0024	1930.0	6332.0	0.00	0.00	0.00	453	0.13	1.70	0.01	0.06	0.07	0	57	186	0.05	12.16	12.20

Well	BGS sample number	Depth (m)	Depth (ft)	S_1 (mg/g)	S_2 (mg/g)	PI	T_{max} (°C)	S_3 (mg/g)	$S_{3'}$ (mg/g)	PC (%)	RC (%)	TOC (%)	HI	OICO	OI	pyroMINC (%)	oxiMINC (%)	MINC (%)
Brigg 1	13003-0025	1930.8	6334.6	0.01	0.01	0.52	418	0.14	4.20	0.01	0.05	0.06	17	50	233	0.11	11.75	11.87
Brigg 1	13003-0026	1931.5	6336.9	0.01	0.05	0.18	429	0.16	2.20	0.01	0.09	0.10	50	20	160	0.06	12.31	12.37
Clitheroe	13003-0027	122.9	403.2	0.65	1.21	0.35	463	0.24	6.40	0.17	1.89	2.06	59	5	12	0.18	4.77	4.95
Clitheroe	13003-0028	127.3	417.7	0.21	0.42	0.34	459	0.17	6.30	0.06	1.02	1.08	39	3	16	0.17	3.41	3.58
Clitheroe	13003-0029	215.05	705.5	0.15	0.25	0.37	455	0.20	8.60	0.04	0.68	0.72	35	10	28	0.23	6.19	6.43
Clitheroe	13003-0030	218.08	715.5	0.15	0.42	0.27	460	0.17	6.20	0.06	1.32	1.38	30	6	12	0.17	2.60	2.78
Clitheroe	13003-0031	222.99	731.6	0.50	1.02	0.33	457	0.27	7.60	0.14	2.16	2.30	44	5	12	0.21	4.32	4.53
Clitheroe	13003-0032	228.2	748.7	0.40	0.71	0.36	456	0.26	8.50	0.11	1.52	1.63	44	7	16	0.23	3.60	3.83
Clitheroe	13003-0033	232.2	761.8	0.14	0.20	0.41	458	0.19	7.60	0.04	0.81	0.85	24	8	22	0.21	6.81	7.02
Grove 3	13003-0034	2305.7	7564.6	0.01	0.00	0.97	496	0.23	9.00	0.01	0.09	0.10	0	10	230	0.25	13.07	13.32
Grove 3	13003-0035	2306.5	7567.3	0.00	0.00	0.00	495	0.32	11.60	0.01	0.11	0.12	0	17	267	0.32	12.92	13.24
Grove 3	13003-0036	2314.66	7594.0	0.00	0.00	0.00	495	0.39	17.00	0.01	0.22	0.23	0	9	170	0.46	12.72	13.19
Heywood	13003-0037	1600.0	5249.2	0.09	0.06	0.59	414	0.36	12.30	0.03	0.58	0.61	10	8	59	0.34	8.92	9.26
Heywood	13003-0038	1601.0	5252.6	0.04	0.06	0.40	352	0.22	8.30	0.02	1.08	1.10	5	5	20	0.23	1.71	1.94
Heywood	13003-0039	1602.4	5257.2	0.01	0.02	0.35	427	0.14	7.40	0.01	0.74	0.75	3	9	19	0.20	0.22	0.42
Heywood	13003-0040	1603.3	5260.2	0.00	0.00	0.96	496	0.25	4.80	0.01	0.10	0.11	0	45	227	0.13	9.94	10.07
High Ings	13003-0041	95.5	313.3	0.11	0.25	0.30	452	0.17	5.20	0.04	0.49	0.53	47	4	32	0.15	11.05	11.20
High Ings	13003-0042	98.0	321.5	0.07	0.37	0.16	455	0.16	7.70	0.05	0.99	1.04	36	6	15	0.21	3.62	3.84
High Ings	13003-0043	99.0	324.8	0.09	0.36	0.20	454	0.13	8.00	0.04	0.85	0.89	40	4	15	0.22	5.62	5.84
High Ings	13003-0044	100.0	328.1	0.13	0.62	0.18	458	0.24	8.30	0.07	1.39	1.46	42	2	16	0.23	2.21	2.44
High Ings	13003-0045	103.6	339.9	0.16	0.60	0.21	435	0.49	7.40	0.09	1.04	1.13	53	13	43	0.20	0.04	0.25
High Ings	13003-0046	105.0	344.5	0.24	1.22	0.17	463	0.18	9.80	0.13	1.76	1.89	65	5	10	0.27	4.85	5.12
High Ings	13003-0047	167.5	549.5	0.11	0.43	0.20	460	0.25	11.00	0.06	1.25	1.31	33	5	19	0.30	2.84	3.14
High Ings	13003-0048	169.0	554.5	0.08	0.42	0.16	463	0.10	4.50	0.05	1.22	1.27	33	6	8	0.12	1.31	1.44
High Ings	13003-0049	217.0	711.9	0.21	1.21	0.15	468	0.16	9.00	0.13	2.39	2.52	48	4	6	0.25	5.18	5.43
High Ings	13003-0050	219.0	718.5	0.29	1.10	0.21	466	0.18	9.90	0.13	1.94	2.07	53	4	9	0.27	7.06	7.33
High	13003-0051	219.3	719.5	0.34	1.78	0.16	468	0.18	9.00	0.19	2.61	2.80	64	4	6	0.25	7.36	7.62

Well	BGS sample number	Depth (m)	Depth (ft)	S_1 (mg/g)	S_2 (mg/g)	PI	T_{max} (°C)	S_3 (mg/g)	$S_{3'}$ (mg/g)	PC (%)	RC (%)	TOC (%)	HI	OICO	OI	pyroMINC (%)	oxiMINC (%)	MINC (%)
Ings+A87																		
Long Eaton	13003-0052		5871	0.18	0.37	0.32	464	0.30	7.20	0.06	1.49	1.55	24	3	19	0.20	0.68	0.88
Long Eaton	13003-0053		5880	0.03	0.05	0.40	461	0.25	6.40	0.01	0.63	0.64	8	5	39	0.17	0.12	0.30
Long Eaton	13003-0054		5885	0.13	0.28	0.32	469	0.22	5.80	0.04	1.38	1.42	20	1	15	0.16	0.28	0.44
Long Eaton	13003-0055		5892	0.19	0.38	0.34	465	0.37	8.50	0.06	1.48	1.54	25	5	24	0.23	1.91	2.14
Long Eaton	13003-0056		5895	0.12	0.30	0.30	466	0.29	6.70	0.05	1.41	1.46	21	4	20	0.18	0.62	0.81
Long Eaton	13003-0057		5898	0.12	0.34	0.26	468	0.30	7.20	0.05	1.48	1.53	22	1	20	0.20	0.67	0.87
Long Eaton	13003-0058		5901	0.04	0.13	0.25	478	0.16	4.40	0.02	0.79	0.81	16	4	20	0.12	0.03	0.15
Nooks Farm	13003-0059		1401	0.08	0.24	0.25	440	0.21	4.30	0.04	0.56	0.60	40	10	35	0.12	0.57	0.68
Nooks Farm	13003-0060		1410	0.28	0.70	0.29	449	0.10	1.20	0.09	1.64	1.73	40	2	6	0.04	0.00	0.04
Nooks Farm	13003-0061		1417	0.23	0.89	0.21	454	0.12	2.20	0.10	1.17	1.27	70	2	9	0.06	0.00	0.06
Nooks Farm	13003-0062		1418	0.35	0.89	0.28	447	0.12	1.20	0.11	1.84	1.95	46	6	6	0.03	0.00	0.04
Nooks Farm	13003-0063		1429	0.25	0.62	0.29	447	0.08	0.90	0.08	1.13	1.21	51	6	7	0.03	0.00	0.03
Nooks Farm	13003-0064		1432	0.32	0.39	0.45	446	0.04	0.60	0.07	0.60	0.67	58	3	6	0.02	0.00	0.02
Nooks Farm	13003-0065		1450	0.30	0.81	0.27	445	0.21	1.90	0.11	2.08	2.19	37	3	10	0.06	0.02	0.08
Nooks Farm	13003-0066		1519	0.23	0.48	0.33	442	0.24	1.90	0.08	1.86	1.94	25	9	12	0.05	0.03	0.08
Nooks Farm	13003-0067		1531	0.19	0.45	0.29	449	0.08	0.80	0.06	1.41	1.47	31	3	5	0.03	0.03	0.05
Old Dalby	13003-0068	1390.6	4562.3	0.91	5.46	0.14	436	0.27	6.70	0.55	2.18	2.73	200	1	10	0.19	2.67	2.86
Old Dalby	13003-0069	1394.3	4574.5	0.97	4.13	0.19	433	0.47	7.80	0.46	3.07	3.53	117	6	13	0.22	0.28	0.50
Old Dalby	13003-0070	1398.5	4588.3	0.80	4.70	0.15	434	0.41	6.00	0.48	2.58	3.06	154	5	13	0.17	0.19	0.36
Old Dalby	13003-0071	1404.6	4608.3	1.79	9.63	0.16	432	0.45	9.60	0.98	4.14	5.12	188	4	9	0.27	1.10	1.38
Old Dalby	13003-0072	1437.5	4716.2	1.61	11.10	0.13	435	0.43	5.50	1.09	4.56	5.65	196	4	8	0.16	0.21	0.37
Old Dalby	13003-0073	1442.5	4732.6	1.12	6.05	0.16	434	0.24	9.30	0.61	1.94	2.55	237	1	9	0.26	7.46	7.72
Old Dalby	13003-0074	1447.8	4750.0	0.80	4.79	0.14	436	0.42	9.50	0.49	2.05	2.54	189	5	17	0.27	1.08	1.35
Old Dalby	13003-0075	1450.8	4759.8	0.93	6.48	0.13	438	0.24	3.10	0.64	2.76	3.40	191	4	7	0.09	0.04	0.13
Old Dalby	13003-0076	1455.0	4773.6	1.45	7.84	0.16	436	0.33	9.70	0.79	2.39	3.18	247	1	10	0.28	4.86	5.14
Ratcliffe on	13003-0077	271.7	891.4	0.51	27.44	0.02	434	0.53	1.90	2.38	6.18	8.56	321	6	6	0.08	0.02	0.10

Well	BGS sample number	Depth (m)	Depth (ft)	S_1 (mg/g)	S_2 (mg/g)	PI	T_{max} (°C)	S_3 (mg/g)	$S_{3'}$ (mg/g)	PC (%)	RC (%)	TOC (%)	HI	OICO	OI	pyroMINC (%)	oxiMINC (%)	MINC (%)
Soar																		
Ratcliffe on Soar	13003-0078	275.0	902.2	0.50	33.51	0.01	435	0.34	1.60	2.86	3.87	6.73	498	6	5	0.06	0.03	0.09
Ratcliffe on Soar	13003-0079	278.2	912.7	1.09	14.07	0.07	423	0.62	11.20	1.31	3.28	4.59	307	7	14	0.33	0.33	0.65
Ratcliffe on Soar	13003-0080	281.7	924.2	0.76	9.74	0.07	424	0.50	9.40	0.91	2.32	3.23	302	6	15	0.27	1.26	1.53
Ratcliffe on Soar	13003-0081	285.0	935.0	0.96	13.47	0.07	422	0.62	9.40	1.25	3.31	4.56	295	7	14	0.27	0.55	0.83
Ratcliffe on Soar	13003-0082	287.5	943.2	0.21	2.92	0.07	416	0.33	3.70	0.30	2.42	2.72	107	14	12	0.11	0.01	0.12
Ratcliffe on Soar	13003-0083	289.5	949.8	0.25	4.44	0.05	422	0.56	12.60	0.43	3.66	4.09	109	11	14	0.35	0.25	0.60
Rempstone	13003-0084	665.0	2181.8	0.86	4.52	0.16	437	0.20	0.50	0.47	2.19	2.66	170	4	8	0.02	0.00	0.03
Rempstone	13003-0085	665.3	2182.7	1.67	25.80	0.06	437	1.15	5.80	2.35	4.96	7.31	353	5	16	0.18	0.01	0.19
Rempstone	13003-0086	666.0	2185.0	1.58	28.53	0.05	438	2.11	25.30	2.59	4.70	7.29	391	6	29	0.70	0.01	0.71
Rempstone	13003-0087	667.0	2188.3	0.92	27.18	0.03	437	0.50	1.50	2.37	3.50	5.87	463	6	9	0.05	0.01	0.06
Rempstone	13003-0088	668.0	2191.6	0.10	0.10	0.50	431	0.74	12.30	0.05	1.72	1.77	6	10	42	0.34	7.30	7.64
Roddlesworth	13003-0089		4226	0.09	0.06	0.62	508	0.72	12.10	0.04	1.71	1.75	3	9	41	0.33	7.38	7.71
Roddlesworth	13003-0090		4239	0.15	0.07	0.69	481	0.16	5.20	0.03	0.16	0.19	37	5	84	0.14	11.07	11.21
Roddlesworth	13003-0091		4250	0.01	0.00	0.99	494	0.12	2.60	0.00	0.07	0.07	0	29	171	0.07	12.07	12.14
Roddlesworth	13003-0092		4256	0.12	0.06	0.66	415	0.29	9.20	0.03	0.23	0.26	23	19	112	0.25	10.51	10.76
Roddlesworth	13003-0093		4268	0.00	0.00	0.67	494	0.09	2.00	0.00	0.07	0.07	0	14	129	0.05	12.44	12.49
Roddlesworth	13003-0094		4277	0.30	0.15	0.66	494	0.22	8.00	0.05	0.33	0.38	39	5	58	0.22	9.73	9.96
Roddlesworth	13003-0095		4281	0.02	0.02	0.48	474	0.15	1.90	0.01	0.06	0.07	29	43	214	0.05	11.88	11.94
Swinden 1	13003-0096	30.0	98.4	0.28	0.66	0.30	447	0.22	8.80	0.09	1.55	1.64	40	8	13	0.24	4.58	4.83
Swinden 1	13003-0097	33.0	108.3	0.27	0.70	0.28	458	0.16	7.90	0.09	1.64	1.73	40	8	9	0.22	3.10	3.32
Swinden 1	13003-0098	38.5	126.3	0.25	0.67	0.27	457	0.16	7.10	0.09	1.65	1.74	39	8	9	0.20	3.13	3.32
Swinden 1	13003-0099	40.5	132.9	0.27	0.58	0.32	456	0.15	8.00	0.08	1.42	1.50	39	8	10	0.22	3.11	3.33
Swinden 1	13003-0100	44.7	146.7	0.24	0.67	0.27	455	0.17	8.50	0.09	1.55	1.64	41	5	10	0.23	1.92	2.16
Swinden 1	13003-0101	48.8	160.1	0.25	0.74	0.25	458	0.16	7.60	0.09	2.21	2.30	32	6	7	0.21	2.70	2.91

Well	BGS sample number	Depth (m)	Depth (ft)	S_1 (mg/g)	S_2 (mg/g)	PI	T_{max} (°C)	S_3 (mg/g)	$S_{3'}$ (mg/g)	PC (%)	RC (%)	TOC (%)	HI	OICO	OI	pyroMINC (%)	oxiMINC (%)	MINC (%)
Swinden 1	13003-0102	621.2	2038.1	0.04	0.23	0.15	580	0.20	7.70	0.03	2.49	2.52	9	4	8	0.21	4.28	4.50
Swinden 1	13003-0103	623.0	2044.0	0.03	0.03	0.46	581	0.18	8.70	0.01	0.83	0.84	4	5	21	0.24	7.35	7.58
Swinden 1	13003-0104	626.8	2056.4	0.03	0.04	0.44	331	0.14	10.60	0.01	1.28	1.29	3	5	11	0.29	3.96	4.25
Swinden 1	13003-0105	629.5	2065.3	0.04	0.08	0.31	595	0.23	8.90	0.02	1.36	1.38	6	4	17	0.24	6.24	6.48
Wessenden 1	13003-0106		3505	0.01	0.00	0.98	494	0.19	11.40	0.01	0.29	0.30	0	20	63	0.31	2.45	2.76
Wessenden 1	13003-0107		3510	0.02	0.00	1.00	494	0.20	10.80	0.01	0.25	0.26	0	15	77	0.29	4.53	4.83
Wessenden 1	13003-0108		3512	0.01	0.00	1.00	494	0.14	7.40	0.01	0.26	0.27	0	19	52	0.20	4.09	4.29
Wessenden 1	13003-0109		3513	0.01	0.00	1.00	494	0.18	3.00	0.01	0.29	0.30	0	10	60	0.08	0.46	0.54

Appendix C: Stratigraphic data from key wells penetrating the Bowland-Hodder shales in central Britain

Non-released wells are in red. ***BGS boreholes are in bold italics.*** Note that all depths of subsea, not downhole relative to KB. Conf. = confidential

Well abbrev-iation	Well name	Year spudded	KB elevation (ft above MSL)	GL elevation (ft above MSL) (or DTM)	Base Permian (ft below MSL) (or outcrop)	Top Bowland-Hodder unit (ft below MSL)	Base Bowland-Hodder unit (ft below MSL)	Bowland-Hodder unit thickness (ft)	Net shale upper unit (ft)
ALP	Alport 1	1939	930	(928)	(Nam)	-910	1630+	>2540	?1000
ASK	Askern 1	1957	25.4	(25)	1033	4595	4787.6+	>193	87
BECH	Becconsall 1	2011	27	(19)	conf.	conf.	conf.	conf.	conf.
BLE	Blacon East 1	1981	47	32	1318	4214	7387+	>3173	819
BOS	Bosley 1	1986	1332.4	1308.7	(Nam)	-223.5	4994	5217.5	408
BOT	Bothamsall 1	1957	117.3	(125)	860	3682.7	4566.7+	>884	412
BOU	Boulsworth 1	1963	1408	1385	(Nam)	1752	3448	1696	98
BRA	Bramley Moor 1	1987	725	714	(West)	2376	3208+	>662	527
CAL	Calow 1	1957	420	(413)	(West)	1860	3299+	>1439	475
CLO	Cloughton 1	1986	573	(542)	5969	8535	9527+	>992	317
CRA	Crayke 1	1964	161	(156)	2653	3479	4339+	>860	?
CRO	Croxteth 1	1953	84	(79)	1579	3216	4132+	>916	419
DUF	***Duffield***	1966	202	(216)	(Nam)	-71	3251+	>3322	764
DUG	Duggleby 1	1990	673	650	4869	8393	9351+	>958	324
EAK	Eakring 146	1944	342	(341)	942	1988	4728	2740	?185
EDA	Edale 1	1937	c.850	(845)	(Nam)	-850	-93+	>757	?
EGM	Egmanton 68	1980	126	112.9	1515	3676	6041.9	2365.9	?10
ELL	Ellenthorpe 1	1945	60	(46)	1181	1181	3538+	>2357	?
ERB	Erbistock 1	1986	208	184	(West)	3793	5986+	>2193	236
FLE	Fletcher Bank 1	1958	857	(837)	(Nam)	3400	4658+	>1258	288
FOR1	Formby 1	1940	18	(20)	5862	7122	7662+	>540	73
FOR4	Formby 4	1949	36	(32)	2742	3144	3844+	>700	210
GAI	Gainsborough 2	1959	104.3	(87)	2380	5816	6154.7+	>338.7	0
GRA	Grange Hill 1	2011	73	47.5	conf.	conf.	conf.	conf.	conf.
GRO	Grove 3	1981	210.4	192	1766	4909	7253	2344	90
GUN	Gun Hill 1	1938	1157	1142	(Nam)	-862	2008	2870	510
HAN	Hanbury 1	1990	467	452	1148	2382	3949	1567	110
HATM	Hatfield Moors 3	1983	29	12	1341	5471	5971+	>500	No logs
HAT	Hathern 1	1954	161	(157)	300	657	1602	945	93
HEA	Heath 1	1919	516	(519)	(West)	3034	3484+	>450	?390
HES	Hesketh 1	1990	41	27	2126	2126	4202+	>2076	798
HEY	Heywood 1	1984	393.8	377.7	(West)	4147.9	4917.9+	>770	180
HIG	High Hutton 1	1987	171	151	3908	6854	8829+	>1975	562
HOL	Holme Chapel 1	1974	891	871	(West)	3964	5566	1602	52
ILK	Ilkeston 1	1985	222.37	208.6	(West)	2335.7	3386.7+	>1051	960
INC	Ince Marshes 1	2011	47.2	33	conf.	conf.	conf.	conf.	conf.
IRO	Ironville 5	1984	303.5	290.4	(West)	1439	3452.5	2013.5	95
KIN	Kinoulton 1	1985	147.4	130.9	932	3742.6	4741+	>998.4	369
KRM	Kirby Misperton 1	1985	118	98	5221	6415	11013	4598	868
KRS	Kirk Smeaton 1	1985	123.7	107.6	2.3	4715.5	5243.7	528.2	381
LONC	Long Clawson 1	1943	178	(178)	1222	4022	4527+	>505	85
LONE	Long Eaton 1	1988	129.7	113	382	382	8410	8028	0 (eroded)
MIL	Milton Green 1	1965	63	52.4	(West)	3801	4858	1057	505

Well abbrev-iation	Well name	Year spudded	KB elevation (ft above MSL)	GL elevation (ft above MSL) (or DTM)	Base Permian (ft below MSL) (or outcrop)	Top Bowland-Hodder unit (ft below MSL)	Base Bowland-Hodder unit (ft below MSL)	Bowland-Hodder unit thickness (ft)	Net shale upper unit (ft)
NOO	Nooks Farm 1	1982	997	980	(Nam)	-517	2623+	>3140	824
NORM	Normanby 1	1985	63.7	43.8	2642	6884	7347.7+	>463.7	308
OLD	Old Dalby 1	1988	323	305.8	1128	3587	4532+	>945	268
PRH	Preese Hall 1	2010	25.5	16.7	conf.	conf.	conf.	conf.	conf.
RAN	Ranton 1	1980	407	394	1913	4209	5428	1219	?0
RAT	Ratcliffe-on-Soar 1	1986	124.8	108.1	696	1015.6	5913.2+	>4895	198
REM	Rempstone 1	1985	273.9	259.8	620.1	1912.1	3437	1524.9	297
ROD	Roddlesworth 1	1987	774	754	(Nam)	3369	7332	3963	44
ROO	***Roosecote***	1970	121.4	(127)	397.4	1615	2501.6+	>886.6	420
SCA	Scaftworth 2	1982	45.6	27.2	1062	6814.2	7585.6+	>771.4	474
SES	Sessay 1	1988	95	80	1225	2164	5405+	>3241	331
SOU	South Leverton 1	1960	37.3	(29)	1913.7	4802.7	5087.7+	>285	124
STR	Strelley 1	1986	436.8	422.1	-376	2412.6	4320.4+	>1907.8	205
SWI	Swinden 1	1978	462.6	456	(Tourn)	-	-	>2310[1]	-
THI	Thistleton 1	1987	75	15	2964	4019	6945+	>2926	2096
THO	Tholthorpe 1	1965	80.4	(75)	1489.6	2609.6	2969.6+	>360	?
TOR	Torksey 4	1975	47.2	34.3	2323	5598.8	6019.8+	>421	279
WEE	Weeton 1	1984	166.8	141.7	(Nam)	909	4886	3977	246
WES	Wessenden 1	1987	1631.5	1620	(Nam)	-131	368	499	117
WHM	Whitmoor 1	1966	1024	(1018)	(Nam)	2096	3426	1330	140
WID	Widmerpool 1	1945	266	(261)	754	2234	5934+	>3700	?3700

NB These data present the interpretation used in this study.

[1] >2310 ft of pre Bowland-Hodder unit shales.

Other wells

Well abbrev-iation	Well name	Well abbrev-iation	Well name
ALD	Aldfield 1	MAL1	Malton 1
APL	Apley 1	MAL4	Malton 4
BARD	Bardney 1	MAR	Marishes 1
BART	Barton 1	NET1	Nettleham 1
BEC	Beckering 1	NET2	Nettleham 2 (B2)
BIS	Biscathorpe 1	NEW	Newton Mulgrave 1
BIT	Bittern's Wood 1	NORG	North Greetwell 1
BLW	Blacon West 1	NOR	Northwood 1
BRAF	Brafferton 1	PIC	Pickering 1
BRI	Brigg 1	PLU	Plungar 8A
BRM	Broomfleet 1	PRE	Prees 1
BRO	Broughton B1	RAL	Ralph Cross 1
BUT	Butterwick 1	ROB	Robin Hood's Bay 1
CHE	Cherry Willingham 1	ROS	Rosedale 1
CLE	Cleveland Hills 1	RUD	Rudston 1
COL	Cold Hanworth 1	SAL	Saltfleetby 3
DUN	Dunholme 1	SCAL	Scaling 1
EGT	Egton High Moor 1	SCU	Scupholme 1
ELS	Elswick 1	SEA	Seal Sands
ESK12	Eskdale 12	SPA	Spaldington 1

Well abbrev-iation	Well name	Well abbrev-iation	Well name
FOR	Fordon 1	STA	Stainton 1
FOR5	Formby F5	TET	Tetney Lock 1
GLA	Glanford 1	WEL	Welton 1
HAR	Harlsey 1	WELW	Welton West 1
HEAF	Heath Farm 1	WHEL	Wheldrake 1
HEM	Hemswell 1	WHE	Whenby 1
HUN	Hunmanby 1	WHI	Whitwell on the Hill 1
KED	Keddington 1Z		
KEL	Kelstern 1		
KIR	Kirkleatham 1		
KNU	Knutsford 1		
LAN	Langtoft 1		
LOC2	Lockton 3		
LOCE	Lockton East 1		

Appendix E: Thermal modelling of the Pennine Basin, central Britain

Summary

This report describes a thermal modelling study covering boreholes across the Pennine Basin, central Britain, from the East Irish Sea Basin, across the Bowland Basin, through the Cheshire Basin and the Widmerpool Trough to the Gainsborough Trough. It forms part of a wider study to assess the extent of the region's shale gas resource.

The regional structural history of the area includes Early Carboniferous rifting that resulted in a period of fault-controlled deposition followed by a Late Carboniferous phase of regional subsidence. This is reflected by widespread marine deposition during the Visean, with shallowing marine conditions during deposition of the Millstone Grit Group during the Namurian and shallow marine/paralic delta top deposition of Coal Measures and Warwickshire Group during the Westphalian. Subsequent regional uplift and erosion occurred during the Variscan Orogeny. Sediments were then deposited on this erosional surface during renewed subsidence during the Permian – Cretaceous, though deposition was interrupted by a short hiatus or period of erosion during the Triassic (Hardegsen event). Following the Variscan Orogeny, subsidence resulted in the deposition of Permian and Triassic sediments in shallow marine/deltaic/lacustrine/sabkha environments. Based on evidence from the closest outcrops, deposition during the Jurassic and Cretaceous is likely to reflect a deepening marine environment. Finally, uplift and erosion removed sediments for almost all the basins in this study during the Palaeocene – recent times.

Generally, the present-day heat flow figures calculated from available boreholes are quite modest (50 – 54 mWm^{-2}), however, in the past, during rifting, this would be expected to have been higher, indeed the models in the depocentres of these basins imply heat flows as high as 78 mWm^{-2} during Early Carboniferous rifting and 65 mWm^{-2} during Cretaceous uplift.

The strata penetrated by each borehole were entered into a 1-D model. The eroded thicknesses of Carboniferous strata for the 1-D models were estimated from surrounding boreholes and published sources in order to estimate the model layers needed to represent these eroded sediments. These varied from a few hundred metres to over 1000 m of sediment removed during Variscan uplift and erosion. Some Permian – Triassic deposits were present in the boreholes used in this study; where these sediments had been removed, the eroded Permian – Cretaceous strata thickness was estimated from surrounding boreholes and published sources. These estimated eroded thicknesses were then used to match the modelled maturity to available vitrinite reflectance (VR) data. Where data were sparse, models from nearby boreholes were used to supplement the modelled heat flow.

Finally, these 1-D models were combined to generate three 2-D model sections, these are not as sophisticated as the 1-D models as simplification is required in order to allow the model to run, however, they give a useful overview of the boreholes in context of the depositional basins which contain them. For the 2-D sections, it was assumed that the strata layers have a uniform lithology across each section, the constitution of which was based on the 1-D models.

1. Introduction

BasinMod™ (Platte River Software, Inc.) was used to model the maturity of sediments in selected boreholes in the Pennine Basin. The final 1-D models may be used alongside geological assessments of the basin to consider the geological history of the Pennine Basin from the Carboniferous to the present day.

The approach taken was to model the boreholes individually using BasinMod™ 1-D as these models allow entry of detailed lithology and modelling of the heat flow to achieve the best fit to the vitrinite reflectance (VR) data. These 1-D models were then used to model the burial history and maturity along a 2-D profile between boreholes using interpreted seismic data to complete the section.

The VR data, 1-D and 2-D models give an understanding of the maturity of the basin and indicate which strata have reached sufficient maturity for any organic material which is present to generate oil or gas.

2. Modelling

This report describes the results of 1-D thermal models in the Pennine Basin. BasinMod™ (Platte River Associates, Inc.) was used to model the maturity of sediments in selected boreholes then these boreholes were integrated into three 2-D sections. The report considers the region area through the Carboniferous to the present day, concentrating on the Bowland Shale where maturity data are available.

The boreholes to be modelled were chosen based on availability of data (Table 1) and the location of the boreholes such that the models would contribute to understanding the thermal maturity of these basins (Figure 1).

The 1-D models and 2-D model presented here were produced using Platte River Associates Software BasinMod 1-D version 7.61 and BasinMod 2-D version 4.61. Borehole stratigraphy and rock properties were used to model compaction and temperature through burial over geological time. The modelled maturity and vitrinite reflectance maturity (VR) data were then compared graphically and used to refine the model until the best fit to the available data was achieved. Plots of the maturity, temperature vs. depth and vs. time were produced. The oil and gas windows were changed from the BasinMod defaults after discussion with I. Andrews, BGS.

BasinMod 1-D calculates heat flow curves based on the finite rifting model of Jarvis & McKenzie (1980). This assumes that in an extensional environment there is rapid initial subsidence due to crustal thinning associated with a thermal anomaly i.e., high heat flow. Unlike McKenzie's earlier model, this one recognises that continental basin formation by extension takes a finite time. When crustal stretching ceases, heat is lost by vertical conduction and the slow decay of the heat flow leads to further subsidence due to thermal contraction. For modelling heat flow in basins with limited extension (stretching factor $\beta \leq 2$), the Jarvis & McKenzie (1980) model assumes that the thermal anomaly develops and decays within about 60 Ma.

In order to match the model to the recorded vitrinite data, estimates of the palaeo-heat flow and eroded sediments thicknesses are required. The thickness of sediment removed is estimated based on surrounding sediments and the VR data. The palaeo-heat flow is estimated based on known rifting events and the slope of the scattered VR point data. Boreholes with more complete VR data were used to supplement models where there were fewer VR data available.

Minor modifications were made to the Jarvis & McKenzie palaeo-heat flow curves to improve the fit of the model to the data. The modelled maturity was calibrated graphically against the maturity data for the borehole. The eroded sediment thickness was estimated using vitrinite reflectance (VR) and apatite fission track analysis (AFTA) where available. Palaeozoic stratigraphical ages were taken from the BGS online stratigraphical tables (Powell 2009 pers. comm., Gradstein *et al.* 2004 and ICS 2006). Lithology mixes to best approximate the stratigraphy were constructed from borehole records held by BGS in the National Geological Records Centre (NGRC), and published data. Permo-Triassic deposits are not well preserved at all sites across this region. Finally, estimates of water depth, surface palaeo-temperature and palaeo-sea level were included. The vitrinite reflectance data were then used for final calibration to produce a best-fit, geologically reasonable model.

The 2-D models were generated by combining results from the calibrated 1-D models. Seismic data was used to interpret the horizons between these wells and these profiles were then used to generate 2-D section models of basin maturity. Only faults that cut more than one horizon affect calculated model results. For simplicity the 2-D model the lithologies were assumed to be uniform across the basin. Initially the model was constructed using only the current sediment thickness. The model was 'coupled', (i.e. the lines separating model layers were joined correctly such that the correct rock properties were contained within the appropriate model layers) and successfully run. This initial model was then modified to include the Variscan Unconformity and erosional surface. A simplified heat flow based on those developed for the 1-D models was used, with a high heat flow in the Carboniferous decreasing to present day levels. The broken lines above the Variscan Unconformity and current land surface indicate the modelled eroded sediment thicknesses above the Variscan unconformity and present day surface (see figure for more detail). It should be noted that the 2-D model cannot model the eroded thickness of Carboniferous sediment where the Variscan Unconformity itself has been eroded, instead, the eroded sediment thickness is then added to the layers removed by recent erosion, which slightly degrades the fit of the VR data compared to the more satisfactory fit of the 1-D models. The Sclater & Christie (1980) or exponential method of compaction was chosen. This method was developed from wells on the North Sea Central Graben, which may show some overpressuring; correcting for this tends to result in undercompaction, which may have affected the fit of the model.

In general, the models fit the data well and are geologically reasonable. Using the more sophisticated and detailed 1-D models to produce a 2-D cross section was a successful approach. There is still potential to refine the 2-D model, for example, by varying lithologies across the basin.

3. Boreholes modelled

The boreholes modelled for this report are given in Table 1. Logs and stratigraphic data are available in the BGS NGRC and archives. Vitrinite reflectance data were taken from published papers, confidential reports, PhD theses or new BGS analytical results (Smith *et al.* 2012).

Table 1: Boreholes modelled

WELL NAME	NUMBER	DRILLED DEPTH (m)	EASTING	NORTHING	COMMENTS (TD – total depth, VR – number of vitrinite reflectance data)
Irish Sea	110/2b-10	2540.51	03°44' 34°589' W	53°50' 38°157'	Released well 16VR (confidential report) TD in Millstone Grit (Namurian C Yeadonian – Marsdenian)
Thistleton 1	SD33NE17	2139.69	339760	437000	Released well 16VR (Smith *et al.* 2012) TD in Bowland Shale (Brigantian – Pendleian)
Hesketh 1	SD42NW6	1295.4	343001	425197	Released well 3VR (Smith *et al.* 2012) TD in Lower Bowland Shale (Brigantian)
Upholland 1	SD50SW20	1523.39	350440	402900	Released well 14 VR (Pearson & Russell, 2000) TD in Sabden Shale (Arnsbergian – Kinderscoutian)
Ince Marshes 1		1570	346211	376439	Confidential well 18 VR (courtesy of IGas Energy Plc.) TD in Craven Group
Blacon East 1	SJ36NE23	2265.88	337890	366860	Released well 7 VR (Smith *et al.* 2012) TD in Carboniferous limestone (Visean)
Knutsford 1	SJ77NW4	3045.7	370269	377851	Released well 4 VR (Pearson & Russell, 2000), 5 AFTA (Lewis *et al.* 1992) TD in Westphalian Coal Measures
Gun Hill 1	SJ96SE18	904	397230	361820	Released well 12 VR (confidential report) TD in Carboniferous Limestone
Long Eaton 1	SK43SE161	2752.34	446400	331660	Released well 8 VR (confidential report) TD in Craven Group (Chadian)
Ilkeston 1	SK44NE47	1103.5	447537	345172	Released well 3 VR (confidential report) TD in Millstone Grit (Arnsbergian)
Grove 3	SK78SE30	2933.0	476155	381373	Released well 3 VR (Smith *et al.* 2012) TD in Early Palaeozoic phyllites with Visean (Courceyan) overlying
Gainsborough 2	SK89SW2	1907.74	481774	390785	Released well 39 VR (confidential report) TD in Upper Bowland Shale (with basic igneous extrusive rock as lowest layer)
Kirk Smeaton 1	SE51NW40	1636.0	451142	416097	Released well 30 VR (confidential report) TD in Craven Group (Brigantian)

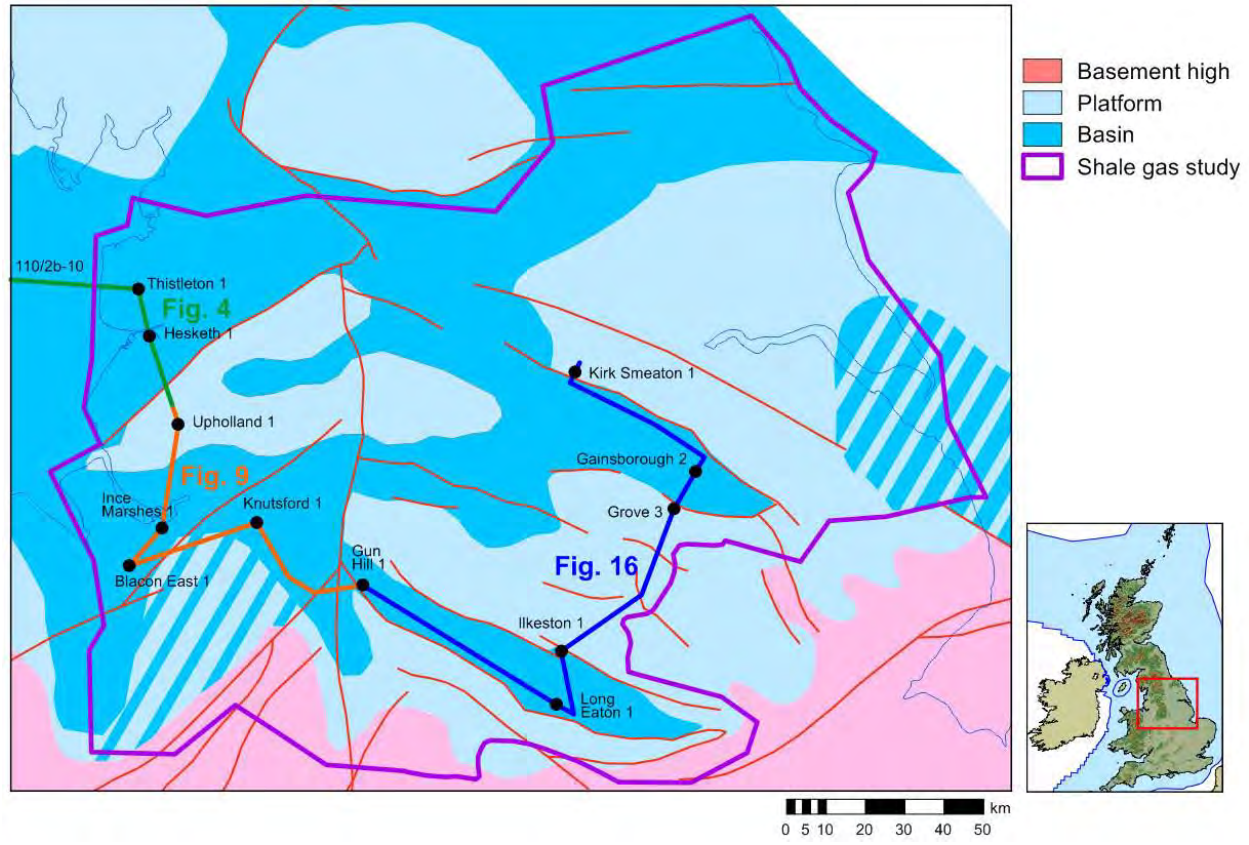

Figure 1. Location of the study area, wells and lines of section

4. East Irish Sea – Craven Basin section

4.1 East Irish Sea geology

The oldest deposits penetrated by the boreholes in this study are of Namurian age. Seismic interpretation extends the 2-D model in this basin to the top of the Chadian in the Bowland-Hodder unit. The East Irish Sea Basin succession comprises Lower Bowland Shale deposited in a deep marine environment in the early Carboniferous (Rowley & White 1998). Rifting and regional extension during the Visean resulted in multiple faults showing syn-depositional deposition of thick marine sediments. Rifting ceased in the late Visean and thermal subsidence occurred through Namurian and Westphalian times and deposition of sediments in paralic and shallow marine environments. This was followed by uplift and erosion during the Variscan Orogeny. A second phase of east-west rifting began during Permian times, resulting in syn-tectonic deposition of thick Permian and early Triassic sediments in a fluvial basin environment followed by marine sediments in the late Triassic. This rifting may have continued to the Late Jurassic. Deposition in deeper marine waters continued through to the Late Cretaceous (Rowley & White 1998). This period of rifting and deposition was again followed by uplift and erosion, most likely due to magmatic underplating.

4.1.1 Well 110/02b-10

This offshore borehole penetrates Namurian to Quaternary sediments and has 16 vitrinite reflectance measurements.

An estimated 800 m of sediment was removed during the Variscan Orogeny and around 1200 m during the later erosional period during the Cretaceous uplift. This figure is in agreement with the estimated thickness of eroded Carboniferous strata in Rowley & White (1998).

A satisfactory fit to the data was achieved. The comparison of model maturity and maturity data is shown in Figure 2c. The heat flow model (Figure 2b) is fairly well constrained by the slope of the VR data curve (Figure 2c). Heat flow appears to have reached 73 mWm^{-2} during the late Carboniferous, resulting in temperatures of around 80ºC in the deepest Westphalian A strata during Carboniferous burial and 140ºC during deep Cretaceous burial. This model implies that the Westphalian A coals achieved a depth of burial of around 3.7 km during the Cretaceous, reaching higher temperatures than during the Carboniferous. A change in the gradient of the line is observed at the Variscan Unconformity. The model indicates that the Carboniferous Coal Measures reached the oil generation window during the Triassic and the gas generation window during the Cretaceous.

4.2 Craven Basin geology

During the Devonian, Old Red Sandstone was deposited in a continental environment. In the early Visean, a marine transgression resulted in deposition of shallow marine sediments and water depths increased to deeper marine in the late Visean as the basin subsided as an asymmetrical southward-tilted graben along the Pendle Fault. The Bowland Shale was deposited in the final stages of Visean sedimentation starting in the Asbian. In the early Namurian, these seas shallowed until during the late Namurian – early Westphalian sediments are of coastal/alluvial/lacustrine/nearshore origin. The Namurian sediments show cyclical deposition and can be correlated across the basin using marine bands. The Millstone Grit Group was deposited in a deltaic environment, sourced from the north. Over 3 km of Devonian – Courceyan sediments are recorded in the basin and over 2.5 km of Visean sediments (Aitkenhead *et al.* 2002). Although the younger rocks have been eroded in the Craven Basin, it was assumed that the younger sediments were also deposited as they are present close to this basin in the region west of the Pennines. The Westphalian Coal Measures were deposited as cyclothems in swampy environment followed by the alluvial/lacustrine Warwickshire Group in the Pennine region.

Sills and dykes in this region are recorded to have ages of 296 ±15 and 302 ±20 Ma.

Carboniferous deposition was followed by uplift and erosion during the Variscan Orogeny. Following this uplift, the basin subsided and Permian and Triassic sediments were deposited in a major rift system. The Craven Basin (previously Bowland Basin or West Lancashire Basin) was contiguous with the East Irish Sea Basin and Cheshire Basin during the Carboniferous and Permian-Triassic (Rowley & White 1998) during regional subsidence and subsequent uplift. Preserved Permo-Triassic sediments are 1 km thick and locally over 2 km thick. As the top of these sediments are eroded, the thickness of these sediments was initially greater. The Triassic Hardegsen unconformity is believed to be present across this basin (Aitkenhead *et al.* 2002).

The current heat flow in this basin is around 50 mWm^{-2} based on observations in the boreholes at Thornton Cleveley and Weeton Camp (Downing & Gray 1986), so it was assumed the present day heat flow in Thistleton 1 and Hesketh 1 is the same.

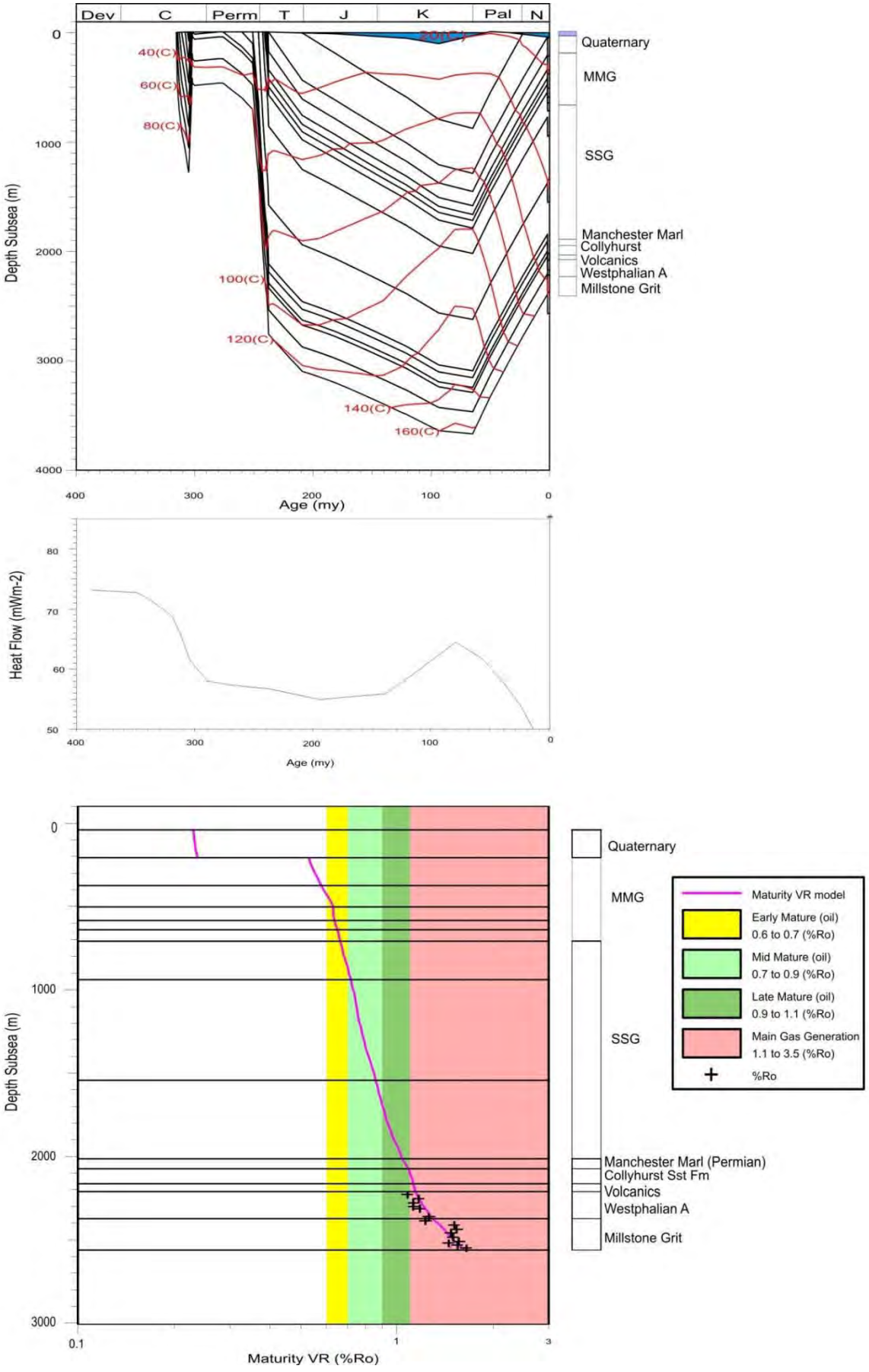

Figure 2. 110/2b-10 model, 2a (top) shows the depositional history and isotherms (isotherms are at 20°C intervals), the blue polygons at the top represent water depth, 2b (centre) shows the modelled palaeo-heat flow and 2c (bottom) compares the modelled VR maturity and VR data.

4.2.1 Thistleton 1

The 16 vitrinite data for Thistleton 1 have quite a broad scatter (Figure 3), the relatively gentle slope implies a low heat flow, but given the scatter of the data, and the heat flow models for the nearby Hesketh 1 and 110/2b-10, the palaeo-heat flow may actually have been higher and the thickness of eroded sediment, lower. However, despite uncertainty in the model, the VR data do indicate that the Bowland Shale reached the oil generation window in this borehole.

The lower part of the Pendleian is offset from the upper part by faulting as shown by the offset of VR data (also A. Carr pers. comm.). Unfortunately, this cannot be modelled without affecting the rest of the model or falsely giving the oldest sediments in this basin a greater age in order to allow sufficient time for these sediments to mature and model the deeper burial of these sediments. It should be noted that due to this, the model indicates that the Bowland Shale only reaches the oil window in this borehole, though the sediments below the fault do reach the gas window (Figure 3c).

The high VR values suggest great quantities of sediment were deposited in the Carboniferous and eroded during the Variscan Orogeny. Near Manchester, over 2.5 km of Coal Measures and Warwickshire Group sediments are recorded. In this model, an additional 3 km of Carboniferous sediments were included in order to fit the data (Figure 3a). This additional thickness may partly be a result of the lower heat flow modelled at this location.

Permian and Triassic sediments are preserved onshore with 600 m of Permian sediments and over 200 m of Triassic Sherwood Sandstone and Mercia Mudstone sediments. The model fits the data when these layers are included as eroded sediments along with a further 3.1 km of deposition during the late Permian to Cretaceous, which was then eroded during the final period of uplift. There is more uncertainty on this final amount of deposition as the model is less sensitive to this layer, however, in order to fit these data, a significant amount of sediment must have been deposited during this period of time.

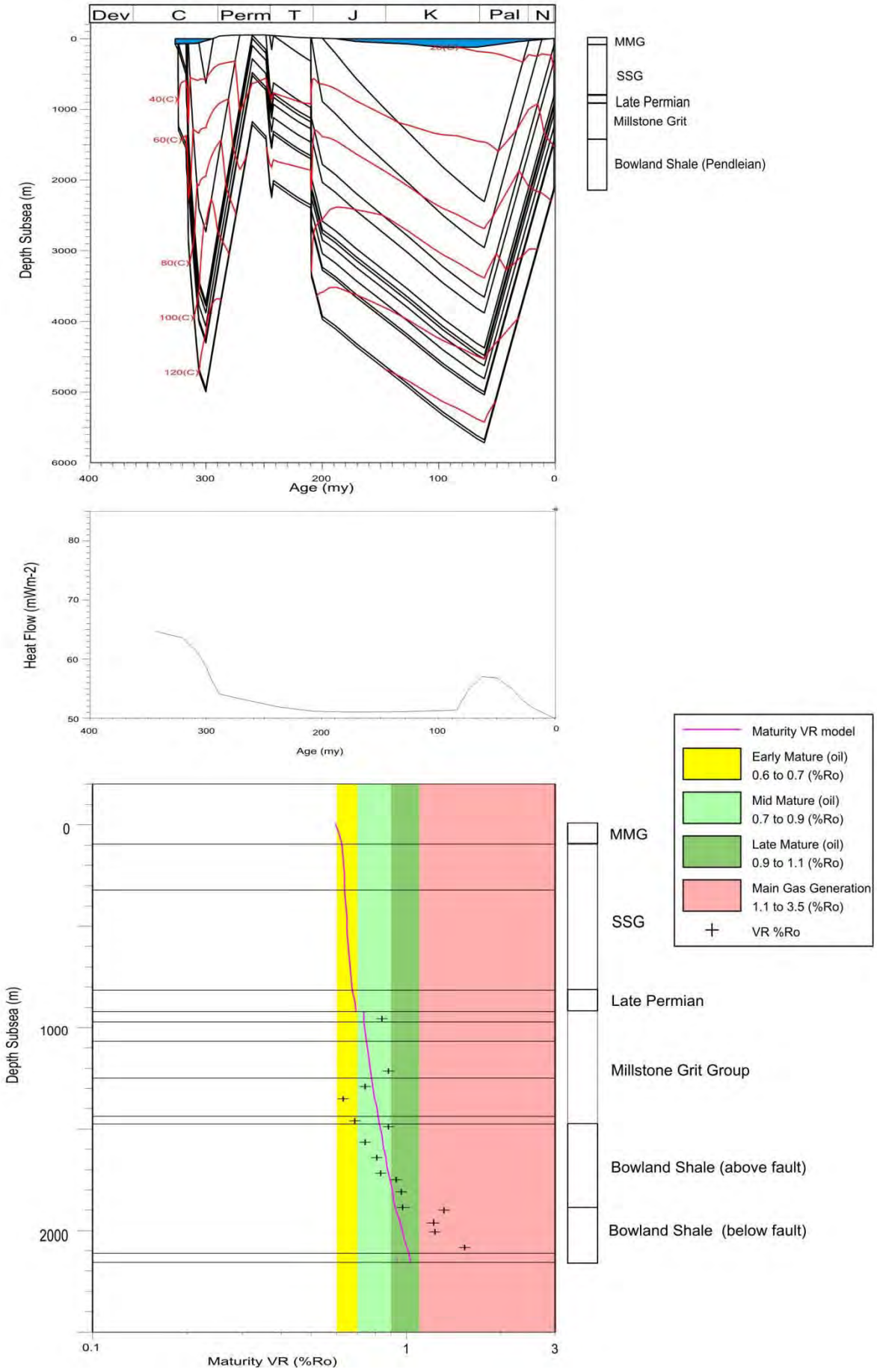

Figure 3. Thistleton model, 3a (top) shows the depositional history, 3b (centre) shows the modelled palaeo-heat flow and 3c (bottom) shows the modelled VR maturity and VR data.

4.2.2 Hesketh 1

As only 3 VR data points are available for this borehole (Figure 4), this model relies heavily on the nearby Thistleton 1 borehole model. The heat flow is subject to the same cautionary note that it may have been higher during Carboniferous rifting and that the thickness of deposited sediment may therefore have been overestimated. However, despite uncertainty in the model, the VR data do indicate that the Bowland Shale reached the oil generation window in this borehole.

In this case, it was estimated that 1500 m of Namurian and 2500 m of Westphalian – Stephanian sediments were deposited during the Carboniferous then eroded from the basin during the Variscan Orogeny. The Bowland Shale reached model temperatures of 120°C and depths of burial of almost 5 km, pushing these sediments into the oil generation window. Following uplift and erosion during the Variscan Orogeny, around 660 m of Permo-Triassic sediments are penetrated by the borehole. The model includes a further 3.9 km of Triassic – Cretaceous sediments which again increased the model temperatures of the Bowland Shales to 120°C and around 5 km depth of burial. These sediments were then removed by the latest uplift and erosion to the present day.

The heat flow for this model was based on the Thistleton model as there are only three VR data points and so the slope of the model is not well constrained outside of this small window.

The model indicates that the Bowland Shale Formation reached the oil generation window during the Carboniferous.

4.2.3 2-D section

Figure 5 and Figure 6 show the 2-D model which was generated using the 1-D models as a basis. Figure 5 shows the current sediment thicknesses across the basin as interpreted from seismic data. These are shown as coloured polygons, dashed lines show missing thicknesses of strata. A reasonable fit to the maturity data was achieved (Figure 6 and Figure 8) and this section shows the great thickness of eroded sediment implied by the models in order to achieve the maturity recorded by the VR data for the Hesketh and Thistleton boreholes in the Bowland Basin. It should be noted that as the lithologies used for the 2-D section are averaged for each formation and as such, the models are less detailed that the 1-D versions, the thickness of sediments over Hesketh and Thistleton is less than shown for the 1D models for this 2-D section. This highlights the need for a combined approach – using the 1-D models to assess the wells in detail and the 2-D model for a basin overview.

The present day gas window is shown in Figure 7. This indicates that most of the Bowland-Hodder unit is currently in the gas generation window (VR 1.1 – 3.5%). It should be noted that the deepest part of the Irish Sea Basin is uncontrolled by VR data and so the maturity model here is unconstrained. This area appears to have undergone rapid syn-depositional faulting so the maturity may in fact be underestimated here since eroded sediment thicknesses were estimated based on nearby boreholes but no VR data were available for this project in order to verify the model in this sub-basin.

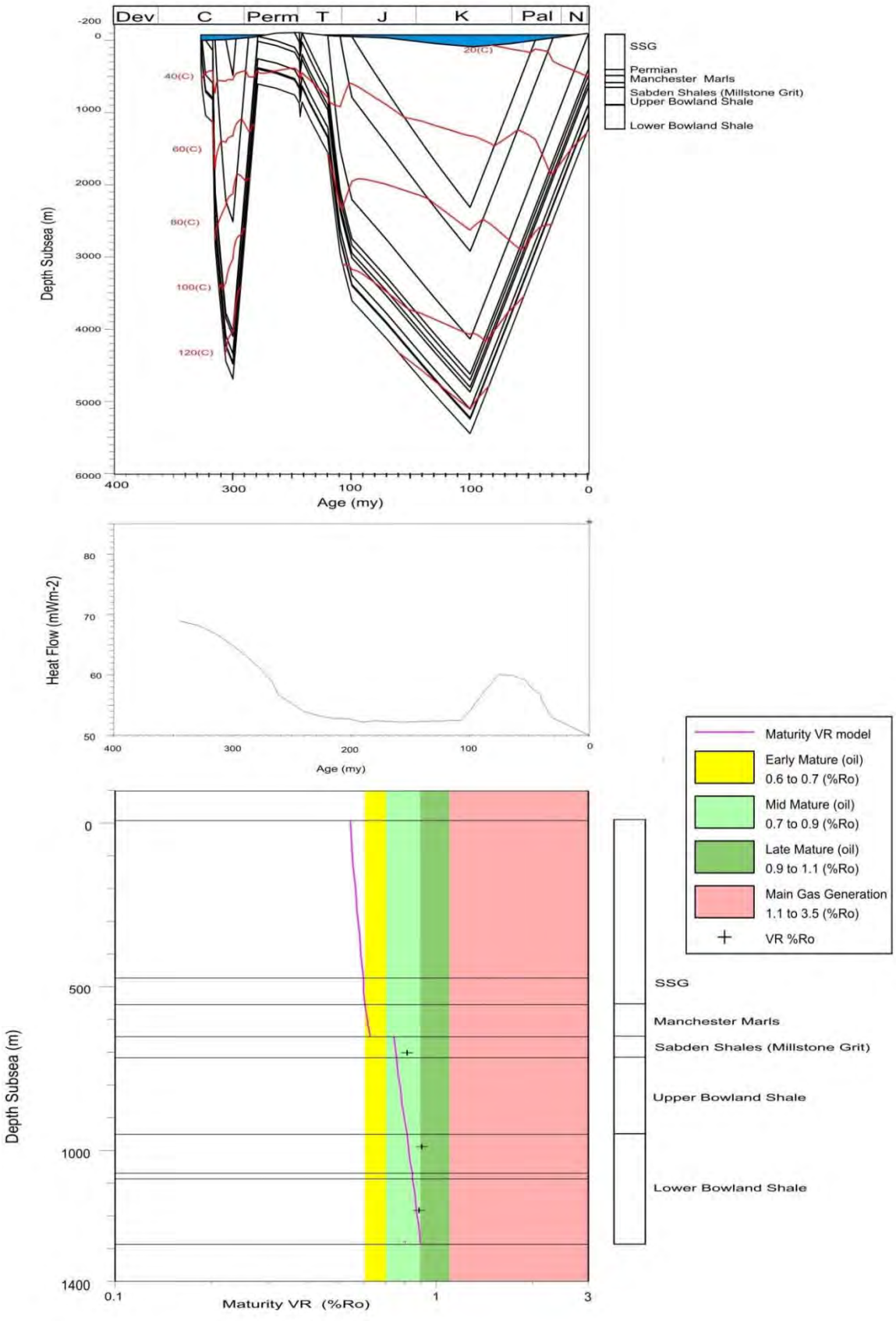

Figure 4. Hesketh model, 4a (top) shows the depositional history, 4b (centre) shows the modelled palaeo-heat flow and 4c (bottom) shows the modelled VR maturity and VR data.

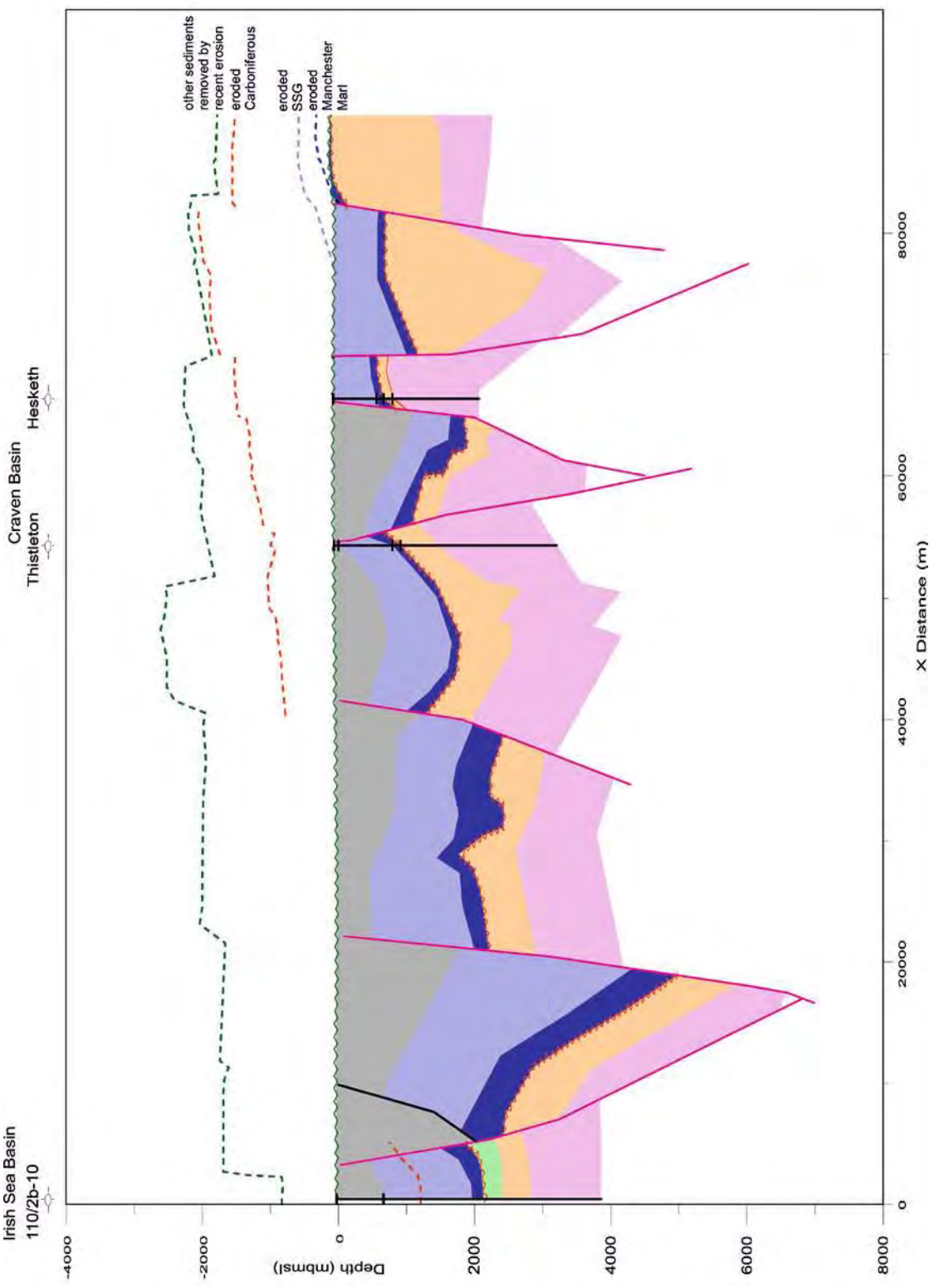

Figure 5. East Irish Sea/Craven Basin 2-D model. Grey is Mercia Mudstone Group, violet is Sherwood Sandstone Group, Dark blue is Manchester Marl, pale green is Westphalian, orange is Millstone Grit, pink is the Bowland-Hodder unit. The dark green unconformity is the current land surface, the red unconformity is the Variscan Unconformity. Dashed lines show eroded thicknesses of strata (the thickness between the unconformity/underlying eroded layer and the dashed line represents the eroded thickness). The bottom of the model is Top Chadian.

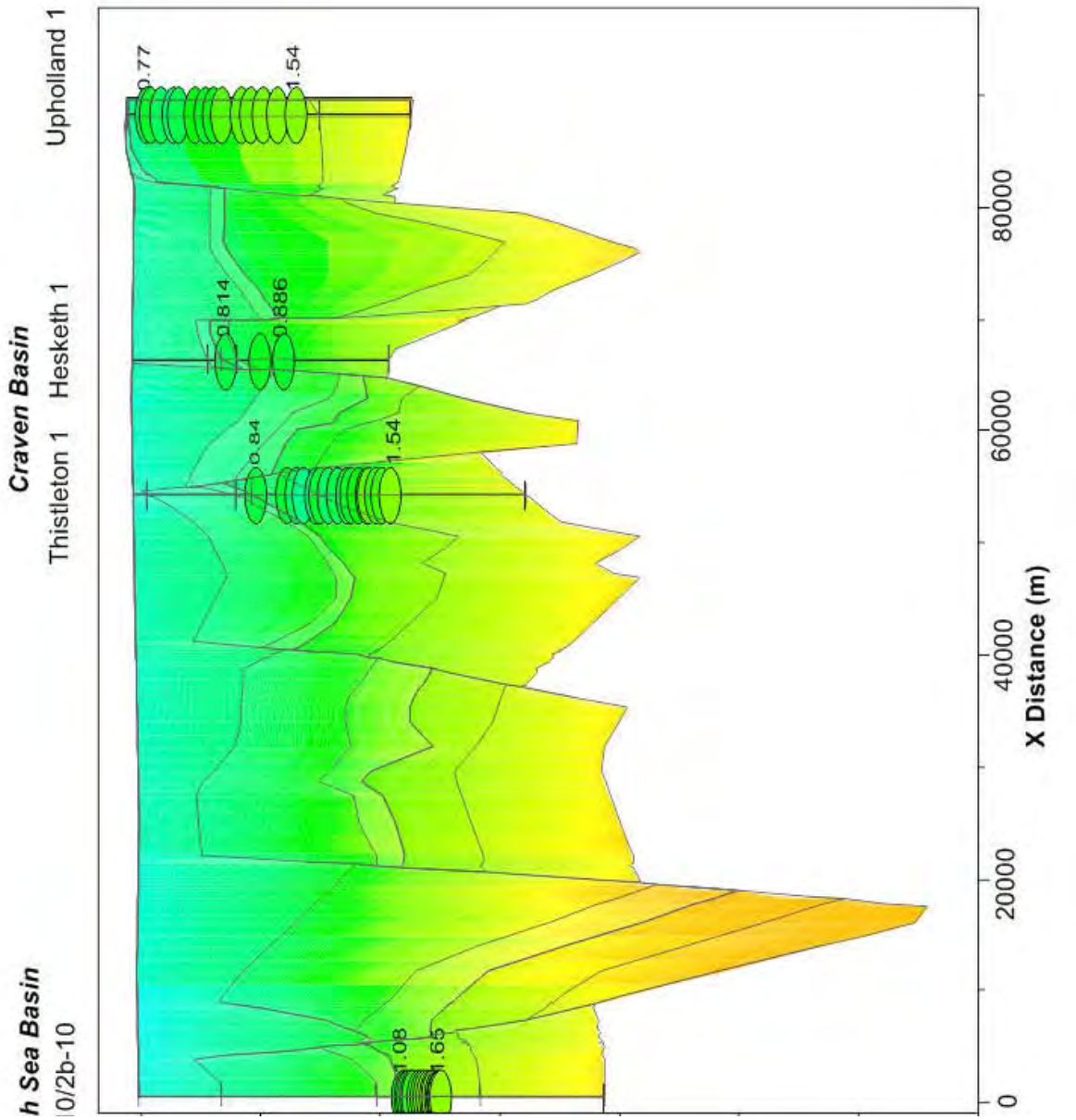

Figure 6. Irish Sea and Craven Basin maturity based on the model is indicated by colour across the whole basin, for comparison, the ovals show the measured VR data at the wells.

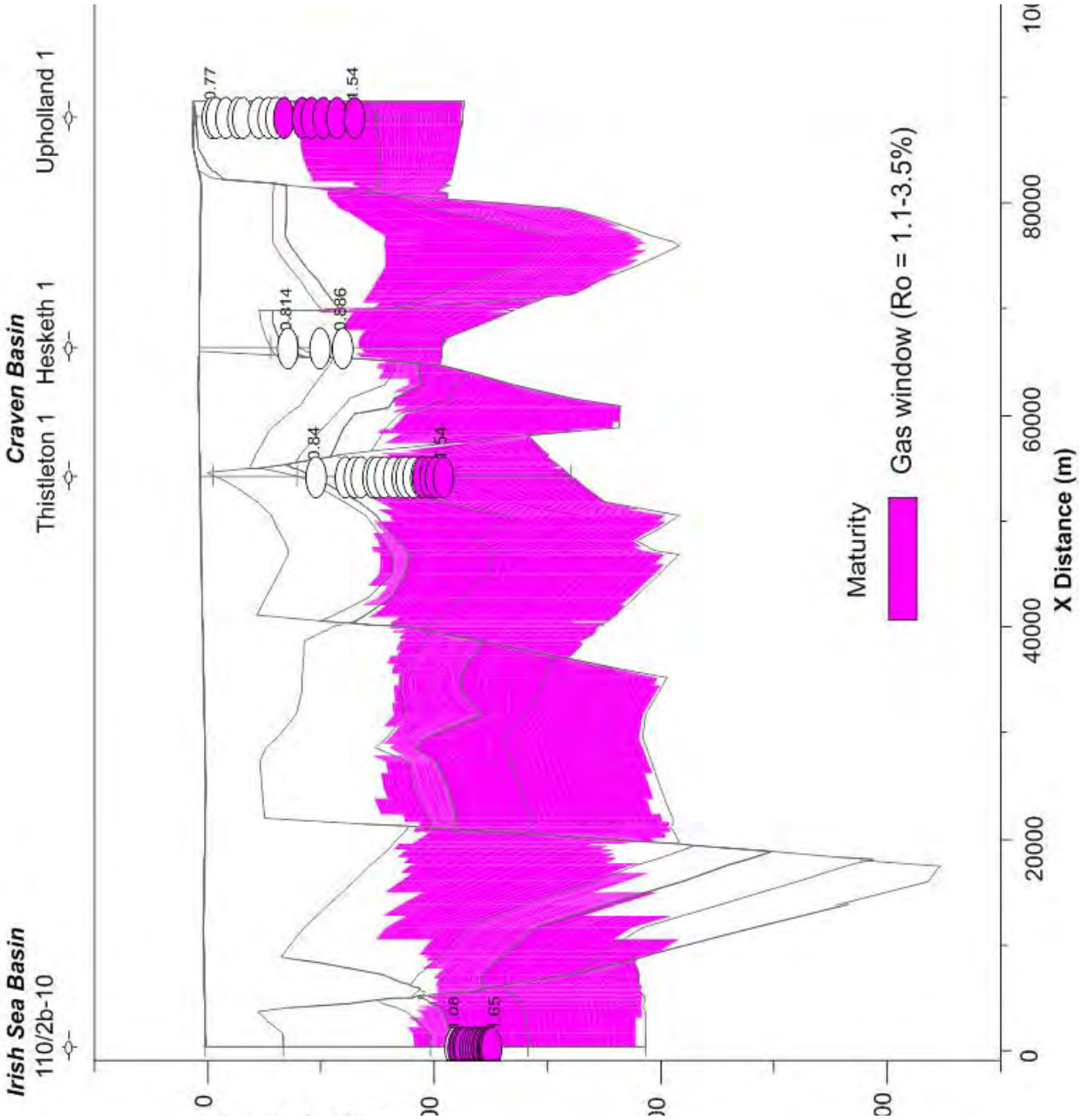

Figure 7. Present day gas window in the Irish Sea and Craven Basin 2-D model

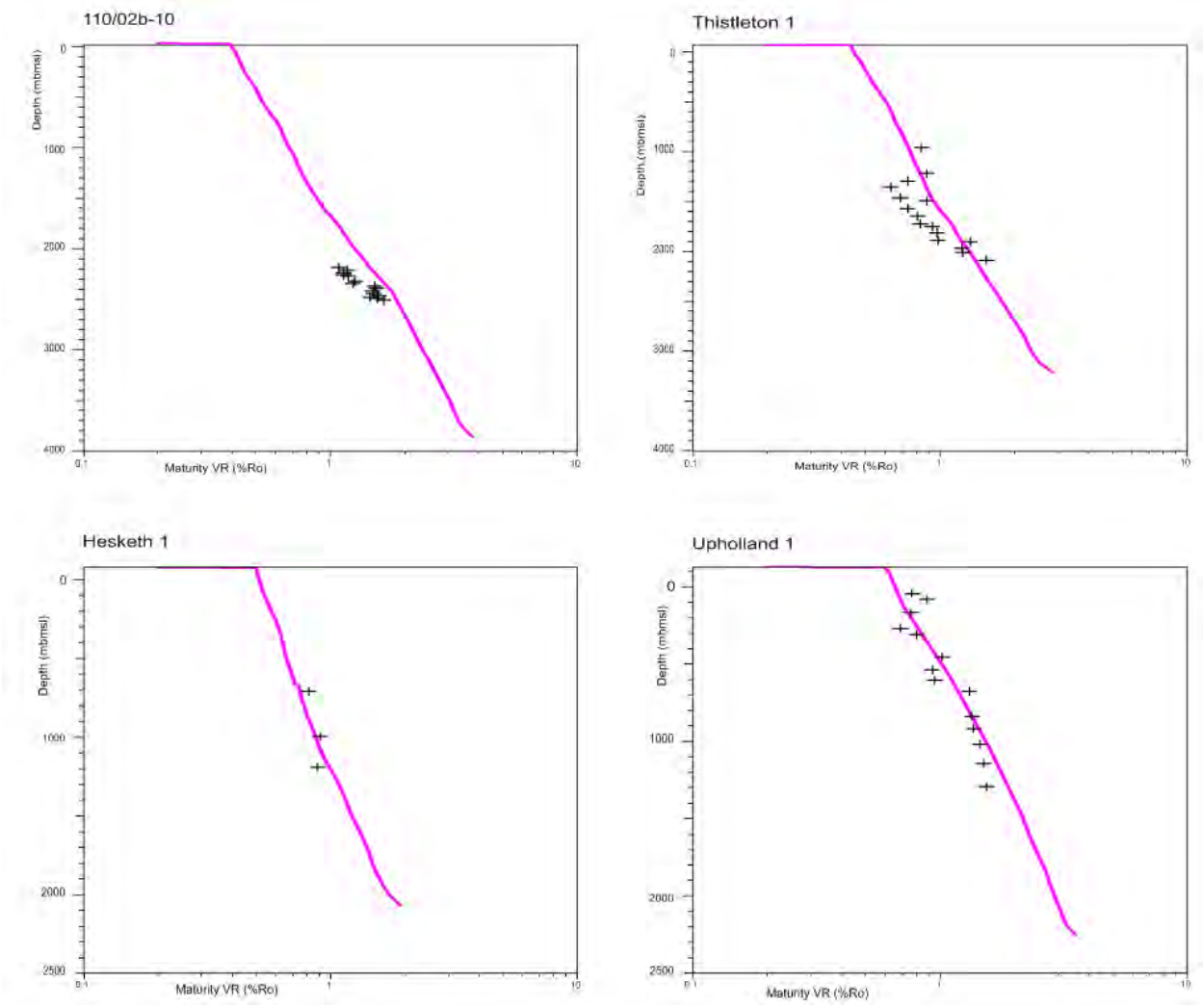

Figure 8. Maturity at well locations across the Irish Sea – Craven Basin 2-D section. The pink line shows model maturity, black crosses show VR data

5. Cheshire Basin section

5.1 Cheshire Basin geology

During most the Devonian, the Cheshire Basin was a region of erosion. Crustal extension began in the late Devonian and continued through the Visean. During the Early Visean, shallow marine deposition occurred in the north of the Cheshire Basin. Subsidence continued into the Late Visean, during which the whole Cheshire Basin region underwent marine deposition with a deeper marine environment prevailing in the north of the region. This was followed by uplift during early Namurian times when the south of the Cheshire Basin became emergent though the north of the basin remained an area of shallow marine deposition until the late Namurian when a more coastal/deltaic environment prevailed (Aitkenhead *et al.* 2002).

The Cheshire Basin is a half-graben formed as one of a series of sedimentary basins during Permo-Triassic rifting. The Permo-Triassic infill of this basin may have been up to four or five kilometres thick prior to geologically recent erosion. The basin is flanked to the east and west by Carboniferous and older rocks. The succession in this region displays widespread uplift and erosion resulting from the Variscan Orogeny (Plant *et al.* 1999).

5.1.1 Upholland 1

The palaeo-heat flow from a previously modelled borehole (Keele 1) was used as a basis for the heat flow for Upholland 1 as the vitrinite reflectance dataset is more complete (Vincent & Merriman 2002). Pearson & Russell (2000) provided VR data for Westphalian A to Pendleian age strata from the Upholland borehole. Stratigraphical data from Plant *et al.* (1999) were used to model the eroded stratigraphy. The VR data were then used to calibrate the model and the heat flow history was assumed to follow a similar pattern to that at Keele 1. Coal Measures in the Westphalian are algal-rich, which may have caused suppression of the VR values and therefore account for the slight difference between the model maturity curve and maturity data points in the Carboniferous coals of Upholland 1 (Figure 9c).

The Upholland 1-D model indicates approximately 800 m of sediment was removed during the Variscan uplift and 50 m during the Hardegsen event (Figure 9a), which agrees with thicknesses estimated in Plant *et al.* (1999). Permo-Triassic cover was calculated to be around 900 m, with a further 500 m deposited during the Jurassic and Cretaceous. The heat flow and temperatures reached are slightly lower than in the centre of the Cheshire Basin; this model shows heat flow of up to 73mWm^{-2} during the early Carboniferous, with temperatures of around 120°C in the Westphalian A coals, and slightly lower temperatures achieved on reaching a depth of about 2 km during the Cretaceous (Figure 9a and b). These results are fairly well constrained by the VR data. Figure 9c indicates that the Coal Measures reached the oil generation window.

5.1.2 Ince Marshes 1

Ince Marshes 1 lies between Knutsford 1 and Blacon East 1 in terms of proximity to the depocentre of the Cheshire Basin. It penetrates the Upper Bowland Shale (Figure 10a). The model achieved a reasonable fit to the data with an estimated 190 m additional Carboniferous strata added then eroded during the Variscan Orogeny and over 1 km of Permian – Triassic strata and 500 m of Jurassic to Cretaceous strata added then eroded during the Hardegsen and Palaeocene – Recent erosion. Model heat flow is shown in Figure 10b. Based on this model, the Upper Bowland Shale reached temperatures over 100°C during Carboniferous burial, and 120°C during deeper Cretaceous burial (Figure 10a), following a similar pattern to Knutsford 1. According to the model, both the Coal Measures and the Upper Bowland Shale reached the oil generation window (Figure 10c) from the Carboniferous onwards.

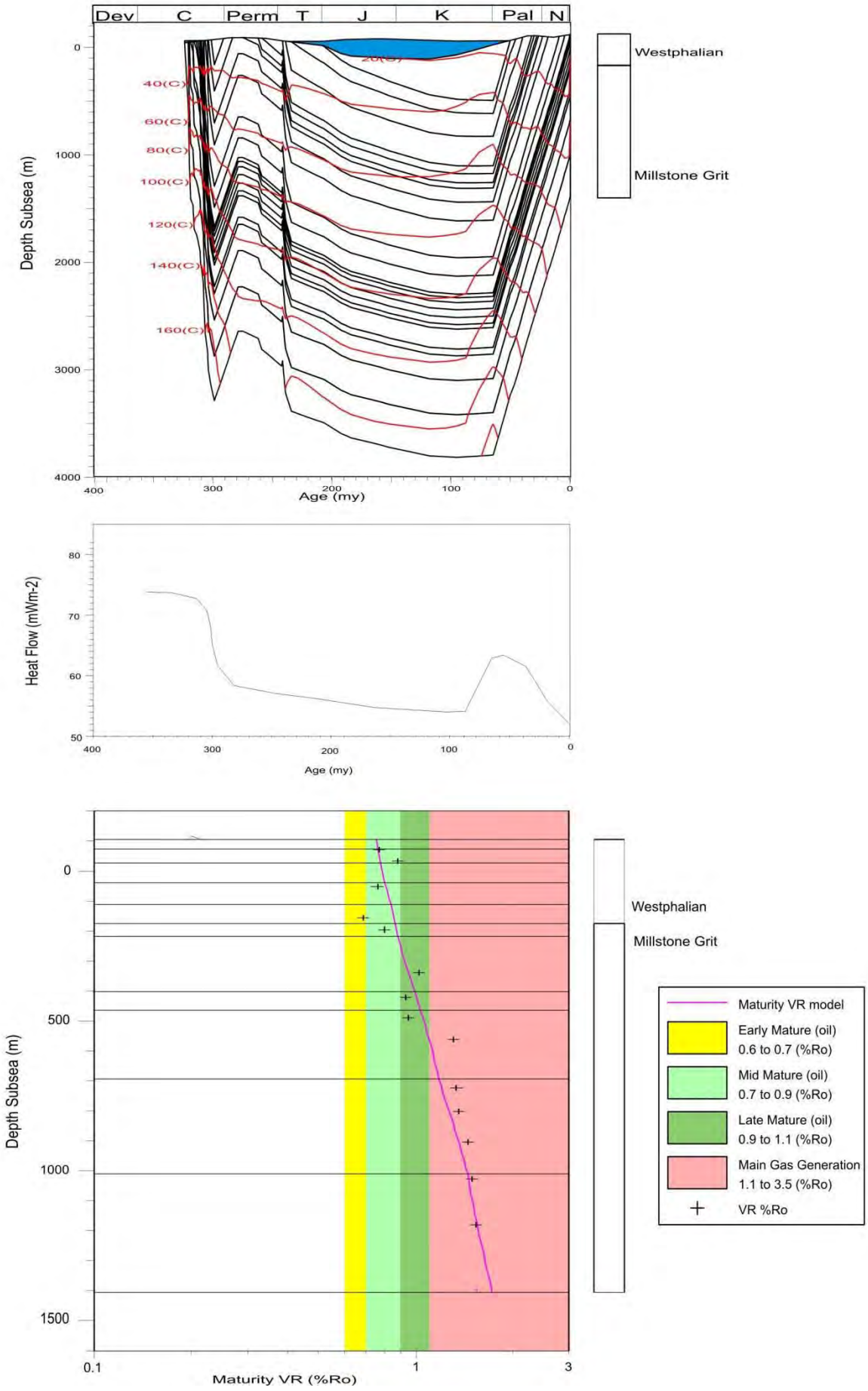

Figure 9. Upholland 1 model, 9a (top) shows the depositional history, 9b (centre) shows the modelled palaeo-heat flow and 9c (bottom) shows the modelled VR maturity and VR data.

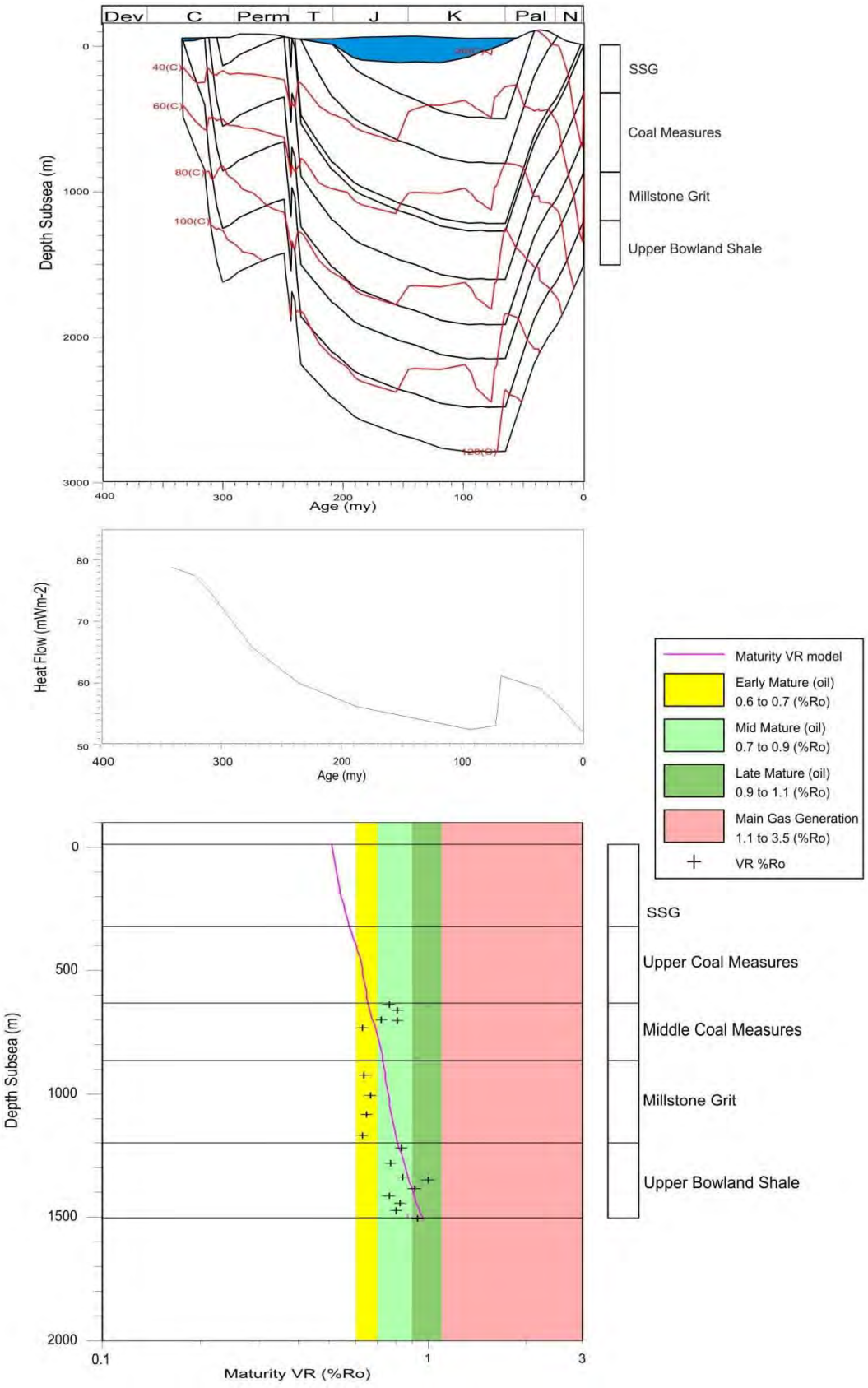

Figure 10. Ince Marshes 1 model, 10a (top) shows the depositional history, 10b (centre) shows the modelled palaeo-heat flow and 10c (bottom) shows the modelled VR maturity and VR data.

5.1.3 Knutsford 1

Limited vitrinite reflectance data are available in Pearson & Russell (2000) for the Knutsford 1 borehole. Porosity data from Plant *et al.* (1999) was also used. Borehole temperature data is also available in Burley *et al.* (1984). Lewis *et al.* (1992) provided AFTA data from the Westphalian, Permian and Triassic. Following the findings in Plant *et al.* (1999), fluid circulation in the basin was included in the model, using the '2-D fluid flow' and 'delta heat' options in BasinMod. '2-D fluid flow' assumes fluid flows through the borehole and surrounding area rather than a closed system with fluid circulation contained within the borehole. It was assumed that most circulation occurred in the porous Permo-Triassic sandstones during the Palaeogene. Borehole data were taken from records held in the NGRC at BGS Keyworth, and the eroded stratigraphy was estimated using information in Plant *et al.* (1999). These data were then used to develop a best-fit model.

The Knutsford 1-D model (Figure 11a) shows a different burial history from that of Keele 1 and Upholland 1, with highest temperatures achieved during the Cretaceous. The model implies removal of approximately 500 m of Carboniferous sediment during Variscan uplift, with deposition recommencing with the Sherwood Sandstone (Figure 11a). An estimated 50 m of overburden was also removed during the Hardegsen event. The model palaeo-heat flow peaked at 78 mWm^{-2} during the late Carboniferous (Figure 11b), with the Westphalian C coals reaching temperatures of around 60°C during the Westphalian and 160°C during Cretaceous/Palaeogene burial. Model calculations imply that late Cretaceous burial beneath 2.8 km of Permo-Triassic strata, with a further 1 km of Jurassic and Cretaceous strata, resulted in these coals experiencing burial of around 4 km and temperatures of 140°C. Figure 11c indicates that the Coal Measures reached the oil generation window during the Triassic and the gas generation window during the Cretaceous.

5.1.4 Blacon East 1

Blacon East 1 is located away from the main Cheshire Basin depocentre and Permo-Triassic sediment thicknesses are therefore thinner than at Knutsford 1. Eroded sediment thicknesses were estimated using Plant *et al.* (1999).

Limited VR data were available for Blacon East 1. The model implies removal of c.600 m of Carboniferous sediment during Variscan uplift, with deposition recommencing with the Sherwood Sandstone (Figure 12a). An estimated 50 m of overburden was also removed during the Hardegsen event. The model palaeo-heat flow peaked at 78 mWm^{-2} during the late Carboniferous (Figure 12b), with the deepest Bowland Shale sediments achieving temperatures of 160°C. Model calculations imply that late Cretaceous burial beneath 220 m of Permo-Triassic strata, with a further 200 m of Triassic, Jurassic and Cretaceous strata, resulted in these coals experiencing burial of around 1.5 km and temperatures of 140°C. Figure 12c indicates that the Bowland Shale reached the gas generation window during the Carboniferous.

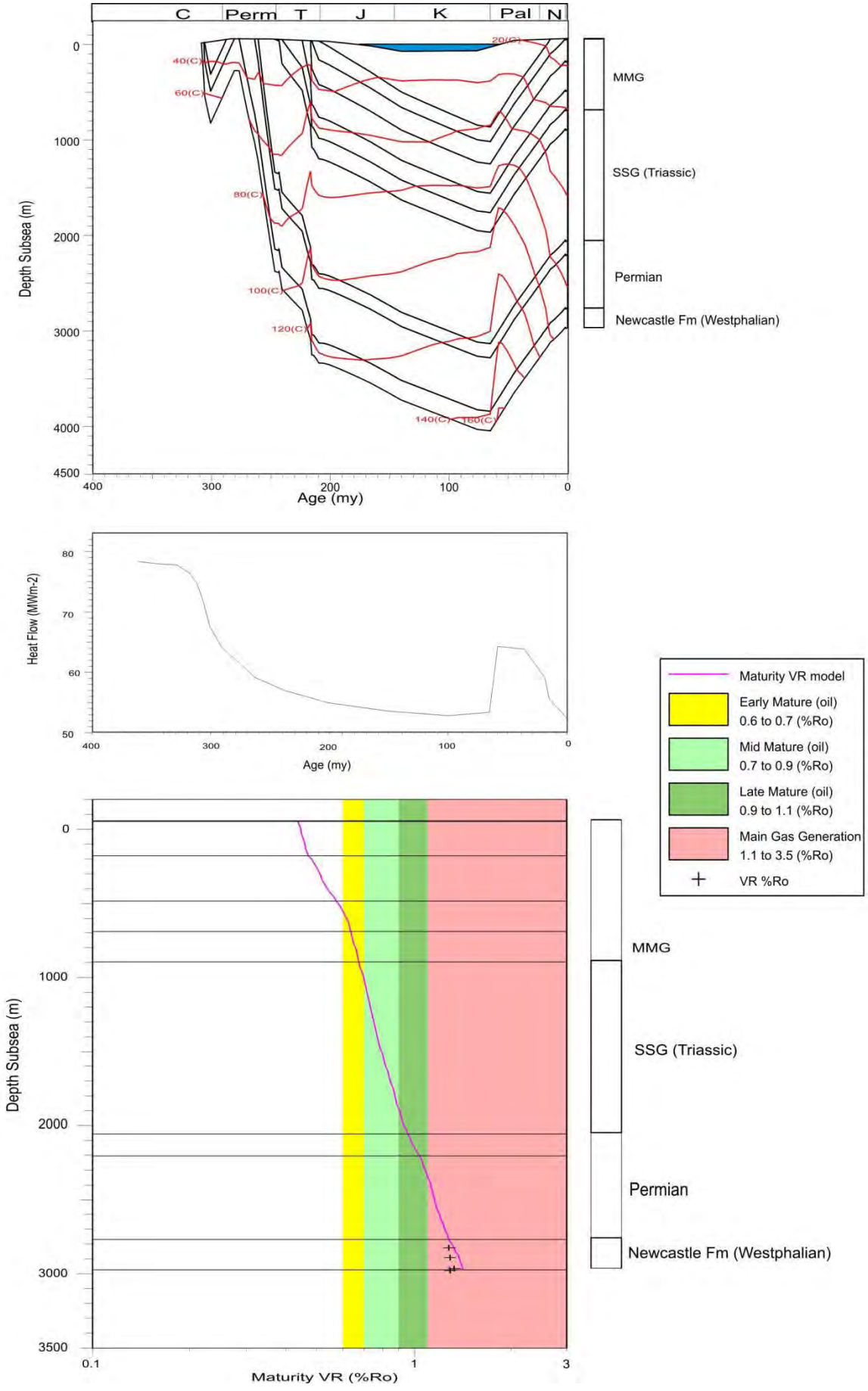

Figure 11. Knutford model, 11a (top) shows the depositional history, 11b (centre) shows the modelled palaeo-heat flow and 11c (bottom) shows the modelled VR maturity and VR data.

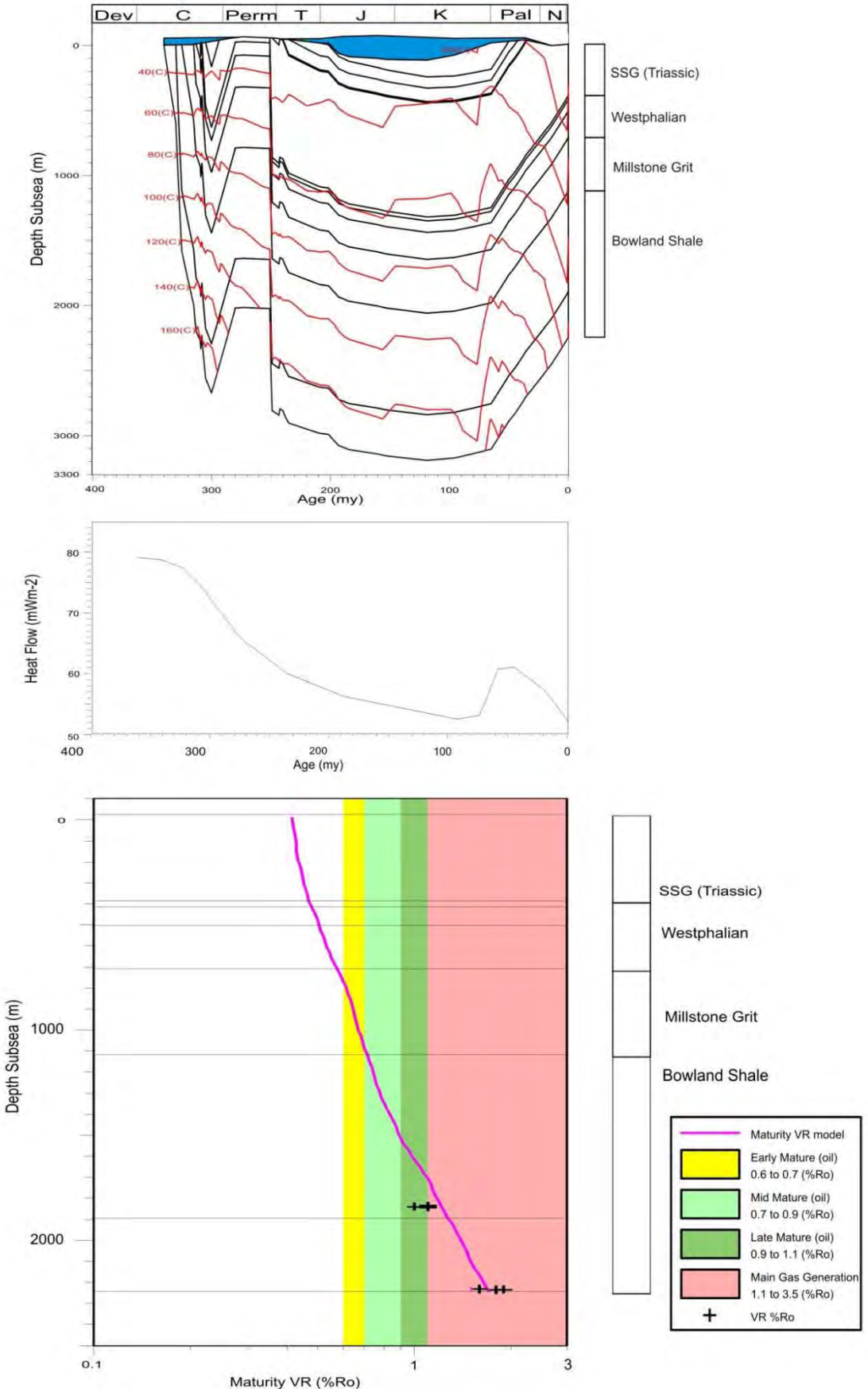

Figure 12. Blacon East 1 model, 12a (top) shows the depositional history, 12b (centre) shows the modelled palaeo-heat flow and 12c (bottom) shows the modelled VR maturity and VR data.

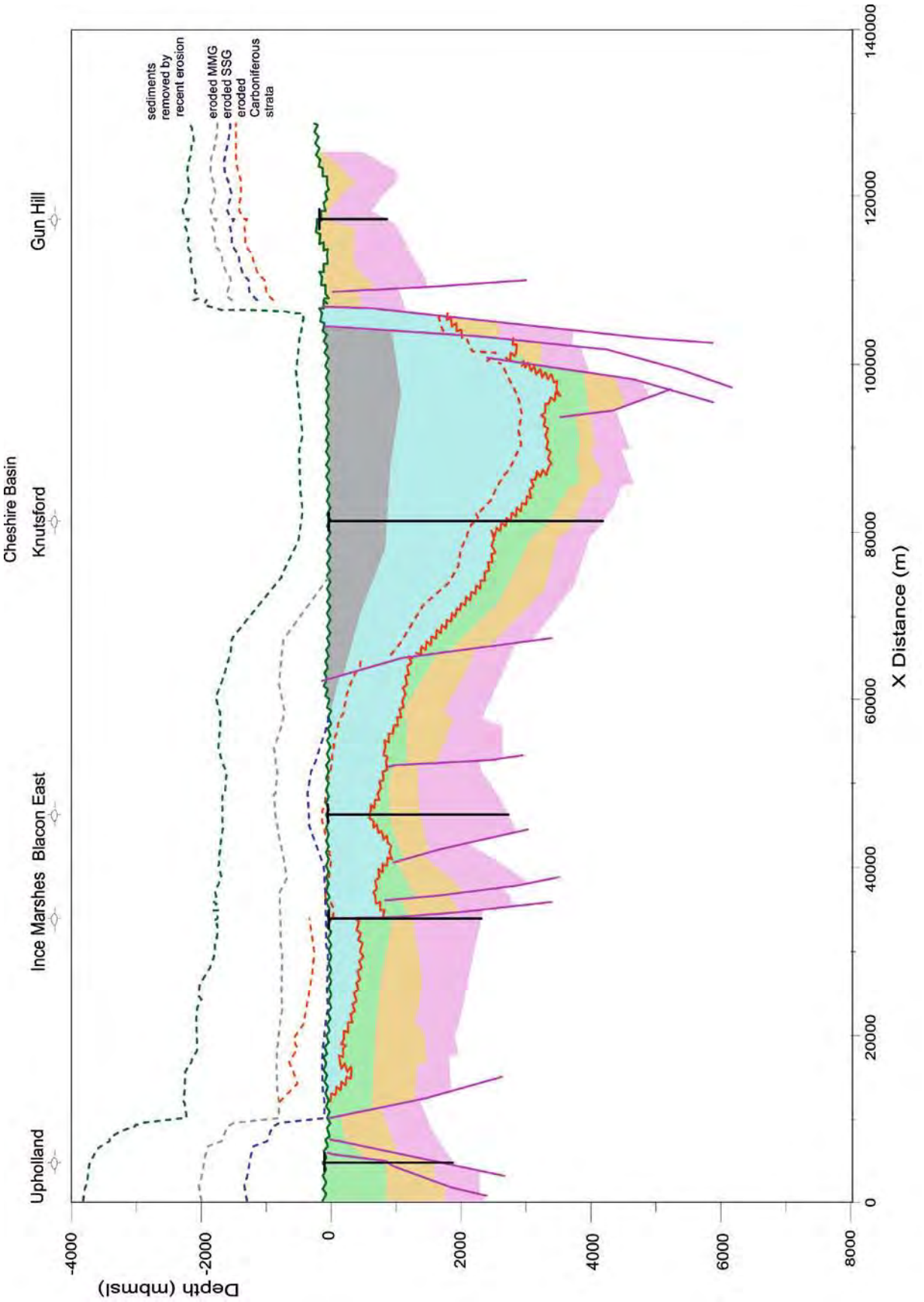

Figure 13. Cheshire Basin 2-D model. Grey is Mercia Mudstone Group, blue is Sherwood Sandstone Group and Permian, green is Westphalian, orange is Millstone Grit, pink is the Bowland-Hodder unit. The green unconformity is the current land surface, the red unconformity is the Variscan Unconformity. Dashed lines show eroded thicknesses of strata (the thickness between the unconformity/underlying eroded layer and the dashed line represents the eroded thickness). The base of the model is top Chadian.

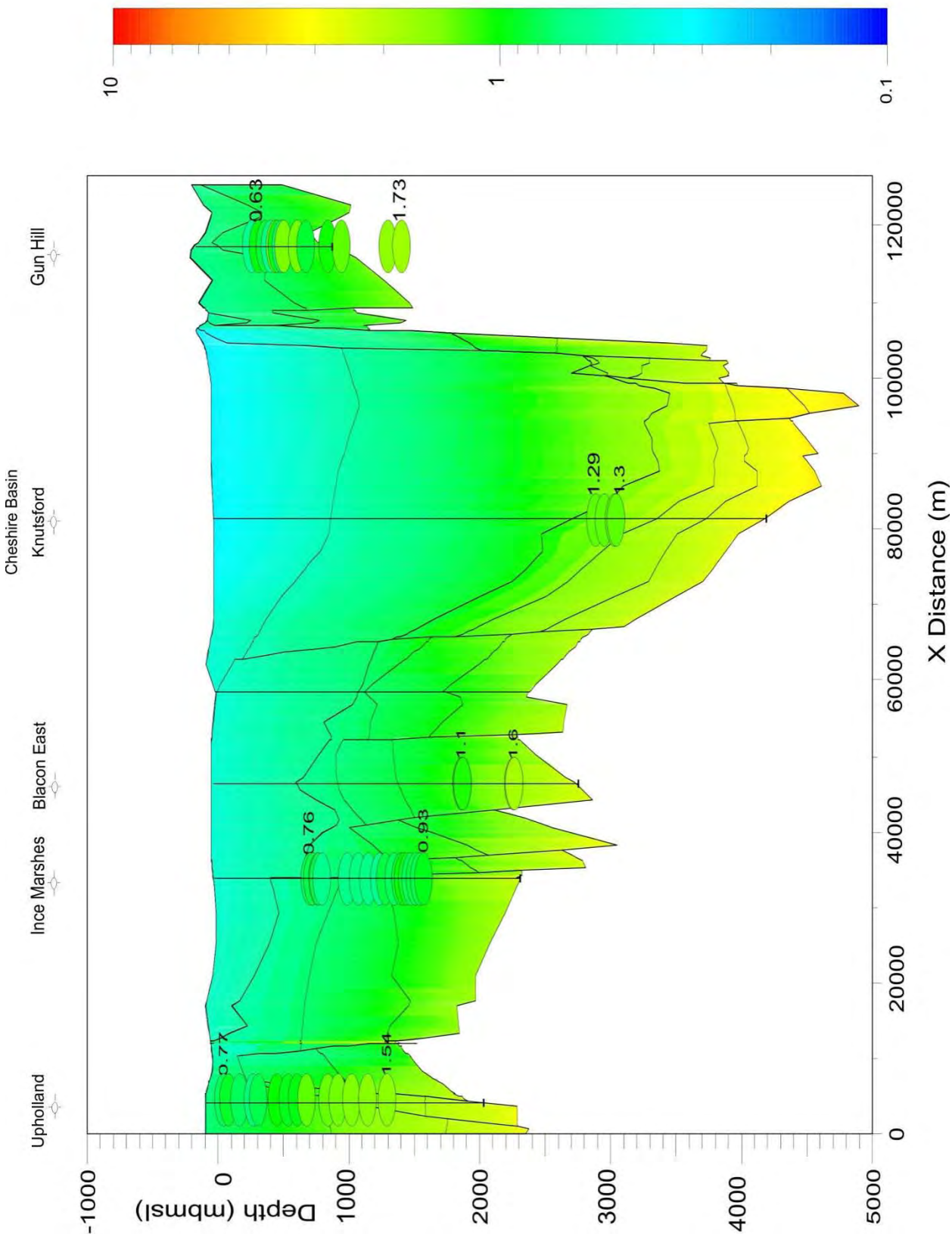

Figure 14. Maturity based on the model is indicated by colour across the whole basin, for comparison, the ovals show the VR data at the wells.

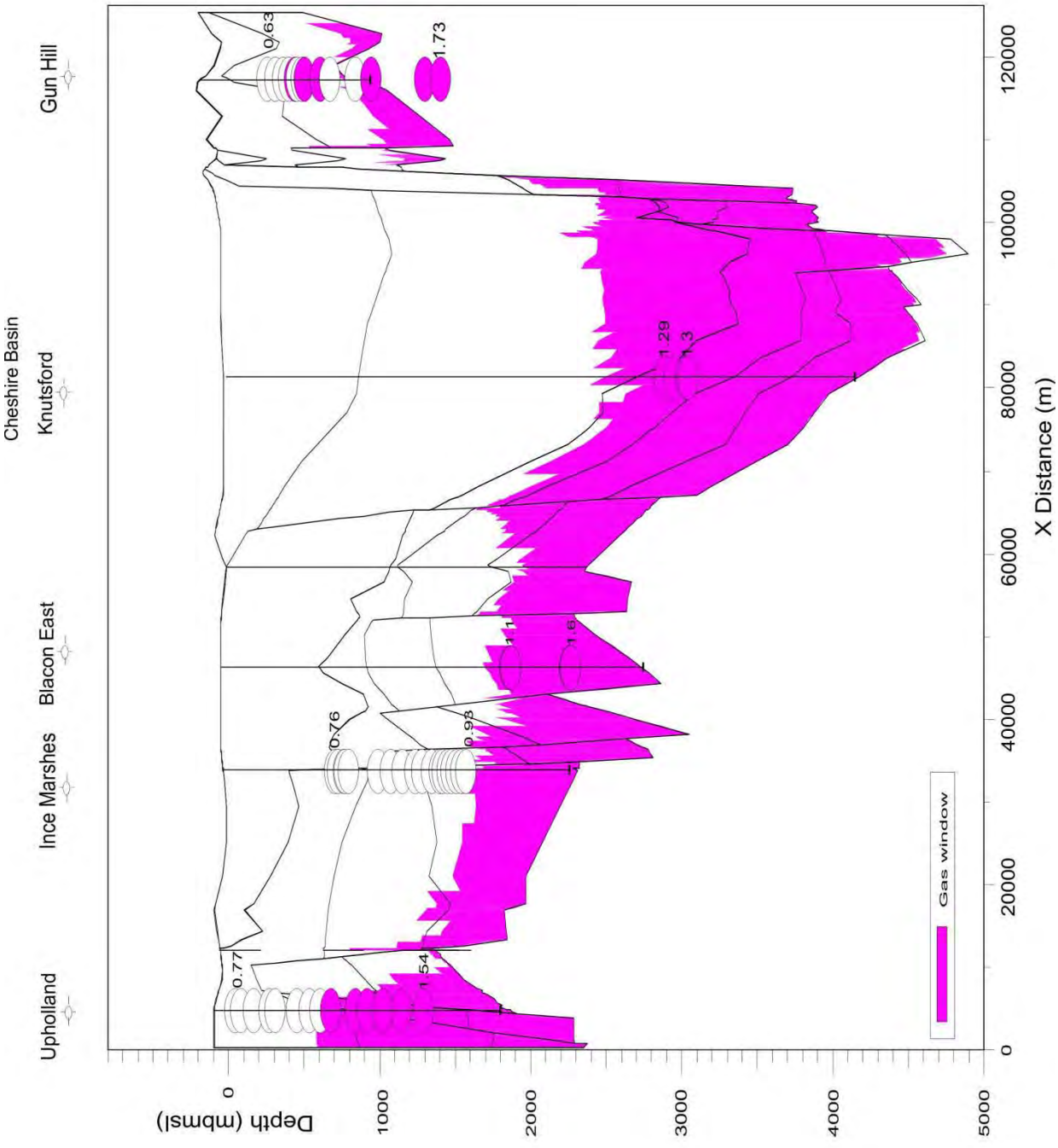

Figure 15. Present day gas window for the Cheshire Basin 2-D section

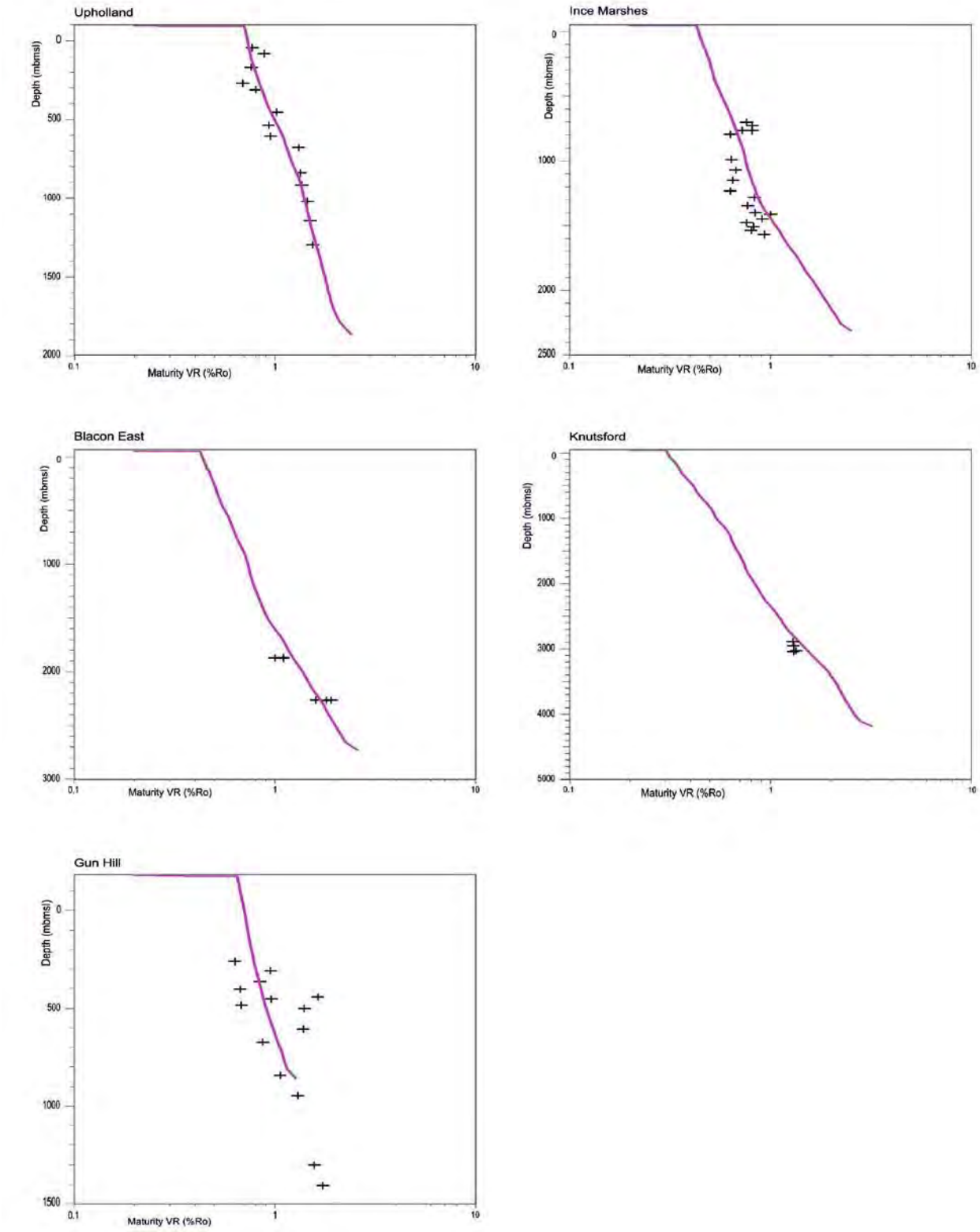

Figure 16. Maturity from the Cheshire Basin 2-D model at the borehole locations across the basin. The pink line shows the model maturity, the black crosses show the VR data

5.1.5 2-D section

Figure *13* and Figure 14 show the 2-D model which was generated for the Cheshire Basin section using the 1-D models as a basis.

Figure 13 shows the current sediment thicknesses across the basin as interpreted from seismic data. A good match to the data was obtained (Figure 14 and Figure 16) given the limitations on entering eroded thicknesses as described in section 2; i.e. that the eroded Carboniferous thickness has been added to the eroded thickness of sediment removed by the latest erosion and the time for the start of this combined erosion was given as the end Carboniferous (Figure *13*). The model indicates that much of the Bowland-Hodder unit of Arundian to Pendleian age is in the gas generation window

6. Widmerpool Gulf – Gainsborough Trough

6.1 Widmerpool Gulf geology

The Bowland Shale is thick in this region, with over 2 km predicted by seismic interpretation (Pharaoh *et al.* 2011). In North Staffordshire, the Millstone Grit shows rhythmic deposition in a deltaic environment and has a recorded thickness of around 1055 m in boreholes in the Widmerpool Gulf. Deposition began in the Marsdenian in South Staffordshire and Widmerpool Gulf became a depocentre for Millstone Grit during the Marsdenian. To the north of the region, the Millstone Grit was more argillaceous. Westphalian Lower and Middle Coal Measures have a recorded thickness of up to 1220 m in North Staffordshire, with Westphalian A sediments being particularly well developed. The oldest Lower Coal Measures are found in the northern part of the region. North Staffordshire coalfields show the maximum development of Upper Coal Measures and Warwickshire Group, including around 335 m Upper Coal Measures and 1320 – 1412 m Warwickshire Group sediments (Hains & Horton 1969).

In this region, the total estimated thickness of the Sherwood Sandstone Group (SSG) varies widely and reaches a maximum thickness in the Cheshire Basin of around 2621 m (Plant *et al.* 1999). Between 30 – 152 m of overlying Mercia Mudstone Group (MMG) has been recorded and around 15 m of Rhaetic sediments occur near East Leake. Jurassic sediments 352 – 527 m thick have been recorded in boreholes and outcrops in this region (Nottinghamshire and the Midlands; Hains & Horton 1969).

In Derbyshire, there are volcanic rocks of Brigantian age and Tertiary intrusions are recorded in Cheshire and Shropshire (Hains & Horton 1969).

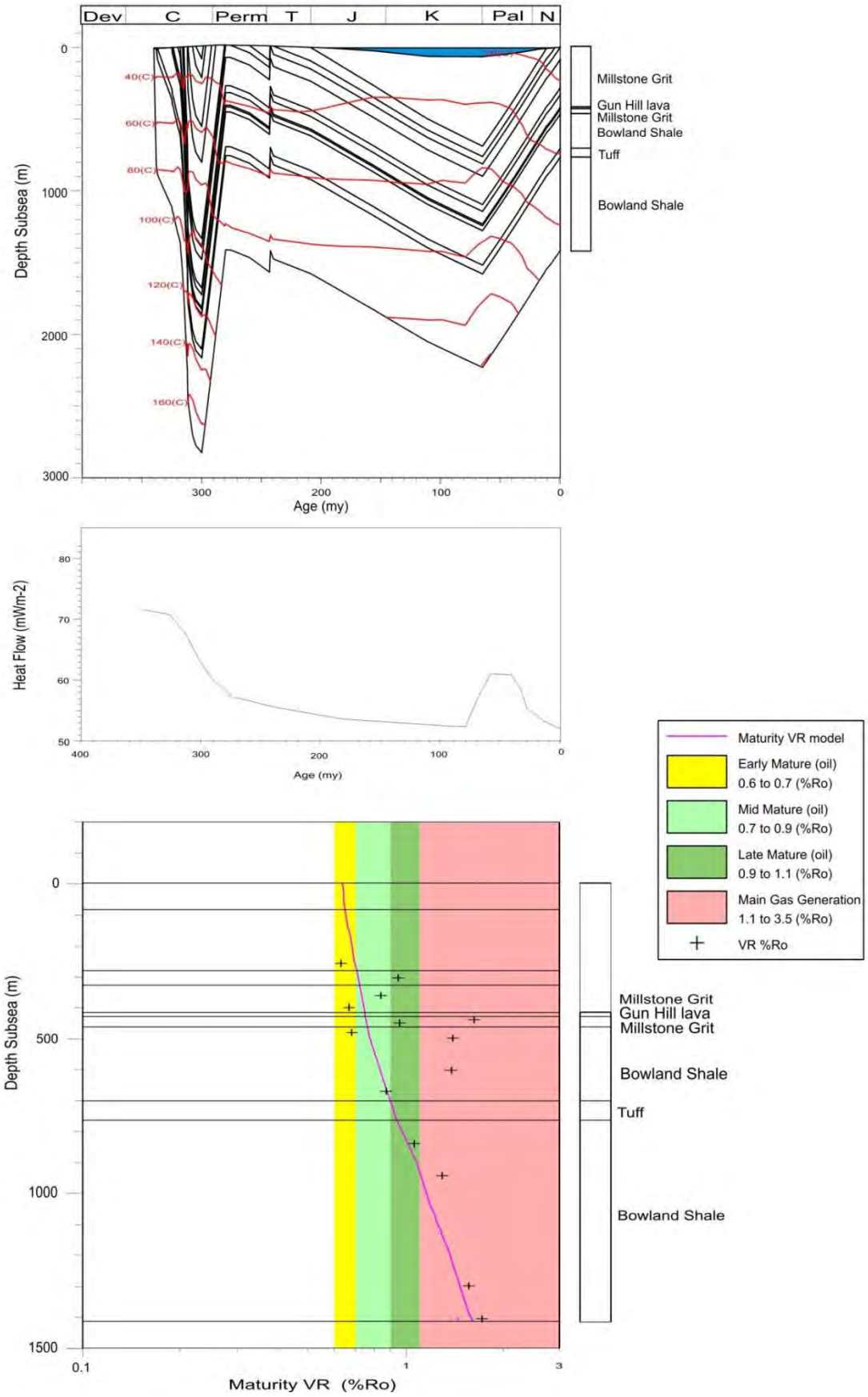

Figure 17. Gun Hill model, 17a (top) shows the depositional history, 17b (centre) shows the modelled palaeo-heat flow and 17c (bottom) shows the modelled VR maturity and VR data.

6.1.1 Gun Hill 1

The Gun Hill 1 borehole shows rapid deposition of thick Carboniferous sequences, with the oldest Bowland Shale reaching temperatures of 160°C (Figure 17a). The model implies removal of approximately 1320 m of Carboniferous sediment during Variscan uplift. The model palaeo-heat flow peaked at 70 mWm^{-2} during the late Carboniferous (Figure 17b). Model calculations imply that late Cretaceous burial beneath 180 m of Permo-Triassic strata, with a further 600 m of Jurassic and Cretaceous strata resulted in temperatures of 120°C in the Bowland Shale.

The VR data indicate that the Bowland Shale reached the gas generation window. Erosion occurred during the Triassic (Hardegsen) and Palaeocene - Recent times exposing Millstone Grit at the surface. The model indicates that the Bowland Shale reached the gas generation window during the Carboniferous (Figure 17c).

The fit of the model to the data may also be influenced by the Gun Hill lava, as the additional heat would have affected the VR readings of layers immediately underneath. In Figure 17c, a high VR reading is recorded immediately underneath the lava flow.

6.1.2 Long Eaton 1

The Long Eaton 1 borehole shows Triassic sediments deposited unconformably on the Widmerpool and Long Eaton Formations of Asbian to Chadian age (Craven Group). These sediments reached maximum depths of burial of around 3 km (Figure 18a) according to the model. The model was constructed with an estimated additional 890 m of Carboniferous sediments removed during erosion associated with the Variscan Orogeny. This was followed by deposition of around 170 m of Permo-Triassic and 340 m of Jurassic – Cretaceous. As there are very few VR data, the heat flow profile from nearby Gun Hill 1 was used as a basis for this model. The model implies that the deepest Craven Group sediments reached the gas generation window and achieved temperatures of up to 200°C during Carboniferous burial.

Given the lack of VR data for this borehole (8 VR data within a very narrow depth range, see Figure 18c) and the fact that this borehole is located in the depocentre of the Widmerpool Gulf, it seems likely that these eroded sediment thicknesses are rather underestimated and confidence in the results of this 1-D model is low.

6.1.3 Ilkeston 1

The Ilkeston 1 borehole penetrates sediments of Westphalian A and Namurian (Yeadonian – Arnsbergian) age (Figure 19a). The model implies that an estimated 600 m of Carboniferous strata were removed during Variscan uplift and erosion. This was followed by deposition of Permo-Triassic sediments, with a modelled thickness of 540 m and Jurassic – Cretaceous sediments with a modelled thickness of 510 m. Limited VR data were available for Ilkeston 1 and the heat flow from Gun Hill 1 formed the basis for this model. The model implies the deepest Bowland Shale sediments achieved temperatures of 120°C during Carboniferous burial (Figure 19a). Figure 19c indicates that the Bowland Shale reached the early oil generation window during the Carboniferous.

Very few VR data are available, so this model should be used with caution; however, the depth of burial seems reasonable for the location (near to the margin of the Widmerpool Trough). It should also be noted that the VR readings are taken from sediments below a fault shown on the borehole log and the data may not give an accurate indication of maturity for this borehole if the rocks have been significantly displaced in depth.

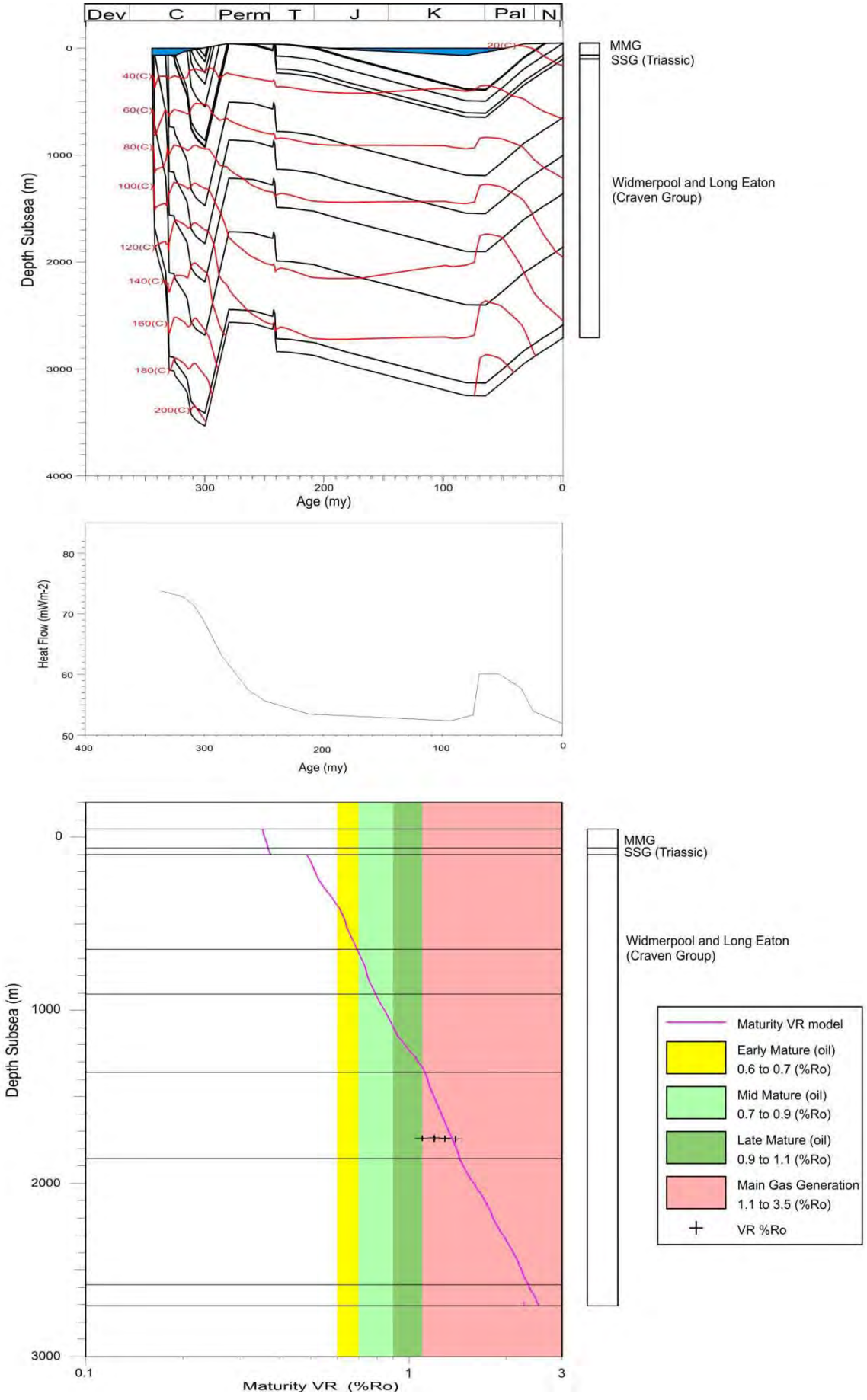

Figure 18. Long Eaton model, 18a (top) shows the depositional history, 18b (centre) shows the modelled palaeo-heat flow and 18c (bottom) shows the modelled VR maturity and VR data.

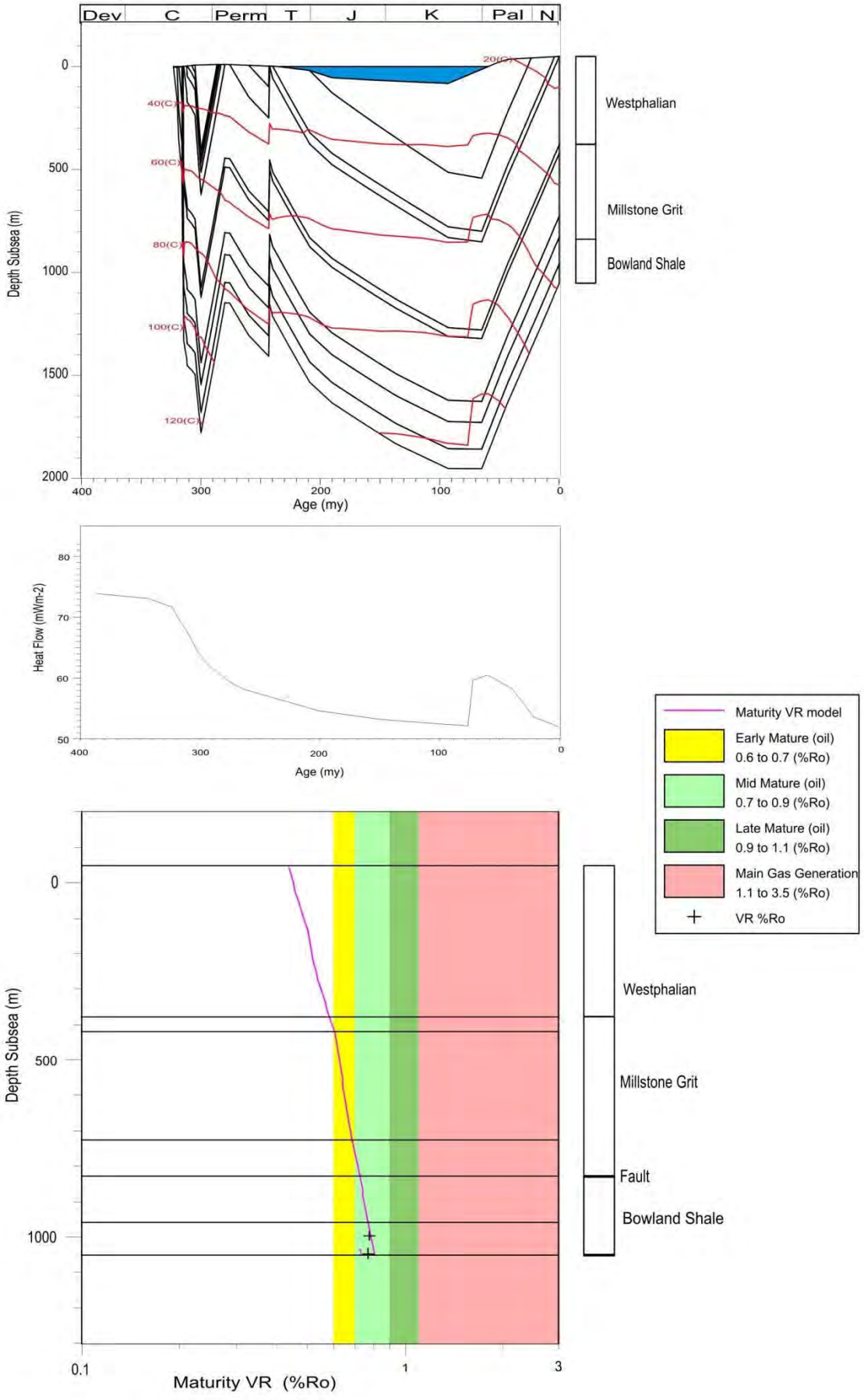

Figure 19. Ilkeston model, 19a (top) shows the depositional history, 19b (centre) shows the modelled palaeo-heat flow and 19c (bottom) shows the modelled VR maturity and VR data.

6.2 Gainsborough Trough geology

The Bowland Shale was deposited in shallowing marine condition, with deep marine conditions during the early Visean and shallow marine conditions during the late Visean. This was followed by deposition of shallow marine/deltaic sediments during the Namurian and Westphalian. Following uplift during the Variscan Orogeny, this region again subsided through the Permian to become fully marine during the Jurassic and Cretaceous. Recent uplift has exposed Permian and Carboniferous rocks in this region.

Recorded thicknesses of Coal Measures are up to 2200 m and the Warwickshire Group reaches thicknesses of up to 140 m east of the Pennine High. Permian sediments in this region are around 88 – 158 m thick, Triassic Sherwood Sandstone Group sediments are around 400 m thick and Mercia Mudstone Group sediments are up to 190 m thick (Aitkenhead *et al.* 2002).

Volcanic activity occurred to the south during latest Namurian times.

The Grove 3 borehole has a heat flow of 54 mWm^{-2} (Downing & Gray 1986), however, other boreholes in this trough such as Ranby 1 and Scaftworth B2 have higher present day heat flows (75 to 83 mWm^{-2}) (Downing & Gray 1986).

Overall, the VR data for the Gainsborough Trough are not as satisfactory as for the other regions modelled for this report. There are very limited data for Grove 3 and the data for Gainsborough 2 and Kirk Smeaton 1 show a broad scatter. Thus confidence in the models is lower than for models previously described. However, it should be noted that a significant number of the VR data for Kirk Smeaton 1 and the VR data for Grove 3 are all in the gas generation window.

6.2.1 Grove 3

Grove 3 penetrates sediments of Permo-Triassic age resting unconformably on sediments of Westphalian C age (Figure 20a). The oldest sediments are Bowland Shales of Courceyan age and the well terminated in Early Palaeozoic phyllites. The model implies deposition and subsequent removal of 900 m of Carboniferous sediment. The deepest Bowland Shale sediments reached temperatures of over 180°C during Carboniferous burial and again during Cretaceous burial. Over 350 m of Permian sediments are recorded in the borehole. An estimated eroded thickness of 1200 m of Permian – Cretaceous sediments was also included in the model. The oldest Bowland Shale in the borehole reached the gas generation window during the Carboniferous.

It should be noted that only 1 VR data point was available, so confidence in this model is low and much of the heat flow model was based on Gainsborough 2 and Kirk Smeaton 1 which have more complete VR datasets (Figure 20c).

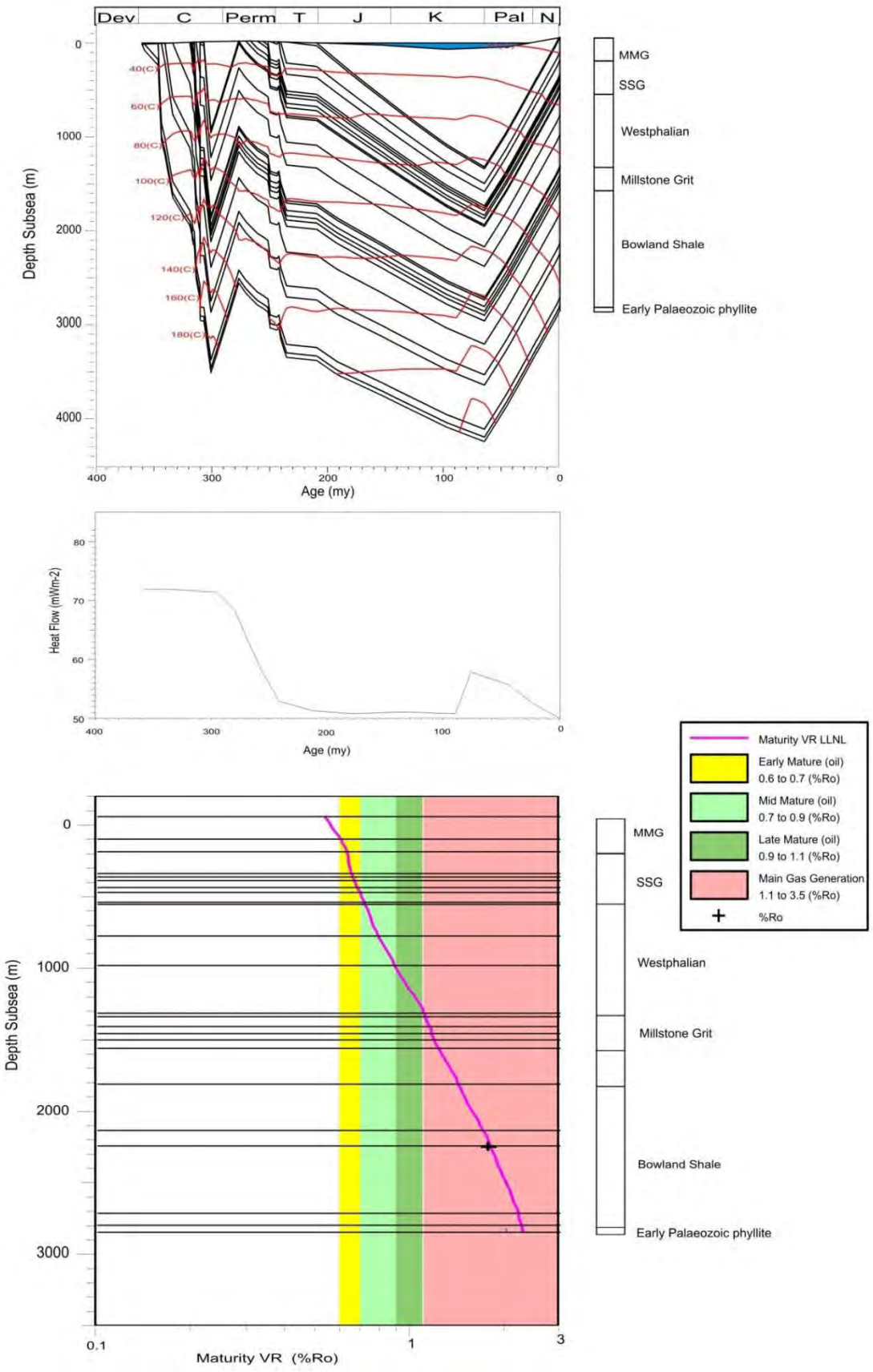

Figure 20. Grove 3 model, 20a (top) shows the depositional history, 20b (centre) shows the modelled palaeo-heat flow and 20c (bottom) shows the modelled VR maturity and VR data.

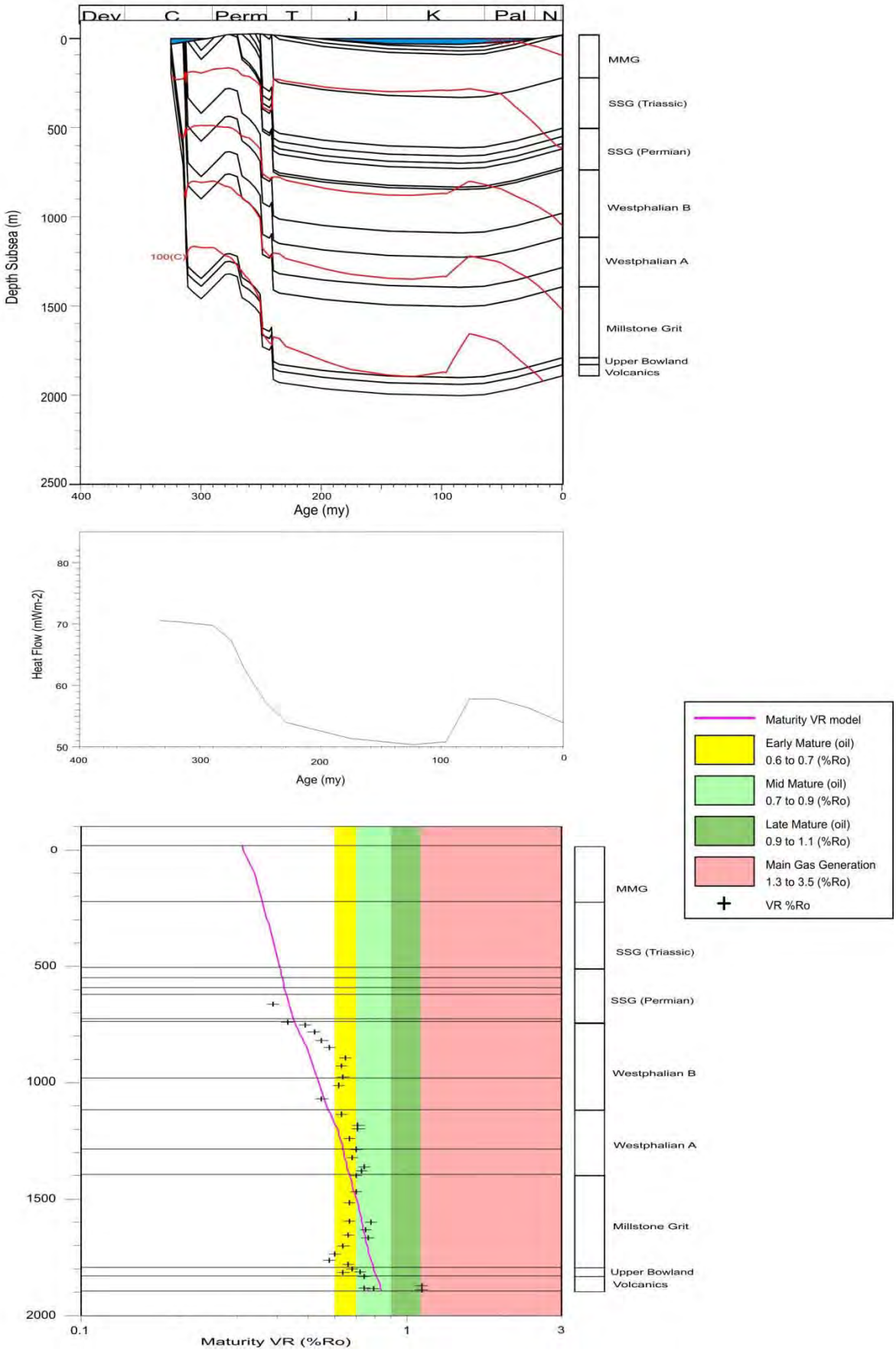

Figure 21. Gainsborough 2 model, 21a (top) shows the depositional history, 21b (centre) shows the modelled palaeo-heat flow and 21c (bottom) shows the modelled VR maturity and VR data.

6.2.2 Gainsborough 2

The Gainsborough 2 borehole penetrates through Permian sediments to the Upper Bowland Shale (Figure 21a). Thirty nine VR data were available and the model fit is reasonable, though there is a broad scatter on the data.

The model heat flow is quite low, having a heat flow of around 70 mWm^{-2} during the late Carboniferous (Figure 21b). The deepest Bowland Shale sediments reached temperatures of over 100°C (Figure 21a). The Upper Bowland Shale reached the oil generation window during Carboniferous burial. An estimated 110 m of Carboniferous sediment was removed during uplift during the Variscan Orogeny. Deposition during the Permian – Cretaceous was quite thin in comparison with other wells in this area; only 515 m is proven in the borehole and a modelled additional 85 m of Permian – Cretaceous sediments eroded by the Hardegsen and Palaeocene – Recent erosion were included in the model. Both the low heat flow and thin sediment deposition seem unusual given the location is not particularly close to the Gainsborough Trough margins. The fit of the 1-D model clearly shows the compromise made here between palaeo-heat flow and eroded sediment thicknesses; if a greater palaeo-heat flow had been modelled to better match the gradient, then the estimated thicknesses of eroded sediment would have been even smaller.

6.2.3 Kirk Smeaton 1

Kirk Smeaton 1 lies on a northern basin bounding fault on the Gainsborough Trough. The modelled heat flow is quite low having a heat flow of around 65 mWm^{-2} during the late Carboniferous. The model indicates that the Lower Bowland Shale reached temperatures of 120°C during Carboniferous burial and 140ºC during Cretaceous burial (Figure 22a). An estimated 1 km of sediment was removed during the Variscan Orogeny. A small remnant of Permian Collyhurst Sandstone is present in the borehole. The removed thicknesses of the Permo-Triassic and Jurassic – Cretaceous layers were 450 m and 800 m respectively. The model fit is reasonable (Figure 22c) and the low heat flow and thin sediments are typical of boreholes closer to the basin margin than the basin depocentre. The fit of the 1-D model clearly shows the compromise made here between palaeo-heat flow and eroded sediment thicknesses; if a greater palaeo-heat flow had been modelled to better match the gradient, then the estimated thicknesses of eroded sediment would have been even smaller.

6.2.4 2-D section

Figure 23 and Figure 24 show the 2-D model which was generated using the 1-D models as a basis. Figure 23 shows the current sediment thicknesses across the basin as interpreted from seismic data. A good fit to the VR data was achieved (Figure 24 and Figure 26). This section clearly shows the impact of the modelled eroded sediments on the maturity of the basins. The deepest parts of the basin have gone through the gas window and are now over-mature (Figure 25). Note that the reverse fault near Eakring has been included as a normal fault in order to model the sediments as BasinMod 2-D cannot include repeated layers in vertical section (Figure 23). Also, where the Variscan erosional surface has been removed, most the eroded thickness of Carboniferous sediments has been added to the thickness removed by the most recent erosion.

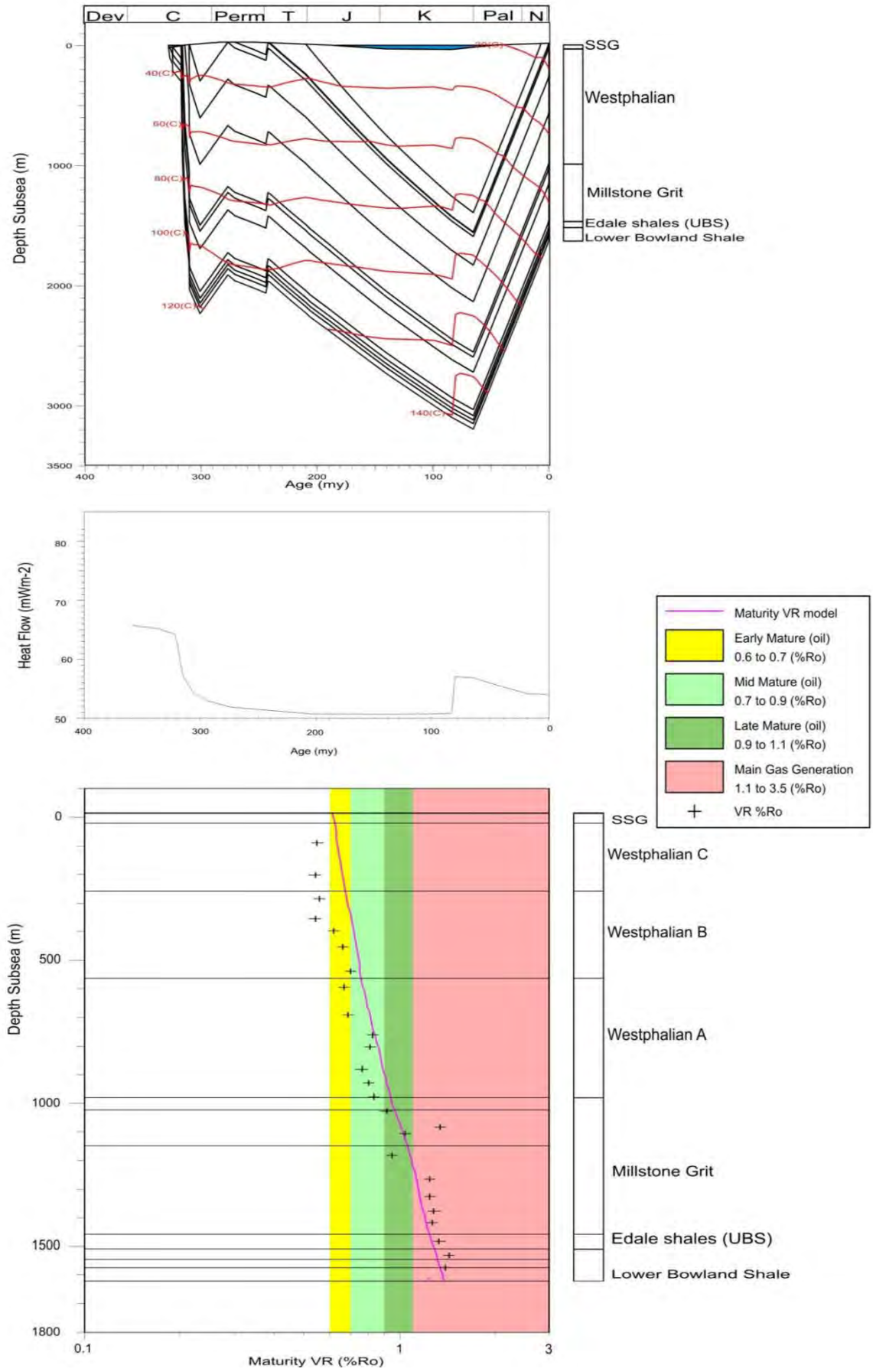

Figure 22. Kirk Smeaton model, 22a (top) shows the depositional history, 22b (centre) shows the modelled palaeo-heat flow and 22c (bottom) shows the modelled VR maturity and VR data.

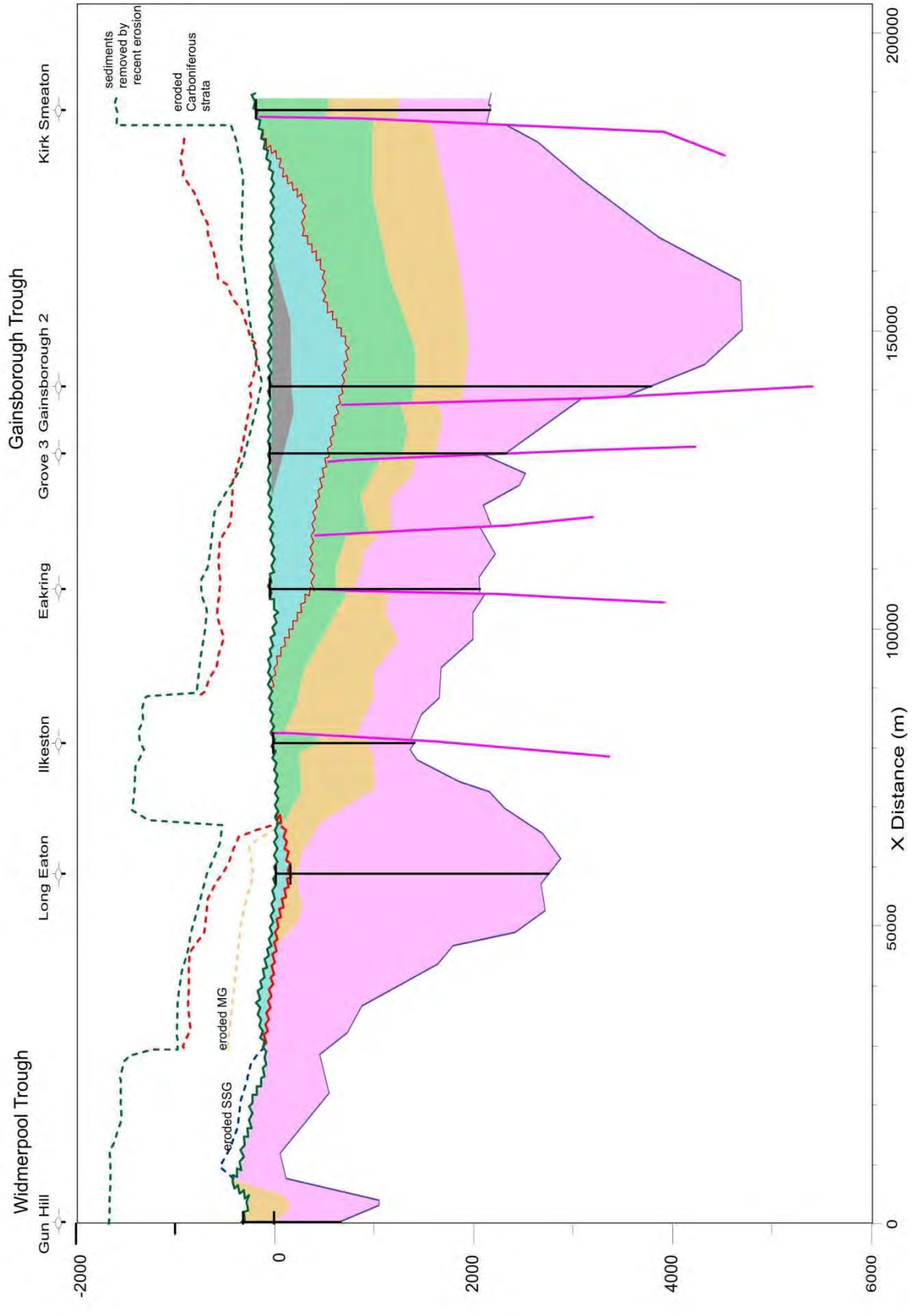

Figure 23. 2-D section across the Widmerpool Gulf and Gainsborough Trough. Grey is MMG, blue is SSG and Permian, green is Westphalian, orange is Millstone Grit, pink is the Bowland-Hodder unit. The green unconformity is the current land surface, the red unconformity is the Variscan Unconformity. Dashed lines show eroded thicknesses of strata (the thickness between the unconformity/underlying eroded layer and the dashed line represents the eroded thickness). The bottom of the model is Top Chadian.

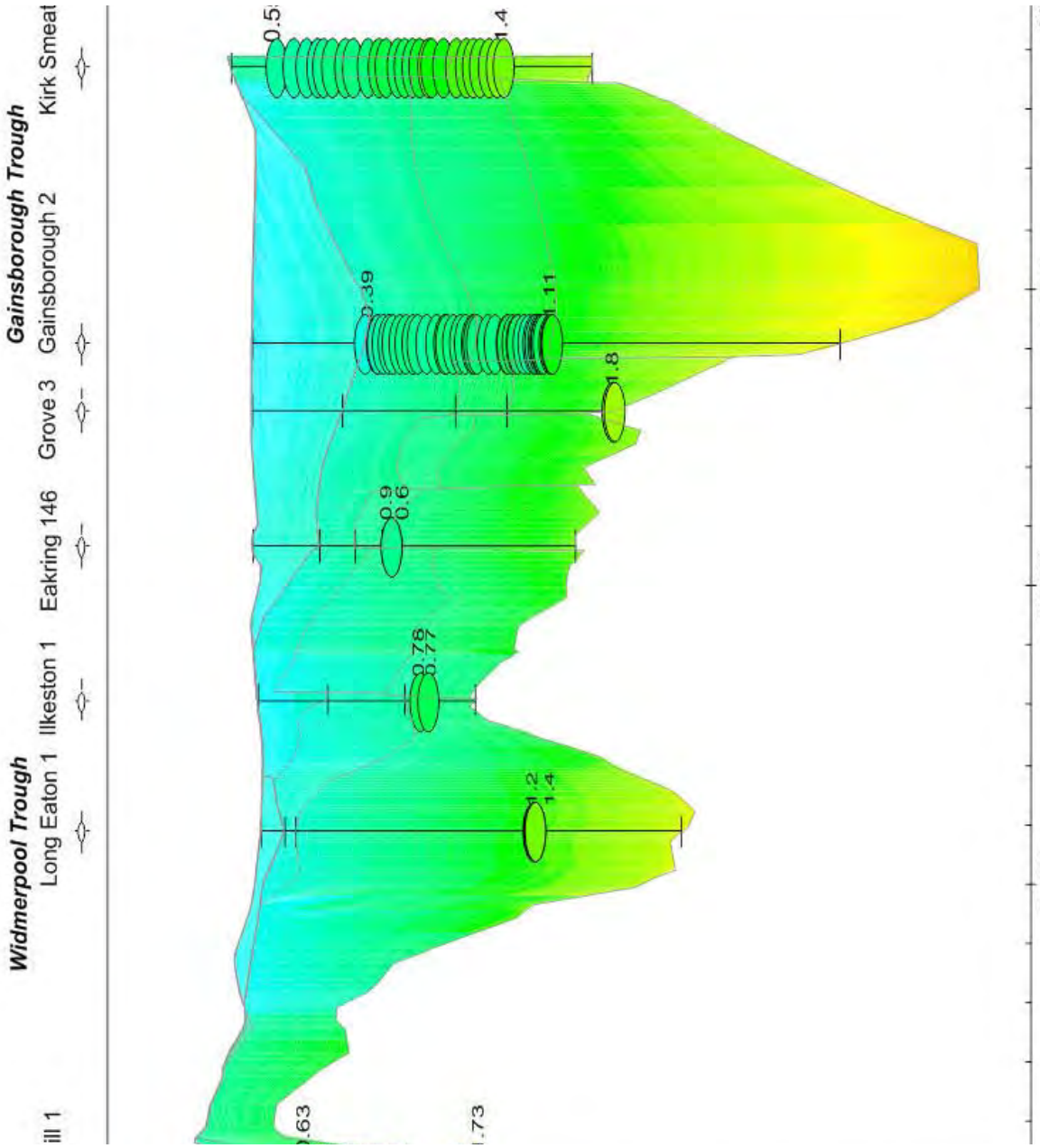

Figure 24. Maturity for the Widmerpool Trough – Gainsborough Trough 2-D section, the continuous colour shows the maturity based on the model, for comparison, the ovals show the measured VR data at the wells.

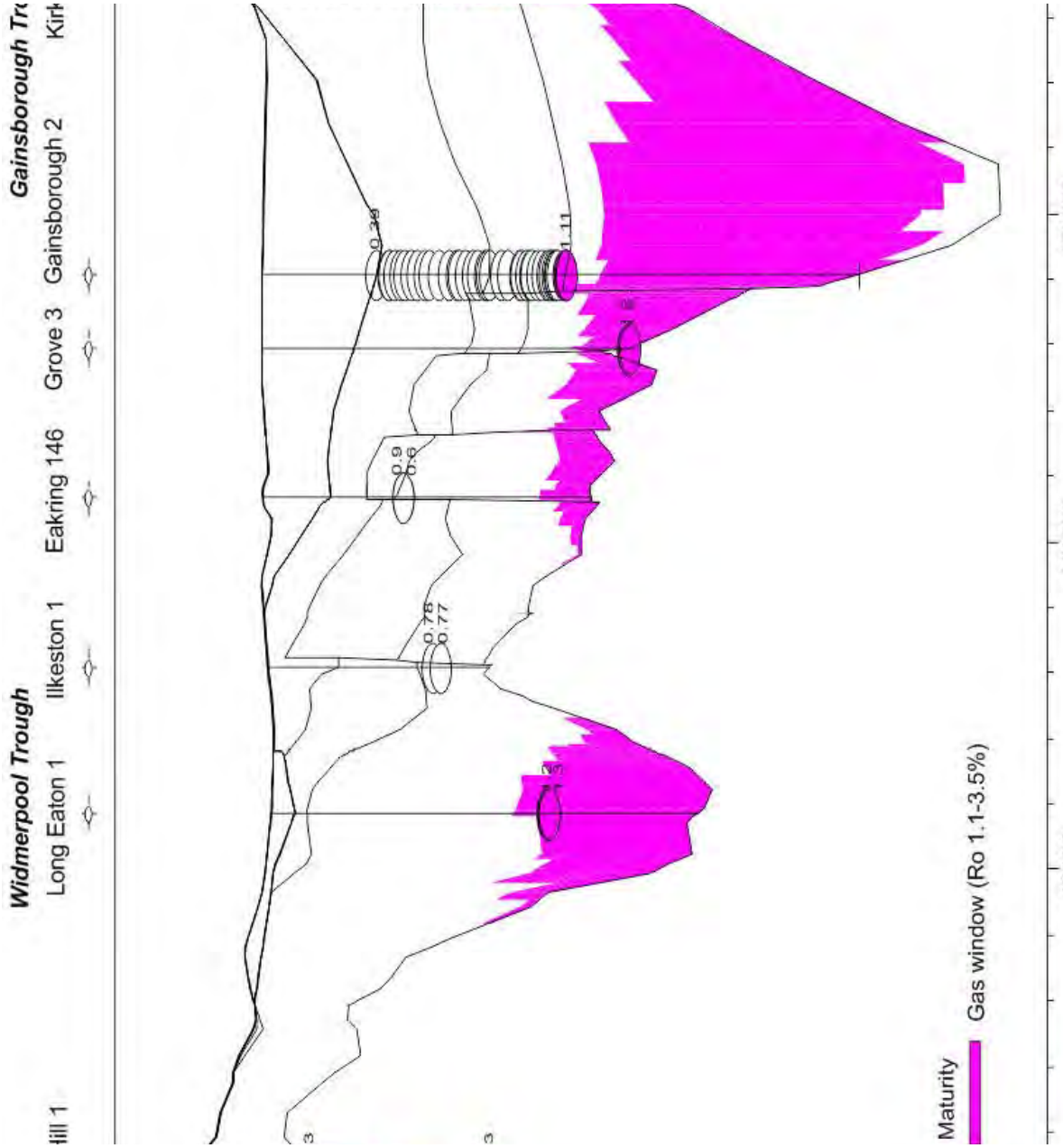

Figure 25. Present day gas window for the Widmerpool Trough - Gainsborough Trough 2-D section model.

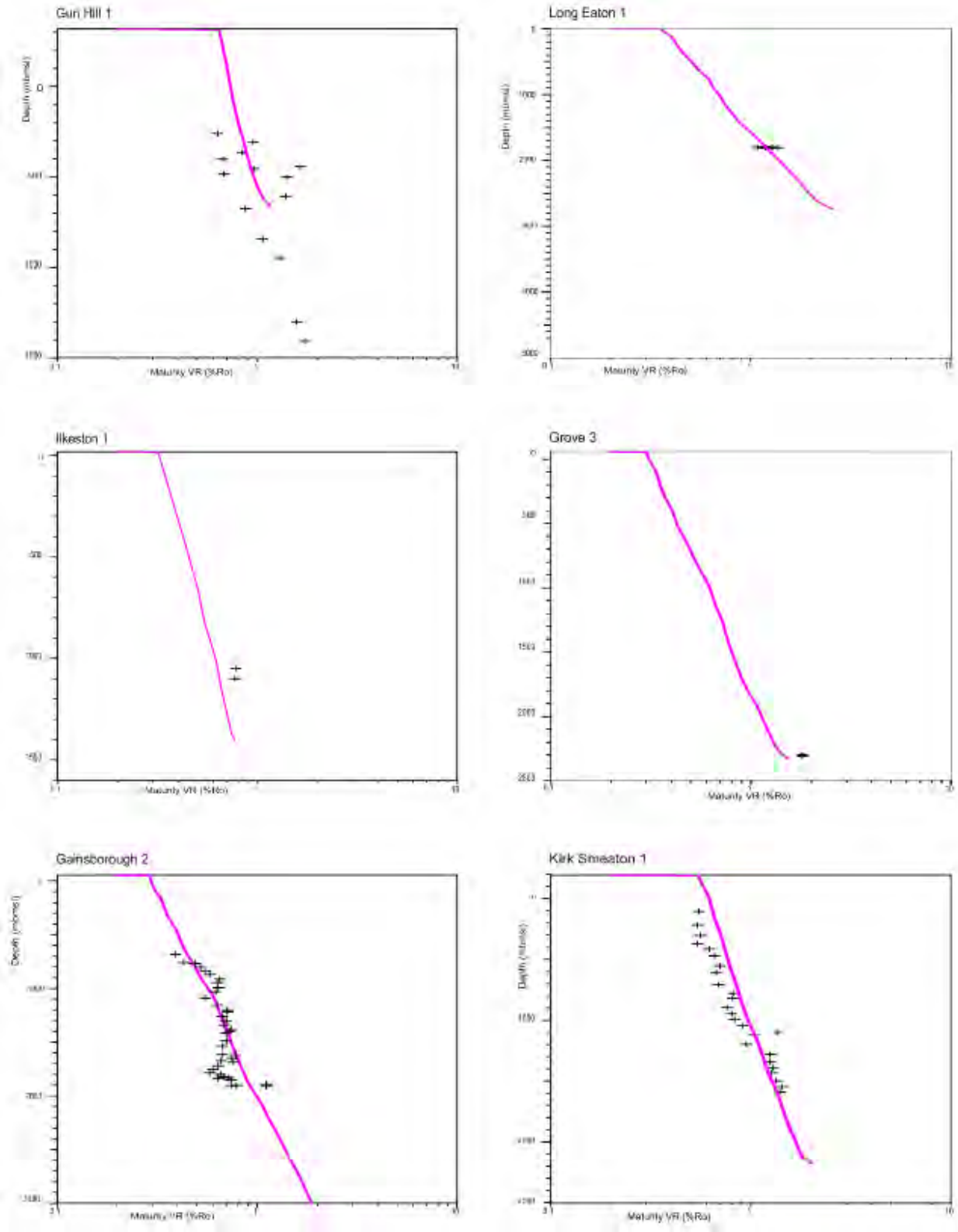

Figure 26. Maturity model at borehole locations across the Widmerpool Trough - Gainsborough Trough 2-D section. Pink line shows the modelled maturity, black crosses show VR data.

Glossary

LBS Lower Bowland Shale

MG Millstone Grit Group

MMG Mercia Mudstone Group

SSG Sherwood Sandstone Group

UBS Upper Bowland Shale

VR Vitrinite reflectance

References

British Geological Survey holds most of the references listed below, and copies may be obtained via the library service subject to copyright legislation (contact libuser@bgs.ac.uk for details). The library catalogue is available at: http://geolib.bgs.ac.uk.

AITKENHEAD, N., BARCLAY, W. J., BRANDON, A., CHADWICK., R. A., CHISHOLM, J, I., COOPER, A. H. AND JOHNSON, E. W. 2002. British Regional Geology. The Pennines and adjacent areas. Fourth Edition. *British Geological Survey, Nottingham*

BGS 2009, Geological Time Chart, version 6 March 2009

BURLEY, A. J., EDMUNDS. W. M. AND GALE. I. N. 1984. Investigation of the geothermal potential of the UK. Catalogue of geothermal data for the land area of the United Kingdom. Second revision. *British Geological Survey, Nottingham*

DOWNING, R. A. AND GRAY, D. A. (EDITORS) 1986. Geothermal Energy – the potential of the United Kingdom. *Her Majesty's Stationary Office, London*

GRADSTEIN., F. M., OGG., J. G. AND SMITH, A. G. (EDITORS) 2004. A geologic time scale. *Cambridge University Press, Cambridge*.

HAINS, B. A. AND HORTON, A. 1969. British Regional Geology. Central England (Third Edition). *Her Majesty's Stationary Office, London*

INTERNATIONAL COMMISSION ON STRATIGRAPHY (ICS), 2006. International Stratigraphic Chart 2006. www.**stratigraphy**.org/

JARVIS, G. T. AND MCKENZIE, D. P. 1980. Sedimentary Basin Formation with Finite Extension Rates. *Earth and Planetary Science Letters **48,** 42-52.*

LEWIS. C. L. E., GREEN, P. F., CARTER, A. AND HURFORD A. J. 1992. Elevated K/T palaeotemperatures throughout Northwest England: three kilometres of Tertiary erosion? *Earth and Planetary Science Letters **112,** 131-145.*

PEARSON, M. J., AND RUSSELL, M. A. 2000. Subsidence and erosion in the Pennine Carboniferous Basin, England: lithological and thermal constraints on maturity modelling. *J. Geol. Soc. Lond. Vol **157**, 471-482*.

PHARAOH, T. C., VINCENT, C. J., BENTHAM, M. S., HULBERT, A., WATERS, C. N. AND SMITH N. J. P. 2011. Structure and evolution of the East Midlands Region of the Pennine Basin. British Geological Survey Subsurface Memoir. *BGS, Keyworth* 144pp

PLANT, J. A., JONES, D. G. AND HASLAM, H. W. (ed.) 1999. The Cheshire Basin. Basin evolution, fluid movement and mineral resources in a Permo-Trias rift setting. *Keyworth, Nottingham: British Geological Survey*.

ROWLEY, E. & WHITE, N. 1998 Inverse modelling of extension and denudation in the East Irish Sea and surrounding areas. *Earth and Planetary Science Letters* **161,** 57–71.

SCLATER, J. G. AND CHRISTIE, P. A. F. 1980. Continental Stretching: An Explanation of the post-mid-Cretaceous Subsidence of the Central North Sea Basin. *J. Gephys. Res.* ***85****, 3711-3739*.

SMITH, N., VANE, C. & MOSS-HAYES, V. 2012. Rock-Eval geochemical analysis of 109 samples from the Carboniferous of the Pennine Basin, including the Bowland-Hodder unit. Appendix to DECC final report.

STACH, E., MACKOWSKY, M.TH., TEICHMULLER, M.,TAYLOR, G. H., CHANDRA, D., TEICHMULLER, R. 1982. Stach's Textbook of Coal Petrology (3rd ed.) *Gebruder Borntraeger, Berlin, Stuttgart*

VINCENT, C. J. AND MERRIMAN, R. J. 2002. Thermal Modelling of the Cheshire Basin using BasinMod™. *British Geological Survey Internal Report*, IR/03/092. 223pp.

C.J. Vincent & I.J. Andrews

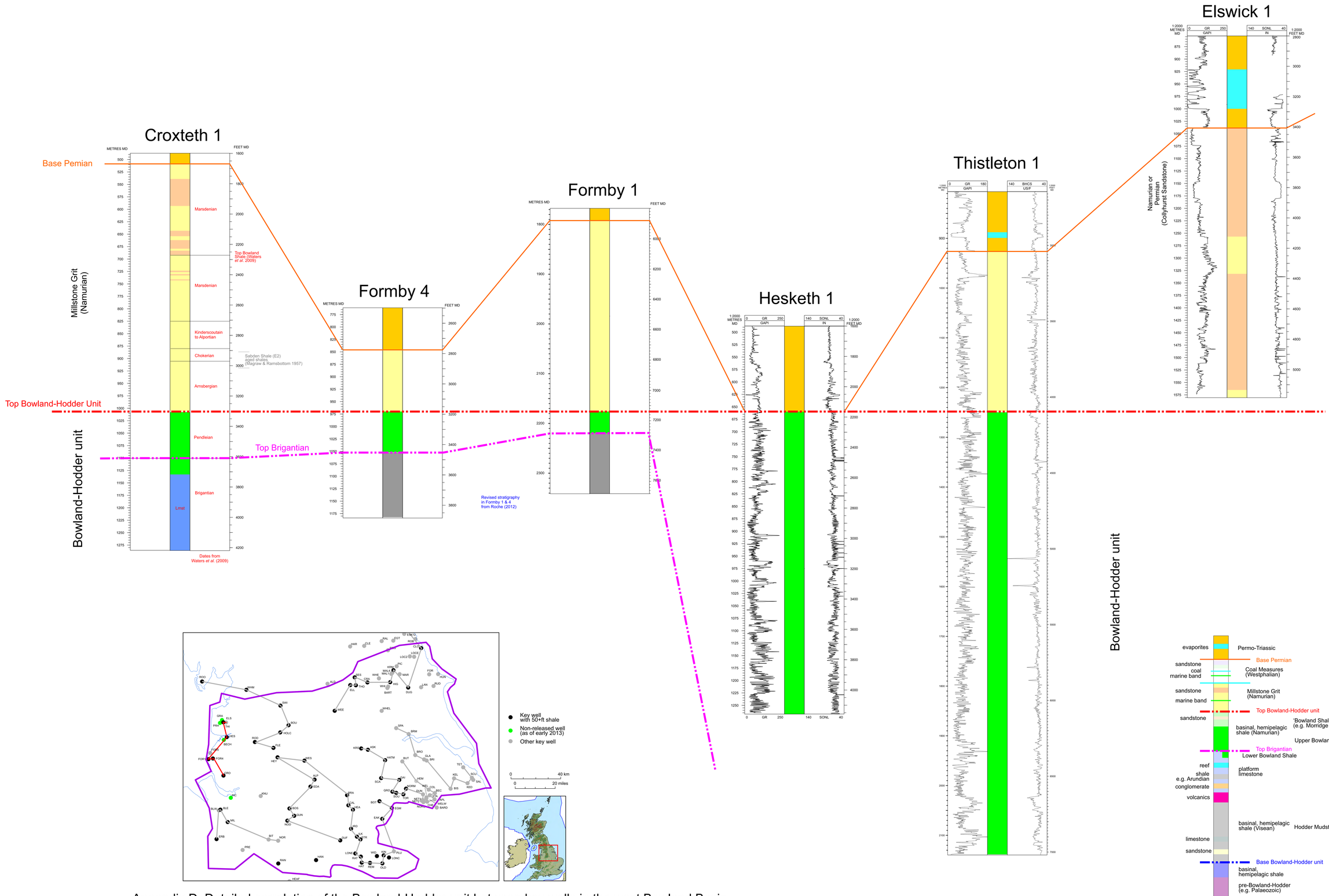

Appendix D. Detailed correlation of the Bowland-Hodder unit between key wells in the west Bowland Basin.

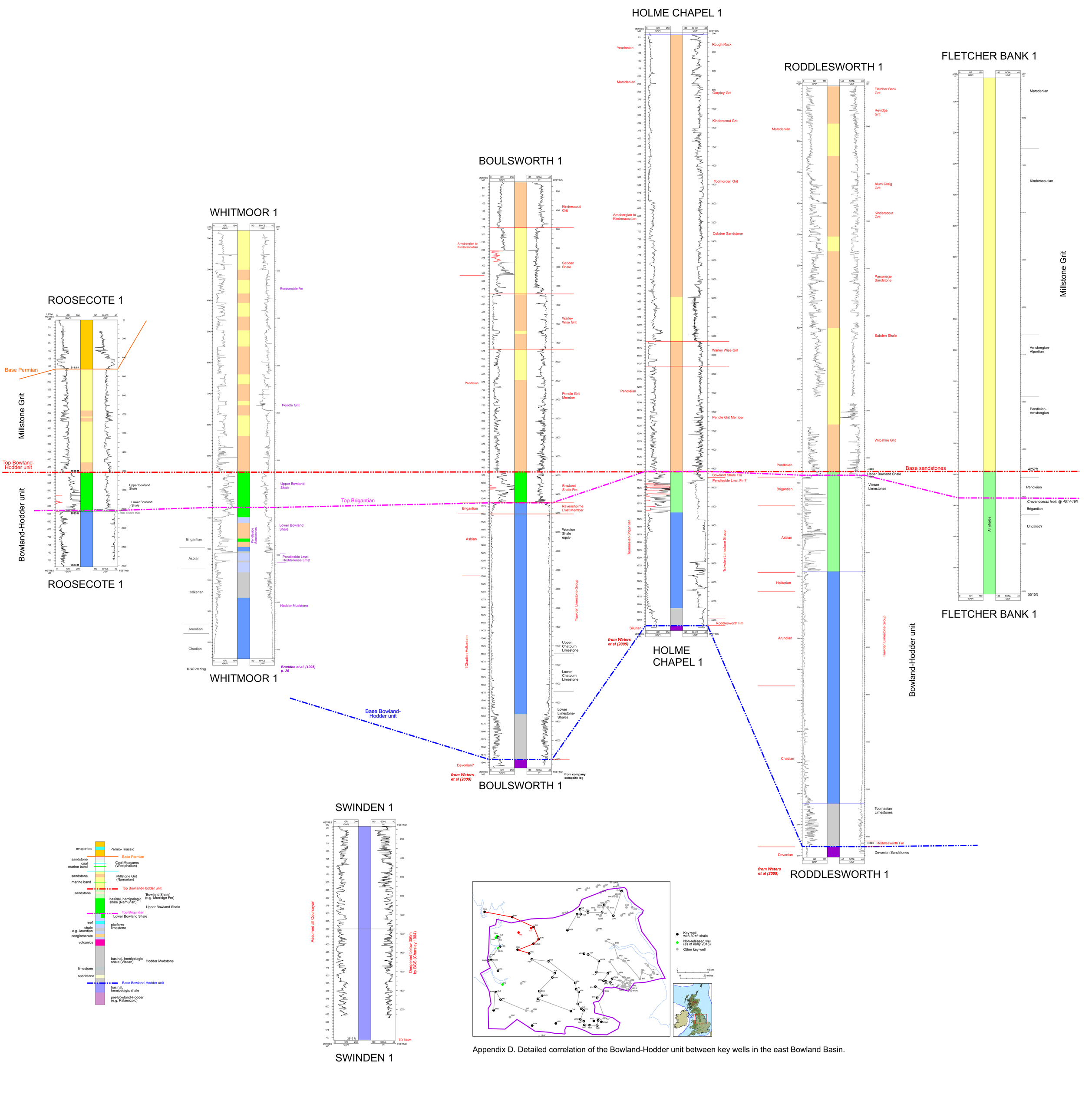

Appendix D. Detailed correlation of the Bowland-Hodder unit between key wells in the east Bowland Basin.

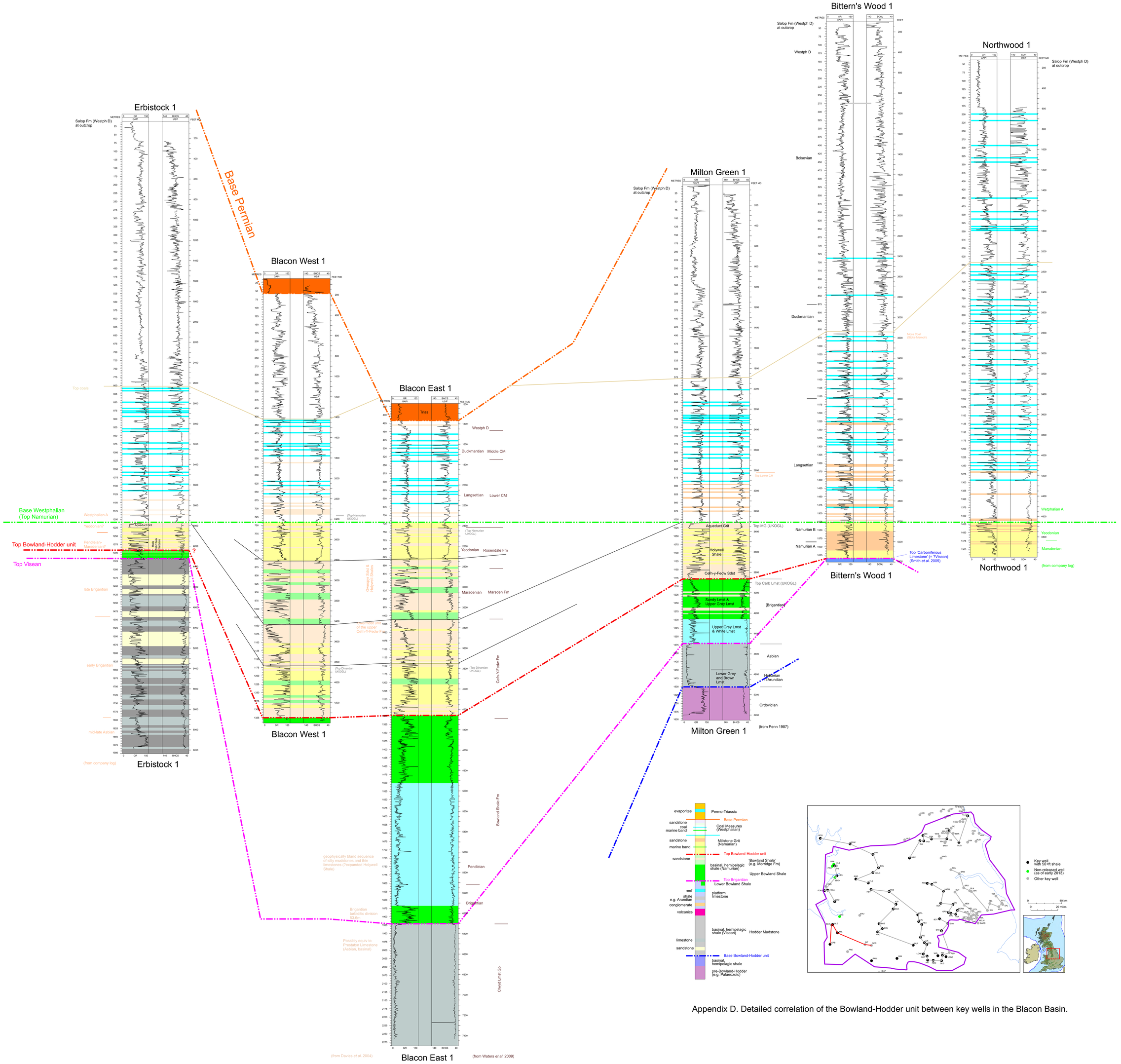

Appendix D. Detailed correlation of the Bowland-Hodder unit between key wells in the Blacon Basin.

Appendix D. Detailed correlation of the Bowland-Hodder unit between key wells in the Widmerpool and Edale basins.

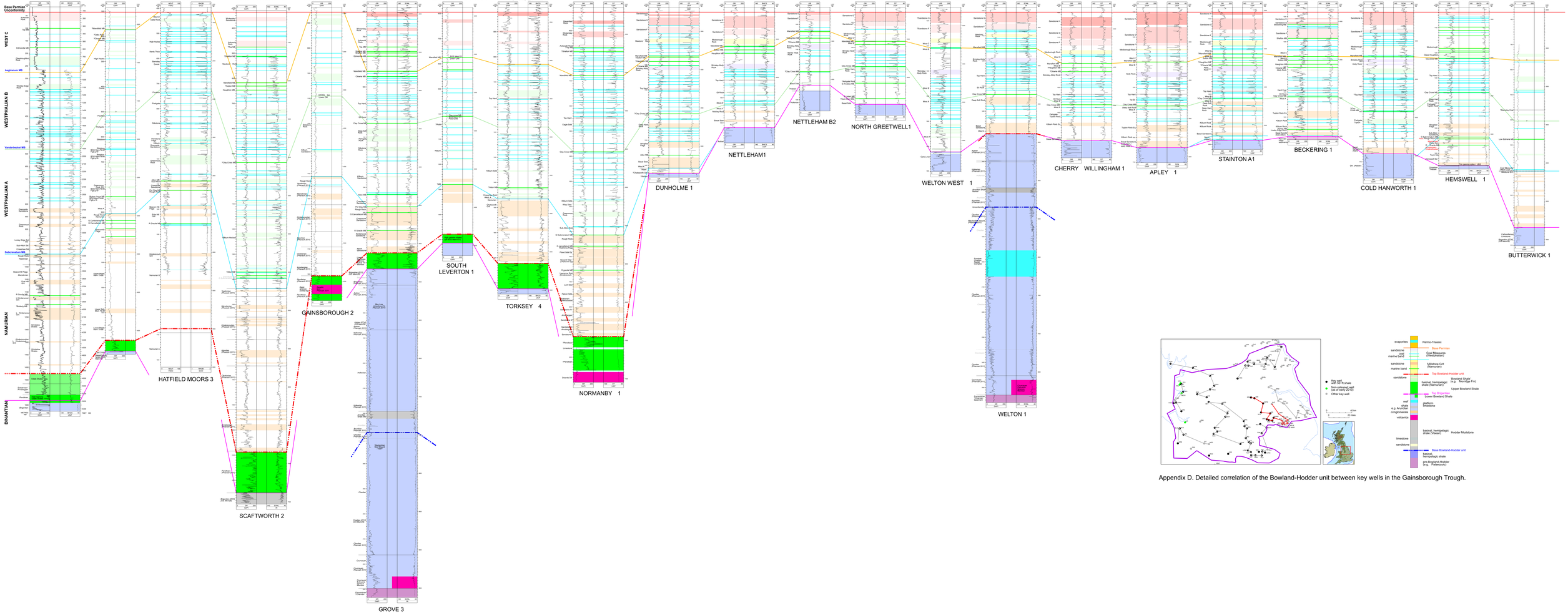

Appendix D. Detailed correlation of the Bowland-Hodder unit between key wells in the Gainsborough Trough.

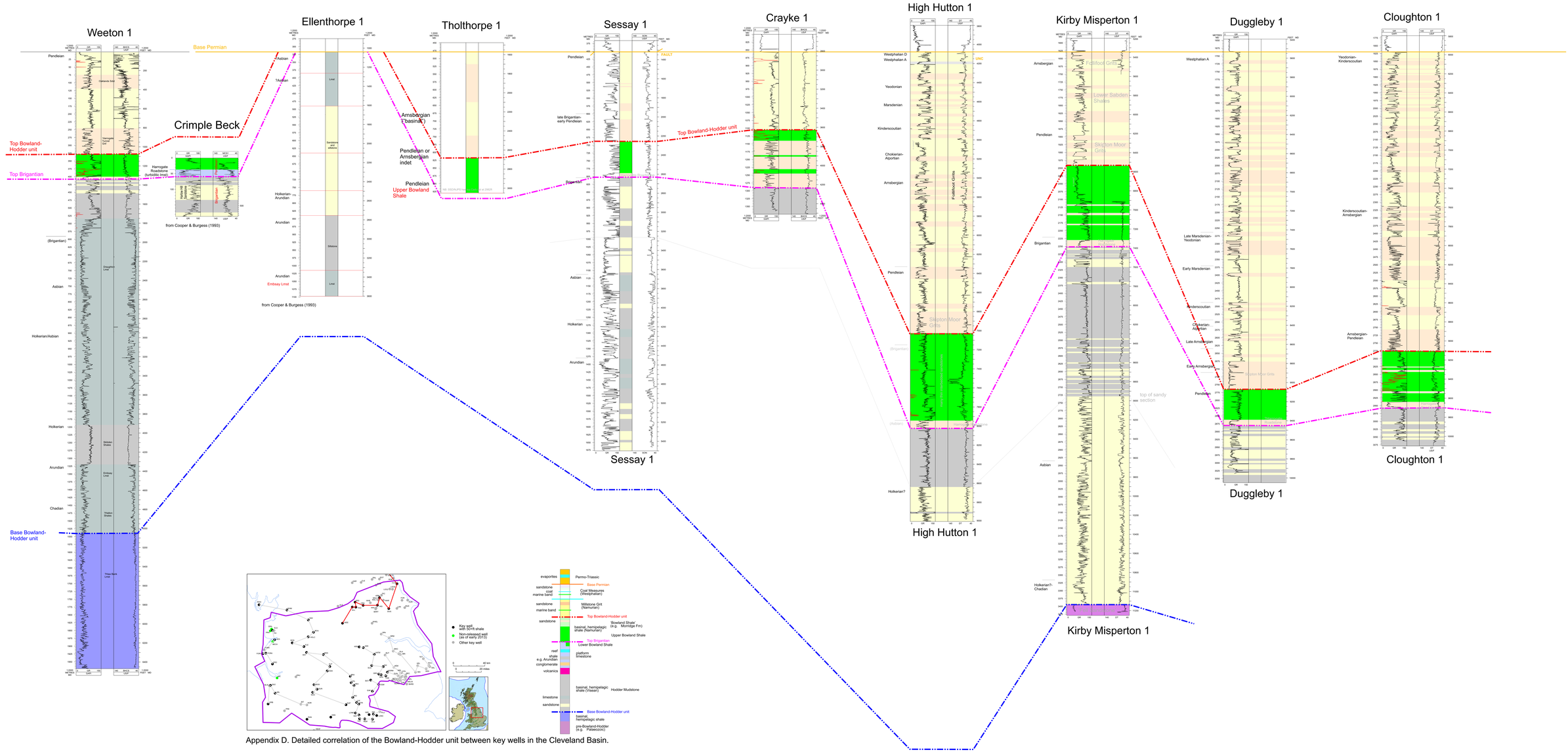

Appendix D. Detailed correlation of the Bowland-Hodder unit between key wells in the Cleveland Basin.

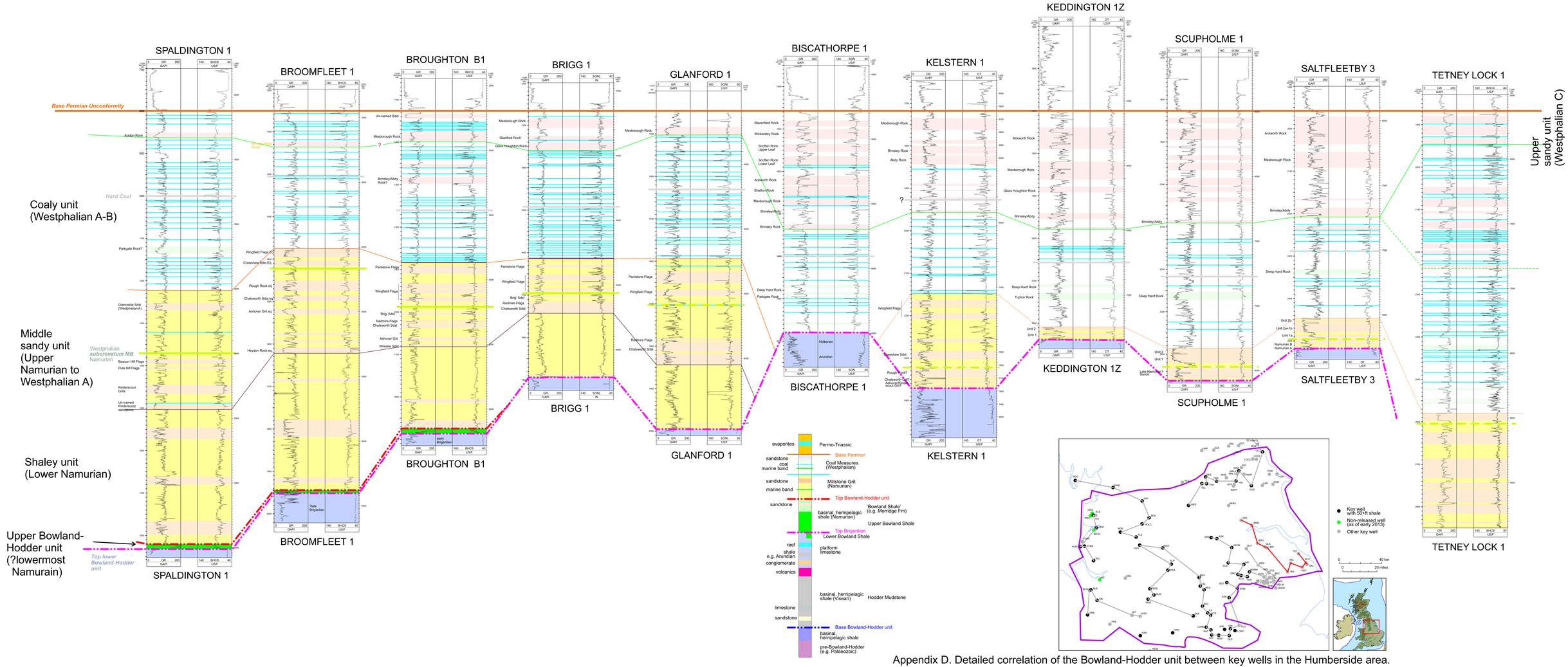

Appendix D. Detailed correlation of the Bowland-Hodder unit between key wells in the Humberside area.